eman ta zabal zazu

Universidad del País Vasco
Euskal Herriko Unibertsitatea
University of the Basque Country

Molecular recognition and Host-Pathogen interactions Unit CIC bioGUNE

Inflammation and Macrophage plasticity laboratory

PhD Thesis

Surface receptors that mediate the interaction of *Borrelia burgdorferi* with macrophages: Death and Inflammation

Ana Carreras González

Supervisors:

Dr. Juan Anguita Castillo

Dra. Ana María Zubiaga Elordieta

eman ta zabal zazu
Universidad del País Vasco
Euskal Herriko Unibertsitatea
University of the Basque Country

CIC bioGUNE
CENTER FOR COOPERATIVE RESEARCH IN BIOSCIENCES

Molecular recognition and Host-Pathogen interactions Unit CIC bioGUNE

Inflammation and Macrophage plasticity laboratory

PhD Thesis

Surface receptors that mediate the interaction of *Borrelia burgdorferi* with Macrophages: Death and Inflammation

Ana Carreras González

Supervisors

Dr. Juan Anguita Castillo

Dr. Ana María Zubiaga Elordieta

Unveiling *Borrelia burgdorferi* phagocytosis mediated by Macrophages and their implication on the inflammatory response

Agradecimientos / Acknowledgements

Voy a dedicar este espacio a agradecer a todas las personas que me han apoyado incondicionalmente a lo largo de estos años, personal y profesionalmente, haciendo posible la realización de este proyecto.

Lo primero de todo, agradecer especialmente a mis codirectores de tesis, Juan Anguita y Ana Zubiaga, por guiarme y aconsejarme durante mi tesis. Gracias Juan por tu paciencia, por darme la libertad para probar cosas nuevas, fracasar y volverlo a intentar. Por apoyarme cuando me he sentido perdida, y por acompañarme con tu peculiar sentido del humor. Contigo he aprendido a buscar respuestas por mi cuenta, a valerme por mi misma y a recoger y guardar los sobrenadantes de las fagocitosis siempre, siempre y por siempre jamás. Gracias a ti también, Ana, por darme consejos sobre el proyecto y escuchar pacientemente mis largas presentaciones en la UPV. De ti me llevo aprendido que con esfuerzo y perseverancia todo se puede lograr.

Creo que no es necesario decirlo, pero guardo y guardaré un espacio especial en mi corazón para el "Inflammation and Macrophage plasticity laboratory". Nos solo me llevo un poco de cada uno de vosotros conmigo, si no que entre todos me habéis hecho crecer como científica, como persona, y como elemento peculiar de la sociedad.

La primera con la que tuve contacto fue Itzi, que me enseñó el laboratorio y me presentó a sus integrantes. Gracias Itzi por toda la paciencia, por enseñarme tanto, por mostrarme que sin Quartzy no hay tesis, y que debería tatuarme cada PNT en la piel. Y gracias por apoyar todos mis planes de disfrazar el labo, sin duda hemos marcado la diferencia. La segunda en acogerme fue Estiti testa di chorlo. Necesitaría varias páginas para agradecerte todo lo que me gustaría. Gracias por todas las risas, por todas las locuras. Por aquel "Estrella" "Estría" que nos marcó. Por ser tan buena compañera y tan buena amiga. Hay amistades que te marcan para siempre, la tuya es sin duda una de ellas. El tercero en discordia fue Nico, que me enseñó la importancia de tener las células siempre en buen estado, para poder tener resultados consistentes. Gracias por apoyarme en los comienzos, que son siempre duros. Y apareció Julen, con su melodiosa voz y sus ganas de comerse el mundo. Tú has sido sin duda mi hermano mayor, me has apoyado y aconsejado, pero también vacilado y molestado. Da igual lo lejos que te vayas, no podrás librarte de mí.

Y la familia creció. Llegó Miguel Ángel, con su peculiar energía vital, su motivación y su risa contagiosa. Siempre dispuesto a echar una mano, a apoyar a todo el mundo. El que construye el Biogune por las mañanas, jeje. Poco después vino la primera dama, Leti. Sin duda hubiera tardado el doble en escribir la tesis si ella hubieras estado vigilándome en el despacho y apartando a los moscardones (H y Aize, jeje). Muchas gracias por tu apoyo, me ha quedado claro que me tengo que sacar el carnet ASAP.

Gracias Rafa por tu apoyo y por tu peculiar sentido del humor. Por la ayuda prestada, y por tus ganas de probar cosas nuevas. Allá adonde vayas te irá bien, seguro. Y qué decir del gran mago Pendergast, Bubbi blomindale, H para el labo, o Hector para el mundo. Gracias por enseñarme que cuanto más diferente, mejor. Me llevo tu frase: "Cualquier aportación al caos es bienvenida". Por otro lado tenemos a Leti2, o Leti samFrodo, que llegó como un rayo de luz, siempre risueña y con energía. Gran seguidora de mi foforeligión. Gracias por todas las cenas gochas que hemos organizado y por estar ahí cuando lo necesitaba.

Poco después llegó Diegu, Gallu, la locura personificada, tan ruidoso y divertido. Llenando el labo como si se tratara de 5 personas en vez de una. Gracias por todos los momentos que hemos pasado. Ainhoa! Contigo conecté muy rápido, de una manera tan natural que espanta. Eres muy grande! Trabajadora, espontánea y directa. Me alegro de haberte conocido, no cambien nunca. Y ya voy llegando poco a poco al final dela lista. Gracias Ainize por llevarme a todas partes, por las risas que echamos en Amsterdam (Minino Minino) y por enseñarme lo que es una mancuerna! No he visto a nadie tan loca por las hamburguesas jeje. Martius! Llevas menos tiempo, pero me has demostrado lo genial que eres, espero haberte podido transmitir lo necesario para que triunfes en tu tesis. Con tu perseverancia puedes con todo. Y por último, Aize, tú llegaste como una brisa de aire fresco en un día de verano. Mi compañero del frikismo, por fin alguien que entiende mis bromas y guiños. Gracias también por toda la ayuda que me has prestado. Vuelve pronto!! May the FO be with you.

Me va a costar separarme de vosotros. Gracias por apoyarme en mis locuras. Gracias por las risas. Sois un grupo perfecto y no lo olvidaré jamás.

Table of contents:

Chapter 3: Regulation of macrophage activity by *Borrelia burgdorferi*-regulated surface receptors

Summary

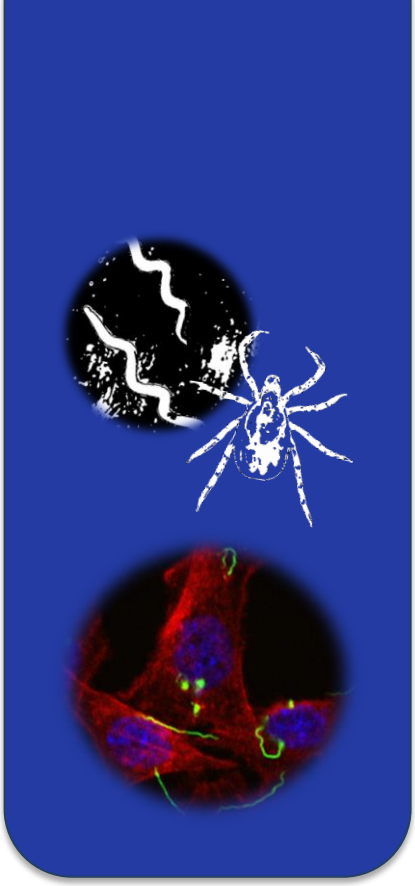

Summary

Lyme disease is the most prevalent vector-borne disease in the Northern hemisphere, with a recent estimate of 650,000-850,000 affected people in Europe (1) and 300,000 in the U.S (2). The increase in Lyme disease cases reported in the last decade in the US and Europe along with climate change-associated shifts in tick populations predicts that this disease will be a major public health concern in the near future. The variety of symptoms associated with the infection and the difficulties in its diagnosis, together with the absence of an effective vaccine underscores the emerging need for more detailed knowledge about the disease and the mechanisms of the immune responses involved.

The importance of macrophages in the control of *B. burgdorferi* infection is two-fold: first, they control spirochetal numbers by phagocytosis; and second, they are greatly responsible for the inflammatory response as a result of infection. Both aspects of the macrophage response are intimately related and therefore, the search for phagocytic receptors also involve the identification of pathways associated with the overall inflammatory output of these cells. In this work, we proposed as a **general aim** the study of macrophage responses to *Borrelia burgdorferi*, focusing on the elements involved in their phagocytic activity and the subsequent cell-mediated inflammatory response, in order to understand more deeply the interaction of this cell type and the bacterium as well as the functional consequences of such interactions.

Using large-scale analytical approaches such as transcriptomics and proteomics, we have studied innate immune responses to the spirochete using both murine macrophages and human monocytes and macrophages. Using RNAseq and micro arrays, we compared the global transcriptional profile of primary murine macrophages (BMM) and human peripheral blood monocytes (hMon) after exposure to *B. burgdorferi.* In both cases, the main transcriptional traits involved in the response resulted in an overlapping pro-inflammatory profile that, nevertheless, reveals distinct transcriptional specificities based on differences both in cell type and species. Overall, similar proinflammatory pathways were found to be activated, such as TLRs, MyD88, NF-κB complex, TNF, IL-1β and IL-1α. Conversely, in both cases, the response suggested the inhibition of IL-10Rα-induced pathways, which have been shown to temper the inflammatory response.

We completed our studies using proteomics analyses: a proteomic profile of BMMs in response to the spirochete; and the identification of proteins present within *B. burgdorferi*-containing phagosomes in human macrophages. Together, the results obtained identified the complex array of signaling components that are involved in the inflammatory output of macrophages, provided clues to the long-term consequences of the encounter of these cells with the spirochete, and allowed us to identify a group of receptors that are involved in the internalization and/or induction of inflammatory factors in response to the bacterium.

Arising from the information obtained in these approaches, we invested a significant effort elucidating the surface receptors and signaling mediators involved in the complex process of *B. burgdorferi* phagocytosis. We discovered that some surface receptors play a regulatory role, while others are directly implicated in the process. Phagosome analysis confirmed that phagocytosis involves several receptors and signaling mediators, distinctly triggering a signaling/inflammatory response.

Apart from confirming the implication in the internalization of the spirochete of receptors already described such as MARCO (4) and uPAR (5), our data allowed us to define a set of receptors that modulate the uptake and/or proinflammatory cytokine production of macrophages in response to *B. burgdorferi.* In particular, we describe the regulation of CD180 in response to *B. burgdorferi*. Our results show that CD180 modulates both phagocytosis and inflammation in response to *B. burgdorferi* through the transcriptional repression of complement receptor 3 (CR3). CD180 is known to play a role in both enhancing and suppressing TLR responses that seem to vary with cell type (6); therefore, our data suggest a tight control on macrophage behavior that is, at the same time, specific to the pathogen. It also indicates that there could be multiple mechanisms of phagocytic and proinflammatory control that may be relevant at different phases of the response.

Our work has led to the identification of the Fc gamma receptor family as phagocytic receptors for *B. burdorferi* in the absence of antibodies. Although the importance of the common FcR γ-chain in the control of spirochetal burdens in mice has been previously demonstrated in the presence of antibodies (7), the alpha chain (CD64) has never been previously related to direct phagocytosis. The results obtained suggest that the role played by these receptors may not be solely mediated by antibodies. Furthermore, the behavior of other members of the pathway, such as CD45 and FcRG3 (low affinity α chain) confirms the relevance of this pathway.

We also elucidated the importance and behavior of different signaling molecules, such as SHIP1, FcRγ, Syk and MyD88. The inhibitory phosphatase SHIP1, the kinase Syk and the common gamma chain, FcRγ do not only signal in response to the Fc Receptor pathway, but have also been demonstrated to interact with activator ITAMs and inhibitory ITIMs present in some C-type lectins (8), many of them described in our studies. SHIP1 can also be recruited by certain C-type lectins, involving FCRγIIB, which can result in an anti-inflammatory response (9).

On the other hand, MyD88 is known to play and important role in *B. burgdorferi* phagocytosis, since is responsible for a large percentage of spirochetal internalization (9); however, although we demonstrate its presence in bacteria-containing phagosomes, we could not identify the receptor(s) that signal through this effector molecule. Several C-type lectins have been reported to crosstalk with TLRs, such as Dectin-1 and TLR2 (11) or DC-SIGN and TLR4 (12). Therefore, since the precise role of each C type lectin remains unknown, we cannot dismiss the possibility that one or various of the described receptors might be indirectly implicated in the MyD88-dependent phagocytosis of *B. burgdorferi*. Overall, the data presented reveal the intricated network and crosstalk between receptor families that intervene in the phagocytic process.

Apart from MARCO, uPAR and CR3, no further receptor has been previously associated with *B. burgdorferi* phagocytosis so far, but many of the receptors described in this thesis play a role in

the ingestion of other pathogens. It is possible that the role played by some of them, such as GPI anchored proteins, might be accessory, as shown in the case of CD14 during CR3-mediated phagocytosis (12).

The overall signature response to a specific pathogen is dictated by the addition of the signals emanating from surface receptors that recognize pathogen components, which is further modulated by the interaction of intracellular signaling molecules, resulting in both the internalization of the pathogen and the induction of cytokines and chemokines. We also describe the complex array of signals that are triggered by the interaction between *B. burgdorferi* and macrophages. Thus, our results will set the basis to elucidate the contribution that each receptor plays in the overall response of macrophages to the spirochete and the assignment of the relationship between receptors and signaling pathways that lead to the functional output on these cells. This knowledge will lead to a better understanding of macrophage function in response to *B. burgdorferi*, clarifying the inflammatory responses observed during human Lyme borreolisis, and revealing new targets of intervention.

REFERENCES

1. EC. Parliament calls for “alarming” spread of Lyme disease to be tackled | News | European Parliament. 2018 (Nov 29). Available from: http://www.europarl.europa.eu/news/en/press-room/20181106IPR18328/parliament-calls-for-alarming-spread-of-lyme-disease-to-be-tackled.
2. Schotthoefer AM, Frost HM. 2015. Ecology and Epidemiology of Lyme Borreliosis. Clin Lab Med 35:723-43.
3. Hawley, K. L., Olson, C. M., Iglesias-Pedraz, J. M., Navasa, N., Cervantes, J. L., Caimano, M. J., … Anguita, J. (2012). CD14 cooperates with complement receptor 3 to mediate MyD88-independent phagocytosis of Borrelia burgdorferi. *Proceedings of the National Academy of Sciences of the United States of America*, *109*(4), 1228–32. http://doi.org/10.1073/pnas.1112078109
4. Petnicki-Ocwieja, T., Chung, E., Acosta, D. I., Ramos, L. T., Shin, O. S., Ghosh, S., … Hua, L. T. (2013). TRIF mediates toll-like receptor 2-dependent inflammatory responses to borrelia burgdorferi. *Infection and Immunity*, *81*(2), 402–410. http://doi.org/10.1128/IAI.00890-12
5. Hovius, J. W. R., Bijlsma, M. F., Van Der Windt, G. J. W., Wiersinga, W. J., Boukens, B. J. D., Coumou, J., … Van Der Poll, T. D. (2009). The urokinase receptor (uPAR) facilitates clearance of Borrelia burgdorferi. *PLoS Pathogens*, *5*(5). http://doi.org/10.1371/journal.ppat.1000447
6. Schultz TE, Blumenthal A. The RP105/MD-1 complex: molecular signaling mechanisms and pathophysiological implications. *J Leukoc Biol* 2017; **101:** 183-192.
7. Belperron AA, Liu N, Booth CJ, Bockenstedt LK. 2014. Dual role for Fcgamma receptors in host defense and disease in Borrelia burgdorferi-infected mice. Front Cell Infect Microbiol 4:75.
8. Mayer, S., Raulf, M. K., & Lepenies, B. (2017). C-type lectins: their network and roles in pathogen recognition and immunity. *Histochemistry and Cell Biology*, *147*(2), 223–237. http://doi.org/10.1007/s00418-016-1523-7

9. Köhl, G., Kilchenstein, R., Figge, J., Strait, R. T., Karsten, C. M., Ludwig, R., … Winkler, A. (2012). Anti-inflammatory activity of IgG1 mediated by Fc galactosylation and association of FcγRIIB and dectin-1. *Nature Medicine*, *18*(9), 1401–1406. http://doi.org/10.1038/nm.2862
10. Petnicki-Ocwieja, T., Chung, E., Acosta, D. I., Ramos, L. T., Shin, O. S., Ghosh, S., … Hua, L. T. (2013). TRIF mediates toll-like receptor 2-dependent inflammatory responses to borrelia burgdorferi. *Infection and Immunity*, *81*(2), 402–410. http://doi.org/10.1128/IAI.00890-12
11. K M. Dennehy, G Ferwerda, I Faro-Trindade, E Pyz, J A. Willment, P R. Taylor, A Kerrigan, S. V Tsoni, S Gordon, F Meyer-Wentrup, G J. Adema, BJ Kullberg, E Schweighoffer, V Tybulewicz, H M. Mora-Montes, N A. R. Gow, D L. Williams, M G. Netea and G D. Brown (2008). Syk kinase is required for collaborative cytokine production induced through Dectin-1 and Toll-like receptors.
European Journal of Immunology, *38*(2), 500–506. http://doi.org/10.1002/eji.200737741
12. Feng, D., Wang, Y., Liu, Y., Wu, L., Li, X., Chen, Y., … Zhou, T. (2018). DC-SIGN reacts with TLR-4 and regulates inflammatory cytokine expression via NF-κB activation in renal tubular epithelial cells during acute renal injury. *Clinical and Experimental Immunology*, *191*(1), 107–115. http://doi.org/10.1111/cei.13048
13. Hawley, K. L., Martín-Ruiz, I., Iglesias-Pedraz, J. M., Berwin, B., & Anguita, J. (2013). CD14 targets complement receptor 3 to lipid rafts during phagocytosis of Borrelia burgdorferi. *International Journal of Biological Sciences*, *9*(8), 803–810. http://doi.org/10.7150/ijbs.7136

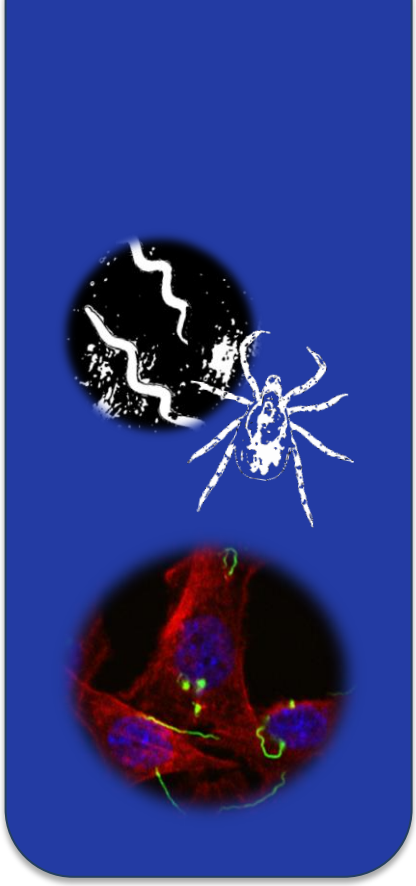

Resumen

La enfermedad de Lyme es la enfermedad transmitida por artrópodos más prevalente en el hemisferio norte, con una estimación reciente de 650,000-850,000 personas afectadas en Europa (1) y 300,000 en los EE. UU. (2). Esta enfermedad es causada por una bacteria llamada *Borrelia burgdorferi* que es transmitida al ser humano a través de la picadura garrapatas pertenecientes al género *Ixodes*. El aumento en los casos de enfermedad de Lyme diagnosticados en la última década en los EE. UU. y Europa, junto con los cambios en las poblaciones de garrapatas debidos al cambio climático, predice que esta enfermedad será un problema importante de salud pública en un futuro cercano. Las dificultades en el diagnóstico y la ausencia de una vacuna eficaz frente a la enfermedad de Lyme apuntan a que existe una necesidad apremiante de obtener un conocimiento más detallado sobre la enfermedad y los mecanismos de la respuesta inmune involucrada. La investigación en esta área de estudio podría contribuir al desarrollo de terapias efectivas y herramientas de diagnóstico específicas que faciliten el tratamiento de esta enfermedad, que en muchos casos sigue mal o poco diagnosticada.

La importancia de los macrófagos en el control de la infección por *B. burgdorferi* es doble: primero, intervienen en la eliminación de las espiroquetas mediante el proceso de fagocitosis; y segundo, son responsables de la respuesta inflamatoria provocada en respuesta la infección. Ambos aspectos de la respuesta están íntimamente relacionados y, por lo tanto, la búsqueda de receptores fagocíticos también conlleva la identificación de vías de señalización asociadas a la respuesta inflamatoria mediada por estas células. En este proyecto, propusimos como objetivo general el estudio de la respuesta inmune de los macrófagos a *B. burgdorferi*, centrándonos en los elementos involucrados en su actividad fagocítica y la posterior respuesta inflamatoria mediada por estas células, a fin de comprender más profundamente la interacción de este tipo de células y la bacteria.

Mediante enfoques analíticos de gran escala, como la transcriptómica y la proteómica, hemos estudiado la respuesta inmune innata frente a la espiroqueta utilizando macrófagos de ratón y monocitos y macrófagos humanos. A través de los análisis de RNAseq y microarray, hemos comparado el perfil transcripcional global de macrófagos murinos primarios (BMM) y de

monocitos sanguíneos periféricos humanos (hMon) en respuesta a *B. burgdorferi*. En ambos casos, los principales rasgos transcripcionales involucrados en la respuesta presentan un perfil proinflamatorio que, sin embargo, muestran especificidades debidas a diferencias en el tipo celular y especie. A grandes rasgos, se encontró la activación de vías proinflamatorias similares, tales como TLR, MyD88, el complejo NF-B, TNF, IL-1β e IL-1α. Por el contrario, en ambos casos la respuesta provocó la inhibición de las vías inducidas por IL-10Rα, que se ha demostrado que atenúan la respuesta inflamatoria.

Completamos nuestro estudio realizando dos análisis proteómicos: un análisis proteómico de BMM en respuesta a la espiroqueta; y la identificación de proteínas presentes dentro de los fagosomas de macrófagos humanos tras fagocitar *B. burgdorferi*. Juntos, los resultados obtenidos identificaron el conjunto de componentes de señalización que participan en la respuesta inflamatoria de los macrófagos. Los datos proporcionaron pistas sobre las consecuencias a largo plazo de la estimulación de estas células con la espiroqueta y nos permitieron identificar un grupo de receptores que están involucrados en la internalización y / o inducción de factores inflamatorios en respuesta a la bacteria.

Partiendo de la información obtenida en estos ensayos, tratamos de describir los receptores de superficie y los mediadores de señalización involucrados en el complejo proceso de fagocitosis de *B. burgdorferi*. Descubrimos que algunos receptores de superficie desempeñan un papel regulador, mientras que otros están directamente implicados en el proceso. El análisis de los fagosomas confirmó que la fagocitosis involucra varios receptores y mediadores de señalización, lo que desencadena claramente una respuesta de señalización / inflamatoria.

Además de confirmar la implicación en la fagocitosis de la espiroqueta de receptores ya descritos, como MARCO (4) y uPAR (5), nuestros datos nos permitieron definir un conjunto de receptores que modulan la captación y/o la producción de citoquinas proinflamatorias por los

macrófagos en respuesta a *B. Burgdorferi*. En particular, describimos el papel regulador de CD180 en respuesta a la bacteria. Nuestros resultados muestran que CD180 modula tanto la fagocitosis como la inflamación en respuesta a *B. burgdorferi* a través de la represión transcripcional del receptor del complemento 3 (CR3). Se sabe que CD180 desempeña un papel tanto en la activación como en la represión de las respuestas mediadas por los receptores tipo Toll (TLRs). El papel desempeñado por CD180 parece variar dependiendo del tipo celular y del tipo de patógeno (6); por lo tanto, nuestros datos sugieren que hay un estricto control sobre el comportamiento del macrófago que es, al mismo tiempo, dependiente del tipo de patógeno. También indican que podría haber múltiples mecanismos de control sobre la fagocitosis e inflamación que pueden ser relevantes en diferentes fases de la respuesta inmune.

Gracias a nuestra investigación hemos identificado a la familia de receptores Fc gamma como mediadores fagocíticos de *B. burgdorferi* en ausencia de anticuerpos. Aunque la importancia de la cadena FcRγ en la respuesta a la espiroqueta ha sido demostrada previamente en ratones aunque en presencia de anticuerpos (7), la cadena alfa (CD64) no se ha relacionado previamente con la fagocitosis no opsónica. Los resultados obtenidos en nuestro estudio sugieren que el papel desempeñado por estos receptores puede no estar mediado únicamente por anticuerpos. Además, el comportamiento de otros miembros de la ruta de señalización, tales como como CD45 y FcRG3 (cadena α de baja afinidad) confirma la implicación de esta ruta en la respuesta inmune a este patógeno.

También esclarecimos la importancia y el comportamiento de diferentes factores de señalización, como SHIP1, FcRγ, Syk y MyD88. La fosfatasa inhibitoria SHIP1, la quinasa Syk y la cadena gamma, FcRγ, no solo transducen las señales de la ruta de señalización de los Fc, sino que se ha demostrado que interactúan con dominios intracelulares ITAM (activadores) e ITIM (inhibidores) presentes en algunas lectinas de tipo C (8) , muchos de ellos descritos en nuestro estudio. SHIP1 también puede ser reclutado por ciertas lectinas de tipo C, que, involucrando al receptor FCRγIIB, desencadenan una respuesta antiinflamatoria (9).

Por otro lado, se ha demostrado que MyD88 juega un papel importante en la fagocitosis de *B. burgdorferi*, siendo responsable de un gran porcentaje de la internalización de las espiroquetas (9); sin embargo, aunque hemos identificado su presencia en los fagosomas de *B. burgdorferi*, no hemos podido identificar los receptores que actúan a través de este elemento de señalización. Se ha descrito que varias lectinas de tipo C interactúan con los TLRs, tales como como Dectin-1 y TLR2 (11) o DC-SIGN y TLR4 (12). Por lo tanto, dado que el papel exacto que desempeña cada lectina de tipo C sigue siendo desconocido, no podemos descartar la posibilidad de que uno o varios de los receptores descritos en nuestro estudio puedan estar implicados en la fagocitosis dependiente de MyD88. En conclusión, los datos obtenidos revelan que existe una compleja conexión entre las familias de los receptores que intervienen en el proceso de fagocitosis de este patógeno.

Además de MARCO, uPAR y CR3, hasta ahora no se había asociado ningún otro receptor con la fagocitosis de *B. burgdorferi*, sin embargo, muchos de los receptores descritos en esta tesis desempeñan un papel en la eliminación de otros patógenos. Es posible que la implicación de algunos de ellos, como las proteínas ancladas a GPI, pueda ser accesoria, como se muestra en el caso de CD14 durante la fagocitosis mediada por CR3 (12).

La respuesta inmune global a un patógeno está dictada por la integración de las señales que emanan de los receptores de superficie que reconocen los componentes del patógeno. Estas señales son moduladas por la interacción entre los factores de señalización intracelular, lo que resulta en la internalización del patógeno y la inducción de citoquinas y quimiocinas. Nuestro estudio describe la complejidad de las señales que se activan tras la interacción entre *B. burgdorferi* y los macrófagos. Por lo tanto, nuestros resultados establecen la base para entender la contribución que cada receptor desempeña en la respuesta general de los macrófagos a la espiroqueta y la relación entre los receptores y las vías de señalización.

Este conocimiento conducirá a una mejor comprensión del rol de los macrófagos en respuesta a *B. burgdorferi*, arrojando luz sobre los síntomas inflamatorios observados durante la borreolisis de Lyme y revelando nuevas dianas terapéuticas para un tratamiento más efectivo de la enfermedad.

REFERENCIAS

1. EC. Parliament calls for “alarming” spread of Lyme disease to be tackled | News | European Parliament. 2018 (Nov 29). Available from: http://www.europarl.europa.eu/news/en/press-room/20181106IPR18328/parliament-calls-for-alarming-spread-of-lyme-disease-to-be-tackled.
2. Schotthoefer AM, Frost HM. 2015. Ecology and Epidemiology of Lyme Borreliosis. Clin Lab Med 35:723-43.
3. Hawley, K. L., Olson, C. M., Iglesias-Pedraz, J. M., Navasa, N., Cervantes, J. L., Caimano, M. J., … Anguita, J. (2012). CD14 cooperates with complement receptor 3 to mediate MyD88-independent phagocytosis of Borrelia burgdorferi. *Proceedings of the National Academy of Sciences of the United States of America*, *109*(4), 1228–32. http://doi.org/10.1073/pnas.1112078109
4. Petnicki-Ocwieja, T., Chung, E., Acosta, D. I., Ramos, L. T., Shin, O. S., Ghosh, S., … Hua, L. T. (2013). TRIF mediates toll-like receptor 2-dependent inflammatory responses to borrelia burgdorferi. *Infection and Immunity*, *81*(2), 402–410. http://doi.org/10.1128/IAI.00890-12
5. Hovius, J. W. R., Bijlsma, M. F., Van Der Windt, G. J. W., Wiersinga, W. J., Boukens, B. J. D., Coumou, J., … Van Der Poll, T. D. (2009). The urokinase receptor (uPAR) facilitates clearance of Borrelia burgdorferi. *PLoS Pathogens*, *5*(5). http://doi.org/10.1371/journal.ppat.1000447
6. Schultz TE, Blumenthal A. The RP105/MD-1 complex: molecular signaling mechanisms and pathophysiological implications. *J Leukoc Biol* 2017; **101:** 183-192.
7. Belperron AA, Liu N, Booth CJ, Bockenstedt LK. 2014. Dual role for Fcgamma receptors in host defense and disease in Borrelia burgdorferi-infected mice. Front Cell Infect Microbiol 4:75.
8. Mayer, S., Raulf, M. K., & Lepenies, B. (2017). C-type lectins: their network and roles in pathogen recognition and immunity. *Histochemistry and Cell Biology*, *147*(2), 223–237. http://doi.org/10.1007/s00418-016-1523-7

9. Köhl, G., Kilchenstein, R., Figge, J., Strait, R. T., Karsten, C. M., Ludwig, R., … Winkler, A. (2012). Anti-inflammatory activity of IgG1 mediated by Fc galactosylation and association of FcγRIIB and dectin-1. *Nature Medicine*, *18*(9), 1401–1406. http://doi.org/10.1038/nm.2862
10. Petnicki-Ocwieja, T., Chung, E., Acosta, D. I., Ramos, L. T., Shin, O. S., Ghosh, S., … Hua, L. T. (2013). TRIF mediates toll-like receptor 2-dependent inflammatory responses to borrelia burgdorferi. *Infection and Immunity*, *81*(2), 402–410. http://doi.org/10.1128/IAI.00890-12
11. K M. Dennehy, G Ferwerda, I Faro-Trindade, E Pyz, J A. Willment, P R. Taylor, A Kerrigan, S. V Tsoni, S Gordon, F Meyer-Wentrup, G J. Adema, BJ Kullberg, E Schweighoffer, V Tybulewicz, H M. Mora-Montes, N A. R. Gow, D L. Williams, M G. Netea and G D. Brown (2008). Syk kinase is required for collaborative cytokine production induced through Dectin-1 and Toll-like receptors.
European Journal of Immunology, *38*(2), 500–506. http://doi.org/10.1002/eji.200737741
12. Feng, D., Wang, Y., Liu, Y., Wu, L., Li, X., Chen, Y., … Zhou, T. (2018). DC-SIGN reacts with TLR-4 and regulates inflammatory cytokine expression via NF-κB activation in renal tubular epithelial cells during acute renal injury. *Clinical and Experimental Immunology*, *191*(1), 107–115. http://doi.org/10.1111/cei.13048
13. Hawley, K. L., Martín-Ruiz, I., Iglesias-Pedraz, J. M., Berwin, B., & Anguita, J. (2013). CD14 targets complement receptor 3 to lipid rafts during phagocytosis of Borrelia burgdorferi. *International Journal of Biological Sciences*, *9*(8), 803–810. http://doi.org/10.7150/ijbs.7136

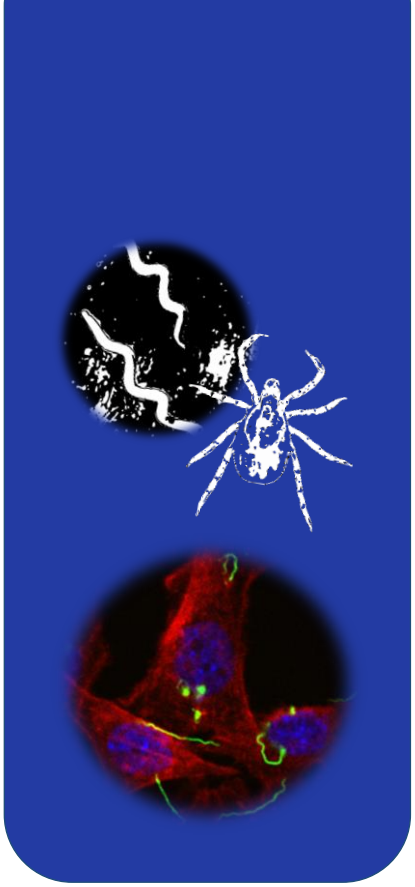

Chapter 1

Introduction

1.1 Introduction to Lyme disease

Lyme disease is a multisystemic illness caused by spirochetes of the genus, *Borrelia* and transmitted by ticks. It is the most prevalent vector-borne disease of the northern hemisphere. The incidence of the disease is estimated to be 300,000 cases per year in the US (CDC) and up to 850,000 cases is Europe (CisiD); however, these numbers could be higher because Lyme disease is not always reported due to the lack of mandatory reporting in several areas, including Europe. Most cases in Europe are located in areas of Central and Eastern Europe (Slovenia, Lithuania, Bulgaria, Estonia, Poland and the Czech Republic). The incidence of Lyme disease has increased during the last decades due to climate change as increasing temperatures have expanded the habitat range for the tick vectors of Lyme disease.

Lyme disease, also known as Lyme borreolisis, was first described in 1975 in Lyme, Connecticut, where a group of children presented symptoms related to juvenile rheumatoid arthritis, therefore the disease was at first called “Lyme arthritis” (1). In June 1982, Willy Burgdorfer discovered a previously unidentified bacterium in a nymphal *Ixodes scapularis* tick, further research demonstrated that this microorganism was also present in sera from patients diagnosed with Lyme disease. After he published his findings the spirochete was named *Borrelia burgdorferi* in his honour (2). The symptoms of the disease have been described along the past centuries in regions of USA and Europe. Moreover, the 2010 autopsy of Ötzi the Iceman, a 5,300-year-old mummy, revealed the presence of the DNA of *Borrelia burgdorferi*, making him possibly the earliest known human with Lyme disease (3).

Lyme disease is a zoonotic disease transmitted between humans and other animals by hard-bodied tick belonging to the *Ixodes* genus, namely *Ixodes scapularis* and *Ixodes pacificus* in US and *Ixodes ricinus* in EU (4) (Figure 1). In addition to *B. burgdorferi*, *I. scapularis* can also act as the vector for other pathogens including *Anaplasma phagocytophilum* and *Babesia microti*. Different *Borrelia* genospecies are known to cause the disease, *B. burgdorferi sensu stricto* (hereafter referred to as *B. burgdorferi*) is the only genospecies that cause the disease in North America, while *B. afzelii* and *B. garinii* are most prevalent in Eurasia (5). Together, all 3 Borrelia genospecies are collectively referred to as *B. burgdorferi sensu lato*. The genus comprises 30 genospecies, albeit at least three species are known to cause the disease in Europe (*B. burgdorferi s.l., B. spielmanii,* and *B. bavariensis*), leading to a wider

variety of clinical manifestations in Europe than in North America. A further three species (*B. bissettii, B. lusitaniae* and *B. valaisiana*) have been very occasionally detected in European patients, but are not recognised as disease causing pathogens (4). Other members of the *Borrelia* genus are known to cause relapsing fever, which are also transmitted by ticks but with a different geographical distribution and inducing distinct symptomatology (6).

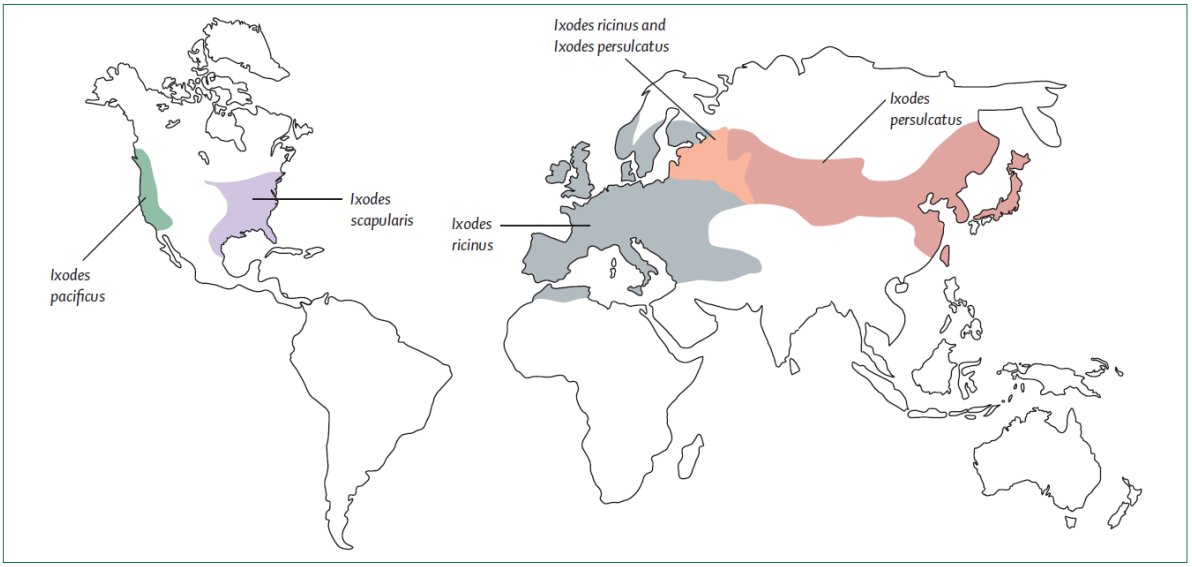

Figure 1: Global distribution of the vectors (*Ixodes ricinus* species complex) of Lyme disease. Modified from Stanek G. *et al., 2012.*

Transmission of the spirochete occurs through the bite of ticks. A feeding period of more than 40-48 hours is usually needed for transmission of *B. burgdorferi* by *I. scapularis* or *I. pacificus* ticks (1). Transmission of *B afzelii* by *I. ricinus*, however, may require less time (7). The clinical manifestations of the disease vary depending on the strain that causes the infection; While *B. afzelii* localizes to the skin, *B. garinii* is usually associated with nervous system disorders (4). *B. burgdorferi* rarely causes this disease in Europe; nevertheless, it is the sole agent of Lyme borreliosis in the United States, presenting with symptoms more associated with arthritic lesions in the northeaster region (4, 5). Furthermore, *B. burgdorferi* induces a broader symptomatology compared to the other two species, and more frequent hematogenous dissemination (8). The only hallmark symptom associated with the infection with these three species is a skin rash, *erythema migrans*, which appears at the site of infection within 7 to 10 days after the tick bite (Figure 5).

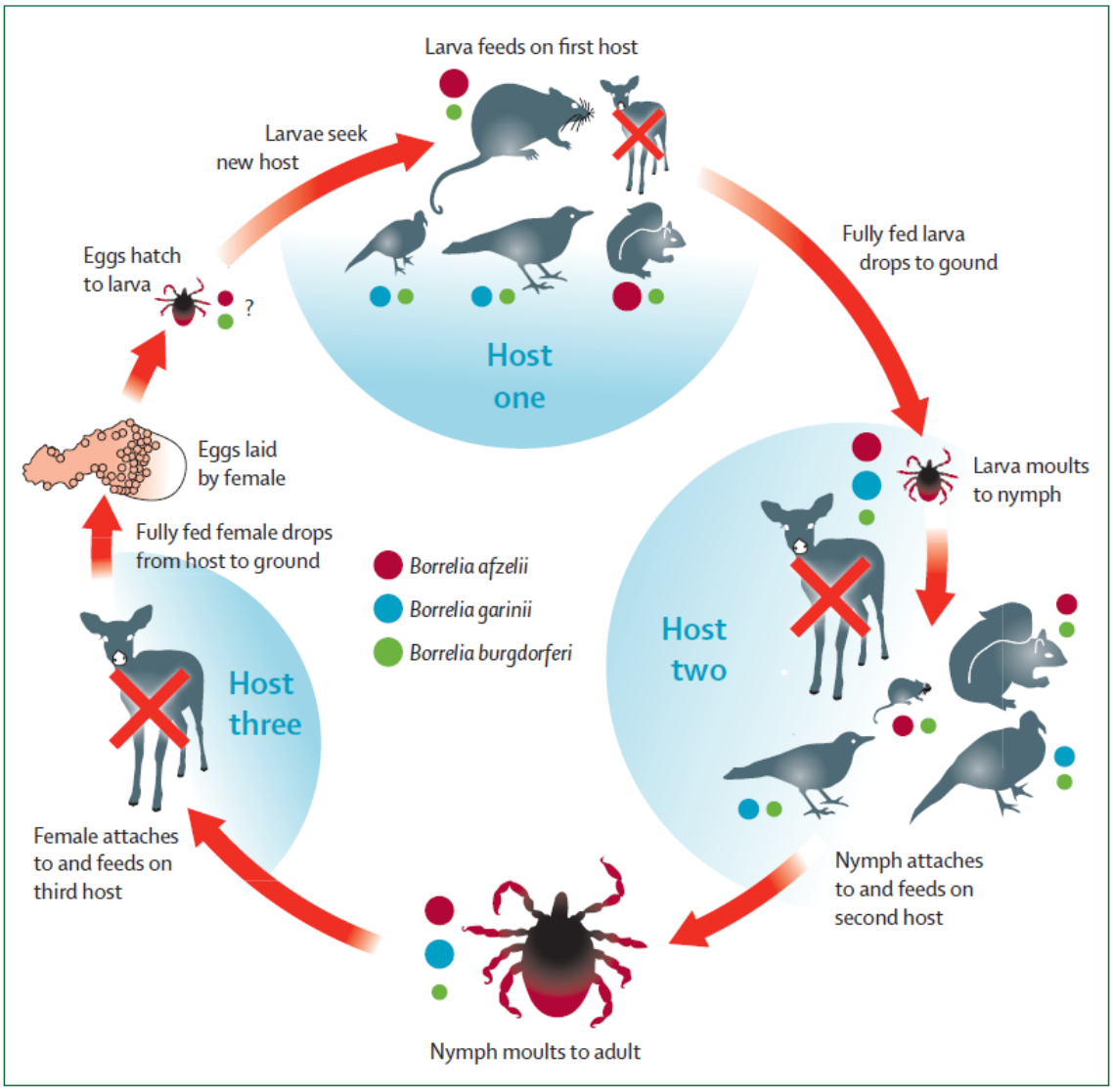

***Figure 2*: Infectious cycle of the European *Borrelia burgdorferi sensu lato* genospecies**: Coloured circles represent each of the *Borrelia* genospecies, and their size indicates the implication of each vertebrate as a reservoir for the different genospecies. A red cross indicates a non-reservoir host. Figure modified from Steere A.C. *et al., 2016.*

The epidemiology of Lyme disease is complex. The life cycle of *B. burgdorferi* depends intimately on the two-year life cycle of *Ixodes* ticks (Figure 2, 3), which consists of three developmental stages: larva, nymph and the adult. *B. burgdorferi* is maintained in Nature via transmission cycles between mammalian hosts and tick vectors. The host animals are small rodents and birds. The tick acquires the bacteria by feeding on a previously infected host and transmitting the bacteria to the subsequent host (2, 9). Mating of adult tick requires large animals, such as deer, which are essential for tick population maintenance.

Afterwards, the female tick lays the eggs, dies, and the cycle starts again. Larval ticks are not infected with *B. burgdorferi,* since the spirochete is not transmitted transovarially (1). Tick nymphs are the most responsible for spirochetal transmission to humans and dogs; however, they are not part of the enzootic life cycle of *B. burgdorferi* and they are considered dead-end hosts.

Figure 3: Developmental stages of *Ixodes ricinus*. From left to right: larva, nymph, adult female, adult male. Figure modified from Stanek G. *et al., 2012*

1.2 Clinical manifestations of the disease

The hallmark symptom of Lyme borreliosis is a skin rash that appears at the site of infection in 70–80% of cases, called *erythema migrans* (*EM*) (11) (Figure 4, A). EM develops within 7 to 10 days of infection and may be accompanied by flu-like symptoms, such as fatigue, malaise, fever, chills, myalgia and headache. In Europe, *B. burgdorferi s. l.* infection causes *EM* as well, but does rarely present other associated symptomatology (12). In rare cases, early Lyme borreolisis in Europe presents a skin manifestation called *borrelial lymphocytoma* that is most often caused by *B. afzelii* infection (Figure 4, C). *EM* lesions consist of perivascular infiltrates of lymphocytes, dendritic cells (DC), macrophages, and a small numbers of plasma cells (13). *EM* spontaneously resolves within weeks even in the absence of antibiotic treatment.

If not properly treated, *B. burgdorferi* may then disseminate systemically via the lymphatic system or blood to the joints, nervous and cardiovascular system causing a variety of inflammatory symptoms such as arthritis, carditis and nervous system defects (i.e.

meningitis). During the early dissemination stage patients may experience numbness, Bell's palsy, palpitations, chest pain or shortness of breath. The colonization of tissues occurs in a matter of weeks or a few months after infection (11).

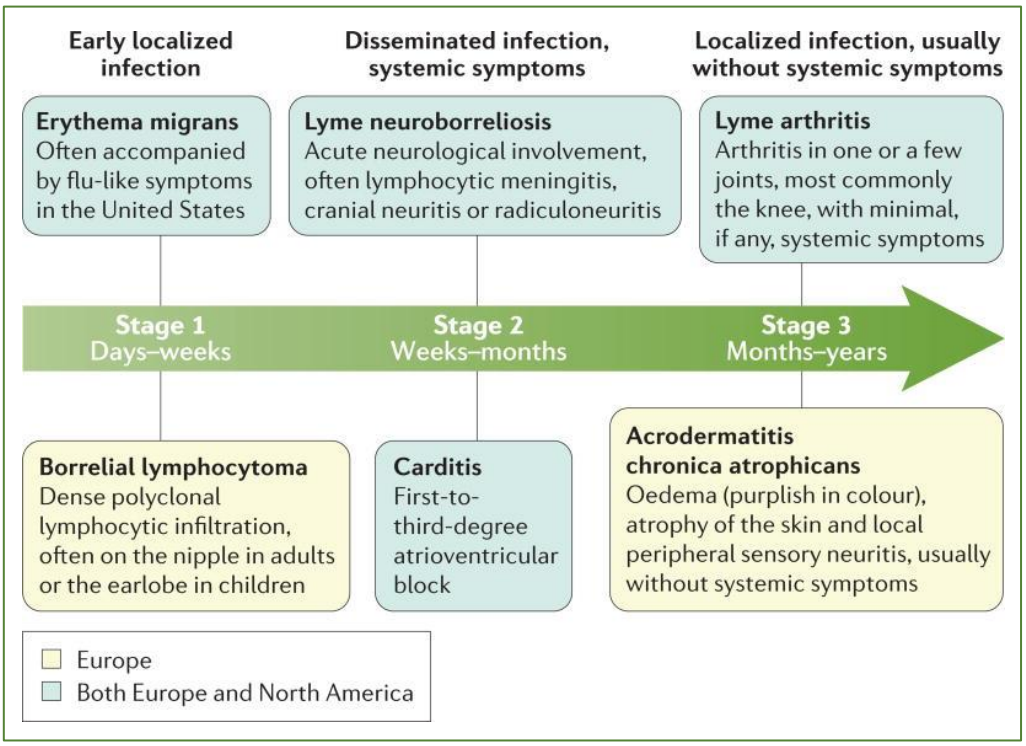

Figure 4: The stages and most common clinical features of Lyme borreliosis: Clinical manifestation of Lyme borreliosis in Europe or Europe and US. We can differentiate three stages, with different clinical manifestations at each stage. The initial symptoms are localized to the skin, however, as the disease progresses and as the immune response matures, the infection typically becomes more localized, such as to the knee joint, and is accompanied by minimal, if any, systemic symptoms. Figure modified from Steere A.C. *et al.,* 2016.

Late stage symptoms include chronic arthritis, neuroborreliosis, or cutaneous lesions such as *acrodermatitis chronica atrophicans* (14) (Figure 4, D). *B. burgdorferi* s.s. is most associated to arthritis, while in Europe and Asia, *B. afzelii* persists in the skin resulting in *acrodermatitis chronica atrophicans*, a skin condition that occurs primarily on sun-exposed surfaces (15). *B. garinii* appears to be the most neurotropic of the three *Borrelia* genospecies. It may cause an exceptionally wide range of neurologic abnormalities (16), including *borrelial encephalomyelitis*, a multiple sclerosis–like illness.

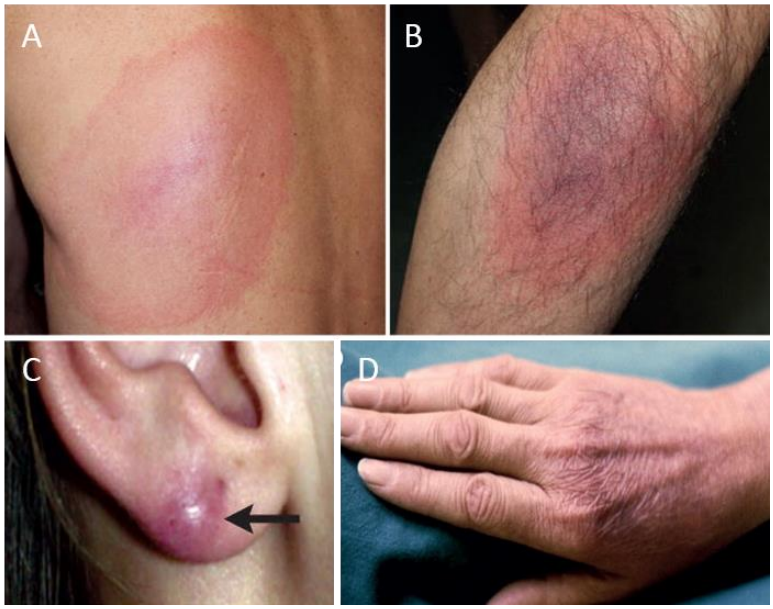

Figure 5: Dermatological manifestations of Lyme borreliosis. **A and B)** Skin lesion known as erythema migrans, which occurs at the site of the tick bite. The rash presents a brighter red outer border, partial central clearing and a bull's eye centre. **C)** *Borrelial lymphocytoma* (arrow) is a subacute lesion that typically occurs on the nipple in adults or on the earlobe in children. **D)** *Acrodermatitis chronica atrophicans* is the most common late manifestation of Lyme borreliosis in Europe. These lesions have an inflammatory phase followed by fibrotic characteristics. Figure modified from Steere A.C*. et al.,* 2016.

1.3 Lyme disease diagnosis

Because of the high antigen variability within *B. burgdorferi* genospecies and the lack of standardized test methods, the diagnosis of Lyme disease presents interpretation difficulties. Therefore, serological results should always be interpreted in the context of the patient's clinical condition and the course of the disease. In general, Lyme disease diagnosis follows a two-tiered sero-diagnostics procedure: the first step searches for specific anti-borrelial IgM and IgG by enzyme-linked immunosorbent assay (ELISA) as a screening test; then, positive or borderline results are confirmed using a immunoblot assay. Nevertheless, the interpretation of the Western blot varies between United States and Europe as no criteria provides results with high sensitivity and specificity for all countries.

Due to the often delayed immune response, results may be false negative in the early stage of the disease; however, the presence of erythema and a reported tick bite is sufficient to initiate treatment without prior serological confirmation (17).

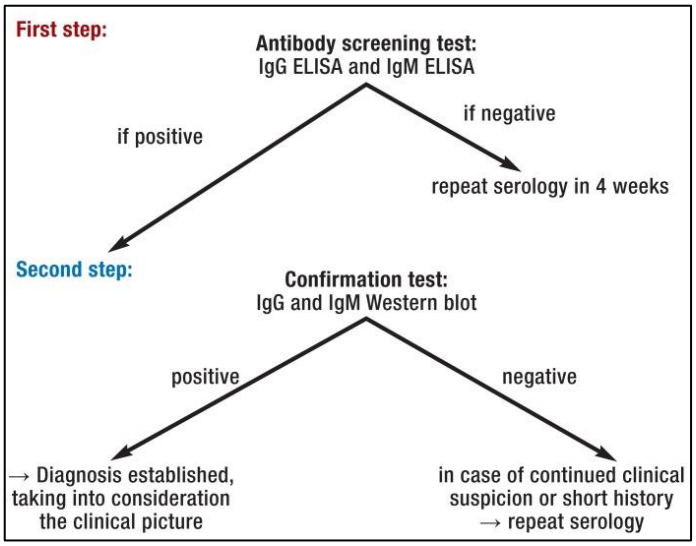

Figure 6: Lyme disease diagnosis; two tiered sero-diagnosis method. Image modified from Scheffold et al., 2015 (17).

1.4 Treatment

During the early stages of Lyme disease oral administration of doxycycline (100 mg twice daily) or amoxicillin (500 mg thrice daily) for two weeks is recommended. When the disease is in a more advanced phase in which other organs are involved, the treatment might be oral or intravenous depending on the organ involved and the disease manifestation. The antibiotics used in these cases are ceftriaxone or cefotaxime, and the doses are variable (17).

1.5 *Borrelia* cellular characteristics, genome and metabolism

B. burgdorferi is a complex microaerophilic Gram-negative bacteria. It is 0.3 µm wide and 5 to 30 µm in length (Figure 7, A). Nevertheless, it differs from the typical Gram-negative bacteria: the outer membrane does not contain lipopolysaccharide but is composed of phospholipids and glycolipids (18). Other components of the outer membrane are lipoproteins, which present a high variability and play a critical role in the interaction of the spirochete with the immune system.

B. burgdorferi is a highly motile spirochete due the presence of axial filaments, a type of flagella attached to each pole that run lengthwise around the cell cylinder in the periplasm,

between the peptidoglycan layer and the outer membrane. This characteristic causes the twisting movement and typical shape of the bacterium (19). The flagellar motors are located at the cell poles along with chemotaxis proteins that sense nutrient concentration and direct the spirochete movement towards chemoattractants and away from harmful elements (20) (Figure 7, b).

The genome of *B. burgdorferi* was the third microbial genome sequenced (21). The spirochete presents one of the most complex genomes known among prokaryotes, containing a linear chromosome of approximately 1 Mb in size as well as at least 12 linear and 9 circular plasmids totalling approximately 600 kb. The linear chromosome carries the majority of housekeeping genes, and is highly conserved among *B. burgdorferi* genospecies, whereas the plasmids show a high degree of variation, being some of them absent between genospecies.

More than 90% of the plasmid-encoded genes are unique to *B. burgdorferi s.l.*, without homologs in other organisms, suggesting that they encode proteins with functions pertinent to the distinctive lifestyle of the spirochete. The plasmids encode most of the expressed outer surface lipoproteins, and therefore, differences in plasmids among *B. burgdorferi s.l.* are thought to contribute to the clinical variability of Lyme borreolisis in different geographical regions (22).

A large portion of the genome encodes lipoproteins, which suggests that they may be important for the survival and host colonization by the spirochete. Specifically, 5% of the chromosomal ORFs and 14.5 to 17% of plasmid ORFs of *B. burgdorferi* encode putative lipoproteins. (21). These lipoproteins include Outer surface proteins (Osp), A-F. The *B. burgdorferi* genome lacks any known toxins. *B. burgdorferi* presents very limited metabolic capabilities as a result of the adoption of a lifestyle that involves parasitizing nutrients from its hosts, therefore, it is highly dependent on its tick vector and vertebrate host for many essential factors (23). The bacterium is an auxotroph for all amino acids, nucleotides and fatty acids. To obtain these factors, the *B. burgdorferi* genome encodes 16 distinct membrane transporters, many of which have broad substrate specificity (Fraser et al., 1997). It also lacks genes encoding enzymes for the tricarboxylic acid cycle and oxidative phosphorylation, relying exclusively on glycolysis for energy production and fermentation of sugars to lactic acid via the Embden–Meyerhof pathway (23).

1.6 Invasion, dissemination and immune evasion

B. burgdorferi survival and adaptation to different host environments depends of gene expression. Adaptive changes occurring during the transmission of the bacterium from the tick midgut to the mammalian host occur in response to signals emanating from tick engorgement, such as temperature increase, the availability of nutrients, changes in oxygen tension and decreased pH (9). This process requires que combined action of the RNA polymerase alternative σ-factor (RpoS) and the *Borrelia* oxidative stress regulator (BosR) (24, 25).

The majority of genes targeted by this two factors encode surface lipoproteins, and, in a fine tuned process, RpoS activates the transcription of mammalian-phase-specific genes (for example, *ospC*) (26). At the same time, BosR transcriptionally represses tick-phase-specific genes (for example, *ospA*) (27). OspA plays an important role in the location of the spirochete within the vector through its interaction with the tick receptor for OspA (TROSPA) in the gut (28). The replacement of OspA by OspC is crucial for mammalian colonization by *B. burgdorferi* (29). Nevertheless, not all lipoprotein regulation is due to the activity of the RpoS/ BosR system. Other components essential for the survival of the spirochete, such as VlsE and complement regulator-acquiring surface proteins (CRASPs) are regulated by still unknown mechanisms (Figure 7c).

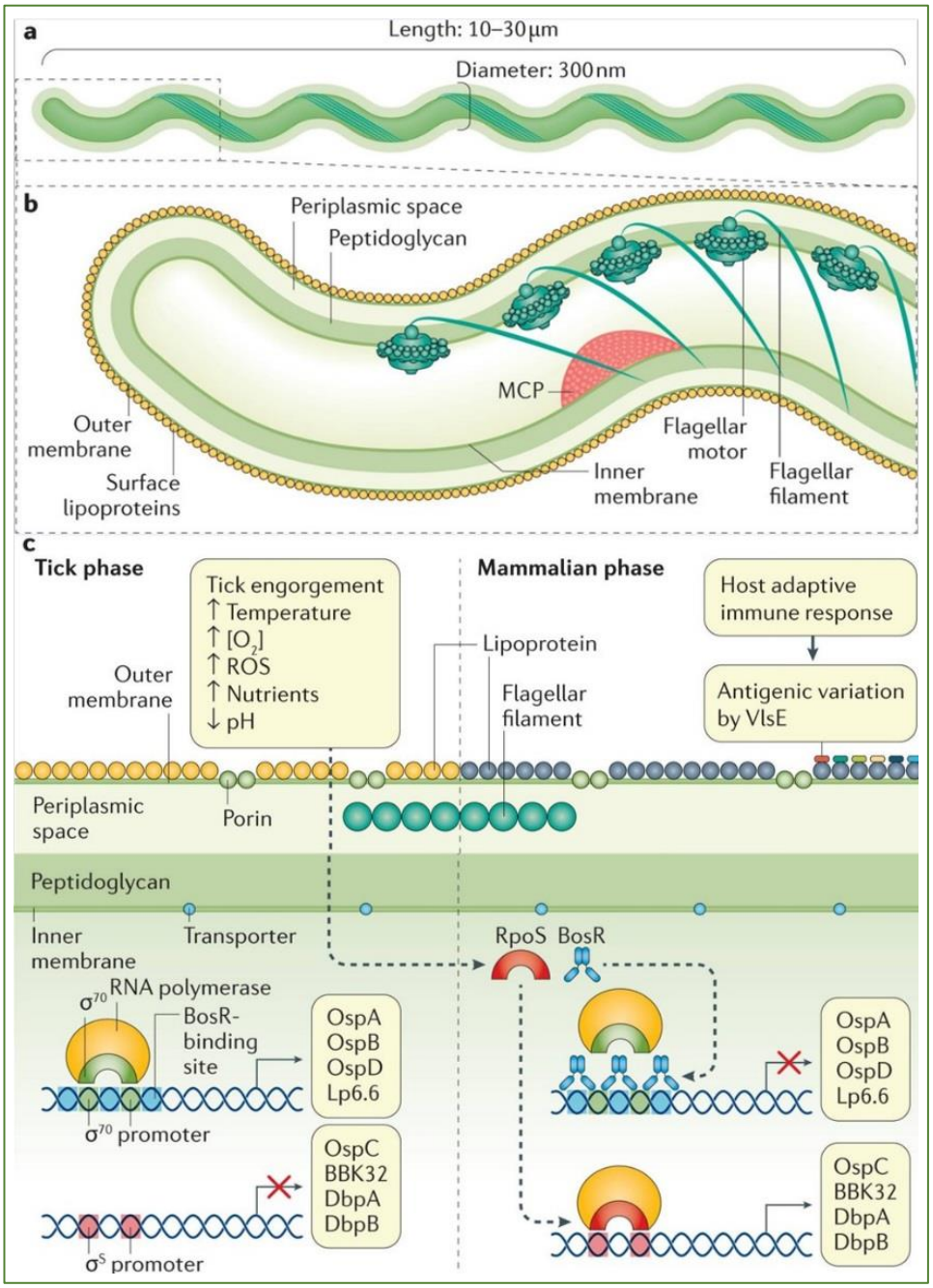

Figure 7: A) *Borrelia burgdorferi* morphology: ~300 nm in diameter and 10–30 µm in length. **B)** 3D model of the spirochete: The flagellar filaments are confined to the periplasmic space and are anchored to each cell pole by the flagellar motors, which are located next to methyl-accepting chemotaxis proteins (MCPs) that direct movement. **C)** The outer membrane of *B. burgdorferi* show different sets of lipoproteins in the tick or mammalian environments. This fine-tuned machinery is mediated by *Borrelia* oxidative stress regulator (BosR) and the RNA polymerase alternative σ-factor RpoS. Figure modified from Steere A.C. *et al.,* 2016.

The colonization of the mammalian host by *B. burgdorferi* is aided by the tick both mechanically and biochemically. The insertion of the tick proboscide during feeding enables

the delivery of the spirochete deep into the dermis, close to blood vessels. Furthermore, tick saliva presents an armoury of proteins and molecules that can impede various mammalian defence responses, which the bacteria exploit to help establish infection (31). For example, the salivary protein, Salp15 binds *B. burgdorferi* OspC and protects the spirochete from antibody-mediated killing, Salp15 also inhibits T cell activation, (31) while sialostatin L blocks neutrophil chemotaxis (32, 33).

B. burgdorferi can prevent host defence responses including complement-mediated killing. *B. burgdorferi* activates the classical and alternative pathways of the complement cascade which play a role in infection control by increasing opsonization and phagocytosis of the spirochete (34), although some *Borrelia* genospecies show resistance to this process. *B. afzelii* is particularly complement-resistant while *B. garinii* show complement-sensitivity, *B. burgdorferi s.s.* isolates are intermediate complement-sensitive (35). A group of surface lipoproteins called CRASPs (complement regulator-acquiring surface proteins) bind complement factor H recruiting a protease (factor I) that cleaves and inactivates the complement serum proteins, C3b and C4b. This process protects the bacterium against complement-mediated killing by preventing the activation of the alternative complement pathway (37, 37). *B. burgdorferi* also express a CD59-like molecule on the outer membrane that can inactivate the membrane attack complex (MAC) and prevent complement-mediated lysis (38). More recently, it has been shown that *B. burgdorferi* expresses a protein on its surface, BBK32, that prevents activation of the classical pathway by blocking activation of the C1 Complement Complex (39).

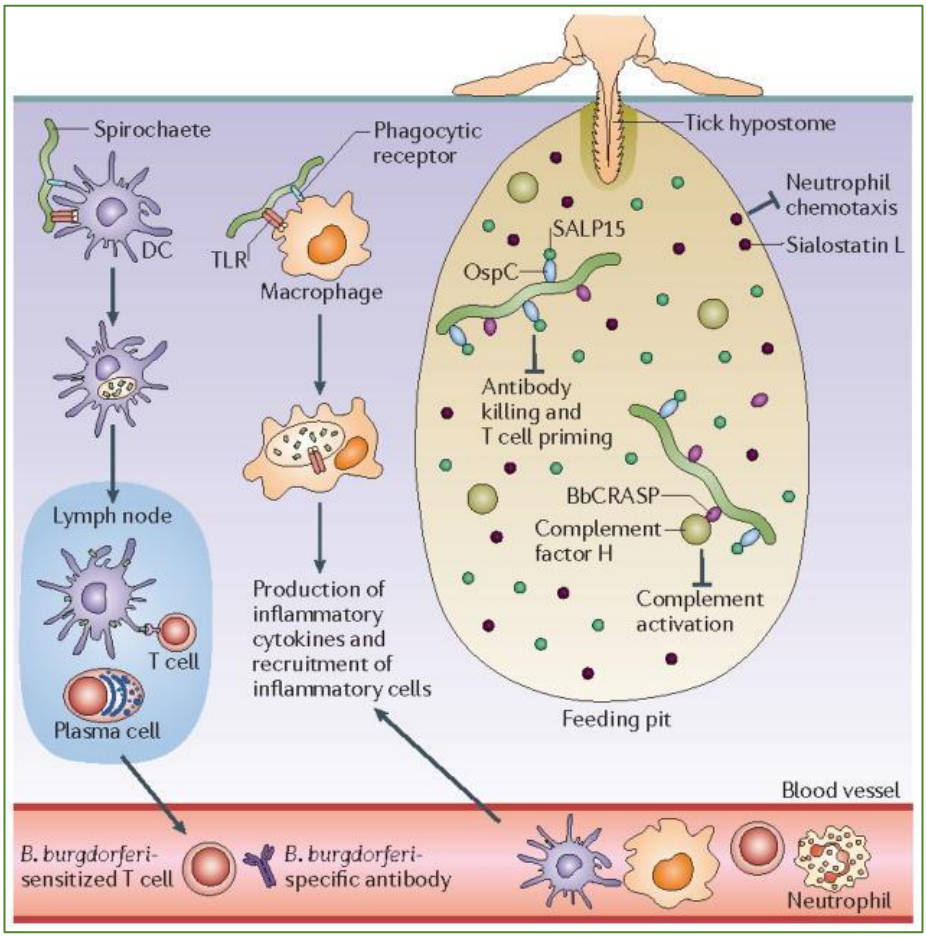

Figure 8: The tick–mammal interface. The tick creates a feeding pit using a barbed protuberance called hypostome as an anchor to the skin of its host. While feeding, the tick secretes saliva containing a high variety of immune-regulator proteins, which help host colonization by *B. burgdorferi*. Some of these bioactive agents are represented in the figure, as SALP15 and Sialostatin L. A group of borrelial surface lipoproteins, called BbCRASPs, also play an important role by complement inhibitor. The spirochete is recognized by local immune cells as macrophages, neutrophils and dendritic cells (DCs). Pro-inflammatory cytokine production that will lead to the recruitment of more effector cells that will eventually lead to the development of erythema migrans. Modified from Radolf JD. *et al*., 2012.

Once deposited in the skin, *B. burgdorferi* multiplies locally, penetrates the matrix between cells and spreads to blood vessels, allowing their migration to distant tissues (40). The motility presented by the spirochete and the adherence to host molecules and extracellular matrix components are critical for *B. burgdorferi* dissemination, evading immune responses and successfully colonizing the host. Many lipoproteins of the mammalian-phase play an important role in this process, since they are responsible for the interaction with components of the extracellular matrix and host tissues. For example, decorin-binding

protein A (DbpA) and DbpB can bind decorin, the main component of the matrix (41), while ErpX and BmpA bind to laminin (42, 43) and p66 and BBB07 can attach to cell surface integrins (44). Another critical lipoprotein is BBK32, which binds fibronectin and glycosaminoglycans and is responsible for the anchoring of the circulating spirochete to vascular surfaces allowing *B. burgdorferi* to transmigrate across the endothelium and disseminate into tissues (45).

During the hematogenous dissemination phase, the major threat to the survival of the spirochete is the potential presence of circulating antibodies. As a mechanism to avoid them, the spirochete undergoes antigenic variation by altering the surface lipoproteins, replacing OspC by VlsE. These two lipoproteins share structural similarities, and therefore might serve the same purpose. Nevertheless, VlsE, presents high antigenic variability, since its gene sequence suffers random *vsl* cassette insertion generating many *vlsE* alleles (46). Therefore, the highly variable region of VlsE is located towards the cells surface allowing *B. burgdorferi* to evade host antibodies to one VlsE variant by expressing a different version. This is a very sophisticated method to avoid host adaptive immune responses that is responsible for the persistent infectious feature of this pathogen (Figure 7, C).

Once in the joints and heart, clearance of the spirochete may be more dependent on cellular responses (such as macrophages in the heart), than antibodies, which are less able to penetrate into deep tissues.

1.7 Host immune response

Despite all the mechanisms that *B. burgdorferi* presents to avoid host immune defences, the spirochete is still recognized and killed by both innate and adaptive immune responses. Since this bacterium does not contain toxins or proteases, the majority of Lyme disease symptoms and tissue damage are caused by pro-inflammatory responses. During the early infection by *B. burgdorferi*, the majority of the response is mediated by T cells, neutrophils, dendritic cells and monocytes or macrophages. Cytokines produced at this stage are predominantly TNF, IL-2, IL-6 and type I IFN, as well as chemoattractants. In both, human and mice, neutrophils are absent in Erythema migrans (47).

During the dissemination stage, both innate and adaptive immune responses are important for controlling bacterial burdens and inflammation (50). Nevertheless, the sole action of the immune system is not sufficient to eradicate infection and *B. burgdorferi* colonizes distant tissues, generating infiltration of immune cells and developing a complex inflammatory symptomatology.

A distinct innate cellular infiltration profile has been observed in *B. burgdorferi*-infected tissues. Carditis in mice and humans is predominantly caused by infiltration of monocytes or macrophages (48). In contrast, arthritic joints show a predominance of neutrophils, with some presence of macrophages and lymphocytes. In susceptible strains of mice, IFNγ appears to modulate carditis (48), whereas type I IFNs may be particularly important for the development of arthritis (49). This tissue-specific tropism complicates our understanding of the host defense against the spirochete, but might suggest that macrophages are more efficient at preventing successful colonization of *B. burgdorferi,* because carditis is a less frequent manifestation of Lyme disease.

Since all Lyme borreolisis symptoms share a common pro-inflammatory signature, a great amount of research has been done trying to elucidate the mechanism by which *B. burgdorferi* causes inflammation, primarily mediated by recognition and phagocytosis by macrophages.

1.8 *Borrelia burgdorferi* recognition by phagocytic cells

The early recognition and inflammatory response to *B. burgdorferi* is mediated by pathogen-associated molecular patterns (PAMPs) that are detected by pattern recognition receptors (PRR), such as Toll-like receptors (TLRs) and (NOD)-like receptors. TLRs receptors are expressed by leukocytes including dendritic cells, macrophages, natural killer cells, cells of the adaptive immunity (T and B lymphocytes) and non-immune cells (epithelial and endothelial cells, and fibroblasts). Most TLRs work as homodimers, except for TLR2, which can dimerize with TLR1 and TLR6. When activated, TLRs recruit adapter molecules within the cytoplasm in order to propagate the signal. Four adapter molecules are known to be

involved in signalling: MyD88, TIRAP (also called Mal), TRIF, and Tram (TRIF-related adaptor molecule). All TLRs except TLR3 utilize MYD88, leading to NF-kB activation and resulting in the production of pro-inflammatory cytokines such as IL-1β, TNF, IL-6, IL-8 and IL-18. TRIF recruitment by TLR3 and TLR4 results in type I IFN production.

Different PAMPs of *B. burgdorferi* are recognized by TLRs, including but not limited to lipoproteins (detected by TLR1/ TLR2 heterodimers) (51), flagellin (detected by TLR5) (52), RNA (detected by TLR7 and TLR8) (53) and CpG DNA (detected by TLR9) (52). It is remarkable that all PAMPS recognized by macrophages are only accessible once *B. burgdorferi* has been degraded inside the phagolysosomes, and thus, none of the TLR described play a role in the surface recognition of the spirochete. Specifically, TLR1/ TLR2 heterodimers recognize tri-acylated lipoproteins, which are embedded in *B. burgdorferi* membrane and therefore only accessible to TLR1/2 after bacterial degradation.

As mentioned before, all TLRs involved in *B. burgdorferi* recognition signal through MyD88 (52). Furthermore, it has been demonstrated that the adaptor protein MyD88 is responsible for a considerable percentage of *B. burgdorferi* phagocytosis in mice, with no effect on the humoral response or antigen production (54). Hence, MyD88 triggers the inflammatory responses through both its effects on phagocytosis and its role in transducing signals from TLR. However, the phagocytic receptor mediating this effect remains unknown.

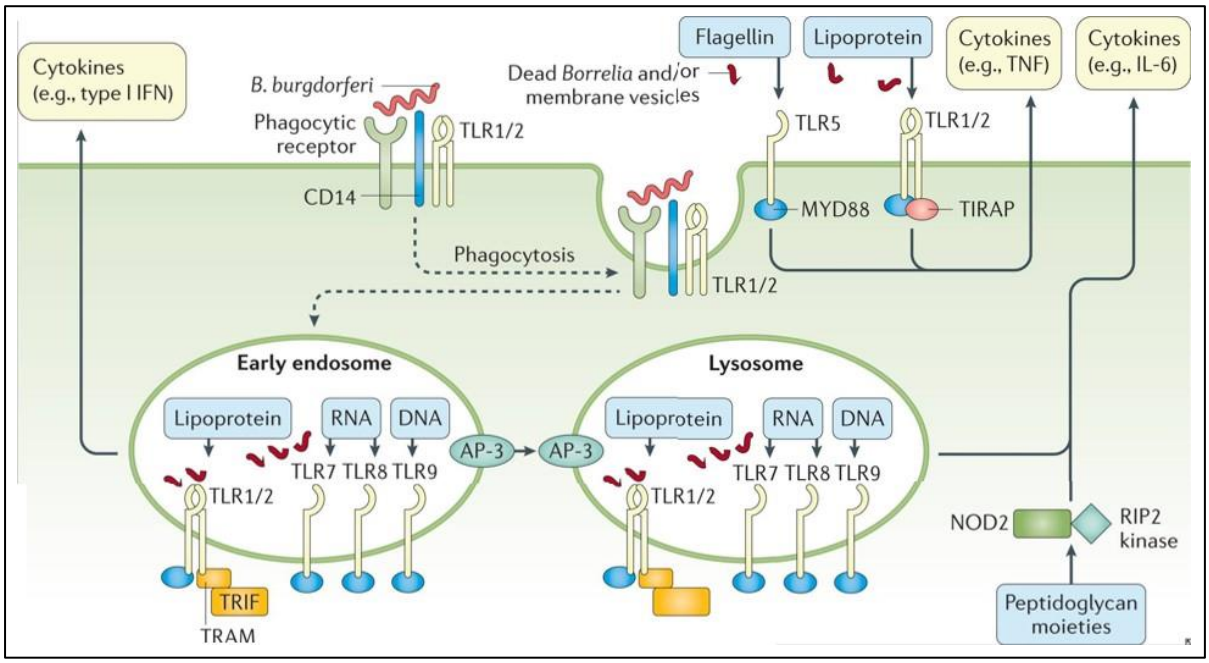

Figure 9: Mechanisms of innate immune recognition of *Borrelia burgdorferi*

The initial innate immune response is triggered by recognition of *Borrelia burgdorferi* or its pathogen-associated molecular patterns (PAMPs) by Toll Like Receptors (TLR) of host immune cells.

Figure modified from Steere A.C. *et al.,* 2016.

1.9 Phagocytosis mediated by macrophages

Phagocytosis is the cornerstone of the innate immune system. It is a complex, fine-tuned process that bridges the innate and adaptive immunity, not only in charge of the clearance of the invading pathogens, but orchestrating the actuation of the downstream cells of the immune system. It only occurs in specialized cells such as macrophages, DCs and neutrophils.

Defined as the engulfment of particles of 0.5 µm or bigger, phagocytosis is a multifarious process that requires the participation of several components in concert, from surface receptors to signalling elements that drive the internalization of the pathogen. Once the pathogen is internalized, the phagosome matures and fuses with lysosomes, becoming a phagolysosome, where the pathogen is killed by reactive oxygen and nitrogen intermediates and hydrolases. Afterwards, microbial peptides belonging to the pathogen are bound to the Major Histocompatibility complex (MHC) class II molecules and transported to the cell surface, where the peptide/MHC class II complex are presented to T cells to trigger the stimulation of the adaptive immune system. At the same time, macrophages activated by pathogen recognition via TLR will secrete inflammatory mediators, including cytokines that will further recruit and instruct the adaptive immune response (Figure 10).

The stating point of phagocytosis is the recognition of the pathogen by cell surface receptors. Phagocytic receptors that recognize patterns on pathogens include the mannose receptor and DEC-205 that recognize mannans, dectins that recognizes b-glucans and integrins (e.g., CD11b/CD18), and scavenger receptors that recognize surface components on bacteria (55). Opsonin molecules (antibodies and complement proteins) also intervene in the recognition and phagocytosis of pathogens. Phagocytic cells contain Fc and Complement receptors, which are able to recognize the opsonin-pathogen complexes and trigger their internalization.

Up to date, few receptors are known to mediate *B. burgdorferi* phagocytosis: The scavenger receptor Macrophage Receptor with Collagenous Structure (MARCO), which plays a role in the internalization of a variety of microbial ligands, is involved in *B. burgdorferi* phagocytosis. MARCO is significantly up-regulated upon *B. burgdorferi* stimulation, a process that requires MyD88-induced signals (56). On the other hand, the absence of uPAR (a GPI-anchored protein) results in the impaired phagocytosis of the spirochete (57), although the signals and co-receptors mediating this function are unknown. Additionally, Mannose Receptor 1 (MRC1, CD206) has been involved in binding of Bb to human monocytes (58), although it is still unclear whether this receptor is involved in the internalization of the bacterium. Another GPI-anchored protein, CD14 collaborates with the integrin, CR3, inducing its translocation to lipid rafts (59). CR3 is a bona-fide phagocytic receptor for *B. burgdorferi* that does not require MyD88-induced signals to mediate the internalization of the spirochete (60). Interestingly, phagocytosis by CR3/CD14 results in a decreased inflammatory output by macrophages (60). Overall, our understanding of the phagocytic uptake of *B. burgdorferi* is still very limited, including the full complement of receptors involved, their contribution to the inflammatory response of innate immune cells, and the signals that mediate these processes. Particularly intriguing is the identity of the receptor(s) involved in the MyD88-dependent internalization of *B. burgdorferi*, since a large proportion of the process requires the adaptor protein.

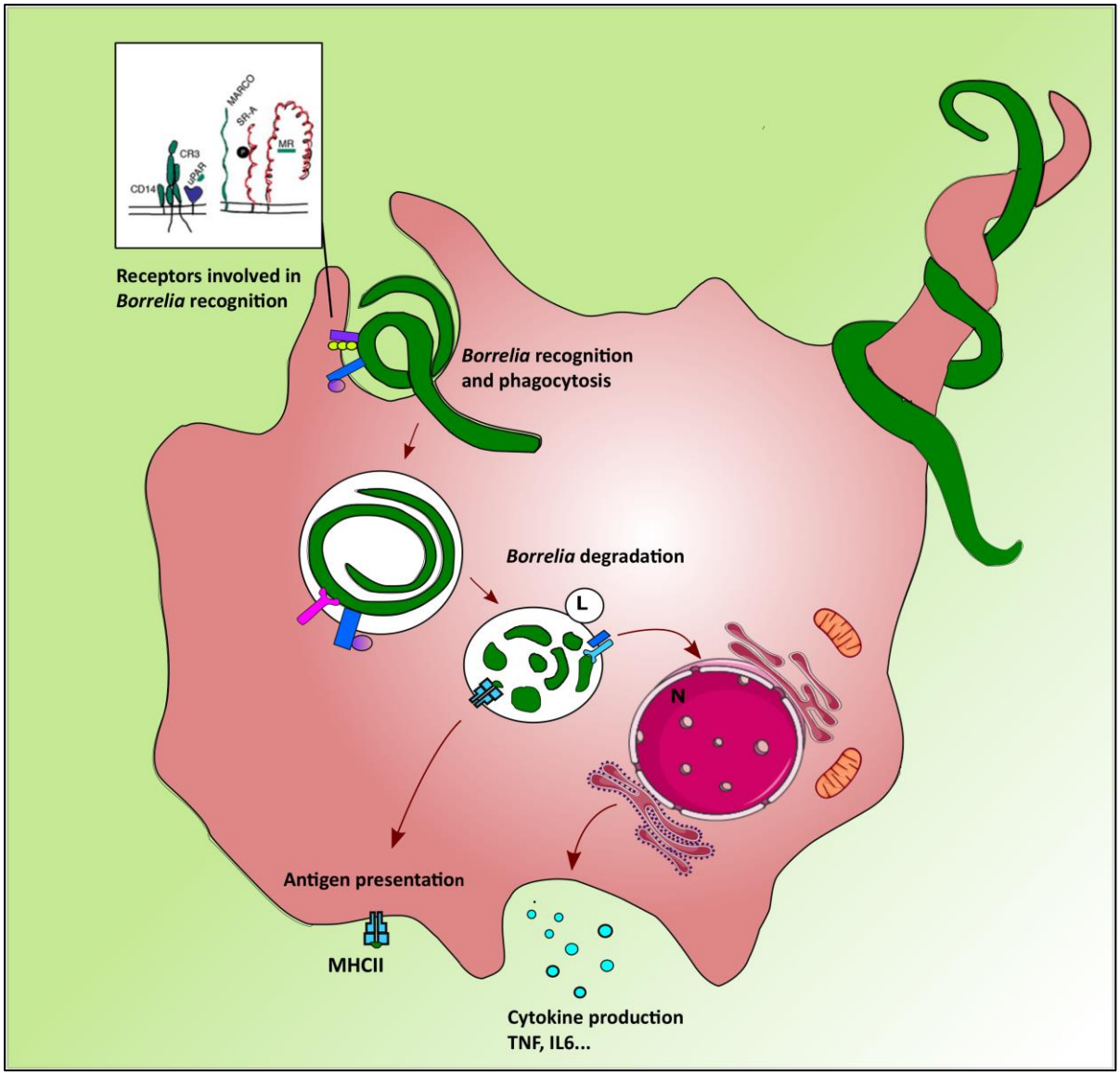

Figure 10: Schematic representation of *B. burgdorferi* phagocytosis mediated by macrophages and the subsequent immune processes. The recognition of the spirochete by TLRs leads to macrophage activation and cytokine/chemokine production (IL-6, TNF). Bacteria degradation in the phagolysosome generates antigen presentation on the cell surface by MHCII molecules, activating downstream components of the immune response as T cells.

1.10 Bibliography

1. Steere, A. C., Coburn, J., Glickstein, L., Steere, A. C., Coburn, J., & Glickstein, L. (2004). The emergence of Lyme disease Find the latest version : Review series The emergence of Lyme disease. *The Journal of Clinical Investigation*, *113*(8), 1093–1101. http://doi.org/10.1172/JCI200421681.

2. Burgdorfer, W., Barbour, A. G., Hayes, S. F., Benach, J. L., & Jannasch, H. W. (1982). Lyme Disease--A Tick-Borne Spirochetosis *Science*, *216*(4552), 1317–1319.

3. Keller, A., Graefen, A., Ball, M., Matzas, M., Boisguerin, V., Maixner, F., … Zink, A. (2012). New insights into the Tyrolean Iceman's origin and phenotype as inferred by whole-genome sequencing. *Nature Communications*, *3*. http://doi.org/10.1038/ncomms1701

4. Gerold Stanek, Gary P Wormser, Jeremy Gray, F. S., & Lyme. (2012). Lyme borreliosis. *Lancet*, *379*(1), 461–473. http://doi.org/10.1016/S0140-6736(11)60103-7

5. Wang, G., Van Dam, A. P., Schwartz, I., & Dankert, J. (1999). Molecular typing of Borrelia burgdorferi sensu lato: Taxonomic, epidemiological, and clinical implications. *Clinical Microbiology Reviews*, *12*(4), 633–653. http://doi.org/10.1016/j.aprim.2013.04.004

6. Margos G, Gofton A, Wibberg D, Dangel A, Marosevic D, Loh S-M, et al. (2018) The genus Borrelia reloaded. *PLoS ONE* 13(12): e0208432. https://doi.org/10.1371/journal.pone.0208432

7. Kahl, O., Janetzki-Mittmann, C., Gray, J. S., Jonas, R., Stein, J., & De Boer, R. (1998). Risk of infection with Borrelia burgdorferi sensu lato for a host in relation to the duration of nymphal Ixodes ricinus feeding and the method of tick removal. *Zentralblatt Fur Bakteriologie*, *287*(1–2), 41–52. http://doi.org/10.1016/S0934-8840(98)80142-4

8. Steere, A. C., Strle, F., Wormser, G. P., Hu, L. T., Branda, J. A., Hovius, J. W. R., … Mead, P. S. (2016). Lyme borreliosis. *Nature Reviews Disease Primers*, *2*(9814), 16090. http://doi.org/10.1038/nrdp.2016.90

9. Anguita, J., Hedrick, M. N., & Fikrig, E. (2003). Adaptation of Borrelia burgdorferi in the tick and the mammalian host. *FEMS Microbiology Reviews*, *27*(4), 493–504. http://doi.org/10.1016/S0168-6445(03)00036-6

10. Matuschka, F. R., & Spielman, A. (1986). The emergence of Lyme disease in a changing environment in North America and Central Europe. *Experimental & Applied Acarology*, *2*(4), 337–353. http://doi.org/10.1007/BF01193900

11. Steere AC, Sikand. V. K. (2003). The Presenting Manifestations of Lyme Disease and the outcomes of treatment. *New England Journal of Medicine,* 348(24), 2472–2474.

12. Cerar, T., Strle, F., Stupica, D., Ruzic-Sabljic, E., McHugh, G., Steere, A. C., & Strle, K. (2016). Differences in genotype, clinical features, and inflammatory potential of borrelia burgdorferi sensu stricto strains from Europe and the United States. *Emerging Infectious Diseases,* 22(5), 818–827. http://doi.org/10.3201/eid2205.151806

13. Mullegger, R.R. (2004). Dermatological manifestations of Lyme borreliosis J Dermatol 14(5):296-309

14. Olson C. M., E. Fikrig, J. Anguita. (2013). Host defenses to spirochetes. In: *Clinical Immunology* 4th Ed. (Rich, Shearer, Fleisher, Schoroeder, Weyand and Frew).

15. Müllegger, R. R., McHugh, G., Ruthazer, R., Binder, B., Kerl, H., & Steere, A. C. (2000). Differential expression of cytokine mRNA in skin specimens from patients with erythema migrans or acrodermatitis chronica atrophicans. *Journal of Investigative Dermatology*, *115*(6), 1115–1123. http://doi.org/10.1046/j.1523-1747.2000.00198.x

16. Oschmann P, et al. (1998) Stages and syndromes of neuroborreliosis. J. Neurol. 1998; 245:262–272.

17. Scheffold, N., Herkommer, B., Kandolf, R., & May, A. E. (2015). Diagnostik, Therapie und Prognose der Lyme-Karditis. *Deutsches Arzteblatt International*, *112*(12), 202–208. http://doi.org/10.3238/arztebl.2015.0202

18. Stübs G, Fingerle V, Wilske B, Göbel UB, Zähringer U, Schumann RR, Schröder NW (2009) Acylated cholesteryl galactosides are specific antigens of borrelia causing lyme disease and frequently induce antibodies in late stages of disease. *J Biol Chem. 284(20):13326-34.*

19. Charon NW, Cockburn A, Li C, Liu J, Miller KA, Miller MR, Motaleb MA, Wolgemuth CW (2012) The unique paradigm of spirochete motility and chemotaxis. *Annu Rev Microbiol*. 66():349-70.

20. Shi W, Yang Z, Geng Y, Wolinsky LE, Lovett MA (1998) Chemotaxis in Borrelia burgdorferi. *J Bacteriol*. 180(2):231-5.

21. Fraser CM, Casjens S, Huang WM, Sutton GG, Clayton R, Lathigra R, White O, Ketchum KA, Dodson R, Hickey EK, Gwinn M, Dougherty B, Tomb JF, Fleischmann RD, Richardson D, Peterson J, Kerlavage AR, Quackenbush J, Salzberg S, Hanson M, van Vugt R, Palmer N, Adams MD, Gocayne J, Weidman J, Utterback T, Watthey L, McDonald L, Artiach P, Bowman C, Garland S, Fuji C, Cotton MD, Horst K, Roberts K, Hatch B, Smith HO, Venter JC, (1997) "Genomic sequence of a Lyme disease spirochaete, Borrelia burgdorferi", *Nature* 390(6660):580-6.

22. Casjens SR, Eggers CH, Schwartz I. (2010) Borrelia: Molecular Biology, Host Interaction, and Pathogenesis. *Caister Academic Press*; pp. 27–53.

23. Gheradini F, Boylan J, Lawrence K, Skare J. (2010) Borrelia: Molecular Biology, Host Interaction, and Pathogenesis. *Caister Academic*;. pp. 103–138.

24. Samuels, D. S. (2010). Gene Regulation in Borrelia burgdorferi . *Annual Review of Microbiology*, *65*(1), 479–499. http://doi.org/10.1146/annurev.micro.112408.134040

25. Radolf, J. D., Caimano, M. J., Stevenson, B., & T, H. L. (2012). Of Ticks, mice and Men. *Nature Reviews. Microbiology*, *10*(2), 87–99. http://doi.org/10.1038/nrmicro2714.Of

26. Hübner A, Yang X, Nolen DM, Popova TG, Cabello FC, Norgard MV (2001) Expression of Borrelia burgdorferi OspC and DbpA is controlled by a RpoN-RpoS regulatory pathway. *Proc Natl Acad Sci U S A.* 98(22):12724-9.

27. Wang P, Dadhwal P, Cheng Z, Zianni MR, Rikihisa Y, Liang FT, Li X (2013)

Borrelia burgdorferi oxidative stress regulator BosR directly represses lipoproteins primarily expressed in the tick during mammalian infection. *Mol Microbiol*. 89(6):1140-53.

28. Pal, U., Li, X., Wang, T., Montgomery, R. R., Ramamoorthi, N., DeSilva, A. M., … Fikrig, E. (2004). TROSPA, an Ixodes scapularis receptor for Borrelia burgdorferi. *Cell*, 119(4), 457–468. https://doi.org/10.1016/j.cell.2004.10.027

29. Grimm D, Tilly K, Byram R, Stewart PE, Krum JG, Bueschel DM, Schwan TG, Policastro PF, Elias AF, Rosa PA (2004) Outer-surface protein C of the Lyme disease spirochete: a protein induced in ticks for infection of mammals. *Proc Natl Acad Sci* U S A. 101(9):3142-7.

30. Steere, A. C., Strle, F., Wormser, G. P., Hu, L. T., Branda, J. A., Hovius, J. W., Li, X., … Mead, P. S. (2016). Lyme borreliosis. *Nature reviews*. Disease primers, 2, 16090. doi:10.1038/nrdp.2016.90

31. Anguita, J., Ramamoorthi, N., Hovius, J. W. R., Das, S., Thomas, V., Persinski, R., … Fikrig, E. (2002). Salp15, an Ixodes scapularis salivary protein, inhibits CD4+T cell activation. *Immunity*, *16*(6), 849–859. http://doi.org/10.1016/S1074-7613(02)00325-4

32. Kotsyfakis M, Sá-Nunes A, Francischetti IM, Mather TN, Andersen JF, Ribeiro JM (2006) Antiinflammatory and immunosuppressive activity of sialostatin L, a salivary cystatin from the tick Ixodes scapularis. *J Biol Chem*.; 281(36):26298-307.

33. Ramamoorthi, N. et al. (2005) The Lyme disease agent exploits a tick protein to infect the mammalian host. *Nature* 436:573-577.

34. Kochi, S. K. & Johnson, R. C. (1988) Role of immunoglobulin G in killing of Borrelia burgdorferi by the classical complement pathway. *Infect Immun*;56:314-321

35. Breitner-Ruddock S, Wurzner R, Schulze J, Brade V. (1997) Heterogeneity in the complement-dependent bacteriolysis within the species of Borrelia burgdorferi. *Med Microbiol Immunol* ;185:253–60.

36. Kraiczy P, et al. (2004) Complement resistance of *Borrelia burgdorferi* correlates with the expression of BbCRASP 1, a novel linear plasmid-encoded surface protein that interacts with human factor H and FHL 1 and is unrelated to Erp proteins. *J Biol Chem*.;279:2421–2429.

37. Madar, M. *et al.* (2015) Exploitation of complement regulatory proteins by Borrelia and Francisella. *Mol Biosyst*;11:1684-1695.

38. Pausa, M. *et al.* (2003) Serum-resistant strains of *Borrelia burgdorferi* evade complement-mediated killing by expressing a CD59-like complement inhibitory molecule*. J Immunol*; 170:3214-3222

39. Garcia, B. L., Zhi, H., Wager, B., Hook, M. & Skare, J. T. (2016) Borrelia burgdorferi BBK32 Inhibits the Classical Pathway by Blocking Activation of the C1 Complement Complex. *PLoS Pathog* 12:e1005404.

40. Shih CM, Pollack RJ, Telford SR 3rd, Spielman A(1992) Delayed dissemination of Lyme disease spirochetes from the site of deposition in the skin of mice*. J Infect Dis*.; 166(4):827-31.

41. Guo BP, Norris SJ, Rosenberg LC, Höök M (1995)Adherence of Borrelia burgdorferi to the proteoglycan decorin. *Infect Immun*. 63(9):3467-72.

42. Brissette CA, Verma A, Bowman A, Cooley AE, Stevenson B. (2009)The *Borrelia burgdorferi* outer-surface protein ErpX binds mammalian laminin. *Microbiology*.;155:863–872.

43. Verma A, Brissette CA, Bowman A, Stevenson B (2009) Borrelia burgdorferi BmpA is a laminin-binding protein. *Infect Immun*. Nov; 77(11):4940-6.

44. Behera AK, Durand E, Cugini C, Antonara S, Bourassa L, Hildebrand E, Hu LT, Coburn J (2008) Borrelia burgdorferi BBB07 interaction with integrin alpha3beta1 stimulates production of pro-inflammatory mediators in primary human chondrocytes. *Cell Microbiol*.; 10(2):320-31

45. Seshu J, et al. (2006) Inactivation of the fibronectin-binding adhesin gene *bbk32* significantly attenuates the infectivity potential of *Borrelia burgdorferi*. *Mol Microbiol*. ;59:1591–1601.

46. Zhang JR, Hardham JM, Barbour AG, Norris SJ.(1997) Antigenic variation in Lyme disease *Borreliae* by promiscuous recombination of VMP-like sequence cassettes. Cell. ;89:275–285.

47. Salazar JC, Pope CD, Sellati TJ, Feder HM Jr, Kiely TG, Dardick KR, Buckman RL, Moore MW, Caimano MJ, Pope JG, Krause PJ, Radolf JD, (2003) Lyme Disease Network. Coevolution of

markers of innate and adaptive immunity in skin and peripheral blood of patients with erythema migrans. *J Immunol*. 171(5):2660-70.

48. Olson, C. M. Jr., Bates, T. C., Izadi, H., Radolf, J. D., Huber, S. A., Boyson, J. E., et al. (2009). Local production of IFN-gamma by invariant NKT cells modulates acute Lyme carditis. J. Immunol. 182, 3728–3734. doi: 10.4049/jim- munol.0804111

49. Miller JC, Ma Y, Bian J, Sheehan KC, Zachary JF, Weis JH, Schreiber RD, Weis JJ. (2008)A critical role for type I IFN in arthritis development following Borrelia burgdorferi infection of mice. *J Immunol*. 181(12):8492-503.

50. Weis JJ, Bockenstedt LK. (2010) Borrelia: Molecular Biology, Host Interaction, and Pathogenesis. *Caister Academic*; pp. 413–441.

51. Lien E, Sellati TJ, Yoshimura A, Flo TH, Rawadi G, Finberg RW, Carroll JD, Espevik T, Ingalls RR, Radolf JD, Golenbock DT. (1999) Toll-like receptor 2 functions as a pattern recognition receptor for diverse bacterial products. *J Biol Chem*. 274(47):33419-25.

52. Shin OS, Isberg RR, Akira S, Uematsu S, Behera AK, Hu LT (2008) Distinct roles for MyD88 and Toll-like receptors 2, 5, and 9 in phagocytosis of Borrelia burgdorferi and cytokine induction. *Infect Immun.* 76(6):2341-51.

53. Petzke MM, Brooks A, Krupna MA, Mordue D, Schwartz I, (2009) Recognition of Borrelia burgdorferi, the Lyme disease spirochete, by TLR7 and TLR9 induces a type I IFN response by human immune cells. *J Immunol*. 183(8):5279-92.

54. Liu N, Montgomery RR, Barthold SW, Bockenstedt LK. (2004). Myeloid differentiation antigen 88 deficiency impairs pathogen clearance but does not alter inflammation in *Borrelia burgdorferi*-infected mice. *Infect Immun* 72:3195-203.

55. Underhill DM, Ozinsky A. (2002) Phagocytosis of microbes: complexity in action. *Annu Rev Immunol* 20:825–52.

56. Petnicki-Ocwieja T, Chung E, Acosta DI, Ramos LT, Shin OS, Ghosh S, Kobzik L, Li X, Hu LT. (2013). TRIF mediates Toll-like receptor 2-dependent inflammatory responses to Borrelia burgdorferi. Infect Immun 81:402-10.

57. Hovius JW, Bijlsma MF, van der Windt GJ, Wiersinga WJ, Boukens BJ, Coumou J, Oei A, de Beer R, de Vos AF, van 't Veer C, van Dam AP, Wang P, Fikrig E, Levi MM, Roelofs JJ, van der Poll T. (2009). The urokinase receptor (uPAR) facilitates clearance of Borrelia burgdorferi. PLoS Pathog 5:e1000447.

58. Cinco, M., Cini, B., Murgia, R., Presani, G., Prodan, M., & Perticarari, S. (2001). Evidence of involvement of the mannose receptor in adhesion of Borrelia burgdorferi to monocyte/macrophages. *Infection and Immunity*, *69*(4), 2743–2747. http://doi.org/10.1128/IAI.69.4.2743-2747.2001

59. Hawley KL, Martin-Ruiz I, Iglesias-Pedraz JM, Berwin B, Anguita J. (2013). CD14 targets complement receptor 3 to lipid rafts during phagocytosis of Borrelia burgdorferi. *Int J Biol Sci* 9:803-10.

60. Hawley KL, Olson CM, Jr., Iglesias-Pedraz JM, Navasa N, Cervantes JL, Caimano MJ, Izadi H, Ingalls RR, Pal U, Salazar JC, Radolf JD, Anguita J. (2012). CD14 cooperates with complement receptor 3 to mediate MyD88-independent phagocytosis of Borrelia burgdorferi. *Proceedings of the National Academy of Sciences of the United States of America* 109:1228-1232.

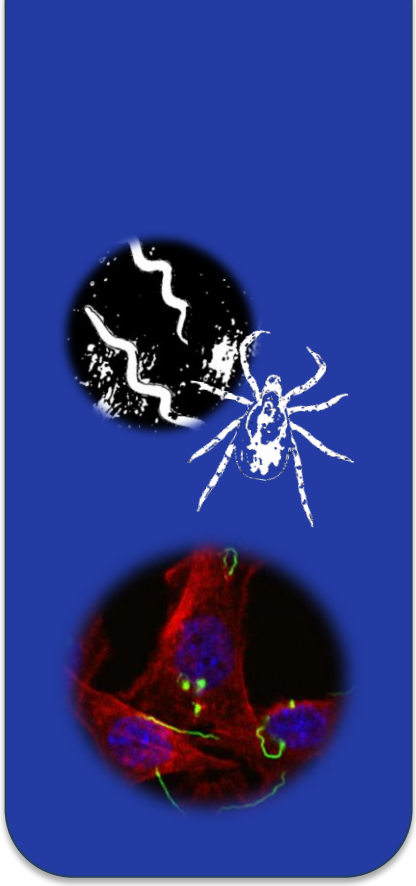

Aim of

the study

The increase of Lyme disease cases reported in the last decade in US and Europe along with climate changes favouring tick population growth predicts that this disease will be a public health concern. A recent publication estimates between 650,000 and 850,000 Lyme patients in Europe. The diagnosis difficulties and the absence of an effective vaccine clarifies that there is an emerging need for more detailed knowledge about the disease and the mechanisms of the immune response involved. The research in this area of study could contribute to the development of fully effective therapies, and specific diagnostic tools that facilitate the management of this disease, which remains in many cases underdiagnosed and ineffectively treated.

We proposed as a **general aim** a multifaceted study of the macrophage response to *Borrelia burgdorferi*, focusing on the elements involved in the phagocytic activity and cell-mediated inflammatory response, to deepen into the understanding of the infections caused by this bacterium. Our starting **hypothesis** was that the response of macrophages to *B. burgdorferi* is mediated by a set of defined surface receptors that either directly or indirectly initiate signaling cascades that determine the overall inflammatory output of these cells.

The **specific objectives** of this study were the following:

1. To analyze the traits of Macrophage and Monocyte response to *B. burgdorferi* at proteomic and transcriptomic level, along with their differences upon the stimulation with the spirochete.

2. To describe the full set of elements involved in the phagocytosis process mediated by Macrophages.

3. To characterize new surface receptors directly implicated in the ingestion of the spirochete, along with their inflammatory signature, as novel targets for macrophage activity.

EC. Parliament calls for “alarming” spread of Lyme disease to be tackled | News | European Parliament. 2018 (Nov 29). Available from: http://www.europarl.europa.eu/news/en/press-room/20181106IPR18328/parliament-calls-for-alarming-spread-of-lyme-disease-to-be-tackled.

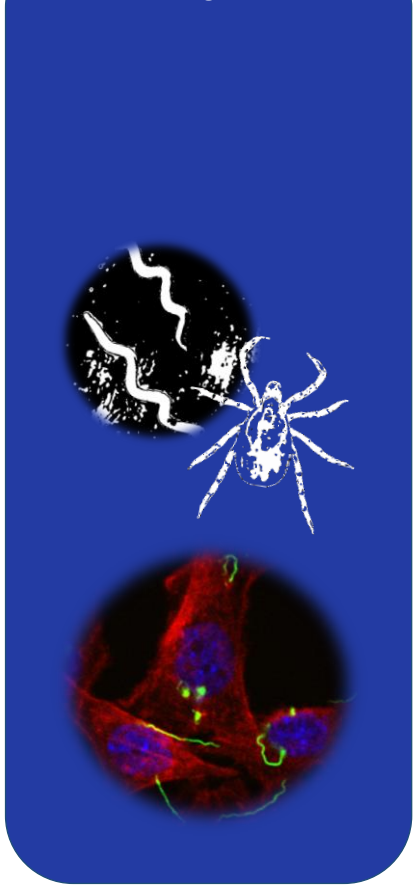

Chapter 2

The regulatory role of CD180 during the response of macrophages to *Borrelia burgdorferi*

Results published in:

Carreras-González, A. *et al.* A multi-omic analysis reveals the regulatory role of CD180 during the response of macrophages to *Borrelia burgdorferi* article. *Emerg. Microbes Infect.* **7,** (2018).

1. INTRODUCTION

Innate immune responses constitute the first host defense mechanism against infection. Phagocytic cells, particularly macrophages and dendritic cells, recognize and internalize bacteria by phagocytosis (1). In addition to the elimination of invading pathogens, the internalization of microorganisms via phagocytosis is the starting point for several downstream signaling pathways, including proinflammatory cascades, as well as those associated with antigen presentation and the activation of cells involved in acquired immune responses. Thus, phagocytosis has critical consequences for the overall response to an invading pathogen, and its coupling to inflammation must be tightly regulated. Innate immune responses to pathogens occur via the activation of different families of receptors, which collectively are referred to as pattern recognition receptors (PRRs). The best-known examples of PRRs are the families of toll-like receptors (TLRs), C-type lectin receptors, NOD-like receptors, and RIG-I-like receptors (2). These molecules respond to specific pathogen components and (3) are ideal candidates as couplers of phagocytosis to inflammation since they are recruited to phagosomes.

Extensive research has been performed in the last several years to identify the receptors and signals related to the internalization and immune responses to *B. burgdorferi*. TLRs play an important role in sensing spirochete constituents and triggering immune responses (12). The involvement of other surface receptors such as CR3-CD14 (13), MARCO (14) or uPAR (15) in both internalization and macrophage-dependent immune modulation has also been recently described. The importance of the phagocytic process during infection with *B. burgdorferi* is two-fold: first, it allows the control of spirochetal numbers during infection, especially in those organs susceptible to developing an inflammatory process, such as the heart, in which phagocytosis seems to outperform the elimination of the bacteria by circulating antibodies (16, 17); second, phagocytosis modulates both the quality and quantity of the inflammatory response by allowing the interaction of pathogen-associated molecular patterns (PAMPs) with their cognate PRRs upon degradation of the bacteria in phagolysosomal compartments (18-21). Phagocytosis of *B. burgdorferi* by macrophages and other cell types is, therefore, probably one of the most important mechanisms of control of the bacteria in the mammalian host.

Large-scale analytical approaches to quantify gene expression (transcriptomics), proteins (proteomics) and metabolites (metabolomics) have emerged with a potential to advance the identification of biomarkers in early, disseminated and post-treatment disease stages (22). These technologies may permit a definition of the disease stage and facilitate its early detection to improve diagnosis. In this chapter, we employed different omic techniques to study innate immune responses to the spirochete using both murine macrophages and human monocytes to reveal new immune treats that are involved activation of macrophages upon *B. burgdorferi* stimulation.

2. MATERIALS AND METHODS

2.1 Mice

C57Bl/6 (B6) mice were purchased from Charles River Laboratories (Barcelona, Spain) and bred at CIC bioGUNE. All work performed with animals was approved by the competent authority (Diputación de Bizkaia) following European and Spanish directives. The CIC bioGUNE´s Animal Facility is accredited by AAALAC Intl.

2.2 Bacteria

B. burgdorferi Bb914, a clone derived from strain 297 that contains a constitutively expressed GFP reporter stably inserted into cp26 (23), along with wild-type *B. burgdorferi* 297 were used for BMMs and RAW264.7 cells. *B. burgdorferi* clone 5A15 of strain B31 was used to stimulate human monocytes and monocyte-derived macrophages. Bacteria were grown in 5-ml tubes at 34 ºC in BSK-H medium (Sigma Aldrich Quimica SL, Madrid, Spain). All stimulations were performed for a period of 16 h unless otherwise stated.

2.3 Cell culture

The macrophage-like RAW264.7 cell line was maintained in DMEM (Lonza, Barcelona, Spain) supplemented with 10% FCS, 2.4 mM L-glutamine and 10% penicillin-streptomycin (Thermo Fisher Scientific, Waltham, MA). RAW264.7 cells were washed and resuspended in FCS- and penicillin-streptomycin-free DMEM 2 hours before use.

Bone marrow-derived macrophages (BMMs) were generated from 8-12-week-old C57Bl/6 (B6) mice as described (16). Bone marrow cells were collected from the femoral shafts and incubated in 100 mm x 15 mm Petri dishes (Thermo Fisher Scientific) for 8 days in DMEM supplemented with 10% FCS and 10% penicillin-streptomycin plus 30 ng/ml of M-CSF (Miltenyi Biotec, Bergisch Gladbach, GE). Following incubation, non-adherent cells were eliminated, and adherent macrophages were scraped, counted and seeded in 6-well tissue-culture plates for stimulation at a density of 10^6 cells/ml. Macrophages were allowed to rest overnight prior to stimulation.

Lentiviral particles containing shRNA targeting *Clec4e* (Sigma Aldrich) and *Cd180* (OriGene Technologies, Rockville, MD) were produced as previously described (24). Supernatants containing the virus were used to infect RAW264.7 cells, followed by incubation with puromycin at 3 µg/ml to generate stable lines. Cells containing the empty vector pLKO.1 were used as controls.

Human monocytes were purified from buffy coats of healthy blood donors by positive selection using a human CD14 purification kit (Miltenyi Biotec). Peripheral blood monocytic cells were isolated by Ficoll density centrifugation at 400 xg for 30 min without brakes. The monocyte layer was recovered, washed and processed according to the manufacturer´s protocol. Monocytes were allowed to rest for at least 4 h before stimulation. To obtain macrophages, purified human monocytes were incubated for 8 days in RPMI 1640 medium (Lonza) supplemented with 10% FCS, 2.4 mM L-glutamine, 10% penicillin-streptomycin and 30 ng/ml of human M-CSF (Miltenyi Biotec). The cells were rested overnight before stimulation. All human samples were obtained after approval by the Basque Country's Ethics committee following the Helsinki convention. Donors signed an informed consent form and were anonymized to the authors.

2.4 Phagocytosis assays

Phagocytosis assays were performed as previously described (13). Experiments were performed in DMEM medium without serum or antibiotics. The day before the assay, the cells were seeded at a density of 1 x 10^6 cells/ml. After 24 hours, *B. burgdorferi* was added to the cells at a multiplicity of infection (m.o.i.) of 25 and incubated at 4 ºC for 15 min followed by 37 ºC for 1.5 h. The cells were then washed to eliminate surface bacteria and analyzed by flow cytometry or confocal microscopy.

2.5 Confocal microscopy

Following incubation of the cells with bacteria, the cells were washed extensively, fixed in 3.7% paraformaldehyde for 7 minutes and then washed with PBS. The cells were then permeabilized with 0.1% Triton-X for 5 minutes and washed. After blocking non-specific binding with 5% BSA for 60 minutes, the cells were stained with rhodamine phalloidin for 10 minutes to visualize the actin cytoskeleton followed by DAPI for 10 minutes to stain the

nuclei (Thermo Fisher Scientific), both at 37 ºC. After extensive washing in PBS, the cells were mounted with Prolong Gold Anti-fade mounting reagent (Thermo Fisher Scientific). Photomicrographs were obtained using a Zeiss LSM 880 Confocal System.

2.6 TNF ELISA

The levels of TNF produced by *B. burgdorferi* stimulation were determined by capture ELISA using the DuoSet II kit (R&D Systems, Minneapolis, MN) according to the manufacturer's recommendations.

2.7 RNA extraction

Total RNA was extracted using the NucleoSpin® RNA kit (Macherey-Nagel, Düren, GE). The quantity and quality of the RNAs were evaluated using the Qubit RNA Assay Kit (Thermo Fisher Scientific) and RNA Nano Chips in a 2100 Bioanalyzer (Agilent Technologies, Santa Clara, CA), respectively.

2.8 RNAseq transcriptomics

Libraries for sequencing were prepared using the TruSeq RNA Sample Preparation Kit v2 (Illumina Inc., San Diego, CA) following the manufacturer´s instructions. Single-read 50-nt sequencing of pooled libraries was carried out in a HiScanSQ platform (Illumina Inc.). The data were generated from macrophages differentiated from 3 independent mice.

2.9 Gene expression array

Total-RNA (200 ng) was used to characterize gene expression with *Illumina Human HT12 v4 BeadChips* (GPL10558) containing 48,804 probes derived from Human RefSeq build 36.2. The cRNA synthesis, amplification, labeling and hybridization of the RNAs were performed following the *Whole-Genome Gene Expression Direct Hybridization* protocol (Illumina Inc.). cRNAs were then hybridized to the diverse gene-probes of the array, and the gene expression levels of the samples were detected using a HiScan scanner (Illumina Inc.). Raw data were extracted with GenomeStudio analysis software (Illumina Inc.) in the form of GenomeStudio's Final Report (sample probe profile). The data were generated using purified monocytes from 3 donors.

2.10 Data analysis

Quality control of the RNAseq sequenced samples was performed using FASTQC software (www.bioinformatics.babraham.ac.uk/projects/fastq). Reads were mapped against the whole mouse (*mm10*) reference genome by Tophat (25) to account for splice junctions. The resulting BAM alignment files for the samples were the input for the Differential Expression (DE) analysis carried out by DESeq2 (26) to account for differentially expressed genes between *B. burgdorferi*-stimulated and unstimulated macrophages. Alignment files were taken as input to generate a table of read counts via R/Bioconductor package GenomicAlignments through the *sumarizeOvelaps* function in 'union' mode for single reads/experiment. The number of uniquely mapped reads ranged from 23 to 25 x 10^6 per sample.

For array data analysis, first, raw expression data were background-corrected, log_2-transformed and quantile-normalized using the *lumi* R package (27) available through the Bioconductor repository. Probes with a "detection p-value" lower than 0.01 in at least one sample were selected. For the detection of differentially expressed genes between *B. burgdorferi*-stimulated and unstimulated monocytes, a linear model was fitted to the probe data, and empirical Bayes moderated t-statistics were calculated using the *limma* package (28) from Bioconductor. Only genes with a differential fold change (FC) >2 or <-2 and a p-value < 0.05 were considered differentially expressed.

GO enrichment was tested using the clusterProfiler (29) Bioconductor package and the Panther Database (30). Gene Ontology enrichment assessment was achieved according to GO (31) and KEGG (32) database terms. The data were also analyzed using QIAGEN´s Ingenuity® Pathway Analysis (IPA, QIAGEN, Red Wood City, CA).

2.11 Real-time RT-PCR

RNA was reverse-transcribed using M-MLV reverse transcriptase (Thermo Fisher Scientific). Real-time PCR was then performed using SYBR Green PCR Master Mix (Thermo Fisher Scientific) on a QuantStudio 6 real-time PCR System (Thermo Fisher Scientific). The fold induction of the genes was calculated using the $2^{\Delta\Delta Ct}$ method relative to the reference

genes, *Rpl19* (mouse) or *RNABP1* and *PLXNC1* (human). The primers used are listed in Table 1.

2.12 Label-free (LF) mass spectrometry proteomics analysis

Total protein from *B. burgdorferi*-stimulated and unstimulated BMMs (from 3 independent mice) was extracted using 3.5 M urea, 1 M thiourea and 2% CHAPS. The samples were incubated for 30 min at RT under agitation and digested following the filter-aided sample preparation (FASP) protocol described by Wisniewski et al (33) with minor modifications. Trypsin was added at a trypsin:protein ratio of 1:10, and the mixture was incubated overnight at 37 °C, dried in an RVC2 25 speedvac concentrator (Christ), and resuspended in 0.1% formic acid.

The equivalent of approximately 500 ng of each sample was analyzed by LC-MS label-free analysis. Peptide separation was performed on a nanoACQUITY UPLC System (Waters, Cerdanyola del Vallès, Barcelona, Spain) connected on-line to an LTQ Orbitrap XL mass spectrometer (Thermo Fisher Scientific). An aliquot of each sample was loaded onto a Symmetry 300 C18 UPLC Trap column (180 µm x 20 mm, 5 µm -Waters-). The pre-column was connected to a BEH130 C18 column (75 µm x 200 mm, 1.7 µm (Waters) and equilibrated in 3% acetonitrile and 0.1% FA. Peptides were eluted directly into an LTQ Orbitrap XL mass spectrometer (Thermo Finnigan, Somerset, NJ) through a nanoelectrospray capillary source (Proxeon Biosystems, Thermo Fisher Scientific) at 300 nl/min and using a 120 min linear gradient of 3–50% acetonitrile. The mass spectrometer automatically switched between MS and MS/MS acquisition in DDA mode. Full MS scan survey spectra (m/z 400–2000) were acquired in the orbitrap with a mass resolution of 30000 at m/z 400. After each survey scan, the six most intense ions above 1000 counts were sequentially subjected to collision-induced dissociation (CID) in the linear ion trap. Precursors with charge states of 2 and 3 were specifically selected for CID. Peptides were excluded from further analysis during 60 s using the dynamic exclusion feature.

Progenesis LC-MS (version 2.0.5556.29015, Nonlinear Dynamics, Newcastle Upon Tyne, UK) was used for the label-free differential protein expression analysis. One of the runs was used as the reference to which the precursor masses in all other samples were aligned. Only

features comprising charges of 2+ and 3+ were selected. The raw abundances of each feature were automatically normalized and logarithmized against the reference run. Samples were grouped in accordance with the comparison being performed, and an ANOVA analysis was performed. A peak list containing the information for all the features was generated and exported to the Mascot search engine (Matrix Science Ltd., London, UK). This file was searched against a Uniprot/Swissprot database, and the list of identified peptides was imported back to Progenesis LC-MS. Protein quantification was performed based on the three most intense non-conflicting peptides (peptides occurring in only one protein), except for proteins with only two non-conflicting peptides. The significance of expression changes was tested at the protein level, and proteins with an absolute value of $\log_2$ (fold change) >= 1 and ANOVA p-value ≤ 0.05 were selected for further analyses.

2.13 Statistical analysis

The results are presented as the means ± SE (standard error). Significant differences between means were calculated with the Student's t test. A p value < 0.05 was considered significant. The Benjamini-Hochberg adjustment method was used for multiple hypothesis testing in DESeq2 (RNAseq) and *limma* (microarray).

2.14 Data availability

The transcriptomic and microarray data are deposited under GEO accession number GSE103483. The proteomics data are deposited in ProteomeXchange under the accession number PXD008228.

Table 1 Primers used

Gene (m = mouse/ h = human)	Forward	Reverse	Tm	Purpose
Rpl19 (m)	GACCAAGGAAGCACGAAAGC	CAGGCCGCTATGTACAGACA	60.0	Reference, RNAseq validation
Clec4e (m)	CAACCACACATTTGACTTCTCTT	TCAGTGAGGTGGATAGGAGCA	59/61	RNAseq validation
Cd14 (m)	ATAGGAACCCTAGCCCAGATGA	ACAAGGCCACTGCTTGGGAT	62.2/60.0	RNAseq validation
Clec4d (m)	GGAAAGTCATTCCAGACCCA	AAGACGCCATTTAACCCACA	58.0/56.0	RNAseq validation
C*d180* (m)	CTTGACTGCACTTGCTCAAACA	CCCACAGCTGCCATACTACA	60.0	RNAseq validation
Siglec5 (m)	TGTGCGTCTTTGTAGCCTGC	*CACTGGAGAGCCGCTGAAT*	60.0/59.0	RNaseq validation
Syk (m)	GATGGGCTCTACCTGCTACG	CCATCAGGTTCCTGGGAGTG	63.0	RNAseq validation
Ptpre (m)	ACCAAGCCTTACTGGAATACTACC	CTGTGCTATGGAGCGTCTGC	64.0/63.0	RNAseq validation
Ly86 (m)	TGGAACATCAAGTCCAGGGT	TCCTATCCCCTTTGTGAGGA	58.0	RNAseq validation
Itgam (m)	TGTACCACTCATTGTGGGCA	GTCCATCAGCTTCGGTGTTG	58/60	qRT-PCR
Clec10a (m)	AACCTTCCGCTGGATCTGTG	GTTGAGACCGGGTAGGAGGA	60.0/63	RNAseq validation
RANBP1 (h)	CATGACCCTCAGTTTGAGCCA	CTCGCTCCTTCCATTCTGGG	60.2	Reference, mArray
PLXNC1 (h)	GGGAGCAAAATGGCTGCTTG	ACAGAAGGGTTCCCACGGTA	60.4	Reference, mArray
CD40 (h)	AGGAGATCAATTTTCCCGACGA	CTCACTGTCTCTCCTGCACT	59.5/58.7	mArray validation
IL1A (h)	AGGCATCCTCCACAATAGCAG	GGACCAATTACTGGCTCAAGGT	59.8/60.2	mArray validation
IL6 (h)	GTGGCTGCAGGACATGACAA	GCCCAGTGGACAGGTTTCTG	60.8	mArray validation
FCGR1A (h)	CTCCTTCTACATGGGCAGCAA	GGCTGCGCTTAAGGACATTT	60/59.1	mArray validation
ITGA5 (h)	GCAGAATTTGGGTTCTGCCT	GGGCACTGGGTCAGATTTATTG	58.7/59.3	mArray validation
FCGR2A (h)	CTTGGGGAAGACGAAGGGATG	CACAGAAGGTGCAGTCAGTCA	60.4/60.2	mArray validation
FCGRT (h)	AGGCCCAGGATGCTGATTTG	AACTAGGCCCAGAACCCCTT	60.4	mArray validation
IL10 (h)	GCTGTTGAGCTGTTTTCCCTG	TCCGAGACACTGGAAGGTGA	60/60.2	mArray validation
LY86 (h)	AAAGAAGCGCCCCCAAAGAG	GGGAGGCGACCAATTAGAGA	60.9/ 59	mArray validation

3. RESULTS

3.1 Global transcriptional response of murine bone marrow-derived macrophages to *B. burgdorferi* stimulation.

To unveil main transcriptional traits involved in the response of macrophages to the spirochete, we performed RNAseq comparing non-stimulated with *B. burgdorferi*-stimulated BMM. Principal component analysis (PCA) (Figure 1A) and sample distance matrix (Figure 1B) showed a clear transcriptional signature derived from BMM exposure to the spirochete. A total of 2066 genes were upregulated and 2315 were downregulated when applying cut-off values of 2-fold induction (absolute value of Log_2 ratio >= 1) and a p value of 0.05 (Figure 2A). Representative upregulated and downregulated genes were validated by qRT-PCR (Figure 3). We then performed an ingenuity pathway analysis (IPA) to obtain information about pathways that were triggered by *B. burgdorferi* exposure. As expected, the stimulation of BMMs with *B. burgdorferi* triggered a pattern of gene expression consistent with the recruitment, activation and proliferation of mononuclear leukocytes (Figure 2B). Overall, a large number of genes that were regulated by *B. burgdorferi* (317 genes) were related to inflammatory responses, and a sizeable amount (64 genes) identified phagocytosis as a hallmark of the response (Figure 2B).

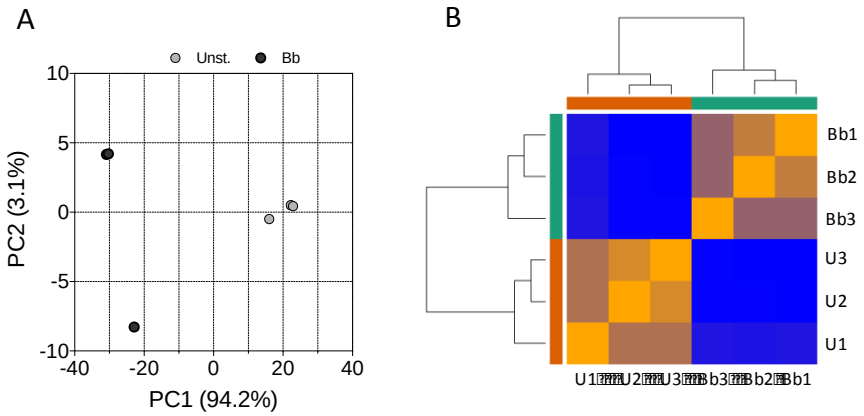

Figure 1 RNAseq analysis of murine bone marrow-derived macrophages stimulated with *B. burgdorferi*. A. Principal component analysis of BMMs stimulated with *B. burgdorferi* (black circles) or left unstimulated (gray circles). B. Sample distance matrix of BMMs stimulated with *B. burgdorferi* (Bb) and unstimulated controls (U)

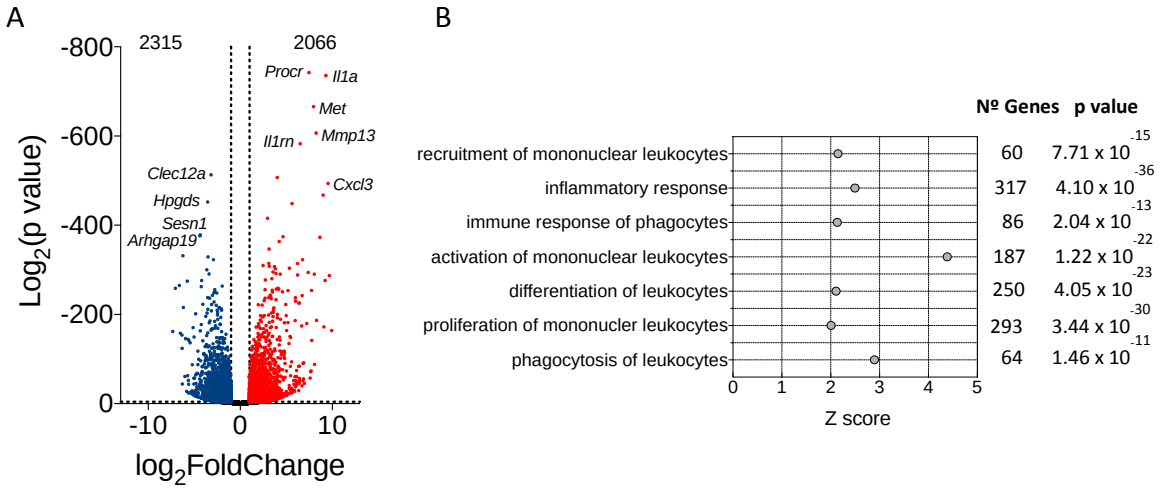

Figure 2 A. Volcano plot showing genes upregulated (red dots) or downregulated (blue dots) upon stimulation of BMMs with *B. burgdorferi*. Ten of the most regulated genes are identified. **B.** Biological processes that are significantly regulated by the stimulation of BMMs with *B. burgdorferi*. The Z scores identify those processes that are differentially regulated (Z > 2). The number of genes corresponding to each process and the p value obtained by IPA is also shown.

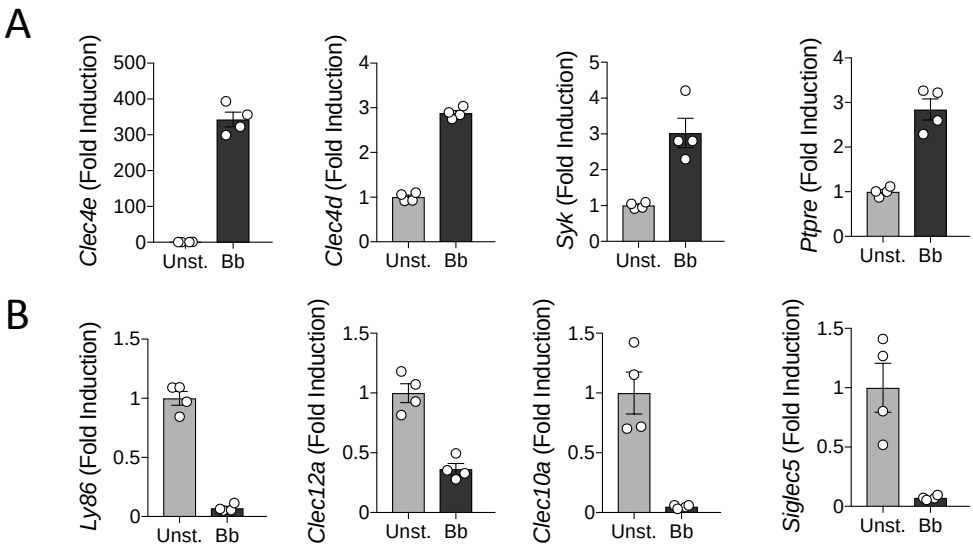

Figure 3 Validation of the RNAseq on selected genes. Fold induction changes by qRT-PCR of a group of selected genes differentially regulated in BMMs from 4 independent mice stimulated with *B. burgdorferi* (black bars) compared to unstimulated controls (grey bars). (A) Genes upregulated. (B) Genes downregulated.

The expression profile of macrophages exposed to the spirochete resembled the transcriptional fingerprint upon recognition of bacteria and viruses by pattern recognition receptors, including Toll-like receptor signaling or activation of IRF by cytosolic pattern recognition receptors (Figure 4A). Furthermore, the expression profile significantly resembled TREM1 receptor signaling events (Figure 4A) upon stimulation. This protein acts as an amplifier of monocyte inflammatory responses triggered by infections by stimulating the release of proinflammatory chemokines and cytokines. In contrast, signaling intermediates induced by PPAR, a well-recognized suppressor of inflammatory responses (34-36), were significantly repressed upon stimulation with *B. burgdorferi* (Figure 4A). We observed a significant overlap of the genes regulated by stimulation of BMMs with *B. burgdorferi* and those associated with gene expression dependent on LPS-, poly rI:C-RNA- and NOD2 (Table 2). These data confirmed the complex nature of the interaction signature between *B. burgdorferi* and PRRs that depends on several receptors. Indeed, although significant overlapping was also found when comparing genes regulated by PMA_3CSK_4 or TLR2-induction with stimulated BMMs (Table 2), the percentage of genes that were shared among these conditions was less than 10%, indicating that the overall response to the spirochete is dependent on a larger array of signaling receptors.

Among the upstream regulators potentially involved in the observed transcriptional response, we found a significant overlap of the cytokines TNF, IL-1β, IL-6, MIF, and IFNβ1, as well as nitric oxide (Table 2, Figure 4B). These responses are probably a secondary activation boost launched after the initial bacterial exposure. Interestingly, even though *Il10* expression was significantly increased upon *B. burgdorferi* stimulation (3.568 Log_2 fold induction, $p = 1.42 \times 10^{-59}$), the overall signature response significantly matched a repressed gene expression profile triggered by the IL-10 receptor (Table 2). These data support a proinflammatory response induced primarily by the interaction of *B. burgdorferi* with macrophages that is further amplified by secreted cytokines or the inhibition of anti-inflammatory pathways.

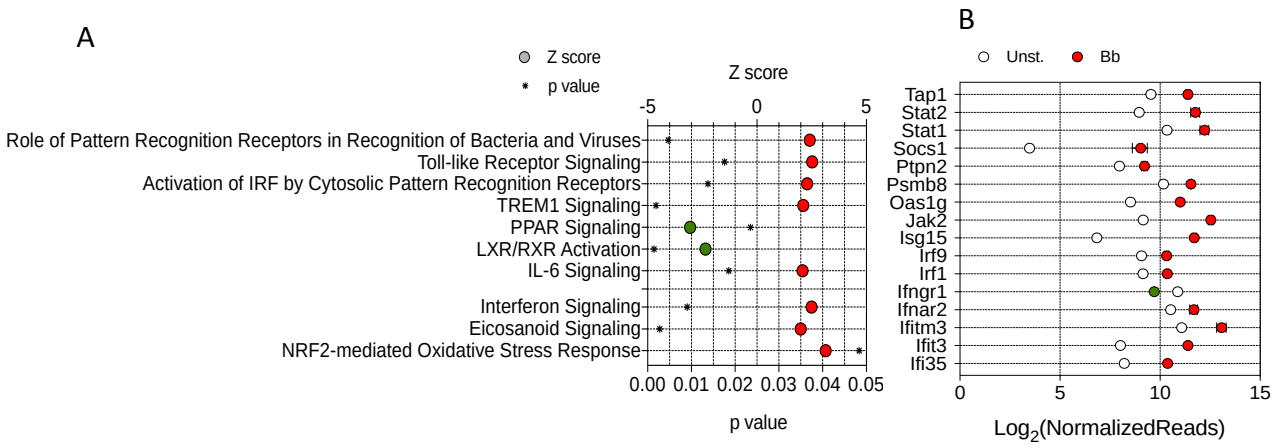

Figure 4 RNAseq analysis of murine bone marrow-derived macrophages stimulated with *B. burgdorferi*. A. Z scores corresponding to genes regulated by *B. burgdorferi* in BMMs in response to specific PRRs and upstream regulators. Z scores >2 or < -2 were considered significant. **B.** Genes that are differentially regulated by B. burgdorferi in BMMs (red circles = upregulated; green circle = downregulated) corresponding to the interferon signaling pathway according to IPA.

Table 2 Selected upstream upregulators showing a significant overlap with the stimulation of BMM with *B. burgdorferi

Regulator	Log2(Fold Induction)	Z score	p value	Nº Molecules	Total (%)
Lipopolysaccharide		11,582	2,07E-97	527	931 (57)
Poly rI:C-RNA		8,706	1,49E-41	161	721 (22)
Nod2	3,373	5,265	2,61E-19	41	743 (6)
NFkB complex		6,403	2,07E-33	185	782 (24)
p38 MAPK		3,655	5,28E-19	110	759 (15)
Tnf	5,200	9,444	1,49E-68	474	837 (57)
Il1b	7,704	7,637	2,90E-55	288	823 (35)
Il6	7,634	4,026	2,96E-40	221	835 (27)
Nos2	6,355	3,853	1,01E-10	59	869 (7)
Mif	1,367	3,255	2,07E-07	36	751 (5)
Ifnb1	2,673	5,798	1,39E-42	123	622 (20)
Il10ra	-0,688	-7,569	3,23E+00	137	498 (28)
PAM3CSK4		4,754	1,47E-17	51	587 (9)
Tlr2	1,556	4,662	2,29E-09	46	616 (8)

* *When appropriate, the induction of the corresponding gene is shown.*

3.2 The human peripheral blood monocyte transcriptional profile shows a similar global response but distinctive species-specific pattern upon *B. burgdorferi* stimulation.

To corroborate the transcriptomic results obtained using murine BMMs and to test their biological relevance in the context of human innate immune responses to the spirochete, human $CD14^+$ peripheral blood monocytes (hMon) were stimulated with *B. burgdorferi*. The transcriptional profile was obtained by microarray analysis and compared with BMM. Overall, 1962 genes were upregulated and 2096 downregulated (absolute value of Log_2 fold induction >= 1; $p < 0.05$; Figure 5A), a selection of which were validated by qRT-PCR (Figure 4) and represented clear patterns of expression (Figure 5B). Reflecting the different cell types and origins (human *vs*. mouse), the transcriptional fingerprints showed a limited number of genes that were regulated and in the same direction in both cell types. Thus, 195 genes were upregulated both in BMMs and hMon upon stimulation with *B. burgdorferi*, while 161 genes were downregulated according to the established criteria (Figure 5C). An additional 168 genes were regulated in opposite directions in both cells types (Figure 5C). In spite of this, IPA showed a regulation of similar expression pathways, including cell movement and recruitment of leukocytes, fatty acid metabolism, endocytosis and phagocytosis, as well as the synthesis of nitric oxide and reactive oxygen species (Figure 5D).

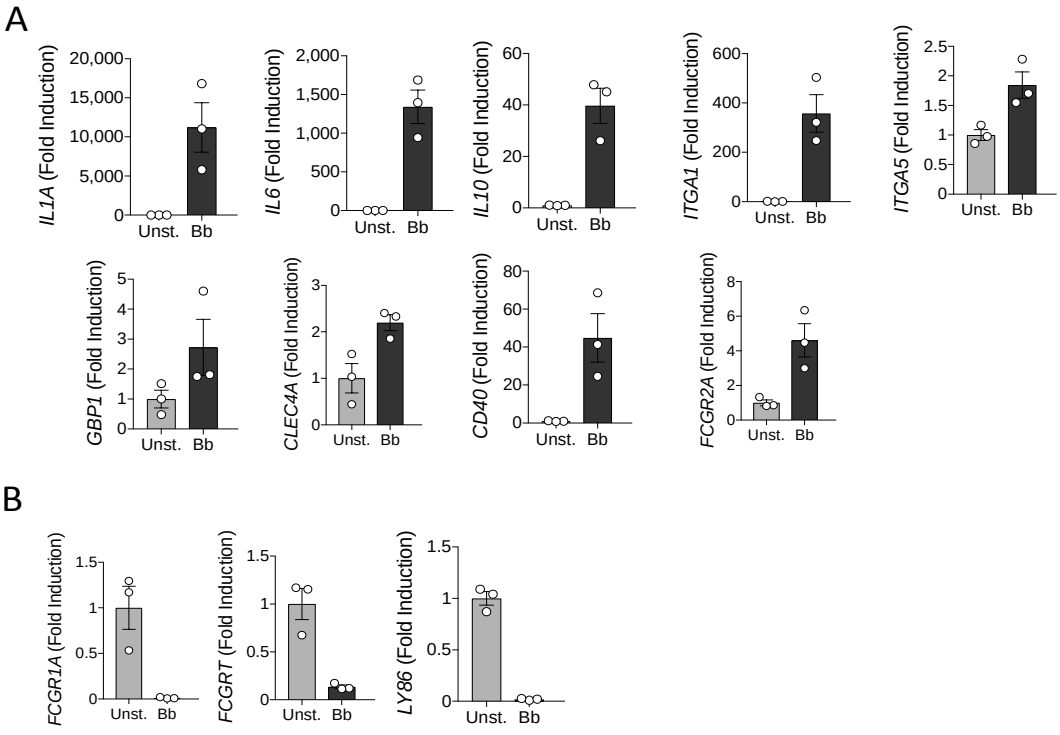

Figure 4 (Previous page) Validation of the µArray on selected genes. Fold induction changes by qRT-PCR of a group of selected genes differentially regulated in human monocytes from 3 independent donors stimulated with *B. burgdorferi* (black bars) compared to unstimulated controls (grey bars). (A) Genes upregulated. (B) Genes downregulated.

Moreover, analysis of upstream regulators showed similar patterns of expression in response to pattern recognition engagement (TLR3, TRL9, TLR7, NOD2), signaling intermediaries (MyD88, NF-κB complex, IKBKB) or secondary metabolites (TNF, IL-1β, IL-1α, IFNα2) (Figure 5E). In both cases, the expression profile resembled the inhibition of gene expression initiated by IL-10Rα, while in a few cases the expression profile followed opposite directions in both cells types (i.e., MITF) (Figure 5E). These results show that in both murine BMMs and hMon, stimulation with *B. burgdorferi* results in an overlapping proinflammatory profile that, nevertheless, reveals distinct transcriptional specificities.

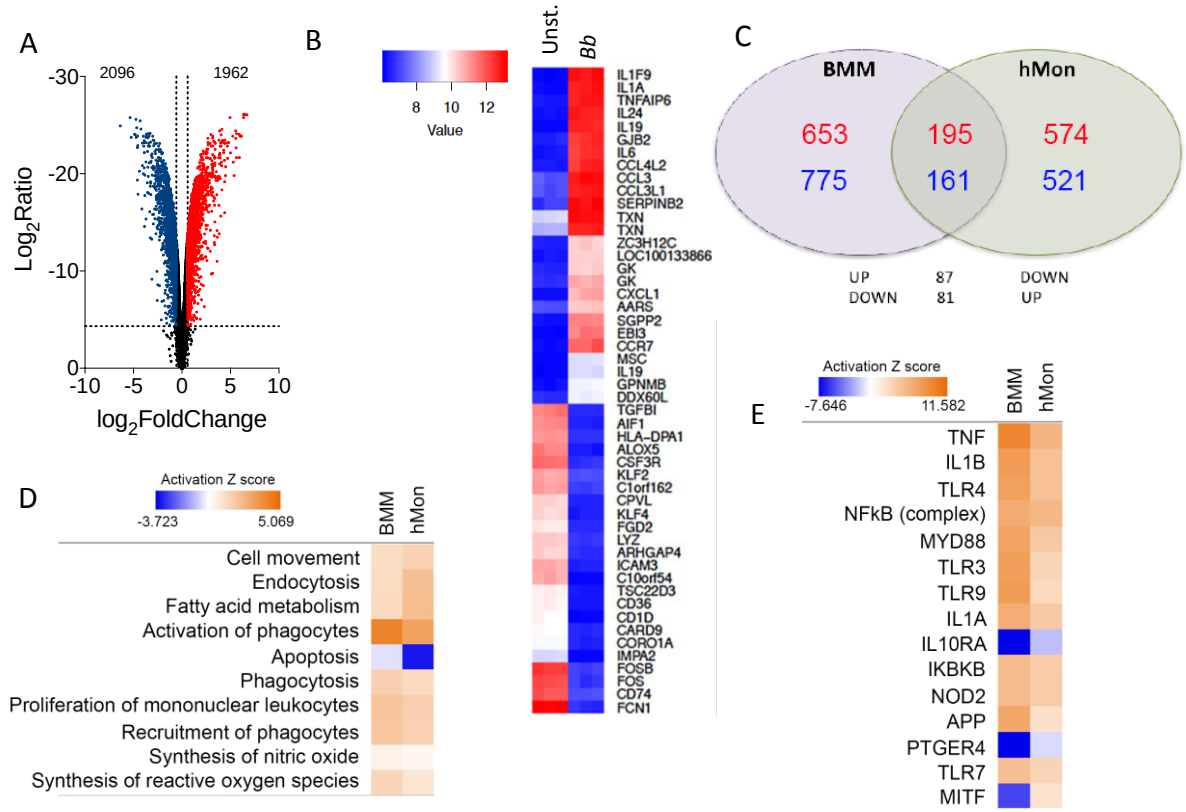

Figure 5 Analysis of genes regulated by *B. burgdorferi* in human CD14$^+$ blood monocytes. A. Volcano plot representing genes that are differentially regulated by stimulation with the spirochete. The red dots represent upregulated genes, while the blue dots correspond to those that are differentially downregulated. **B.** Heat map showing the 50 most regulated genes in response to *B. burgdorferi* stimulation of human monocytes (Bb) compared with unstimulated monocytes (Unst.).**C.** Venn diagram showing the overlap in gene regulation

(***Figure 5 continued***) between BMMs and human monocytes stimulated with *B. burgdorferi*. The number of upregulated genes is represented in red. Downregulated genes are marked in blue. **D.** Comparison of biological processes regulated in BMMs and hMon stimulated with *B. burgdorferi*. Processes that showed activation are indicated in orange, while those that were downregulated are presented in blue. The intensity of the colors is determined by the calculated Z value for each process. **E.** Upstream activator pathways regulated by *B. burgdorferi* in BMMs and hMon. The colors and intensities are presented according to calculated Z values as in D.

3.3 The proteome of BMMs shows a distinct profile upon stimulation of BMMs with *B. burgdorferi*.

We also assessed differences in protein levels between unstimulated and *B. burgdorferi*-stimulated BMMs using label-free MS. We detected 810 proteins represented by at least 2 peptides, 35 of which showed significantly different levels ($p < 0.05$) and were regulated at least 2-fold (absolute value of Log_2 fold induction >= 1; 17 upregulated and 18 downregulated) between unstimulated and *B. burgdorferi*-stimulated BMMs (Figure 6A; Supplementary Table S2). Of the 17 upregulated proteins, 13 corresponded to genes that were significantly upregulated upon stimulation in the transcriptomic approach, while 3 corresponded to genes with no significant transcriptional change and 1 was downregulated at the gene expression level (Figure 6A, Table 3). In contrast, the majority of proteins that were downregulated upon stimulation with *B. burgdorferi* (11 of 18) corresponded to genes without changes in expression, and 7 also showed downregulation at the gene expression level (Figure 6A, Table 3).

Despite the limited amount of proteins that were significantly changed at this time interval of stimulation, IPA showed that the majority corresponded to proteins that are known to be regulated by LPS- (17 proteins), CpG oligonucleotide- (7 proteins) or poly rI:C-RNA-induced stimulation (8 proteins; Figure 6B). Furthermore, several proteins corresponded to NOD2- (5 proteins) or MyD88-induced pathways (8 proteins). The regulated proteins were also related to the stimulation with TNF (15 proteins) or IL-1β (10 proteins) (Figure 6B). As expected, the proteins that were regulated by IL-10Rα engagement (6 proteins) showed that this pathway is inhibited by *B. burgdorferi* stimulation (Figure 6B). Overall, the proteomics analysis of BMMs corroborated the activation pathways initiated by stimulation with the spirochete at the gene expression level both in BMMs and hMon.

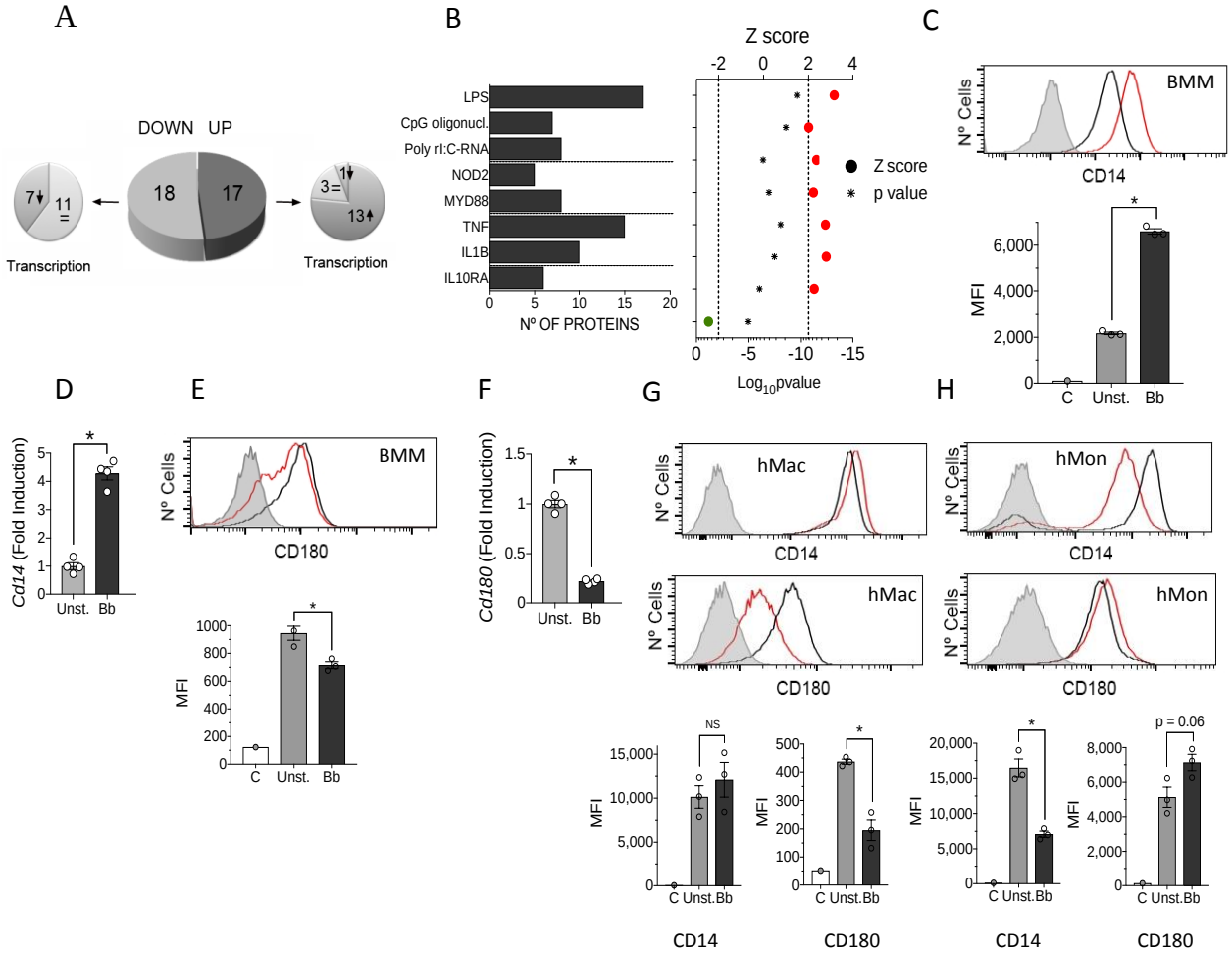

Figure 6 Proteomic analysis of BMMs stimulated with *B. burgdorferi* A. Pie chart showing the upregulated (dark gray) or downregulated proteins (light gray) in response to stimulation with the spirochete. The smaller pie charts on each side represent the direction of the regulation corresponding to the genes encoding the differentially expressed proteins. **B.** Upstream regulators with significant Z scores (> 2, red circles or < -2, green circle) and the number of regulated proteins. .**C.** Flow cytometry analysis of CD14 expression in BMMs stimulated with *B. burgdorferi* (red histogram) compared with unstimulated cells (black histogram). The gray histogram represents the unstained control. The average of the mean fluorescence intensity (MFI) ± SE for 3 independent mice is represented below. The experiment is representative of 3 performed. **D.** Upregulation of *Cd14* expression levels determined by qRT-PCR of RNA extracted from *B. burgdorferi*-stimulated BMMs (black bar) or unstimulated controls (gray bar). The results represent the average ± SE of 4 independent mice and are representative of 3 experiments performed. **E.** Flow cytometry analysis of CD180 expression in BMMs stimulated with *B. burgdorferi* (red histogram) compared with unstimulated cells (black histogram). The gray histogram represents the unstained control. The average of the MFI ± SE for 3 independent mice is shown below and is representative of 3 experiments. **F.** Downregulation of *Cd180* expression levels by qRT-PCR in BMMs stimulated with *B. burgdorferi* (black bar) or unstimulated controls (gray bar). The results are the mean

(***Figure 6 continued***) ± SE of 4 independent mice. **G.** Expression of CD14 (top histograms) and CD180 (bottom histograms) in human monocyte-derived macrophages stimulated with *B. burgdorferi* (red histograms) and unstimulated controls (black histograms). The gray histogram represents the unstained controls. The average of the mean fluorescence intensity (MFI) ± SE for 3 independent determinations is represented below. The results are representative of those obtained with 6 independent samples. **H.** Expression of CD14 (top histograms) and CD180 (bottom histograms) in hMon stimulated with *B. burgdorferi* (red histograms) and unstimulated controls (black histograms. The gray histogram represents the unstained controls. The average of the mean fluorescence intensity (MFI) ± SE for 3 independent determinations is represented below. The results are representative of those obtained with 9 independent samples.

We then sought to identify proteins that are regulated by *B. burgdorferi* in macrophages and that may have a role in the response of these cells to the spirochete. Among the differentially expressed proteins, the majority represented plasma membrane-anchored proteins (12 proteins) (Table 4). Notably, we observed two proteins, CD14 and CD180, which were regulated in opposite directions. The stimulation of BMMs with *B. burgdorferi* resulted in increased levels of both surface CD14 and gene expression (Figure 6 C, D), while the levels of CD180, a non-canonical member of the TLR family of proteins, were significantly reduced (Figure 6 E, F). The downregulation of CD180 was corroborated in *in vitro* differentiated human macrophages (Figure 6G). In contrast, human monocytes isolated from blood showed an opposite phenotype, with reduced levels of CD14 and increased expression of CD180 in response to the spirochete (Figure 6H), evidencing the distinct role of both types of cells in tissue homeostasis and immunity (37).

3.4 CD180 regulates the phagocytosis of *B. burgdorferi* and the production of TNF

Among the surface proteins regulated by the stimulation with *B. burgdorferi*, Clec4e (Mincle) has been shown to be involved in the phagocytosis of several microorganisms (38). To address its potential role in the response of phagocytic cells to the spirochete, we silenced *Clec4e* (Mincle) in RAW264.7 cells by lentiviral infection (Figure 7A). The repression of *Clec4e* gene expression did not result in an appreciable reduction of the phagocytic capacity of RAW264.7 cells (Figure 7B). Furthermore, the analysis of TNF production upon stimulation with *B. burgdorferi* did not result in a differential production of

this cytokine (Figure 7C), indicating that the C-type lectin receptor is not involved in the internalization or proinflammatory cytokine production in response to the spirochete.

Phagocytosis of *B. burgdorferi* is largely dependent on MyD88-mediated signals (13, 39). However, the involved receptor(s) are still unknown. Since the stimulation with *B. burgdorferi* induced the downregulation of CD180 (Table 3), we sought to determine whether this TLR family member is involved in the internalization of the spirochete and/or the induction of proinflammatory responses. Silencing of *Cd180* (Figure 7D) resulted in a significant increase in the capacity of RAW264.7 cells to internalize *B. burgdorferi* (Figure 7E,F).

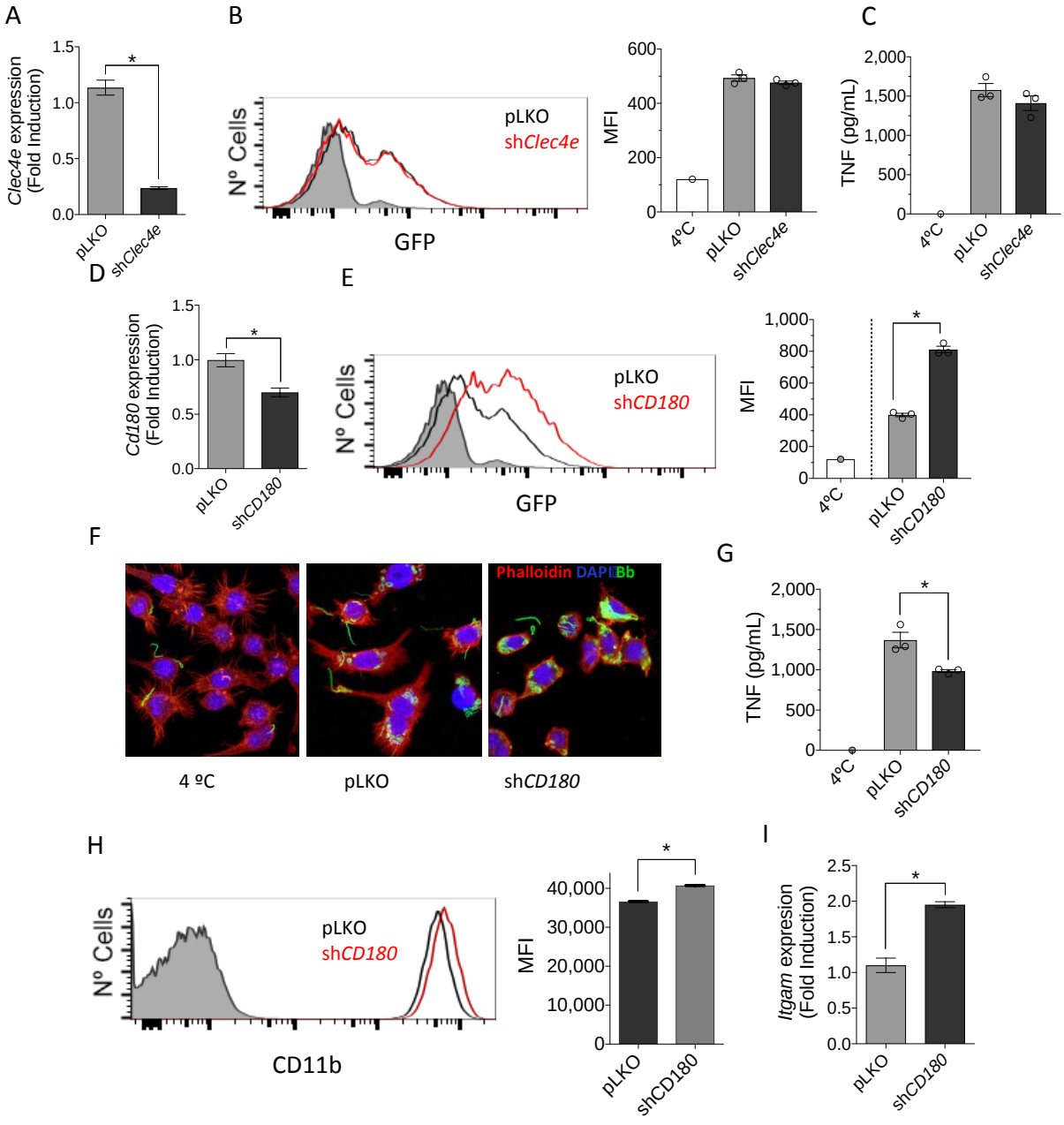

Figure 7 (previous page) CD180 regulates the response of macrophages to *B. burgdorferi* A. Downregulation of *Clec4e* expression in RAW264.7 cells infected with a lentivirus containing specific shRNA (black bar) or an empty vector (pLKO, gray), as determined by qRT-PCR. The results represent the average of 3 determinations. **B.** Phagocytosis of *B. burgdorferi* by RAW264.7 cells containing shRNA specific for *Clec4a* (red histogram) or an empty control (pLKO, black histogram). The gray histogram represents cells incubated at 4 °C (control). The average MFI of 3 determinations is presented on the right. The results are representative of at least 3 independent experiments**. C.** TNF production upon stimulation with *B. burgdorferi* by RAW264.7 cells with silenced *Clec4a* or controls. D. Silencing of *CD180* in RAW264.7 cells (black bar) or pLKO controls (gray bar), as determined by qRT-PCR. The values correspond to the average ± SE of 3 determinations and are representative of 3 experiments. **E.** Phagocytosis of *B. burgdorferi* by sh*Cd180* RAW 264.7 cells (red histogram) or pLKO-infected controls (black histogram). The gray histogram represents the 4 °C control. The average of 3 determinations is presented on the right. The results are representative of at least 3 independent experiments. **F.** Confocal micrograph of RAW264.7 cells containing shRNA specific for *Cd180* (shCD180) or an empty vector (pLKO). The cells were stained with phalloidin (red) and DAPI. *B. burgdorferi* are shown in green. **G.** TNF production upon stimulation with *B.* burgdorferi by RAW264.7 cells containing a shRNA specific for *Cd180* or a vector control (pLKO). The average ± SE of 3 determinations is presented and represent at least 3 independent experiments. **H.** Flow cytometry showing the expression of CD11b in unstimulated RAW264.7 cells containing a shRNA specific for *Cd180* (red histogram) or an empty vector (pLKO, black histogram). The gray histogram represents the unstained control. The average of the mean fluorescence intensity (MFI) ± SE for 3 determinations is represented on the right. **I.** qRT-PCR showing the expression of the *Itgam* gene in unstimulated RAW264.7 cells containing an shRNA specific for *Cd180* (black bar) or the empty vector (pLKO, gray bar). The results represent the average ± SE of 3 determinations.

Table 3 Proteins significantly regulated by *B. burgdorferi* stimulation of BMMs and their corresponding gene transcription profiles

Protein	Gene	*Proteomics*		*Transcriptomics*	
		Log_2(Ratio Borr/Unst)	ANOVA	Log_2Fold (BMM)	p value
PGH2_MOUSE	*Ptgs2*	4,845	2,65E-06	8,664	4,97E-113
IRG1_MOUSE	*Irg1*	4,215	4,48E-04	-5,283	1,27E-07
CTR2_MOUSE	*Slc7a2*	3,036	5,78E-03	6,219	1,89E-95
CLC4E_MOUSE	*Clec4e*	2,907	6,38E-04	5,157	9,73E-08
GBP2_MOUSE	*Gbp2*	2,683	6,24E-04	3,796	1,07E-06
SQSTM_MOUSE	*Sqstm1*	2,668	1,67E-03	2,502	1,62E-15
IL1B_MOUSE	*Il1b*	2,407	4,79E-03	7,704	7,83E-23
DEOC_MOUSE	*Dera*	2,347	1,18E-02	-0,773	3,33E-06
FCGR2_MOUSE	*Fcgr2b*	2,211	7,22E-03	2,708	2,48E-23
HMOX1_MOUSE	*Hmox1*	2,061	2,46E-03	3,722	3,37E-93
ICAM1_MOUSE	*Icam1*	1,673	6,87E-03	2,138	1,48E-03

DDX21_MOUSE	*Ddx21*	1,509	5,48E-03	-0,259	3,74E-01
PRDX5_MOUSE	*Prdx5*	1,437	9,02E-03	3,180	1,35E-28
VPS4B_MOUSE	*Vps4b*	1,261	1,54E-02	-0,198	2,77E-01
CD14_MOUSE	*Cd14*	1,246	6,25E-03	2,320	7,36E-21
ACSL1_MOUSE	*Acsl1*	1,210	2,80E-03	4,649	2,12E-113
4F2_MOUSE	*Slc3a2*	1,135	6,33E-03	1,796	1,65E-16
MYO1F_MOUSE	*Myo1f*	-1,080	3,01E-02	-1,489	3,71E-29
CD36_MOUSE	*Cd36*	-1,110	6,80E-03	0,679	4,99E-02
NPC1_MOUSE	*Npc1*	-1,126	4,35E-02	-0,288	2,73E-02
AGAL_MOUSE	*Gla*	-1,133	4,46E-02	-0,253	6,35E-02
LKHA4_MOUSE	*Lta4h*	-1,138	9,15E-03	-0,446	2,74E-03
AP3B1_MOUSE	*Ap3b1*	-1,147	4,69E-03	0,348	8,58E-03
STOM_MOUSE	*Stom*	-1,150	1,17E-02	0,661	3,95E-05
LRP1_MOUSE	*Lrp1*	-1,166	3,84E-02	-1,059	4,17E-05
CSF1R_MOUSE	*Csf1r*	-1,199	3,12E-02	-0,317	2,74E-02
SCMC1_MOUSE	*Slc25a24*	-1,218	9,82E-03	-0,692	2,25E-07
ACL6A_MOUSE	*Actl6a*	-1,268	3,67E-02	-0,070	7,49E-01
LGMN_MOUSE	*Lgmn*	-1,303	2,37E-02	-2,022	2,11E-26
PP2BA_MOUSE	*Ppp3ca*	-1,349	2,60E-03	-1,163	6,13E-23
CD180_MOUSE	*Cd180*	-1,349	1,65E-02	-1,540	2,28E-15
PLST_MOUSE	*Pls3*	-1,418	4,58E-02	-0,961	6,00E-08
WASP_MOUSE	*Was*	-1,665	4,06E-02	-0,421	1,72E-03
NIBAN_MOUSE	*Fam129a*	-1,951	3,86E-02	-4,056	2,97E-43
LIPL_MOUSE	*Lpl*	-2,430	1,55E-02	-1,376	4,57E-07

* *Proteins and genes that were regulated in the same direction are marked in green (downregulated) or orange (upregulated). IRG1 was regulated in opposite directions at the protein and gene expression levels (marked in gray).*

Strikingly, the repression of *Cd180* also resulted in a significant reduction in TNF production by RAW264.7 cells in response to the spirochete (Figure 7G). The stimulation of Cd180-silenced cells also resulted in lower mRNA levels of *Tnf* and *Il6* (Figure 8). Phagocytosis of *B. burgdorferi* is mediated by several, largely unknown, phagocytic receptors, including complement receptor (CR) 3 (CD11b/CD18) (13). Interestingly, phagocytosis mediated by CR3 results in the attenuation of the inflammatory response, particularly the production of TNF (13). In concordance with our results, CD180 has been associated with the tempering of the proinflammatory response of macrophages (40, 41). We sought to determine whether the increased phagocytosis of *B. burgdorferi* in cells with repressed expression of *Cd180* was

due to the regulation of CR3. The analysis of CD11b surface expression by flow cytometry showed significantly increased levels in sh*Cd180* cells compared with the controls (Figure 7H). Furthermore, the analysis by qRT-PCR of sh*Cd180* cells showed the upregulation of *Itgam* gene expression (Figure 7I).

Overall, these data unravel a new role for CD180 in the regulation of expression of the phagocytic receptor for *B. burgdorferi*, CR3. The inhibition of CR3 expression by CD180 attenuates phagocytosis and promotes proinflammatory responses. These results define CD180 as an important regulator of immune responses mediated by *B. burgdorferi*.

Table 4 Proteins significantly regulated by *B. burgdorferi* stimulation of BMMs that are located in the plasma membrane

Protein	*Gene*	*Name*	*Function*
CTR2_MOUSE	*Slc7a2*	ATRC2	Cationic aminoacid transporter.
CLC4E_MOUSE	*Clec4e*	Mincle	C-type lectin,
FCGR2_MOUSE	*Fcgr2b*	CD32, FC gamma RIIB	Low affinity IgG Fc receptor.
ICAM1_MOUSE	*Icam1*	CD54, Intercepllular adhesion molecule 1	Adhesion molecule.
CD14_MOUSE	*Cd14*	CD14	Cooperates with TLR4 and CR3.
4F2_MOUSE	*Slc3a2*	CD98, Ly10	aminoacid and Ca2+ Transporter.
CD36_MOUSE	*Cd36*	CD36, Fatty acid translocase	lipid binding.
AP3B1_MOUSE	*Ap3b1*	Pearl, Tsap4	Protein targetting to lysosome.
STOM_MOUSE	*Stom*	Stomatin	Regulation of ion channels and transporters.
LRP1_MOUSE	*Lrp1*	CD91, alpha-2-macroglobulin receptor	Lipid homeostasis and clearance of apoptotic cells.
CSF1R_MOUSE	*Csf1r*	CD115, CSF1 receptor	Regulation of macrophage function.
CD180_MOUSE	*Cd180*	RP105, Ly78	Forms dimers with MD-1. Pattern recognition receptor.

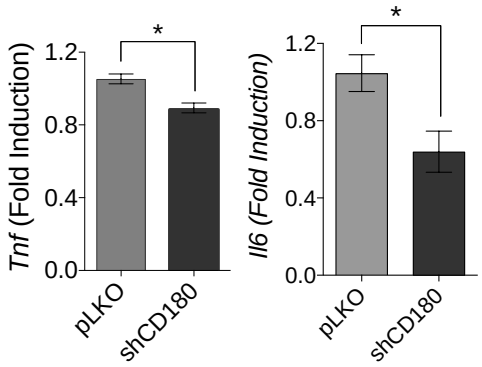

Figure 8 (previous page) *Tnf* and *Il6* gene expression induced by *B. burgdorferi* in RAW264.7 cells with silenced *Cd180*. Control- and *Cd180*-silenced cells (10^6 cells /ml) were stimulated with *B. burgdorferi* at an

m.o.i. of 25 for 4h. Total RNA was then extracted, reverse-transcribed and used to determine by qRT-PCR for the levels of *Tnf* and *Il6* mRNA levels. The results represent the mean ± SE of triplicates.

4. DISCUSSION

Macrophages can recognize, phagocytose, and eliminate invading pathogens and thus have a crucial role in host defense. These cells constitute a key component of the innate immune system with the ability to respond to a wide array of stimuli, both endogenous and pathogen-associated, showing an enormous capacity to adapt and respond to environmental cues. In the presence of pathogens, macrophages produce an array of inflammatory factors upon the engagement of pattern-recognition receptors (PRRs). The response of macrophages is further modulated by environmental signals, including cytokines such as TNF, IL-10, IL-6 or interferons, among other factors. The use of high-throughput (omic) techniques has grown exponentially in recent years driven by marked improvement in analytical platforms, increasing resolution and sensitivity, high-throughput capabilities and reducing costs (42). These methodologies have allowed the elucidation of mechanisms of pathogenesis for disease-causing agents, identified disease biomarkers (biosignatures) or characterized the response to preventative and therapeutic interventions (42, 43). Omic technologies have been used in Lyme borreliosis patients, enabling the determination of a distinctive disease biosignature, particularly at the early disease stages (42-46). Here we employed high-throughput techniques to study biosignatures of both primary murine macrophages and human monocytes exposed to *B. burgdorferi*. Our results showed that while general transcriptional traits are shared between human monocytes and murine macrophages, there are several important differences between both cell types. However, both their expression profiles resemble the transcriptional fingerprint upon recognition of bacteria and viruses by PRRs, including TLR signaling or the activation of IRF, evidencing the complex nature of the interaction signature between *B. burgdorferi* and phagocytic cells, which depends on several receptors. Moreover, comparison of the signaling pathways activated by *B. burgdorferi* on isolated murine macrophages and human peripheral blood monocytes resemble those found in peripheral blood monocytic cells obtained from patients diagnosed with Lyme borreliosis (44) (Figure 9) and correlates with a previous description of the transcriptome induced by *B. burgdorferi* stimulation of the murine cell line J774 (47) (Figure 10). Overall, these data suggest that the identification of transcriptional traits in isolated cells stimulated with the spirochete can represent biosignatures that are present in infected individuals.

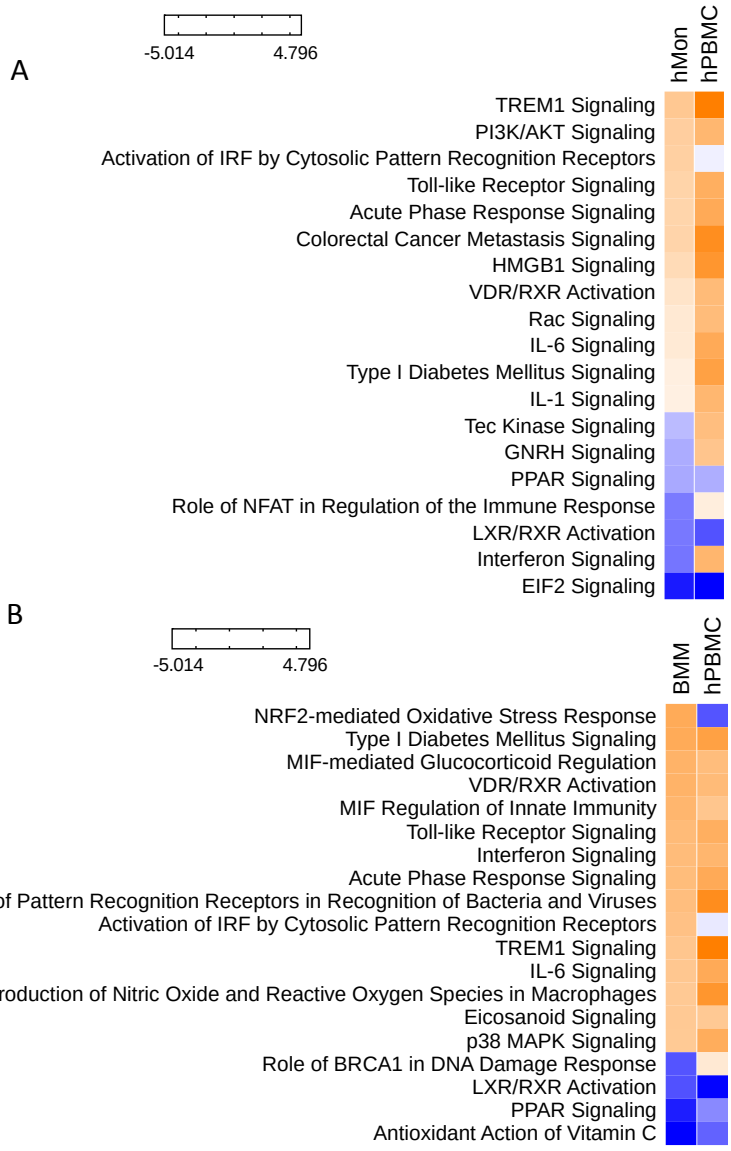

Figure 9 Comparison of the signaling pathways induced by B. burgdorferi in murine BMMs, human monocytes and PBMCs from Lyme borreliosis patients. Pathways identified by IPA induced by the stimulation with *B. burgdorferi* or human peripheral blood monocytes (A) or murine BMMs (B) compared to those identified in PBMCs isolated from diagnosed Lyme borreliosis patients (44). The colors represent the calculated z values and are indicated as activated (orange) or repressed (blue). Pathways marked in white were not identified by IPA as regulated.

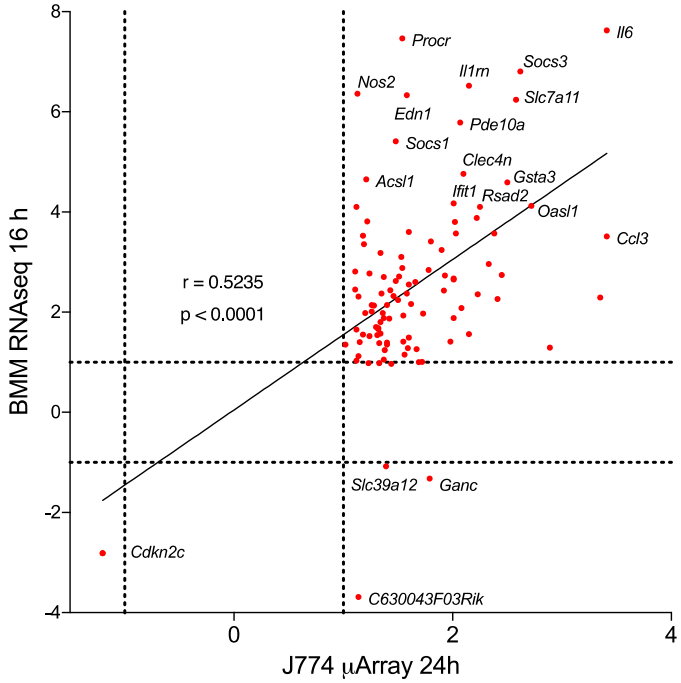

Figure 10 Comparison between the transcriptome of the murine cell line J774 and BMM stimulated with *B. burgdorferi*. Correlation between the transcriptome of the murine macrophage cell line, J774 stimulated with *B. burgdorferi* for 24h (47) and BMMs stimulated with the spirochete for 16h. The data corresponding to the J774 cells correspond to a uArray analysis and extracted from the supplementary materials of the study. The correlation was calculated for those genes in which a change in transcriptional levels between stimulated and unstimulated cells was found, and correspond to those with an absolute value for the $\log_2$FoldInduction >= 1 and $p < 0.05$. The genes most regulated are identified.

Inherent to their killing capacity, macrophages produce numerous molecules that, while exerting functions related to host defenses, are also capable of damaging host tissue (48). Inflammation is, therefore, a two-edged sword and, thus, coupling of phagocytosis to inflammation must be tightly regulated. It is not surprising that many regulatory mechanisms are required to control the inflammatory response by preventing inappropriate activation or by a timely termination of the immune response. *B. burgdorferi* stimulation of TLR-dependent and independent signaling in host cells leads to transcriptional activation, the release of inflammatory mediators, and anti-microbial responses (49-52). The stimulation with *B. burgdorferi* also leads to the induction of several anti-inflammatory pathways, including IL-10 (53-56), PPAR (34-36) or the induction of phagocytic receptors with anti-inflammatory action, such as CR3 (13, 57). The relative contribution of each is unknown, but our results show that even though IL-10 production is highly induced by the

spirochete, IL-10R-dependent signaling is repressed at the time of analysis. However, our data show that the stimulation of macrophages with *B. burgdorferi* induces the downregulation of CD180. Furthermore, this stimulation also results in decreased expression of the *Ly86* gene (encoding the CD180 accessory molecule MD-1; -1.902 Log_2 fold induction, $p = 1.09 \times 10^{-15}$ in *B. burgdorferi*-stimulated BMMs compared with unstimulated cells), which is required for the function and surface expression of CD180 (58). In turn, the repression of CD180 expression results in the secondary upregulation of CR3 and the tempering of the inflammatory response. Overall, these results suggest that the initial stimulation with the spirochete sets the starting point for the control of the proinflammatory output of macrophages, which may be more evident further downstream in the activation process. Whether the sustained exposure of phagocytic cells with *B. burgdorferi* reflects the increased activation of these anti-inflammatory pathways will be the subject of further investigation.

Our results unravel a mechanism involving CD180 to control the response of macrophages to *B. burgdorferi*. CD180 (also known as RP105) is a TLR-like protein that is expressed by B-lymphocytes, macrophages and dendritic cells (59). CD180 is unique in its role in both enhancing and suppressing TLR responses that seem to vary with the cell type (59). CD180 is required for full responsiveness to LPS in B cells (58-60), while it seems to differentially regulate TLR4- and TLR2-induced responses in dendritic cells and macrophages (59). The response to *B. burgdorferi* is more complex than the surface interaction between PAMPs and PRRs and is dependent on the internalization of the spirochete (12). In turn, different phagocytosis pathways lead to proinflammatory responses or the downregulation of the production of cytokines such as TNF (13). Silencing *Cd180* increased *B. burgdorferi* phagocytosis by macrophages while reducing TNF synthesis, suggesting that the TLR molecule modulates the expression of phagocytic receptors. CR3 is a phagocytic receptor that recognizes and phagocytose the spirochete, leading to a decrease in TNF production (13). Similarly, engagement of CR3 during phagocytosis of apoptotic cells downregulates the production and secretion of proinflammatory cytokines (61). Now, we describe a novel functional interaction between CD180 and CR3 upon *B. burgdorferi* recognition. *B. burgdorferi* is able to modulate CD180 expression, which further regulates CR3 expression and subsequent CR3-mediated phagocytosis and cytokine production, providing an

additional mechanism for the regulation of the immune responses triggered by *B. burgdorferi*. This mechanism of inflammation modulation has the advantage of providing an increase phagocytic activity to macrophages (that is required while the presence of spirochetes is still high) while at the same time tempering the induced proinflammatory response.

Overall, our data provide a global view of the intricate response mechanisms associated with the interaction of monocytes/macrophages with *B. burgdorferi*. These data also offer clues to mechanisms of control of the phagocytic and proinflammatory activity of these cells and suggest multiple mechanisms of control that may be relevant at different phases of the response.

5. REFERENCES

1. Nagl M, Kacani L, Mullauer B, Lemberger EM, Stoiber H, Sprinzl GM*, et al.* Phagocytosis and killing of bacteria by professional phagocytes and dendritic cells. *Clin Diagn Lab Immunol* 2002; **9:** 1165-1168.

2. Aderem A. Phagocytosis and the inflammatory response. *J Infect Dis* 2003; **187 Suppl 2:** S340-345.

3. Moretti J, Blander JM. Insights into phagocytosis-coupled activation of pattern recognition receptors and inflammasomes. *Curr Opin Immunol* 2014; **26:** 100-110.

4. Rizzoli A, Hauffe H, Carpi G, Vourc HG, Neteler M, Rosa R. Lyme borreliosis in Europe. *Euro surveillance : bulletin Europeen sur les maladies transmissibles = European communicable disease bulletin* 2011; **16:** 19906.

5. Olson CJ, Fikrig E, Anguita J. Host defenses to spirochetes. In: Rich S, Fleisher, Schoroeder, Weyand and Frew (ed). *Clinical Immunology*, 4th edn. Elsevier2013.

6. Schotthoefer AM, Frost HM. Ecology and Epidemiology of Lyme Borreliosis. *Clin Lab Med* 2015; **35:** 723-743.

7. Kuehn BM. CDC estimates 300,000 US cases of Lyme disease annually. *JAMA* 2013; **310:** 1110.

8. Murray TS, Shapiro ED. Lyme disease. *Clin Lab Med* 2010; **30:** 311-328.

9. Chomel B. Lyme disease. *Rev Sci Tech* 2015; **34:** 569-576.

10. Lelovas P, Dontas I, Bassiakou E, Xanthos T. Cardiac implications of Lyme disease, diagnosis and therapeutic approach. *Int J Cardiol* 2008; **129:** 15-21.

11. Aucott JN, Seifter A, Rebman AW. Probable late lyme disease: a variant manifestation of untreated *Borrelia burgdorferi* infection. *BMC Infect Dis* 2012; **12:** 173.

12. Cervantes JL, Hawley KL, Benjamin SJ, Weinerman B, Luu SM, Salazar JC. Phagosomal TLR signaling upon *Borrelia burgdorferi* infection. *Front Cell Infect Microbiol* 2014; **4:** 55.

13. Hawley KL, Olson CM, Jr., Iglesias-Pedraz JM, Navasa N, Cervantes JL, Caimano MJ*, et al.* CD14 cooperates with complement receptor 3 to mediate MyD88-independent phagocytosis of *Borrelia burgdorferi*. *Proc Natl Acad Sci U S A* 2012; **109:** 1228-1232.

14. Petnicki-Ocwieja T, Chung E, Acosta DI, Ramos LT, Shin OS, Ghosh S*, et al.* TRIF mediates Toll-like receptor 2-dependent inflammatory responses to Borrelia burgdorferi. *Infect Immun* 2013; **81:** 402-410.

15. Hovius JW, Bijlsma MF, van der Windt GJ, Wiersinga WJ, Boukens BJ, Coumou J*, et al.* The urokinase receptor (uPAR) facilitates clearance of *Borrelia burgdorferi*. *PLoS Pathog* 2009; **5:** e1000447.

16. Olson C, Bates T, Izadi H, Radolf J, Huber S, Boyson J*, et al.* Local Production of IFN-gamma by Invariant NKT Cells Modulates Acute Lyme Carditis. *J Immunol* 2009; **182:** 3728-3734.

17. Hawley K, Navasa N, Olson CM, Jr., Bates TC, Garg R, Hedrick MN*, et al.* Macrophage p38 Mitogen-Activated Protein Kinase Activity Regulates Invariant Natural Killer T-Cell Responses During *Borrelia burgdorferi* Infection. *J Infect Dis* 2012; **206:** 283-291.

18. Cervantes JL, Dunham-Ems SM, La Vake CJ, Petzke MM, Sahay B, Sellati TJ*, et al.* Phagosomal signaling by *Borrelia burgdorferi* in human monocytes involves Toll-like receptor (TLR) 2 and TLR8 cooperativity and TLR8-mediated induction of IFN-{beta}. *Proc Natl Acad Sci U S A* 2011; **108:** 3683-3688.

19. Petzke MM, Brooks A, Krupna MA, Mordue D, Schwartz I. Recognition of *Borrelia burgdorferi*, the Lyme disease spirochete, by TLR7 and TLR9 induces a type I IFN response by human immune cells. *J Immunol* 2009; **183:** 5279-5292.

20. Salazar JC, Duhnam-Ems S, La Vake C, Cruz AR, Moore MW, Caimano MJ*, et al.* Activation of human monocytes by live *Borrelia burgdorferi* generates TLR2-dependent and -independent responses which include induction of IFN-beta. *PLoS Pathog* 2009; **5:** e1000444.

21. Cruz AR, Moore MW, La Vake CJ, Eggers CH, Salazar JC, Radolf JD. Phagocytosis of *Borrelia burgdorferi*, the Lyme disease spirochete, potentiates innate immune activation and induces apoptosis in human monocytes. *Infect Immun* 2008; **76:** 56-70.

22. Badawi A. The Potential of Omics Technologies in Lyme Disease Biomarker Discovery and Early Detection. *Infect Dis Ther* 2017; **6:** 85-102.

23. Dunham-Ems SM, Caimano MJ, Pal U, Wolgemuth CW, Eggers CH, Balic A*, et al.* Live imaging reveals a biphasic mode of dissemination of *Borrelia burgdorferi* within ticks. *J Clin Invest* 2009; **119:** 3652-3665.

24. Garcia-Cao I, Song MS, Hobbs RM, Laurent G, Giorgi C, de Boer VC*, et al.* Systemic elevation of PTEN induces a tumor-suppressive metabolic state. *Cell* 2012; **149:** 49-62.

25. Trapnell C, Pachter L, Salzberg SL. TopHat: discovering splice junctions with RNA-Seq. *Bioinformatics* 2009; **25:** 1105-1111.

26. Love MI, Huber W, Anders S. Moderated estimation of fold change and dispersion for RNA-seq data with DESeq2. *Genome Biol* 2014; **15:** 550.

27. Du P, Kibbe WA, Lin SM. lumi: a pipeline for processing Illumina microarray. *Bioinformatics* 2008; **24:** 1547-1548.

28. Ritchie ME, Phipson B, Wu D, Hu Y, Law CW, Shi W*, et al. limma* powers differential expression analyses for RNA-sequencing and microarray studies. *Nucleic Acids Res* 2015; **43:** e47.

29. Yu G, Wang LG, Han Y, He QY. clusterProfiler: an R package for comparing biological themes among gene clusters. *OMICS* 2012; **16:** 284-287.

30. Thomas PD, Campbell MJ, Kejariwal A, Mi H, Karlak B, Daverman R*, et al.* PANTHER: a library of protein families and subfamilies indexed by function. *Genome Res* 2003; **13:** 2129-2141

31. Ashburner M, Ball CA, Blake JA, Botstein D, Butler H, Cherry JM*, et al.* Gene ontology: tool for the unification of biology. The Gene Ontology Consortium. *Nat Genet* 2000; **25:** 25-29.

32. Kanehisa M, Goto S, Kawashima S, Nakaya A. The KEGG databases at GenomeNet. *Nucleic Acids Res* 2002; **30:** 42-46.

33. Wisniewski JR, Zougman A, Nagaraj N, Mann M. Universal sample preparation method for proteome analysis. *Nat Methods* 2009; **6:** 359-362.

34. Henson P. Suppression of macrophage inflammatory responses by PPARs. *Proc Natl Acad Sci U S A* 2003; **100:** 6295-6296.

35. Ricote M, Huang JT, Welch JS, Glass CK. The peroxisome proliferator-activated receptor (PPARgamma) as a regulator of monocyte/macrophage function. *J Leukoc Biol* 1999; **66:** 733-739.

36. Jiang C, Ting AT, Seed B. PPAR-gamma agonists inhibit production of monocyte inflammatory cytokines. *Nature* 1998; **391:** 82-86.

37. Ginhoux F, Jung S. Monocytes and macrophages: developmental pathways and tissue homeostasis. *Nat Rev Immunol* 2014; **14:** 392-404.

38. Patin EC, Orr SJ, Schaible UE. Macrophage Inducible C-Type Lectin As a Multifunctional Player in Immunity. *Front Immunol* 2017; **8:** 861.

39. Shin OS, Isberg RR, Akira S, Uematsu S, Behera AK, Hu LT. Distinct roles for MyD88 and Toll-like receptors 2, 5, and 9 in phagocytosis of *Borrelia burgdorferi* and cytokine induction. *Infect Immun* 2008; **76:** 2341-2351.

40. Yu CH, Micaroni M, Puyskens A, Schultz TE, Yeo JC, Stanley AC*, et al.* RP105 engages phosphatidylinositol 3-kinase p110delta to facilitate the trafficking and secretion of cytokines in macrophages during mycobacterial infection. *J Immunol* 2015; **195:** 3890-3900.

41. Liu B, Zhang N, Liu Z, Fu Y, Feng S, Wang S*, et al.* RP105 involved in activation of mouse macrophages via TLR2 and TLR4 signaling. *Mol Cell Biochem* 2013; **378:** 183-193.

42. Wheelock CE, Goss VM, Balgoma D, Nicholas B, Brandsma J, Skipp PJ*, et al.* Application of 'omics technologies to biomarker discovery in inflammatory lung diseases. *Eur Respir J* 2013; **42:** 802-825.

43. Abu-Asab MS, Chaouchi M, Alesci S, Galli S, Laassri M, Cheema AK*, et al.* Biomarkers in the age of omics: time for a systems biology approach. *OMICS* 2011; **15:** 105-112.

44. Bouquet J, Soloski MJ, Swei A, Cheadle C, Federman S, Billaud JN*, et al.* Longitudinal transcriptome analysis reveals a sustained differential gene expression signature in patients treated for acute Lyme disease. *mBio* 2016; **7:** e00100-00116.

45. Molins CR, Ashton LV, Wormser GP, Hess AM, Delorey MJ, Mahapatra S*, et al.* Development of a metabolic biosignature for detection of early Lyme disease. *Clin Infect Dis* 2015; **60:** 1767-1775.

46. Soloski MJ, Crowder LA, Lahey LJ, Wagner CA, Robinson WH, Aucott JN. Serum inflammatory mediators as markers of human Lyme disease activity. *PLoS One* 2014; **9:** e93243.

47. Gautam A, Dixit S, Philipp MT, Singh SR, Morici LA, Kaushal D*, et al.* Interleukin-10 alters effector functions of multiple genes induced by *Borrelia burgdorferi* in macrophages to regulate Lyme disease inflammation. *Infect Immun* 2011; **79:** 4876-4892.

48. Steevels TA, Meyaard L. Immune inhibitory receptors: essential regulators of phagocyte function. *Eur J Immunol* 2011; **41:** 575-587.

49. Berende A, Oosting M, Kullberg BJ, Netea MG, Joosten LA. Activation of innate host defense mechanisms by *Borrelia*. *Eur Cytokine Netw* 2010; **21:** 7-18.

50. Coleman JL, Benach JL. The urokinase receptor can be induced by *Borrelia burgdorferi* through receptors of the innate immune system. *Infect Immun* 2003; **71:** 5556-5564.

51. Oosting M, Berende A, Sturm P, Ter Hofstede HJ, de Jong DJ, Kanneganti TD*, et al.* Recognition of *Borrelia burgdorferi* by NOD2 is central for the induction of an inflammatory reaction. *J Infect Dis* 2010; **201:** 1849-1858.

52. Radolf JD, Arndt LL, Akins DR, Curetty LL, Levi ME, Shen Y*, et al. Treponema pallidum* and *Borrelia burgdorferi* lipoproteins and synthetic lipopeptides activate monocytes/macrophages. *J Immunol* 1995; **154:** 2866-2877.

53. Brown JP, Zachary JF, Teuscher C, Weis JJ, Wooten RM. Dual role of interleukin-10 in murine Lyme disease: regulation of arthritis severity and host defense. *Infect Immun* 1999; **67:** 5142-5150.

54. Chung Y, Zhang N, Wooten RM. *Borrelia burgdorferi* elicited-IL-10 suppresses the production of inflammatory mediators, phagocytosis, and expression of co-stimulatory receptors by murine macrophages and/or dendritic cells. *PLoS One* 2013; **8:** e84980.

55. Giambartolomei GH, Dennis VA, Lasater BL, Philipp MT. Induction of pro- and anti-inflammatory cytokines by *Borrelia burgdorferi* lipoproteins in monocytes is mediated by CD14. *Infect Immun* 1999; **67:** 140-147.

56. Giambartolomei GH, Dennis VA, Philipp MT. *Borrelia burgdorferi* stimulates the production of interleukin-10 in peripheral blood mononuclear cells from uninfected humans and rhesus monkeys. *Infect Immun* 1998; **66:** 2691-2697.

57. Garcia RC, Murgia R, Cinco M. Complement receptor 3 binds the *Borrelia burgdorferi* outer surface proteins OspA and OspB in an iC3b-independent manner. *Infect Immun* 2005; **73:** 6138-6142.

58. Nagai Y, Shimazu R, Ogata H, Akashi S, Sudo K, Yamasaki H*, et al.* Requirement for MD-1 in cell surface expression of RP105/CD180 and B-cell responsiveness to lipopolysaccharide. *Blood* 2002; **99:** 1699-1705.

59. Schultz TE, Blumenthal A. The RP105/MD-1 complex: molecular signaling mechanisms and pathophysiological implications. *J Leukoc Biol* 2017; **101:** 183-192.

60. Ogata H, Su I, Miyake K, Nagai Y, Akashi S, Mecklenbrauker I*, et al.* The toll-like receptor protein RP105 regulates lipopolysaccharide signaling in B cells. *J Exp Med* 2000; **192:** 23-29.

61. Chung EY, Kim SJ, Ma XJ. Regulation of cytokine production during phagocytosis of apoptotic cells. *Cell Res* 2006; **16:** 154-161.

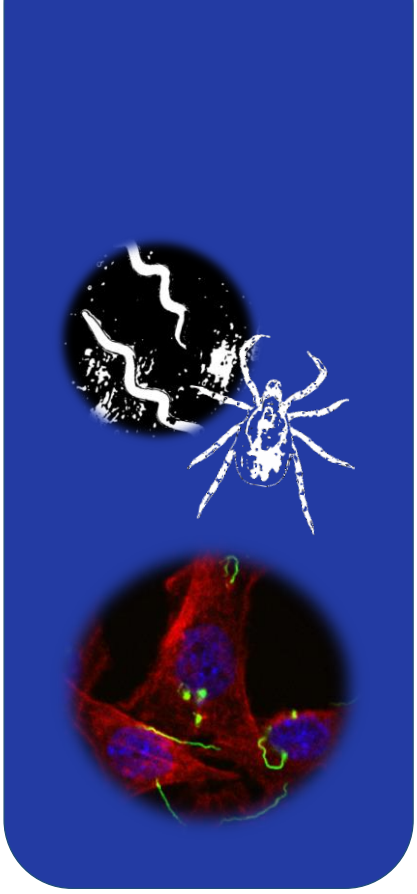

Chapter 3

Regulation of macrophage activity by *Borrelia burgdorferi*-regulated surface receptors

Results submitted for publication:

Carreras-González, A. et al., (2019) Regulation of macrophage activity by surface receptors contained within *Borrelia burgdorferi*-enriched phagosomal fractions. *Submitted for publication*.

1. INTRODUCTION

Innate immune responses, including those by macrophages and neutrophils, not only constitute the first line of defense against the spirochete but also seem to play a critical role once the spirochete has disseminated to distant organs (9). Phagocytosis ensures the degradation of the pathogen and results in the induction of signaling events leading to the generation of pro-inflammatory cytokines and antigen presentation, which leads to the stimulation of adaptive immunity. In spite of its importance, there are large gaps in our understanding of the receptors involved in the process. While a few surface receptors have been nominally associated with the internalization of the spirochete, such as uPAR (10) or MARCO (11), the only *bona fide* phagocytic receptor described for *B. burgdorfei* is composed of the surface proteins Complement Receptor (CR) 3 and CD14 (12-14). A large proportion of phagocytosis of *B. burgdorferi* depends on signals emanating from MyD88. However, the receptors associated with this pathway are currently unknown. MyD88-induced signals are required, however, for the *B. burgdorferi*-induced upregulation of MARCO (11). In contrast, CR3/CD14-mediated phagocytosis is independent of MyD88-induced signals and results in the downmodulation of the proinflammatory responses (14). In fact, the repression of CR3 surface expression by the TLR family member, CD180, results in the effective modulation of both phagocytosis and proinflammatory responses (15). Other signaling pathways have been described to be involved in the internalization of *B. burgdorferi*, including Syk activation elicited by MARCO (16).

A wide array of surface receptors is involved in the phagocytic internalization of microorganisms, including integrins, C-type lectins, scavenger receptors or siglecs (17-19). In the presence of opsonins (complement-derived products and antibodies), phagocytosis can also occur through specific receptors. However, both complement (20) and Fc receptors (21) have been shown to mediate the internalization or cell invasion of pathogens in the absence of opsonins, including enteropathogenic *E. coli* (22), a process that requires the high affinity Fc receptor, CD64. For each particular pathogen, its interaction with phagocytic cells is likely to be complex and involve several independent interactions. These, in turn, would likely result in the initiation of several signaling pathways that converge and provide a specific cellular output. In the case of *B. burgdorferi*, we have previously demonstrated in the Chapter 2 that the response of macrophages to the spirochete is dependent on multiple

signaling pathways (15) indicating that the array of receptors that trigger these responses is more complex than those already described.

In the previous chapter we identified a group of surface receptors that are involved in both the internalization and the induction of cytokines by *B. burgdorferi*. In this Chapter we ought to define a set of receptors that modulate the uptake and/or proinflammatory cytokine production of macrophages in response to *B. burgdorferi* by the analysis of the proteome of phagosome-enriched fractions containing the spirochete plus the use of multi-omic data previously generated.

2. MATERIALS AND METHODS

2.1 Mice

C57Bl/6 (B6) mice were purchased from Charles River Laboratories (Barcelona, Spain) and bred at CIC bioGUNE. CD64-deficient mice (C.129P2-Fcgr1^{tm1Sjv}/Cnrm), in a B6 background (23) were obtained from Dr. J. S. Verbeek and bred at CIC bioGUNE. All work performed with animals was approved by the competent authority (Diputación de Bizkaia) following European and Spanish directives. CIC bioGUNE's Animal Facility is accredited by AAALAC Intl.

2.2 Bacteria

B. burgdorferi wild type 297, Bb914, B31 clone 5A15 and BB0167-deficient clone 5A15 strains were used for cell stimulations. Bb914 constitutively expresses a GFP cassette stably inserted into cp26 (24). Bacteria were grown in 5 ml tubes at 34 °C in BSK-H medium (Sigma Aldrich, Madrid, Spain) for 3-5 days. BB0167 deficient *B. burgdorferi* were obtained from Steven J. Norris (Department of Pathology and Laboratory Medicine, Houston, Texas).

2.3 Cell culture

RAW 264.7 cells were maintained in DMEM (Lonza, Barcelona, Spain) supplemented with 10% FCS and 1% penicillin–streptomycin (Thermo Fisher Scientific, Alcobendas, Madrid, Spain). CHO cells stably transfected with plasmids containing human Fcγ Receptor I Alpha (FcgRI, CD64) were generated using full open reading frames under the CMV promoter (Origene, Herford, Germany). The cells were maintained in Ham's F-12 medium (Sigma Aldrich) supplemented with 10% FCS and 1% penicillin–streptomycin. Bone marrow-derived macrophages (BMMs) were generated from 8–12-week-old C57Bl/6 (B6) mice as described (25). Bone marrow cells were collected from the femoral shafts and incubated in 100 mm x 15 mm Petri dishes (Thermo Fisher Scientific) for 6 days in DMEM supplemented with 10% FCS and 10% penicillin–streptomycin plus 30 ng/ml of M-CSF (Miltenyi Biotec, Bergisch Gladbach, GE). Following incubation, non-adherent cells were eliminated, and adherent macrophages were scraped, counted and seeded in 6-well tissue-culture plates for stimulation at a density of 10^6 cells per ml. Macrophages were allowed to rest overnight prior to stimulation.

Inhibition of Syk kinases was achieved using Piceatannol (26) (30 µM; Sigma Aldrich) one hour prior to the addition of *B. burgdorferi*.

Lentiviral particles containing shRNA targeting different receptors (Mission shRNA, Sigma Aldrich) (Table 1) were produced as previously described (27). Supernatants containing the virus were used to infect RAW 264.7 cells, followed by selection with puromycin at a concentration of 3 µg/ml to generate stable lines. Cell lines infected with the empty vector, pLK0.1, were used as controls. Gene silencing in BMMs was achieved by lentivirus addition at days 3 and 6 of the differentiation process.

The silencing of the genes was tested either by surface staining or qRT-PCR. Total RNA was purified by Trizol extraction and reverse transcribed with the M-MLV Kit (Thermo Fisher Scientific). Real-time PCRs were performed using perfeCTa SYBR Green SuperMix Low ROX (Quantabio, Beverly, MA) on a QuantStudio 6 real-time PCR System (Thermo Fisher Scientific). The mRNA relative quantification was calculated using the ΔΔCt method. PCR efficiency was always between 90 and 110%.

The primers used are listed in Table 2.

Human monocytes were purified from buffy coats of healthy blood donors by positive selection using a human CD14 purification kit (Miltenyi Biotec), as described (15). To obtain macrophages, purified human monocytes were incubated for 8 days in RPMI 1640 medium (Lonza) supplemented with 10% FCS, 2.4 mM L-glutamine, 10% penicillin-streptomycin and 30 ng/ml of human M-CSF (Miltenyi Biotec). The cells were rested overnight before stimulation. Blocking of human Fcγ Receptor I Alpha was performed by incubation of human monocyte-derived macrophages (hMAC) with 2 µg/ml of anti-human CD64 (Antibodies.com, Cambridge, UK) one hour prior to the addition of *B. burgdorferi*. All human samples were obtained after approval by the Basque Country's Ethics committee following the Helsinki convention. Donors signed an informed consent form and were anonymized to the authors.

Table 1 sh*RNA*s used.

Gene	Gene Bank Accession Nº	Mission shRNA catalogue Nº
Fcer1g	NM_010185.4	TRCN0000067588
Fcgr1	NM_010186.5	TRCN0000067678
Ptprc	NM_011210.4	TRCN0000029929
Inpp5d	NM_010566.3	TRCN0000436483
Clec4a3	NM_153197.2	TRCN0000109845
Clec4b1	NM_027218.2	TRCN0000436087
Clec4d	NM_010819.4	TRCN0000304453
Clec4n	NM_020001.2	TRCN0000066787
Clec10a	NM_010796.3	TRCN0000067028
Clec12a	NM_177686.4	TRCN0000249250
Cd302	NM_025422.4	TRCN0000176008
Ly75	NM_013825.3	TRCN0000375342
Stab1	NM_138672.2	TRCN0000215721
Stab2	NM_138673.3	TRCN0000109510
Marco	NM_010766.3	TRCN0000424243
Msr1	NM_031195.2	TRCN0000431188
Siglec5	NM_145581.2	TRCN0000094304
Cd33	NM_021293.1	TRCN0000094368
Siglec1	NM_011426.1	TRCN0000094864
Cd52	NM_013706.2	TRCN0000077003
Ly6e	NM_008529.2	TRCN0000101140
Cd59a	NM_007652.5	TRCN0000329358
Cd24a	NM_009846.2	TRCN0000332785
Plaur	NM_011113.3	TRCN0000362760

Table 2 Primers used. All primers were used at an annealing temperature of 60 ºC, except for *Plaur* (58 ºC).

Gene	Primers	Gene	Primers
Ptprc	5'-GATCCACTGCTGGGCTTCA-3' 5'-GAACATGCTGCCAATGGTTCT-3'	*Stab2*	5'-GCTGCAAGTCCTCATGTCCT-3' 5'-TTCTGTGGCACAAACAGGGT-3'
Inpp5d	5'-CCAGGGCAAGATGAGGGAGA-3' 5'-GGACCTCGGTTGGCAATGTA-3'	*Marco*	5'-TTAGCAGCTATGGAGGTGGC-3' 5'-GACACACTGATGACCTCTCGG-3'
Clec4a3	5'-GGGCAACAGCTCCAGACTT-3' 5'-TCTTATTCTCCGGTGCTCTGA-3'	*Msr1*	5'-ACCTCCTGTTGCTTTGCTGT-3' 5'-ACACGGAACGCTTCCAGAAT-3'
Clec4b1	5'-GGAACCAAGTAGCAGTGGGA-3' 5'-CCTCAGCACCTGTTTCATTG-3'	*Siglec5*	5'-TGTGCGTCTTTGTAGCCTGC-3' 5'-CACTGGAGAGCCGCTGAAT-3'
Clec4d	5'-GGAAAGTCATTCCAGACCCA-3' 5'-AAGACGCCATTTAACCCACA-3'	*Cd33*	5'-CAGAGCCCAAGAATCAGGAG-3' 5'-CCTTCTCTGGAGCAGGTGTC-3'
Clec4n	5'-AGAAGATTTACCTATGAGTGCCTGT-3' 5'-GGCTAGGAAAAGAACGGCCT-3'	*Siglec1*	5'-GTCTCCAGGAAGGTGGTCAG-3' 5'-CAGGGCTGATACTGGCTTCT-3'
Clec10a	5'-AACCTTCCGCTGGATCTGTG-3' 5'-GTTGAGACCGGGTAGGAGGA-3'	*Cd52*	5'-GGTGGAGGTGCTGTTTTTGT-3' 5'-GCCCAGGAAGATTTCAGGAT-3'
Clec12a	5'-GCAAAGGGCCAAGGAAGAAC-3' 5'-TATACAGCTCTCGGCACAGC-3'	*Ly6e*	5'-TCAGGGAATGAACTTGCTCC-3' 5'-TCGGTATTATCTTCGGGGC-3'
Cd302	5'-ATCCAGGATGGTTCCTGTTCTG-3' 5'-ACTTGCCACAAAAACTGAGCC-3'	*Cd59a*	5'-GGAATGCAAGTGTATCAAAGGTGT-3' 5'-CCCCAAGGATCCGTCACTTT-3'
Ly75	5'-GATAAGGCTGGGCACAAAGG-3' 5'-CTGTGACTCCACCGTCATGC-3'	*Cd24a*	5'-CCCCAAATGGCAACCACAAG-3' 5'-TCAAACCTTTCACGCGTCCT-3'
Stab1	5'-AGTTGCCTCCTGATAGCTGC-3' 5'-CCCTCCTTCTGCTCTGTGTC-3'	*Plaur*	5'-AGCTCTGGTCCAAAGAGGTG-3' 5'-CCATGATCATCAGCCTGACA-3'

2.4 Phagocytosis assays

Phagocytosis assays were performed as previously described (14). Experiments were performed in DMEM medium without serum or antibiotics. The day before the assay, the cells were seeded at a density of 3×10^5 cells per ml in complete DMEM media. After 16 h, the cell medium was changed to DMEM without supplements and the cells were rested for 1 h. GFP expressing *B. burgdorferi* were then added to the cells at a multiplicity of infection (m.o.i.) of 25 and incubated at 4 °C for 15 min followed by 37 °C for 2 h. The cells were then washed to eliminate surface bacteria and analyzed by flow cytometry in a BD FACS Canto II cytometer (BD Biosciences, San Agustín de Guadalix, Madrid, Spain). The data were analyzed using FlowJo for Mac, version 10.5.3 (FlowJo, Ashland, OR). The phagocytic index was calculated following the formula: %GFP cells (Test) x MFI (Test) - %GFP cells (4 ºC control) x MFI (4 ºC control) (10).

2.5 Confocal microscopy

Following incubation of CHO cells with *B. burgdorferi*-GFP 297 at 37 ºC, the cells were washed with PBS, fixed with 4% paraformaldehyde for 20 min, permeabilized with PBS containing 0,3% Triton X-100 (VWR, Llinars del Vallés, Barcelona, Spain) and stained with rhodamine phalloidin and DAPI for 10 min at 37 ºC (Thermo Fisher Scientific) (1:300). After extensive washing in PBS, the cells were mounted using the Prolong Gold Antifade mounting reagent (Thermo Fisher Scientific). The images were obtained employing a Leica TCS SP8 confocal system (Leica Microsystems, Madrid, Spain).

2.6 Phagosome purification

Isolation of *B. burgdorferi*-containing phagosomes was performed as previously described (28). Twenty million BMMs were stimulated with *B. burgdorferi*-GFP at an m.o.i. of 50 for 2h. The cells were washed twice with PBS, scraped and centrifuged. The cell pellet was resuspended in 1 ml of homogenization buffer (20mM HEPES, 0.5mM EGTA, 8.5% sucrose plus a protease inhibitor cocktail (Sigma-Aldrich) and lysed by passage through a 27 G needle until at least a 70% of breakage was observed. Cell debris and nuclei were removed by centrifugation at 500 x *g* and treated with DNAse I. The supernatant was layered on top of a discontinuous sucrose gradient (50%, 45%, 40%, 35%, 32%, 15%) and centrifuged at 100,000 x *g* for 1h at 4 ºC. One ml fractions were collected from the top and

centrifuged in 20 ml of homogenization buffer without sucrose at 110,000 x *g* for 1 h at 4 ºC. Each pellet was then resuspended in 100 µl of homogenization buffer without sucrose and analyzed.

For *B. burgdorferi*-containing phagosome purification from hMAC, we followed a protocol from Vinet and Descoteaux (29) with some modifications. The nuclei-free phagosome sample was mixed with an equal volume of 50% sucrose, placed in the sucrose gradient between the 15% and 40% sucrose layers, added an 8.5% sucrose layer, centrifuged at 100,000 x *g* for 1 h and the fractions recovered from the top to the bottom, as before.

2.7 Immunoblotting

Ten µl of each gradient fraction was loaded onto a 4-20% Bis-Tris protein gel (Thermo Fisher Scientific). The separated proteins were then transferred to nitrocellulose membranes and blocked with TBST-5% milk for 1h. The membranes were then incubated with the primary antibody followed by HRP-labeled secondary antibodies, and developed with ECL substrate (Bio-Rad, Alcobendas, Madrid). The following antibodies were used: Anti-human CD64 (Antibodies.com; 1:2000), anti-GFP (Roche, Madrid, Spain; 1:1000), anti-human CD11b (clone 23F-12; Santa Cruz Biotechnology, Heidelberg, Germany; 1:200), anti-mouse CD11b (clone M-19; Santa Cruz Biotechnology; 1:1000), anti-human LAMP1 (clone H4A3; Developmental Studies Hybridoma Bank, University of Iowa, Iowa City, IA; 1:500), anti-mouse LAMP2 (clone GL2A7; Abcam, Cambridge, UK; 1:1000), anti-mouse FcγR (Merk, Tres Cantos, Madrid, Spain; 1:1000), anti-human and mouse MyD88 (clone HFL-296; Santa Cruz Biotechnology; 1:1000), anti-mouse CD14 (clone M-305; Santa Cruz Biotechnology).

For CD64 ligand aproaches*, B. burgdorferi* B31 or BB0167-deficient *B. burgdorferi* were collected, washed and resuspended in PBS. Bacteria lysis was perform by 3 cycles of 30s of sonication pulses. 30µg of Bacteria lysate was loaded onto a 4-20% Bis-Tris protein gel (Thermo Fisher Scientific). The separated proteins were then transferred to nitrocellulose membranes and blocked with TBST-5% milk for 1h. The membranes were then incubated with the primary antibody followed by HRP-labeled secondary antibodies, and developed with ECL substrate (Bio-Rad, Alcobendas, Madrid). The antibodies used were anti-BB0167 mouse serum (1:100) and anti-mouse IgG-HRP.

2.8 Proteomic analysis

***In solution digestion*:** Phagosome-enriched proteins were extracted using 7M urea, 2M thiourea and 4% CHAPS. Samples were incubated for 30 min at RT under agitation and digested following the filter-aided FASP protocol described by Wisniewski et al (30) with minor modifications. Trypsin was added to a trypsin:protein ratio of 1:10, and the mixture was incubated overnight at 37 ºC, dried in an RVC2 25 speedvac concentrator (Christ, Osterode am Harz, Germany), and resuspended in 0.1% Formic Acid.

***Mass spectrometry analysis*:** The samples were submitted to LC-MS label-free analysis using two different platforms. First, peptide separation was performed on a nanoACQUITY UPLC System (Waters, Cerdanyola del Vallés, Barcelona, Spain) connected on-line to an LTQ Orbitrap XL mass spectrometer (Thermo Fisher Scientific) using the same parameters described before (15). In addition, the samples were analyzed in a hybrid trapped ion mobility spectrometry – quadrupole time of flight mass spectrometer (timsTOF Pro with PASEF, Bruker, Rivas Vaciamadrid, Madrid, Spain) coupled online to a nanoElute liquid chromatograph (Bruker). This mass spectrometer takes advantage of a scan mode termed parallel accumulation – serial fragmentation (PASEF), which multiplies the sequencing speed without any loss in sensitivity (31) and has been proven to provide outstanding analytical speed and sensibility for proteomics analyses (32). The samples (200 ng) were directly loaded in a 25 cm, 75 µm ID Odyssey C18 nano column with an integrated emitter (IonOpticks, Parkville, Victoria, Australia) and resolved at 400 nl/min with a 90 min gradient. The column was heated to 50 ºC using an oven.

Searches were carried out using the Mascot search engine (Matrix Science, London, UK) through Proteome Discoverer software 1.4 (Thermo Fisher Scientific). Orbitrap RAW files were directly loaded into the program, whereas mgf files generated by DataAnalysis software (Bruker) were used for timsTOF searches. Orbi searches were carried out with precursor and fragment tolerances of 10 ppm and 0.5 Da, whereas 50 ppm and 0.05 Da were used for TIMS TOF runs. A database consisting of human (Uniprot/Swissprot) and *Borrelia burgdorferi* (Uniprot/Swissprot and Uniprot/TrEMBL) entries (2018_10 release) was used for the searches. Only proteins identified with an FDR < 1% were considered. Spectral counts for each protein (the number of identified spectra matching to peptides from that protein, also named SpC or PSMs) were normalized against protein length. Then, these

values were converted to Normalized Spectral Abundance Factor (NSAF) values by normalizing them against the sum of normalized spectral counts in each of the runs.

2.9 TNF ELISA

The levels of TNF produced by *B. burgdorferi* stimulation were determined by capture ELISA using the DuoSet II kit (R&D Systems, Minneapolis, MN) according to the manufacturer's recommendations.

2.10 Statistical analysis

The results are presented as the means ± SE (standard error). Significant differences between means were calculated with the Student's t test. A p value < 0.05 was considered significant.

2.11 Data availability

The mass spectrometry proteomics data have been deposited to the ProteomeXchange Consortium via the PRIDE (39) partner repository with the dataset identifier PXD012854. All relevant data are within the manuscript and its Supporting Information files.

2.12 Protein expression and purification

His-tagged extracellular region of BB0167 was purchased from DNAsu, Arizona, in the pMCSG7 plasmid. The plasmid was transformed and expressed in *E. coli* BL21 (DE3) as described before (44), except that overnight autoinduction media of Studier was used (45).

BB0167 extracellular peptide sequence:
AIEVEKNNKGINLSFDIEFYPNSFQILQKEYKKIDLIAKLLEKFKKNNILIEGHTEQFGLEEEMHELSEKRARAI
GNYLIKMKVKDKDQILFKGWGSQKPKYPKSSPLKAKNRRVEITILNN

Cells were lysed with hen-egg lysozyme and sonicated in 50 mM Tris-HCl (pH 8.0) buffer, NaCl was added at a final concentration of 500 mM, and cell debris was removed by centrifugation. The supernatant was loaded onto an immobilized metal affinity chromatography column (Histrap HP, Amersham Biosciences) equilibrated in 50 mM HEPES (pH 8.0) containing 500 mM NaCl. The column was washed with 50 mM HEPES (pH 8.0) containing 500 mM NaCl and 20 mM imidazole, and then the protein was eluted with 50

mM HEPES (pH 8.0) containing 500 mM imidazole. The protein was cleaved with thrombin (Novagen) to remove the N-terminal His-tag. The solution was dialyzed against 20 mM sodium acetate buffer (pH 4.6) and purified by cation-exchange chromatography (Resource S, Amersham Biosciences) using a linear gradient of NaCl.

Purified BB0167 was labelled with Alexa Fluor 488 protein labelling kit (Life technologies), following the manufacturer's recommendations.

2.13 *In vivo* experiments

Six to 8 week old B6 or CD64-deficient mice (C.129P2-Fcgr1^{tm1Sjv}/Cnrm), in a B6 background were infected with 10^5 *B. burgdorferi* B31 or BB0167-deficient *B. burgdorferi*, subcutaneously, as described (43). The mice were sacrificed 3 weeks post infection. The hearts were cut in half through bisections across the atria and ventricles to isolate DNA using the AllPrep DNA/RNA/miRNA Universal Kit (QIAGEN) following the manufacturer's recommendations.

Real-time PCRs were performed using perfeCTa SYBR Green SuperMix Low ROX (Quantabio, Beverly, MA) on a QuantStudio 6 real-time PCR System (Thermo Fisher Scientific). The DNA relative quantification was calculated using the ΔΔCt method. Bacterial burdens were measured from heart DNA by qPCR targeting *recA* relative to the murine gene, *Rpl19.*

3. RESULTS

3.1 Isolation and characterization of *B. burgdorferi*-containing, phagosome-enriched fractions.

In order to characterize the protein content of cellular fractions enriched in *B. burgdorferi*-containing phagosomes, we purified protein extracts of bone marrow-derived macrophages that had been exposed to GFP-containing spirochetes for 2 h by sucrose gradient centrifugation. Immunoblotting analysis showed, as expected (13), the presence of CD11b and CD14 in the LAMP-2-enriched fractions. These fractions were also positive for GFP (Figure 1A). Similar results were obtained when analyzing human monocyte-derived macrophages (Figure 1B). Further analysis showed the presence of MyD88 in the LAMP1-enriched fractions (Figure 1B). We therefore hypothesized that these fractions would contain *B. burgdorferi* phagosomes. We determined the proteomic composition of fractions 4, 6 and 8 of the hMac sucrose gradient preparation (Figure 1B). The identification of several borrelial proteins in these fractions confirmed the presence of phagosomes (Figure 1C). In fact, as observed in the immunoblots, the number of spirochetal proteins detected correlated with the level of degradation of *B. burgdorferi* (23 proteins in fraction 4, 50 in fraction 6 and 156 in fraction 8, representing normalized spectral abundance factors -NSAF- of 0.7, 2.4 and 6.7, respectively). This suggested that the differential buoyancy of the *B. burgdorferi*-containing fractions is related to the level of maturation of the phagosome/phagolysosome. A total of 2514 proteins were identified in fractions 4, 6 and 8, of which 961 were shared proteins (Figure 1D). Among the identified proteins, we determined the presence of the two components of the phagocytic receptor for *B. burgdorferi*, CR3 (ITGAM and ITGB2), as well as CD14, which were present in all fractions, confirming a major role for CR3/CD14 in the phagocytosis of *B. burgdorferi* (14). Of note, both TLR2 and TLR8 were present in the three fractions analyzed, while fraction 4 also contained TLR6 and TLR5. The TLR family member CD180, which regulates the phagocytosis of *B. burgdorferi* (15) was also present in the three fractions analyzed (Table 3). Analysis of the proteins identified showed the enrichment of components related to phagosome, endocytosis or antigen processing and presentation, particularly in fraction 6 and the pool of common proteins among the three fractions analyzed (Figure 1E). Surprisingly, 27 identified proteins common to the three fractions belonged to Fc gamma R-mediated phagocytosis

(Figure 1E). Since the phagocytosis assays were performed in the absence of serum, and therefore antibodies, these results suggest a role for this pathway in the internalization of opsonin (antibody)-free spirochetes.

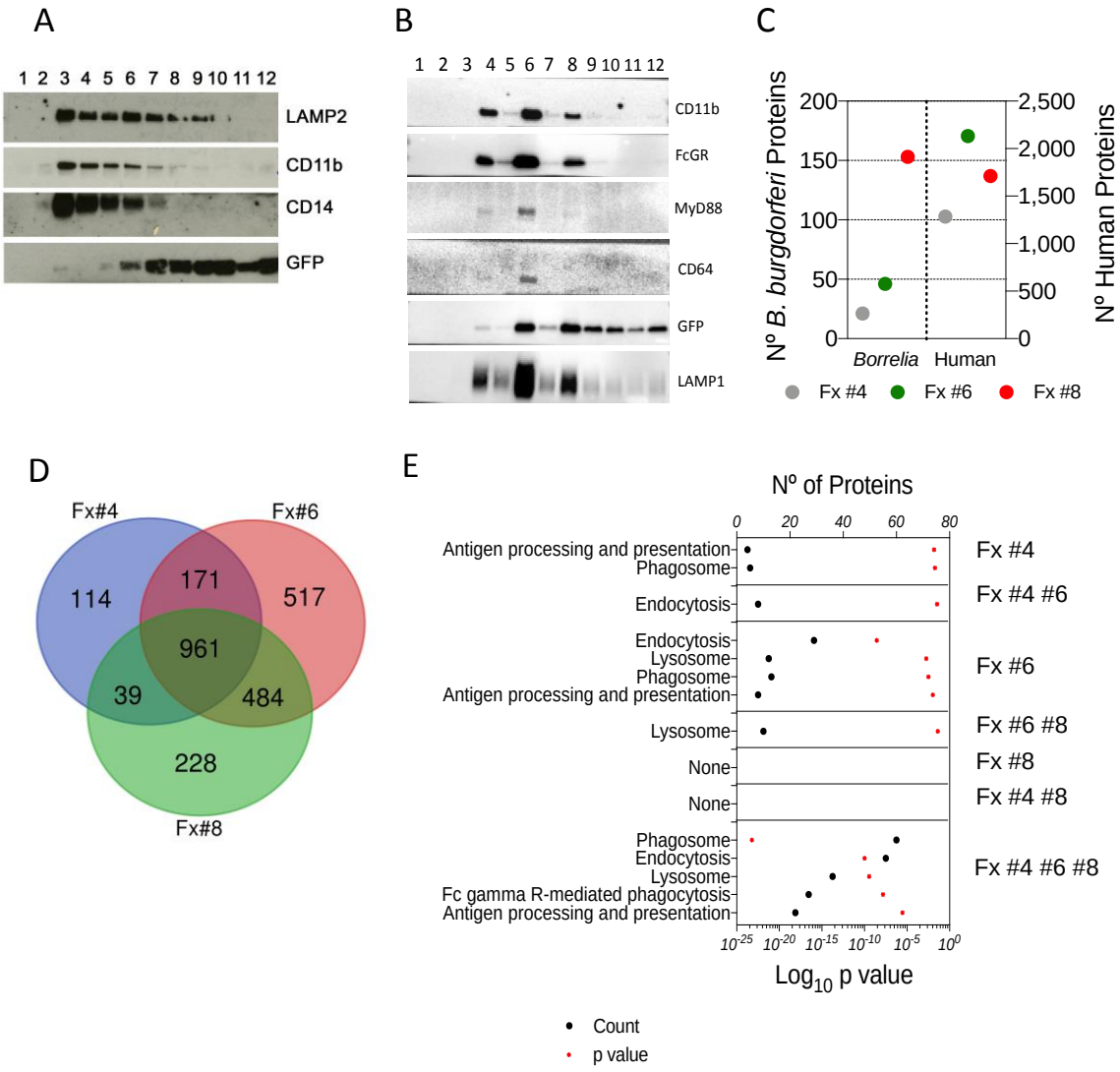

Figure 1 Proteomic characterization of B. *burgdorferi*-containing, phagosome-enriched fractions. Immunoblot analysis of *B. burgdorferi*-containing phagosome enriched sucrose fractions from murine BMMs (A) and human monocyte-derived macrophages (B). The numbers at the top indicate the number of fraction collected from the top. (C) Number of B. burgdorferi and human proteins contained in phagosome-enriched fractions 4, 6 and 8. (D) Venn diagram showing the overlap in protein composition of hMac phagosome-enriched fractions 4, 6 and 8. A total of 2514 proteins were identified in all 3 fractions, with 961 shared proteins. (E) KEGG pathway analysis of the proteins identified in each fraction. The proteins analyzed correspond to those proteins represented only in each individual fraction, those shared by 2 fractions and the 961 common proteins found in all 3, as in Fig. 1D.

Table 3 Identification of components of phagocytosis and TLRs in phagosome-containing fractions of human monocyte derived macrophages. ND, not detected

Uniprot	Description	Fraction #	Σ Coverage	Σ# Proteins	Σ# Unique Peptides	Σ# Peptides	Σ# PSMs	SAF	NSAF
ITAM_HUMAN	Integrin alpha-M	4	16.49	1	14	15	41	0.3226	0.1322
		6	23.78	1	21	22	57	0.4485	0.0746
		8	17.71	1	15	16	43	0.3383	0.0707
ITB2_HUMAN	Integrin beta-2	4	37.58	1	24	25	83	0.9796	0.4016
		6	44.47	1	26	27	125	1.4753	0.2455
		8	40.96	1	26	27	96	1.1331	0.2368
CD14_HUMAN	Monocyte differentiation antigen CD14	4	22.40	1	8	8	32	0.7990	0.3275
		6	32.80	1	10	10	67	1.6729	0.2784
		8	32.80	1	10	10	47	1.1735	0.2452
TLR2_HUMAN	Toll-like receptor 2	4	13.65	1	10	10	32	0.3564	0.1461
		6	24.74	1	15	15	58	0.6460	0.1075
		8	14.80	1	10	10	33	0.3676	0.0768
TLR8_HUMAN	Toll-like receptor 8	4	3.94	1	4	4	4	0.0334	0.0137
		6	8.74	1	9	9	14	0.1169	0.0195

		8	7.01	1	7	7	9	0.0752	0.0157
TLR6_HUMAN	Toll-like receptor 6	4	1.63	1	1	1	2	0.0218	0.0089
		6	ND	ND	ND	ND	ND	ND	ND
		8	ND	ND	ND	ND	ND	ND	ND
TLR5_HUMAN	Toll-like receptor 5	4	0.93	1	1	1	1	0.0102	0.0042
		6	ND	ND	ND	ND	ND	ND	ND
		8	ND	ND	ND	ND	ND	ND	ND
CD180_HUMAN	CD180 Antigen	4	2.42	1	1	1	1	0.0135	0.0055
		6	8.47	1	4	4	7	0.0944	0.0157
		8	2.42	1	1	1	2	0.0270	0.0056

3.2 The analysis of the *B. burgdorferi*-induced transcriptome reveals the regulation of several putative phagocytic receptors.

We have recently described the regulation of macrophage surface receptors in response to the stimulation with *B. burgdorferi* that modulate both the capacity of these cells to phagocytose the spirochete and the ensuing inflammatory response (15). *B. burgdorferi* induces the downregulation of CD180, leading to increased expression of CR3, augmented phagocytosis and reduced pro-inflammatory cytokine production (15). On the other hand, the C-type lectin receptor, MINCL, did not influence either phagocytosis of, or TNF production in response to *B. burgdorferi*. In order to identify additional surface receptors that modulate either aspect of the macrophage response, we further analyzed the multi-omic murine and human data previously reported (15). Table 4 shows the comparative transcriptomic analysis of several members of different classes of receptors that may be involved in the response of monocytes/macrophages to *B. burgdorferi*. We analyzed the regulation of C-type lectins, GPI anchored proteins, Scavenger receptors, Siglecs and Fc receptors. Several receptors belonging to these families where regulated by the stimulation with *B. burgdorferi* (Table 4). The validation by flow cytometry of the surface upregulation of these receptors is presented in Figure 2. Importantly, several of these receptors were found in the phagosome-enriched fractions (Table 4), further suggesting a role in the interaction of macrophages and the spirochete.

3.3 Silencing of the potential receptors in RAW 264.7 shows their implication in *Borrelia burgdorferi* phagocytosis and the inflammatory response.

We next evaluated the role of several of the receptors identified in the response to *B. burgdorferi* by overexpression of specific shRNAs in RAW 264.7 cells (Figure 3). Stable cell lines established after selection of lentivirally infected RAW 264.7 cells were first analyzed for their phagocytic activity compared to vector-transduced controls. The results are presented in Figures 5-8 and summarized in Figure 4A. Of the receptors analyzed, several (CLEC4A3, CLEC13B, CLEC12A, CD52 and SIGLEC1) did not affect the phagocytosis of *B. burgdorferi* (Figure 4A**,** 5-8). Silencing of CLEC4N (Dectin 2), STABILIN 2, MARCO, CLEC13A, uPAR, CLEC4B1 or CD33 however, caused a diminished uptake of *B. burgdorferi* by RAW 264.7 cells to different extents (Figure 4A**,** 5-8). These included receptors previously shown

to be involved in the internalization of the spirochete, such as MARCO (11) and uPAR (10). On the other hand, silencing of CLEC10A, STABILIN1, LY6E, CLEC4D, MSR1, CD24A, CD59A or SIGLEC5 resulted in the increased ability of the cells to internalize the spirochete (Figure 4A**,** 5-8).

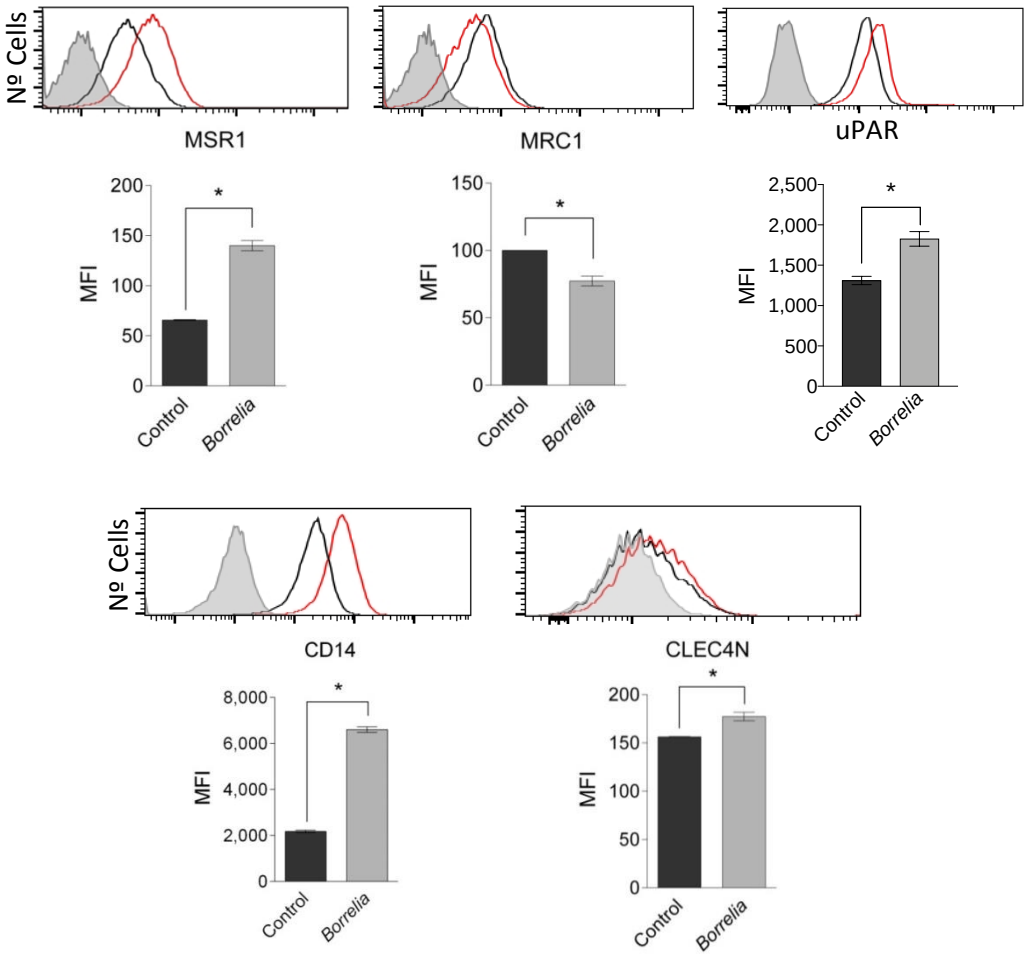

Figure 2 Validation of the transcriptomic analysis of BMM receptors involved in the response to *B. burgdorferi.* Flow cytometry analysis of receptors after 16 h stimulation with *B. burgdorferi* (red histogram / grey bar) or non-treated controls (black histogram / black bar). The gray histogram represents the 4 °C control.

Table 4 Regulation of surface receptors by stimulation of BMMs and hMon with *B. burgdorferi*, as reported (15). The last column indicates the identification of this receptors in phagosome-enriched fractions of hMACs stimulated with the spirochete. WB: immunoblotting, NP, not present.

RNAseq BMM	Fold Change	p Value	Proteomics BMM	Fold Change	Anova (p)	µARRAY hMon	Fold Change	p Value	Phagosome
FcgR asocciated									
Fcer1g	1.03	8.40E-01	FCERG	0.91	8.39E-01	*FCER1G*	2.15	1.23E-04	YES
Fcgr1	1.25	4.92E-01	FCGR1A	0.62	3.79E-02	*FCGR1A*	0.60	1.15E-03	YES (WB)
NP			FCGR2	4.63	7.22E-03	*FCGR2A*	3.72	7.15E-05	YES
Fcgr2b	6.54	2.48E-23	NP			*FCGR2B*	1.54	1.19E-01	YES
Ptprc	0,82	8.54E-02	PTPRC	0.73	2.23E-01	*PTPRC*	0.83	8.94E-03	YES
Syk	1.49	6.54E-24	KSYK	1.18	2.61E-01	*SYK*	0.87	1.06E-01	YES
Inpp5d	0.61	1.03E-08	SHIP1	0.74	2.81E-01	*INPP5D*	0.38	3.49E-06	YES
C-type lectins									
Clec1a	0.09	1.26E-03	NP			*CLEC1A*	0.84	1.72E-02	NO
Clec4a3	0.50	1.89E-03	NP			*CLEC4A*	1.90	2.27E-04	YES
Clec4b1	2.95	5.05E-06	NP			NP			NO
Clec4d	3.79	8.21E-09	NP			*CLEC4D*	1.01	9.64E-01	NO

Clec4e	35.67	9.73E-08	CLC4E	7.50	6.38E-04	*CLEC4E*	2.26	2,.24E-05	NO
Clec4n	27.08	7.15E-33	NP			*CLEC4N*	1.02	8.01E-01	NO
Clec5a	1.95	9.87E-03	NP			*CLEC5A*	2.80	6.97E-06	YES
Clec7a	0.15	1.84E-38	NP			*CLEC7A*	0.71	4.31E-04	YES
Clec10a	0.34	2.29E-03	NP			*CLEC10A*	0.57	3.84E-03	NO
Clec12a	0.11	3.46E-155	NP			*CLEC12A*	2.50	6.01E-03	NO
Cd302 (Clec13a)	4.47	1.36E-08	NP			*CD302*	0.26	1.36E-04	YES
Ly75 (Clec13b)	7.73	9.11E-06	NP			NP			YES
Mrc1	0.11	4.95E-27	MRC1	0.77	5.33E-01				YES
Scavenger receptors									
Stab1	0.45	7.75E-09	NP			*STAB1*	0.27	1.56E+05	YES
Stab2	0.13	2.35E-04	NP			NP			NO
Marco	2.00	4.87E-01	NP			*MARCO*	0.49	4.09E-03	YES
Msr1	5.42	2.52E-61	NP			NP			YES
Siglecs									
Siglec1	1.31	3.80E-01	NP			*SIGLEC1*	0.89	1.80E-01	YES
Siglec5	0.04	1.57E-21	NP			*SIGLEC5*	1.26	3.19E-01	YES

Cd33	2.27	3.08E-04	NP			*CD33*	0.23	4.45E-06	YES
GPI Anchored proteins									
Cd52	0.62	3.23E-02	NP			*CD52*	0.06	5.33E-07	NO
Ly6e	2.57	5.59E-05	NP			NP			NO
Cd59a	0.34	3.67E-10	NP			*CD59*	1.74	1.43E-04	YES
Cd24a	4.74	1.19E-03	NP			NP			NO
Cd14	4.99	3.10E-22	CD14	2.37	6.25E-03	*CD14*	0.85	7.25E-01	YES
Plaur	4.96	1.28E-47	NP			*PLAUR*	2.51	5.17E-05	YES
Integrins									
Itgam	0.80	3.50E-01	ITGAM	1.17	4.27E-01	*ITGAM*	0.11	3.95E-07	YES
Itgb2	1,56	6,69E-06	ITGB2	0,63	2,66E-02	*ITGB2*	0,17	7,19E-07	YES

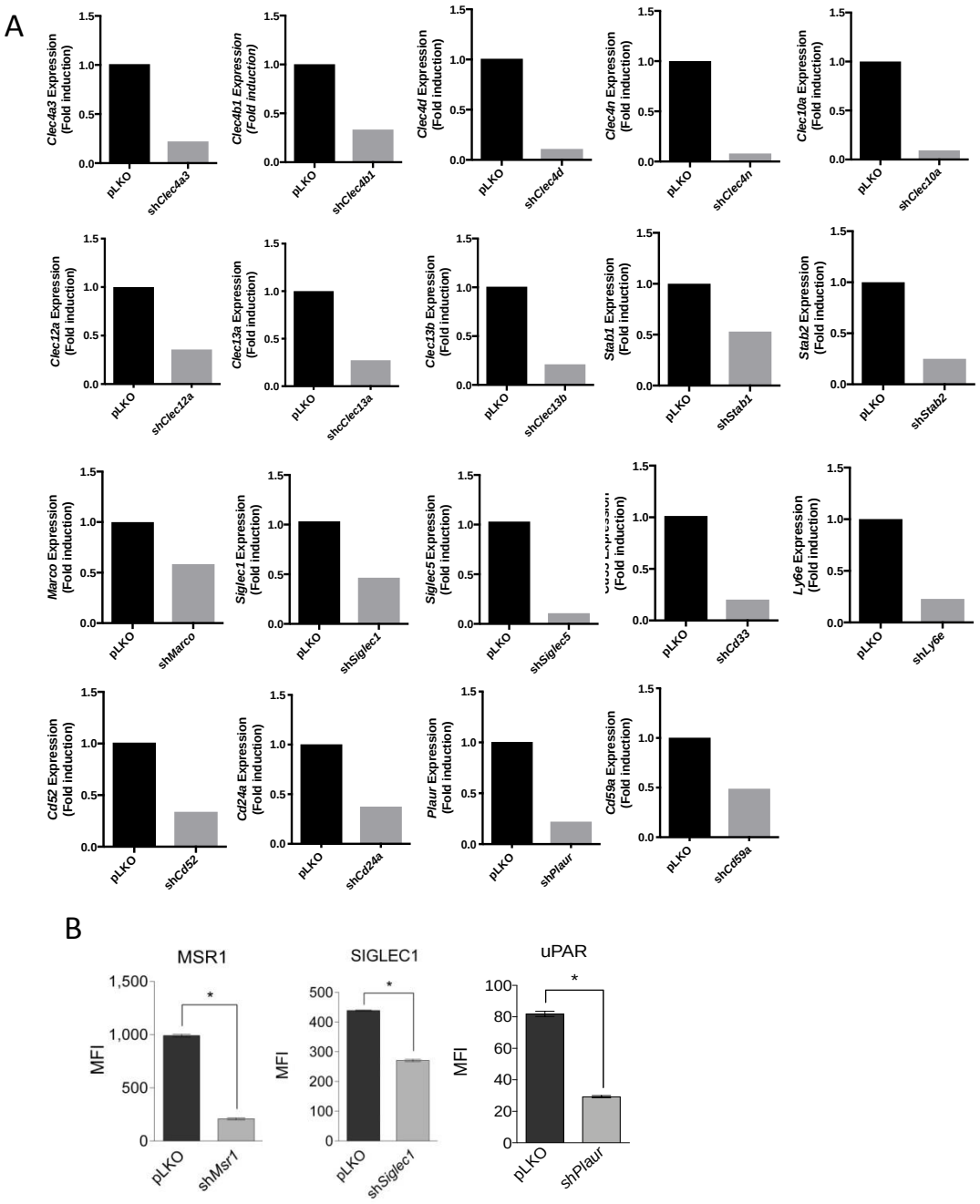

Figure 3 Downregulation of receptor expression in RAW264.7. (A) Downregulation of surface receptors upon lentiviral infection containing specific sh*RNA* (grey bar) compared to lentivirus containing the empty vector (pLKO.1, black), as determined by qRT-PCR. (B) Surface expression (MFI) of MSR1, SIGLEC1 and uPAR in sh*RNA*- (grey bar) and pLKO.1 (black bar)-infected RAW 264.7 cells

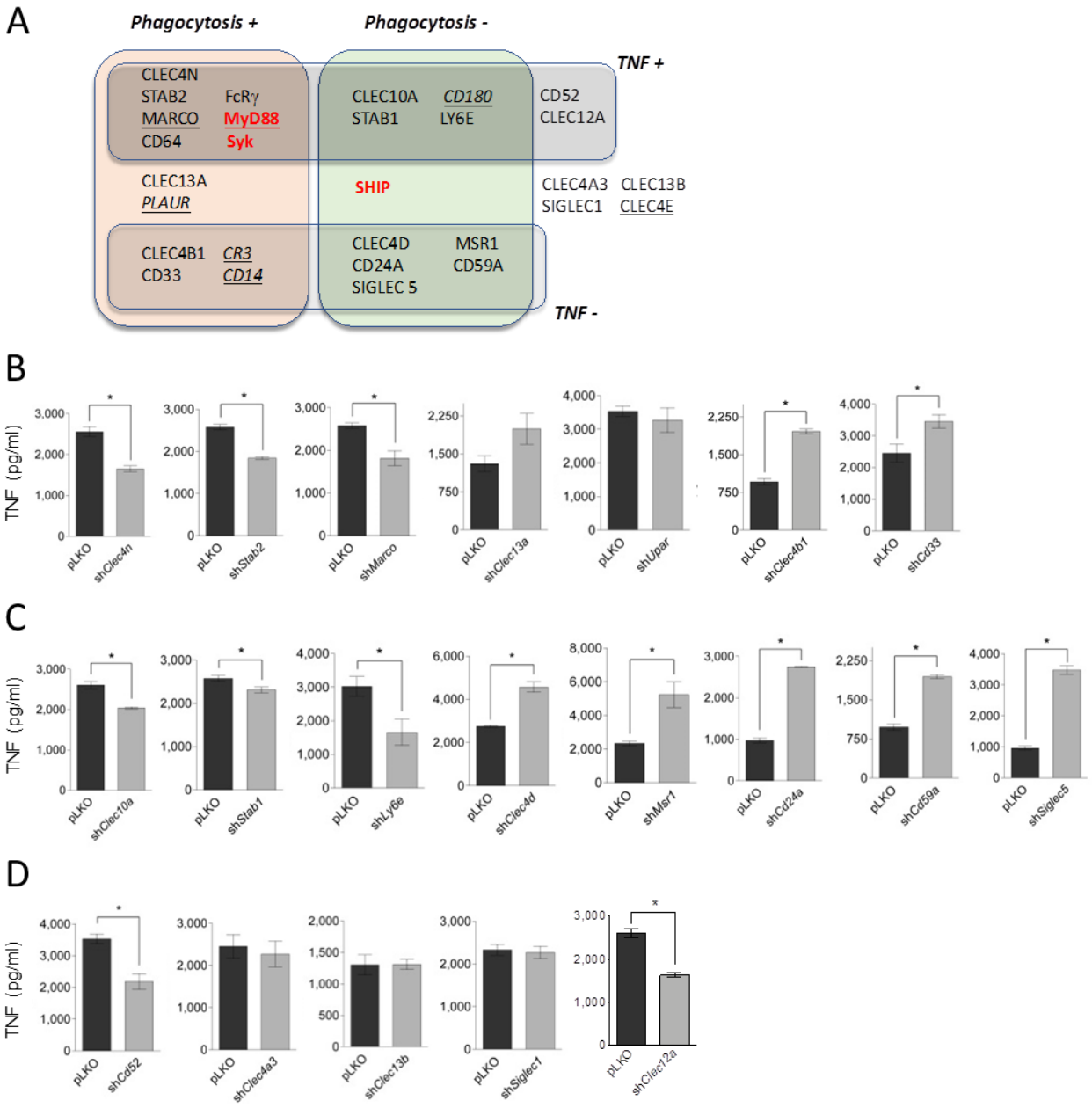

Figure 4 Several surface receptors are involved in the phagocytosis of RAW 264.7 cells to *B. burgdorferi* and the induction of TNF. (A) Schematic representation of the role of the receptors involved positively or negatively in *B. burgdorferi* phagocytosis and the induction of TNF. TNF induction by RAW 264.7 cells silenced for the receptors involved positively (B), negatively (C) or not involved (D) in *B. burgdorferi* phagocytosis upon stimulation with the bacteria. The data corresponds to the average ± SE and are representative of at least 3 independent experiments.

We next analyzed the effect of shRNA overexpression on TNF induction in response to *B. burgdorferi*. Of the receptors positively associated with *B. burgdorferi* phagocytosis, CLEC4N, STABILIN 2 and MARCO were also involved in the positive regulation of TNF (Figure

4A, B), while CLEC4B1 and CD33 negatively regulated the induction of the cytokine (Figure 4A, B). Interestingly, both CLEC13A and uPAR silencing had no effect on the induction of TNF, in spite of their positive regulation of phagocytosis (Figure 4A, B). Of the receptors negatively regulating the uptake of *B. burgdorferi*, CLEC10A, STABILIN 1 and LY6E positively regulated the induction of TNF (Figure 4A, C), while silencing of CLEC4D, MSR1, CD24A, CD59A and SIGLEC5 resulted in increased TNF levels (Figure 4A, C). Of note, although CLEC12A and CD52 silencing did not affect the phagocytic capacity of RAW 264.7 cells, it affected TNF production in response to the spirochete (Figure 4A, D).

Because the regulation of CD11b would cause opposite effects on phagocytosis and TNF induction (14), as demonstrated by the CD180-mediated regulation of the integrin (15), we assessed the levels of expression of this protein on RAW 264.7 cells that showed opposite effects on spirochetal uptake and TNF production. We stained CD11b in RAW 264.7 cells with stable expression of sh*Clec10a*, sh*Stab1*, sh*Ly6e*, sh*Clec4b1* and sh*Cd33* (Figure 4A). A slight decreased on CD11b expression was observed in cells with silenced *Clec4b1*, consistent with the reduced phagocytic activity of these cells and increased TNF production (Figure 9). The rest of the analyzed silenced cells showed no obvious differences in the surface expression levels of CD11b, suggesting an alternative mechanism of modulation of the response.

Overall, these data show that several surface receptors contribute to the overall response of phagocytic cells to *B. burgdorferi*.

Figure 5

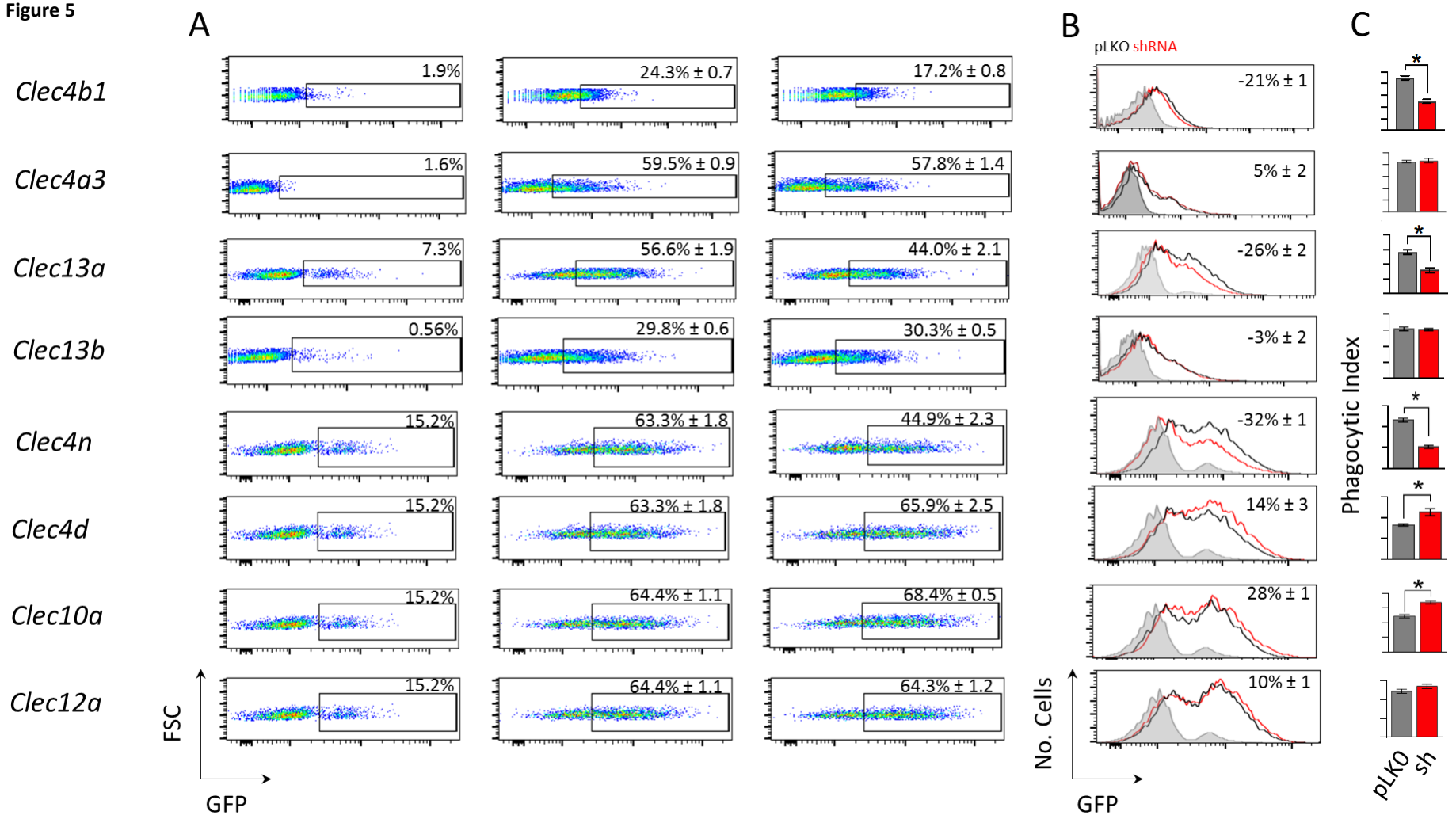
A
B
C
Clec4b1
Clec4a3
Clec13a
Clec13b
Clec4n
Clec4d
Clec10a
Clec12a
1.9%
24.3% ± 0.7
17.2% ± 0.8
1.6%
59.5% ± 0.9
57.8% ± 1.4
7.3%
56.6% ± 1.9
44.0% ± 2.1
0.56%
29.8% ± 0.6
30.3% ± 0.5
15.2%
63.3% ± 1.8
44.9% ± 2.3
15.2%
63.3% ± 1.8
65.9% ± 2.5
15.2%
64.4% ± 1.1
68.4% ± 0.5
15.2%
64.4% ± 1.1
64.3% ± 1.2
FSC
GFP
pLKO shRNA
-21% ± 1
5% ± 2
-26% ± 2
-3% ± 2
-32% ± 1
14% ± 3
28% ± 1
10% ± 1
No. Cells
GFP
Phagocytic Index
*
pLKO
sh

Figure 6

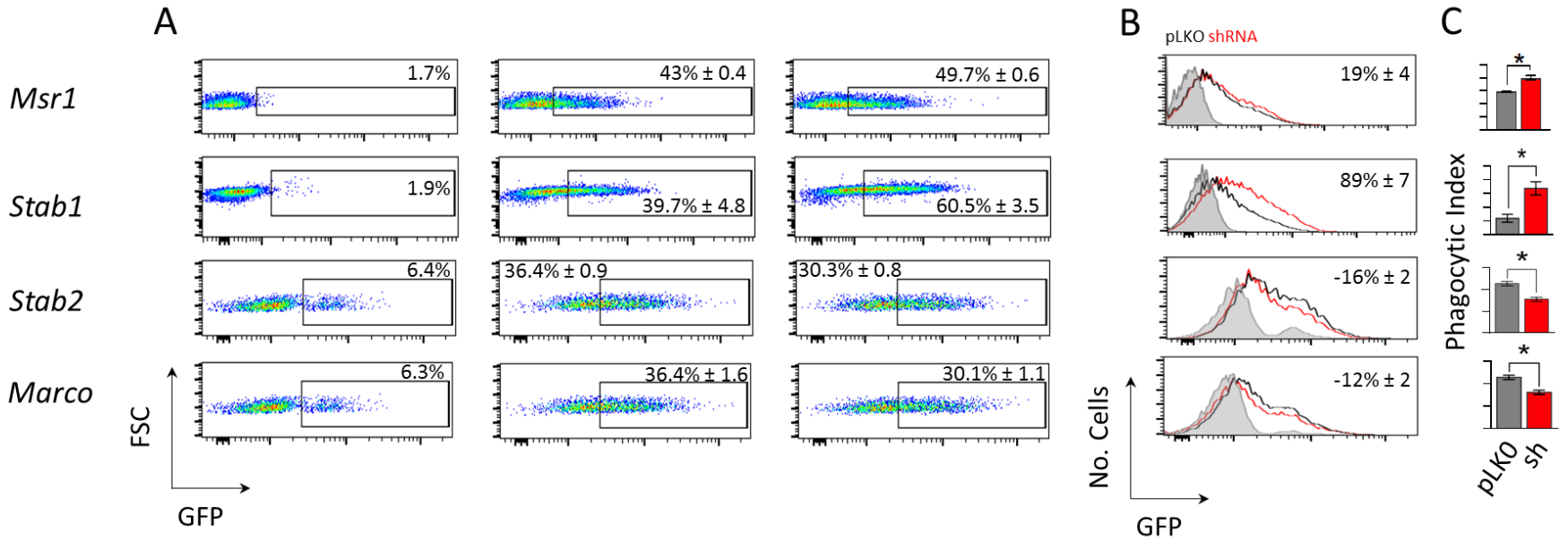

Figure 7

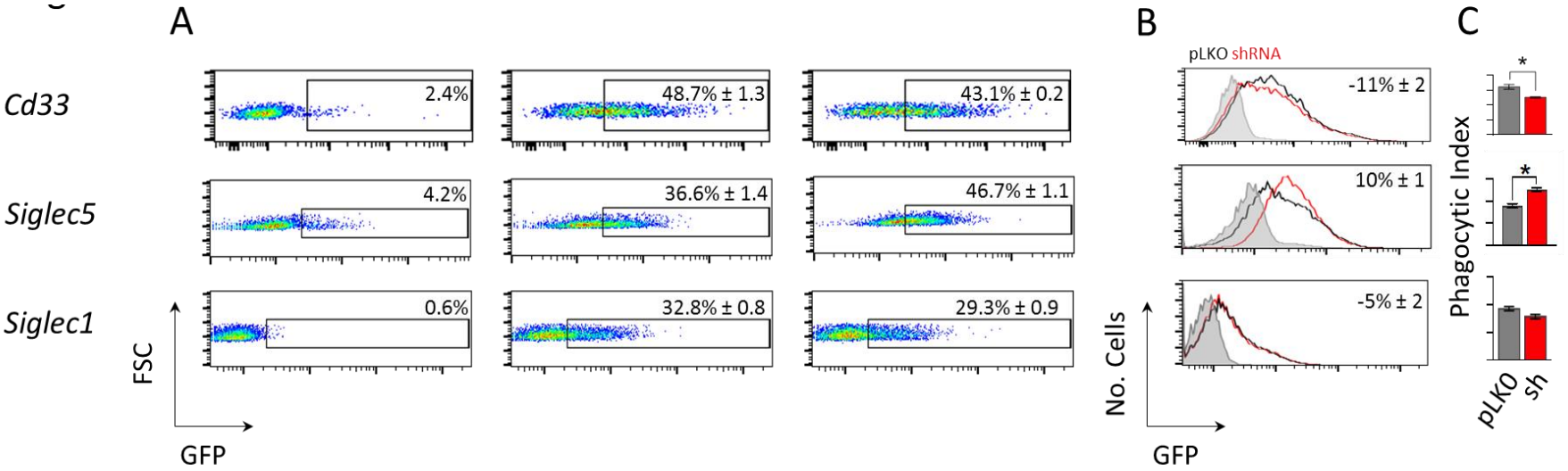

Figure 8

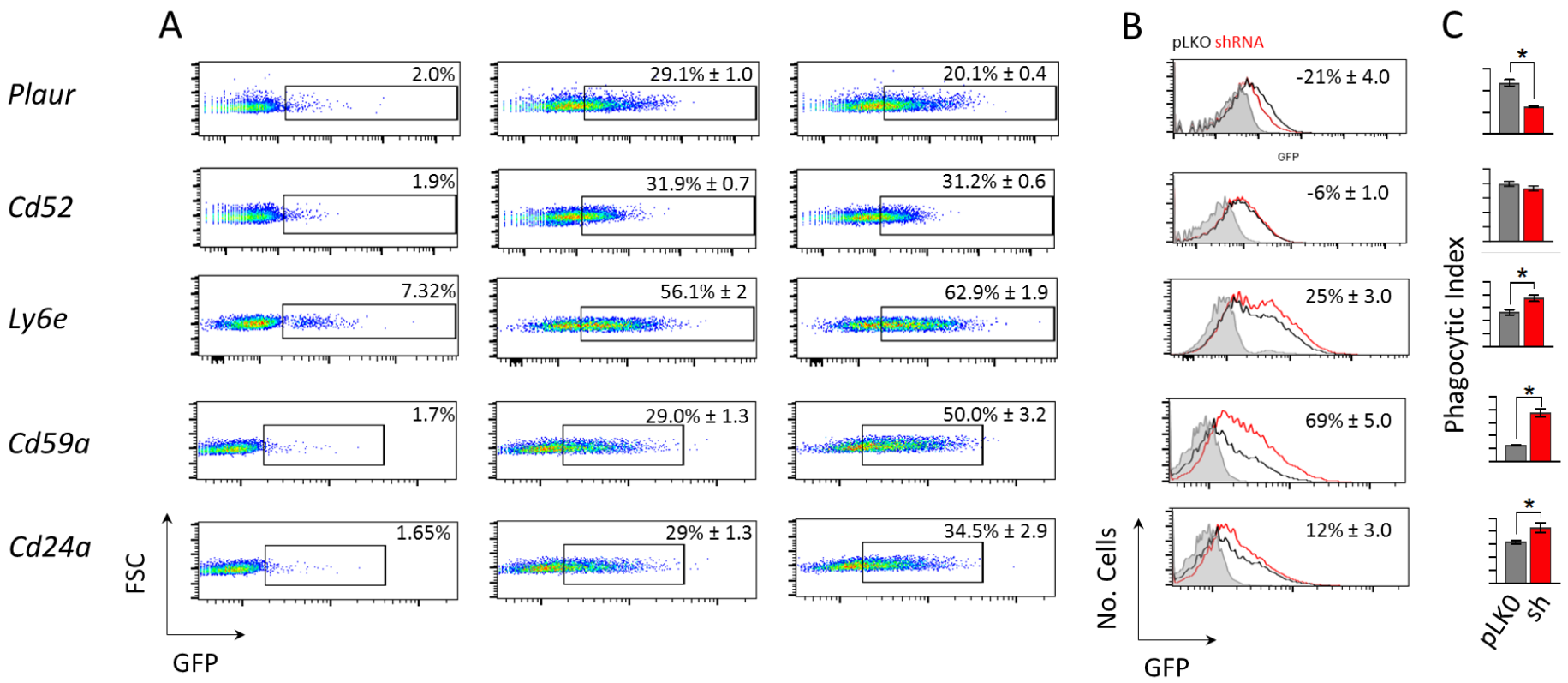

Figures 5-8 Phagocytosis of *B. burgdorferi* by C-type Lectin- (Fig. S3), Scavenger receptors- (Fig. S4), Siglec- (Fig. S5) and GPI-anchored proteins- (Fig. S6), silenced RAW264.7 cells. (A) Percentage of GFP-positive RAW 264.7 cells in sh*RNA*- (right panel) or pLKO.1-infected (middle panel) cells. The 4 ºC control is represented on the left panels. The numbers represent the average ± SE of 3 determinations. (B) Histograms representing phagocytosis by sh*RNA*- (red histogram) and control-infected (black histograms) RAW 264.7 cells. The gray histogram represents the 4 °C control. The numbers represent the average MFI ± SE of 3 determinations. (C) Phagocytic index of sh*RNA*- (grey bars) and pLKO.1-infected (red bars) RAW 264.7 cells. The data represent the average ± SE of 3 determinations.

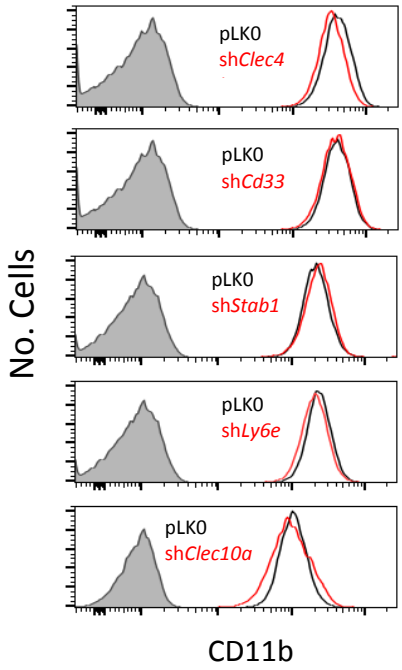

Figure 9 Flow cytometry analysis of CD11b expression in sh*Clec10a*, sh*Stab1*, sh*Ly6e*, sh*Clec4b1* and sh*Cd33* RAW264.7 cell lines. Sh*RNA* infected RAW 264.7 cells (red histogram) and pLKO.1-infected controls (black histogram) were analyzed for CD11b expression by flow cytometry. The gray histogram represents the unstained control. The data represent at least 3 independent determinations.

3.4 CD64 mediates the phagocytosis of *B. burgdorferi* in absence of specific antibodies.

The proteomics analysis of the phagosome-enriched fractions of hMACs showed a significant contribution to components of the Fcγ phagocytosis pathway (Figure 10A), including CD64 (Figure 1B). Because Fcγ Receptor I Alpha (FcgRI, CD64) has been shown to directly recognize *Escherichia coli* by murine macrophages in the context of meningeal infection (22) and to mediate bacterial invasion, we further assessed whether this receptor would mediate the internalization of *B. burgdorferi* in the absence of opsonins (antibodies). Silencing *Fcgr1* in RAW 264.7 cells resulted in decreased phagocytosis of *B. burgdorferi* (Figure 11A) and TNF (Figure 11B). *Cd64*-silenced BMMs (Figure 10B) also showed reduced uptake of the spirochete in serum-free medium (Figure 10C). Furthermore, the use of a blocking antibody targeting CD64 resulted in the reduced phagocytic capacity of human blood monocyte-derived macrophages (Figure 10D). In addition, BMMs from CD64-deficient mice showed a diminished phagocytic capacity (Figure 10E) and TNF production in response to *B. burgdorferi* (Figure 10F). The attenuated capacity of silenced cells to internalize *B. burgdorferi* was not associated with variations in the expression of CD11b or CD14 (Figure 10G). In order to demonstrate the capacity of CD64 to bind the spirochete, we expressed ectopically the receptor in CHO cells (Figure 10H). Compared to non-transfected controls, CHO-CD64 cells were able to bind *B. burgdorferi*, demonstrating the capacity of this receptor to anchor the spirochete (Figure 10I, J).

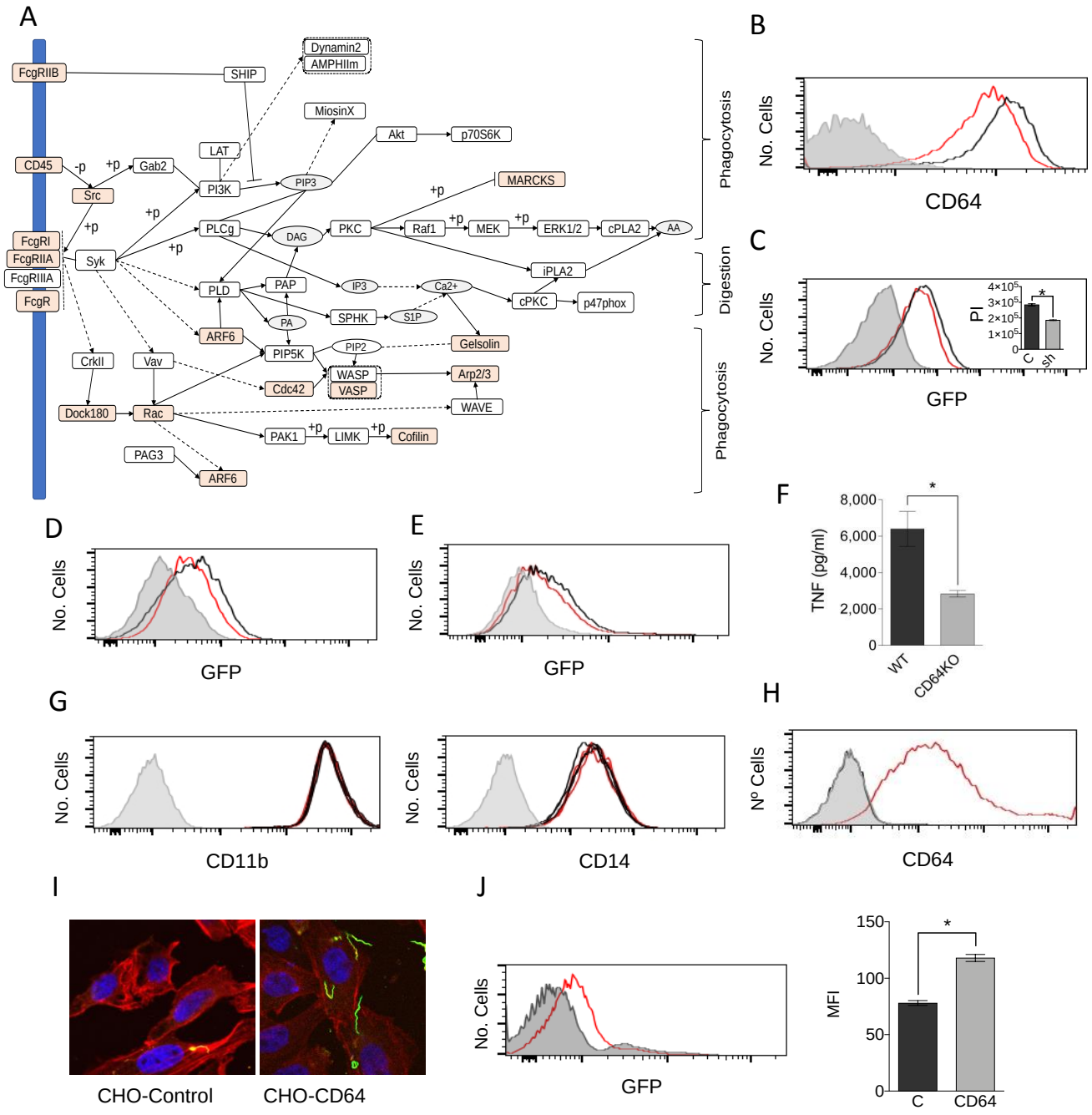

Figure 10 The Fc gamma Receptor phagocytosis pathway is implicated in the response of macrophages to *B. burgdorferi*. (A) Components of the KEGG Fc gamma Receptor pathway identified in the proteomics analysis of the phagosome-enriched fractions of hMAC. (B) Lower expression levels of CD64 on *Fcgr1a*-silenced BMMs (red histogram) compared to pLKO.1 lentivirally infected cells (black histogram), as determined by flow cytometry. The gray histogram represents the unstained control. (C) Phagocytosis of *B. burgdorferi* by sh*Fcgr1a* BMMs (red histogram) or pLKO.1-infected controls (black histogram). The gray histogram represents the 4 °C control. The results are representative of at least 3 independent experiments. (D) Phagocytosis of *B. burgdorferi* by hMACs in the presence of a blocking antibody targeting CD64 (red histogram) or controls (black histogram). The gray histogram represents the 4 °C control. The results are representative of 8 individual

(***continued from previous page***) donors. (E) Phagocytosis of *B. burgdorferi* by BMMs differentiated from CD64-deficient mice (red histogram) or wildtype controls (black histogram). The gray histogram represents the 4 °C control. The results are representative of at least 3 independent experiments. (F) TNF production upon stimulation of BMM from CD64-deficient mice (grey bar) or wildtype controls (black bar) with *B. burgdorferi*. The data represent the average ± SE of 3 mice per group. (G) Flow cytometry analysis showing the expression of CD11b and CD14 in BMMs from CD64-deficient mice (red histogram) or wildtype controls (black histogram). The gray histogram represents the unstained control. (H) Histogram representing the ectopic expression of human CD64 in CHO cells (red histogram) and un-transfected controls (black histogram). The gray histogram represents the unstained control. (I) Confocal micrograph of un-transfected CHO cells (CHO-Control) and CHO cells transfected with human CD64 (left). The cells were stained with phalloidin (red) and DAPI (blue). *B. burgdorferi* are shown in green. (J) Binding of *B. burgdorferi* to CHO cells ectopically expression human CD64 (red histogram) compared to un-transfected cells (black histogram). The gray histogram represents the 4 °C control. The average mean fluorescence intensity (MFI) of 3 determinations is presented on the right, as is representative of at least 3 independent experiments.

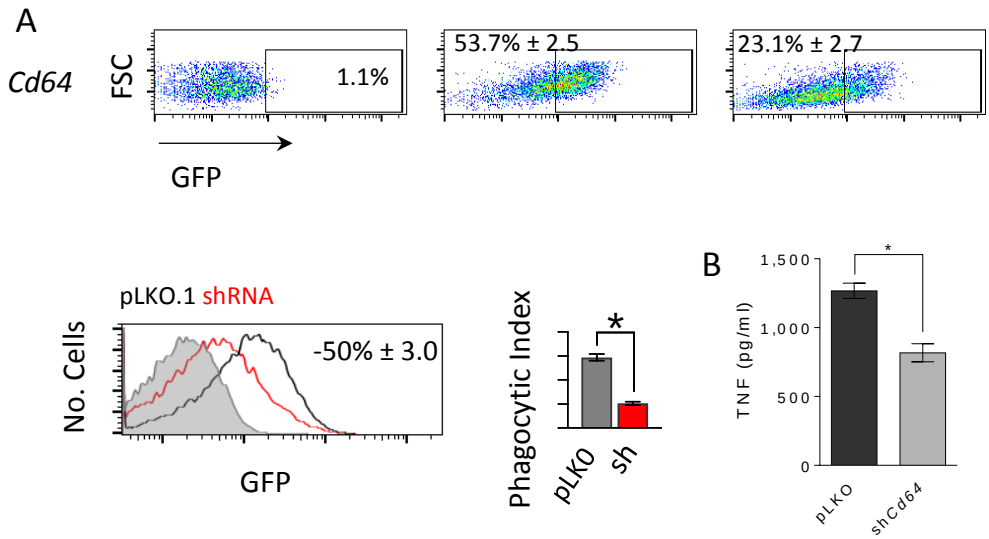

Figure 11 Phagocytosis of *B. burgdorferi* by sh*Cd64* RAW264.7 cells. (Left panels) Percentage of GFP-positive RAW 264.7 cells in sh*RNA*- (right panel) or pLKO.1-infected (middle panel) cells. The 4 ºC control is represented on the left panels. The numbers represent the average ± SE of 3 determinations. (Middle panel) Histograms representing phagocytosis by sh*RNA*- (red histogram) and control-infected (black histograms) RAW 264.7 cells. The gray histogram represents the 4 °C control. The numbers represent the average MFI ± SE of 3 determinations. (right panel) Phagocytic index of sh*RNA*- (grey bars) and pLKO.1-infected (red bars) RAW 264.7 cells. The data represent the average ± SE of 3 determinations. (B) TNF production by sh*Fcgr1a* RAW 264.7 cell (grey bar) and pLKO.1 controls (black bar) upon stimulation with *B. burgdorferi*. The average ± SE of 3 determinations is represented.

3.5 The common gamma chain mediates the phagocytosis of *B. burgdorferi*.

Fc and other receptors, including some C-type lectins require the recruitment and signals elicited by the common gamma chain (FCER1G, FcγR) (19, 21, 33). These include some of those that modulate the internalization of the spirochete, such as CLEC4N, or CLEC4D. We therefore assessed the role of FCER1G in the internalization of the spirochete. RAW 264.7 cells harboring sh*Fcer1g* (**Figure 12A**) showed a diminished capacity to internalize *B. burgdorferi* (**Figure 12B**) and resulted in decreased induction of TNF in response to the spirochete (**Figure 12C**). The same reduction in phagocytosis to *B. burgdorferi* was observed in silenced BMMs (**Figure 13A**).

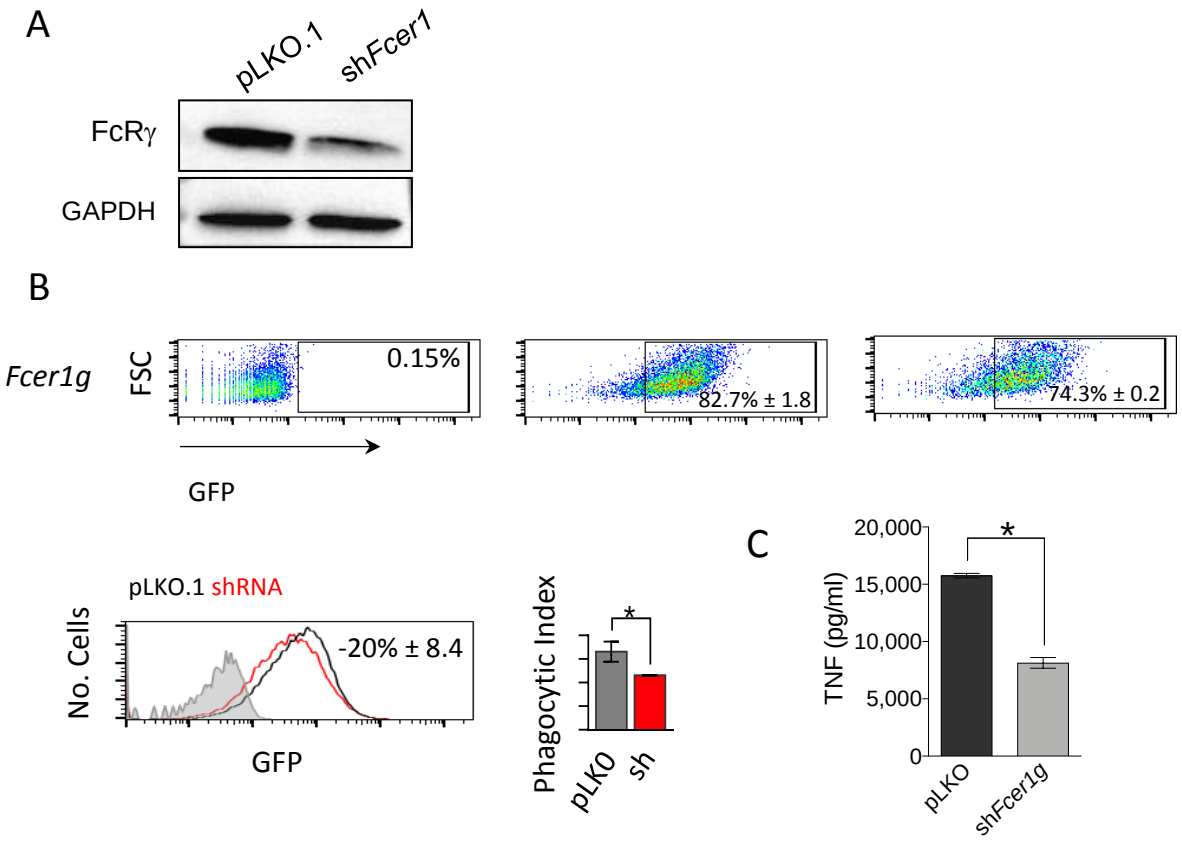

Figure 12 Phagocytosis of *B. burgdorferi* by sh*Fcer1g* RAW264.7 cells. (A) Downregulation of FcγR expression in RAW264.7 cells infected with lentivirus containing sh*Fcer1g* or the empty vector, as determined by Western blot analysis. (B) Phagocytosis of *B. burgdorferi* by sh*Fcer1g* RAW264.7 cells. (C) TNF production by sh*Fcer1g* RAW264.7 (grey bar) or pLKO.1 control (black bar) upon stimulation with *B. burgdorferi*. The data represent the average ± SE of 3 experiments.

The common FcR γ-chain mediates Syk recruitment, which is responsible for downstream signaling activation. Since Syk silencing resulted in the loss of viability of RAW 264.7 cells, we proceeded to the chemical inhibition of the kinase with Piceatannol (16). Both phagocytosis of *B. burgdorferi* (Figure 13B,C) and TNF induction (Figure 13D) were decreased in BMMs, confirming the implication of this enzyme in this process. Furthermore, Syk inhibition in hMac decreased the capacity of these cells to phagocyte *B.burgdorferi* (Figure 13E, F).

FcgR phosphorylation and Syk recruitment requires the participation of CD45 (PTPRC), through the initial dephosphorylation of Src kinases. Since CD45 was present in the phagosome-enriched fractions of hMac (Table 4), we also analyzed the involvement of this phosphatase on the internalization of *B. burgdorferi* and TNF induction. As expected, *Ptprp* silencing in RAW 264.7 cells resulted in diminished internalization of the spirochete (Figure 14). Overall, these data show that the Fc gamma Receptor signaling pathway is involved in the internalization of and proinflammatory output in response to *B. burgdorferi*.

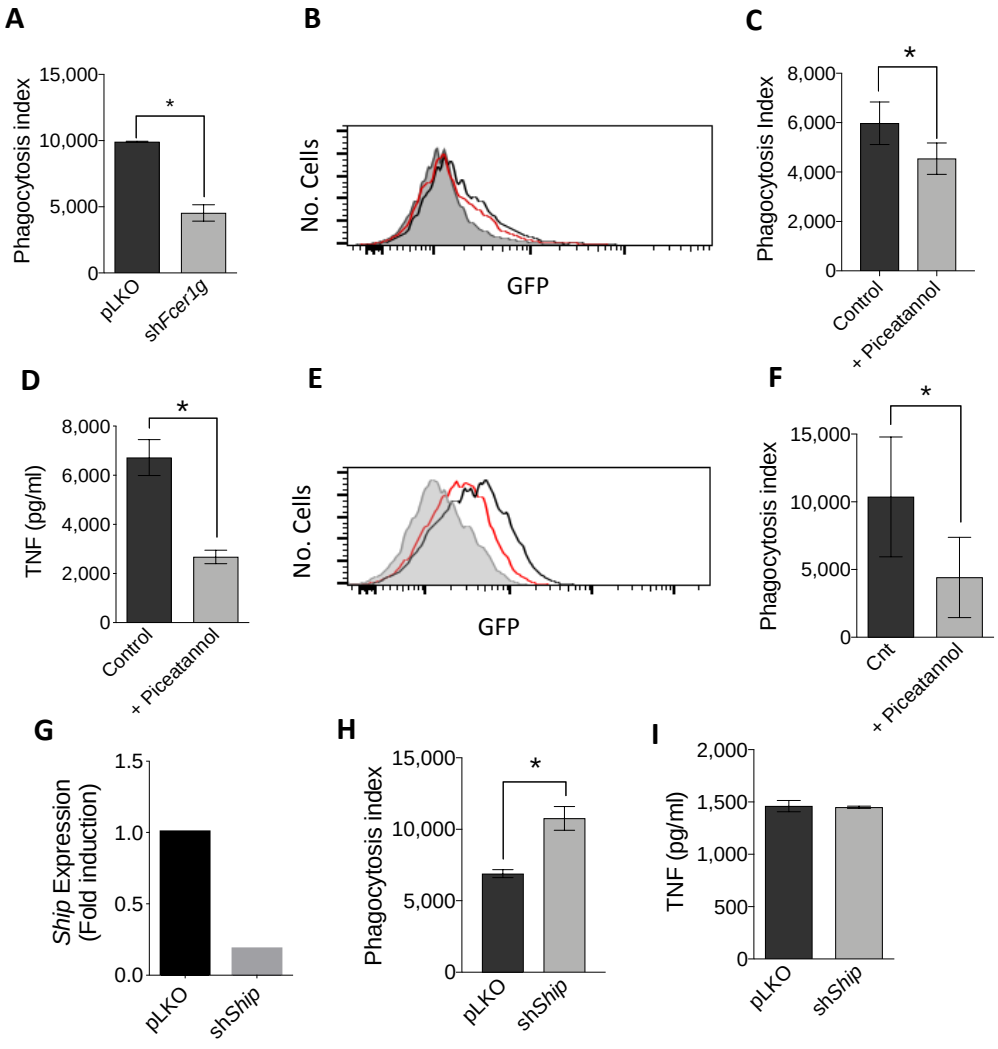

Figure 13 (previous page) The common gamma chain, Syk kinase and SHIP1 phosphatase are mediators of *B. burgdorferi* phagocytosis. (A) Phagocytosis of *B. burgdorferi* by sh*Fcerig* BMMs (grey bar) or controls (pLKO.1 infected, black). The data represent the average ± SE of 3 mice. (B) Phagocytosis of *B. burgdorferi* by BMMs treated with Piceatannol (red histogram) or non-treated controls (black histogram). The gray histogram represents the 4 °C control. (C) Phagocytosis index of BMMs treated with piceatannol (grey bar) or non-treated controls (black bar). The data represent the average ± SE of 3 mice. (D) TNF production of piceatannol treated BMMs in response to *B. burgdorferi* stimulation (grey bar) and controls (black bar). The average ± SE of 3 mice per group is presented. (E) Phagocytosis of *B. burgdorferi* by hMACs treated with Piceatannol (red histogram) and controls (black histogram). The gray histogram represents the 4 °C control. (F) Phagocytosis index of hMACs treated with Piceatannol (grey bar) and controls (black bar). The data represent the average ± SE of 5 donors. (G) Downregulation of *Ship* expression in RAW 264.7 cells infected with a lentivirus containing specific shRNA (grey bar) or an empty vector (pLKO.1, black), as determined by qRT-PCR. (H) Phagocytosis of *B. burgdorferi* by sh*Ship* RAW264.7 cells (grey bar) and pLKO.1-infected controls (black bar). The average ± SE of 3 independent experiments is shown. (I) TNF production upon stimulation with *B. burgdorferi* by sh*Ship* RAW264.7 cells (grey bar) or pLKO.1 controls (black bar). The data represent the average ± SE of 3 independent experiments.

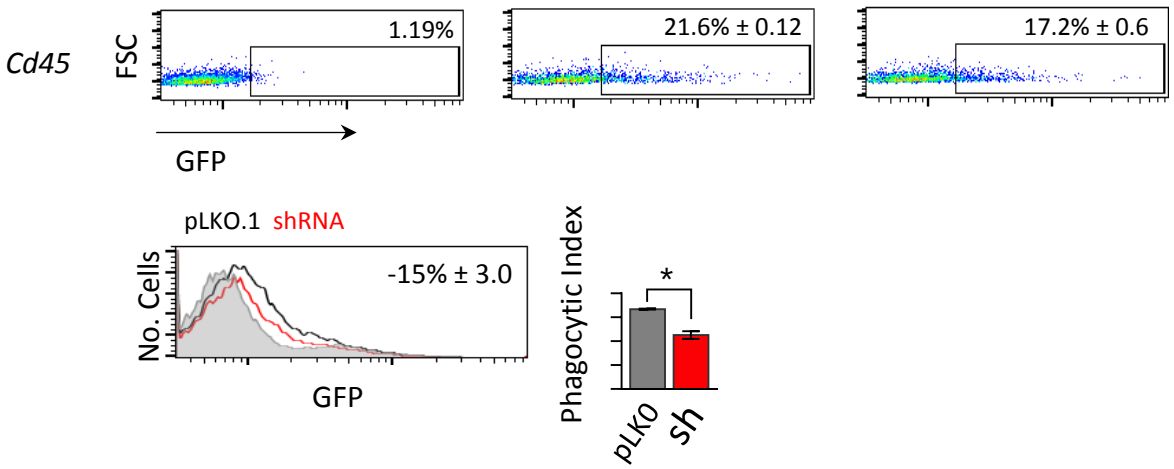

Figure 14 Phagocytosis of *B. burgdorferi* by sh*CD45* RAW264.7 cells. Phagocytosis of *B. burgdorferi* by sh*Ptprc* RAW 264.7 cells. The data were analyzed as in Fig. S8 and represent the average ± SE of 3 experiments.

3.6 The phosphatase, SHIP1, represses the phagocytosis of *B. burgdorferi* but does not affect the induction of TNF.

The myeloid specific phosphatase, SHIP1, modulates several signaling pathways, including those initiated by Fc gamma receptors (34) and other surface receptors (19). The stimulation of BMMs with *B. burgdorferi* induced the downregulation of *Inpp5d* (encoding SHIP1, **Table 4**) and the protein is present in the phagosomal enriched fractions of human macrophages (**Table 4**). To address the potential role of SHIP1 on the response of

macrophages to the spirochete, we silenced *Inpp5d* in RAW264.7 cells (**Figure 13G)**. We observed an increased capacity of silenced cells to phagocyte *B. burgdorferi* (**Figure 15, 13H**). However, the induction of TNF was not different between control and *Inpp5d*-silenced cells (**Fig. 13I**), indicating that the phosphatase is specifically involved in the internalization of *B. burgdorferi*.

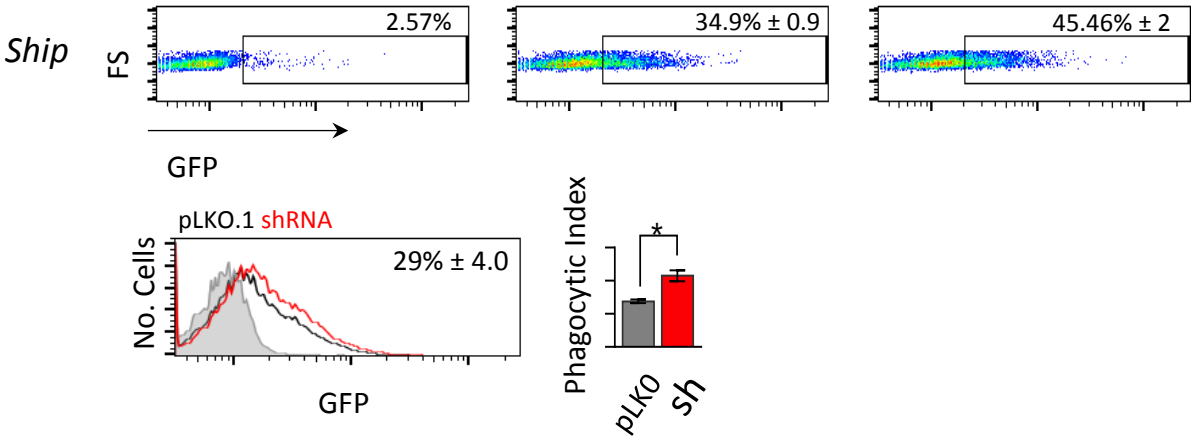

Figure 15 Phagocytosis of *B. burgdorferi* by sh*Ship* RAW264.7 cells. The data were analyzed as in Fig. S8 and represent the average ± SE of 3 experiments.

3.7 The identification of the *B. burgdorferi* ligand that interacts with CD64

We have demonstrated that CD64 binds to *B. burgdorferi* and probably participates in the internalization of the spirochete. We sought to identify the *B. burgdorferi* protein recognized by this receptor. There is only one published evidence describing the ability of CD64 to bind a pathogen in the absence of serum in the context of invasion of macrophages by *E. coli*, which is mediated by the surface protein, OmpA (40). *B. burgdorferi* contains an orthologue of OmpA, designated as BB0167 (Figure 16A).

Intriguingly, mice infected with BB0167-deficient *B. burgdorferi*, generated in an infectious spirochete using a signature-tagged mutagenesis (STM) approach, harbored higher bacteria burdens in the heart (41) (Figure 16B). We therefore, hypothesized that BB0167 mediates the internalization of *B. burgdorferi* mediated by the Fc gamma receptor, CD64.

We cloned and purified the soluble, extracellular region of BB0167 (Figure 17A). The purified protein was also used to immunize mice and generate anti-BB0167 antibodies (Figure 17B).

The recombinant protein was then labeled with Alexa Fluor-488. Labelled BB0167 was added to control and transfected hCD64 transfected CHO cells (Figure 17C). CHO cells expressing hCD64 showed binding of BB0167 while the control cells showed minimal binding (Figure 17C, D), suggesting that the lipoprotein is able to bind to the high affinity Fc receptor. To further confirm these results, we obtained *B. burgdorferi* deficient for BB0167 from Lin and collaborators (41) (Figure 17F). Binding experiments showed that the BB0167-deficient *B. burgdorferi* had a lower capacity to bind to hCD64-expressing CHO cells (Figure 17G, H).

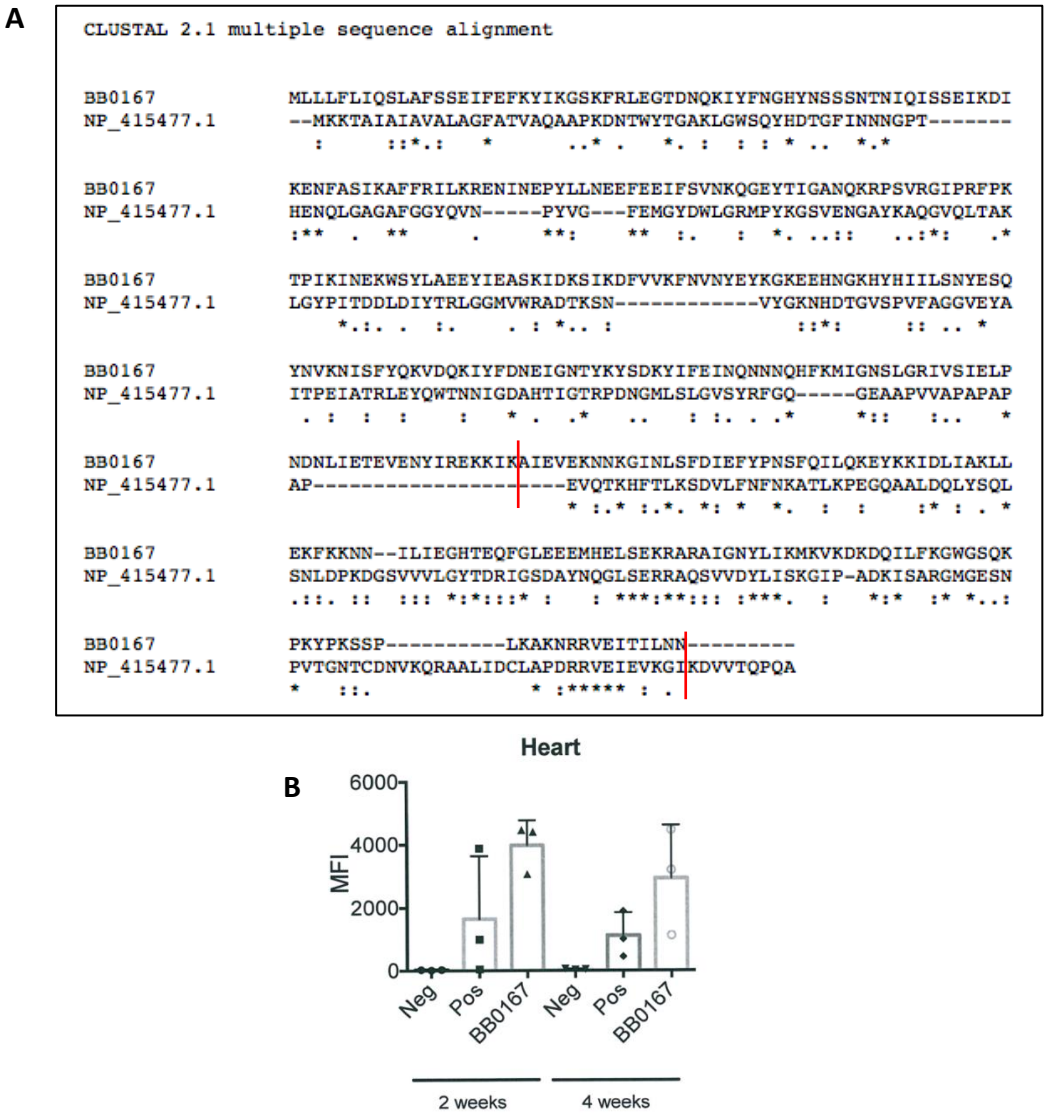

Figure 16 A: Protein sequence alignment of *E. coli* OmpA (NP_415477.1) and *B. burgdorferi* BB0167. The region between the red lines corresponds to the extracellular domain. B: BB0167 deficient *B. burgdorferi* burdens are higher in the heart compared to WT *B. burgdorferi.* Data published by Lin and collaborators (41).

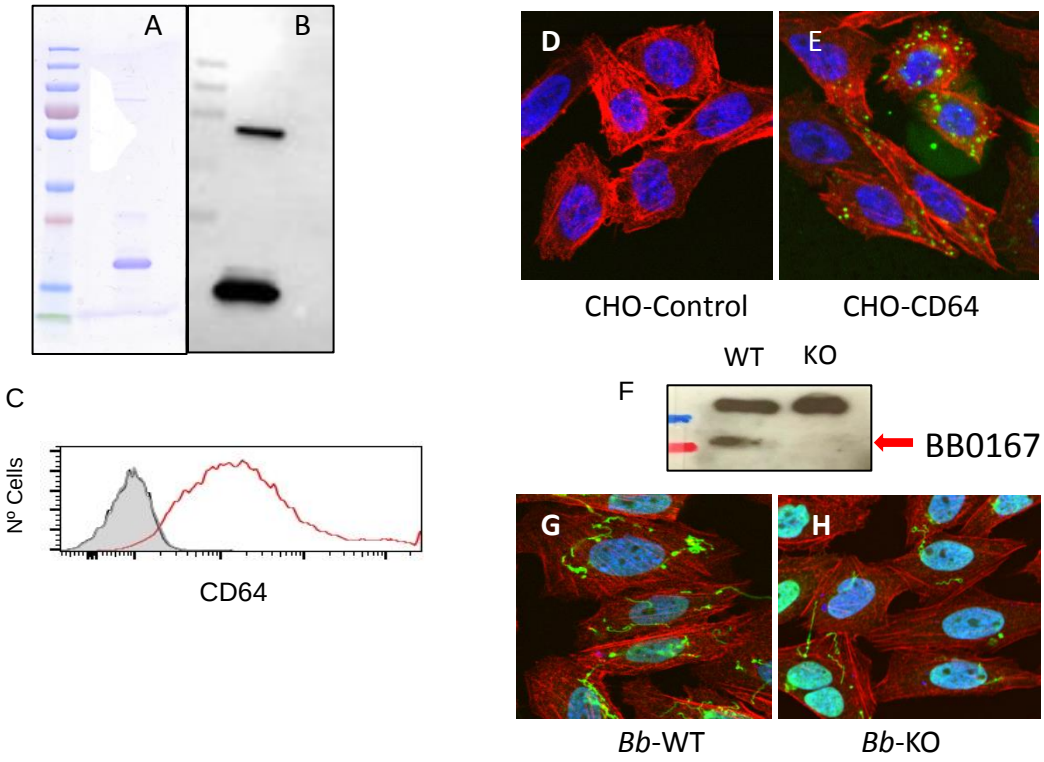

Figure 17 A: Coomasie blue staining of the purified extracellular domain of BB0167. B: Inmunoblot of anti-BB0167 generated antibody in mice. C: CD64 expression in CHO cells (red histogram) and in un-transfected controls (grey histogram). CHO expressing the human version of CD64 show labeled BB0167 bound to the cell surface (E) compared to un-transfected CHO. F: Inmunoblot of BB0167 liproprotein in WT and KO *B. burgdorferi*. The results show non-specific bands since the available antibodies are mice serum. (D). CD64 expressing CHO with *Bb*-WT (G) and *Bb*-KO (H). Confocal micrograph cells were stained with Rhodamine (red) and DAPI (blue), *B. burgdorferi* is shown in green.

We argued that the absence of the CD64 ligand would result in decreased phagocytosis and hence, increased bacterial numbers in the heart of infected mice. We therefore, infected CD64-deficient and WT mice with BB0167-deficient and WT *B. burgdorferi*, and assessed bacterial burdens in the heart after 3 weeks of infection. CD64 deficient mice showed higher *B. burgdorferi* burdens (*recA*) compared to WT mice, confirming that CD64 has a role in bacterial clearance (Figure 18A). In contrast, the levels of BB0167-deficient bacteria (identified by barcode PCR) showed no differences (Figure 18B). These results suggested that the interaction between BB0167 and CD64 mediates the phagocytosis of *B. burgdorferi*.

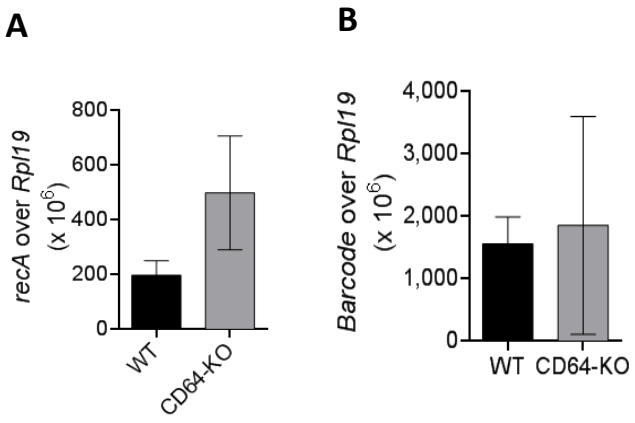

Figure 18 *In vivo* experiments suggest that Bb0167 is the ligand of CD64. A. *B. burgdorferi* burdens (recA) in CD64$^{-/-}$ mice heart (grey bar) versus WT-mice heart (black bar) determined by qRT-PCR. The DNA quantity was normalized to Rpl19 DNA. The data corresponds to the average ± SE of 5 mice. B. Bb0167 deficient *B. burgdorferi* (barcode) burdens in cardiac tissue of CD64$^{-/-}$ and WT mice. The heart DNA quantity was normalized to Rpl19 DNA. The data represent the average ± SE of 5 mice.

1. DISCUSSION

Macrophages are key elements of the immune response; they are not only involved in the clearance of the pathogens, but also act as a bridge between the innate and adaptive arms of the immune response. Macrophages harbor a large number of surface receptors, which confer this cell type a high level of plasticity. Upon engagement of pathogen-recognition receptors (PRRs), macrophages produce an array of cytokine/chemokines that orchestrate the behavior of the downstream components of the inflammatory response. Surface receptors that specifically recognize the pathogen recruit signaling molecules that transduce signals and mediate the internalization and clearance of the pathogen. Multiple receptors may intervene in the phagocytosis of the same pathogen (19, 35). Thus, the overall signature response to a specific pathogen is dictated by the addition of the signals initially emanating from surface receptors, further modulated by the interaction of intracellular signals generated as a result of the internalization of the pathogen (15).

We have identified a variety of receptors implicated in the response of macrophage to *B. burgdorferi*. For this purpose, we first analyzed the proteomic content of phagosome-enriched fractions containing *B. burgdorferi*. We further complemented this approach with the identification of surface receptors regulated by the stimulation of macrophages with the spirochete (15), an approach previously used by Hu and collaborators that led to the identification of MARCO as a phagocytic receptor for *B. burgdorferi* (11). Our approach also allowed us to identify MARCO and uPAR, another receptor previously involved in the uptake of the spirochete (10), as proteins involved in the response of macrophages to *B. burgdorferi*. Furthermore, these results also confirmed the role of CR3/CD14 in the response of phagocytic cells to the microorganism.

Our results show that the repertoire of surface proteins involved in this response is complex and composed of several classes of receptors, including C-lectins, scavenger receptors, siglecs and Fc receptors. The importance of the common FcR γ-chain in the control of spirochetal burdens in mice has been previously demonstrated albeit in the presence of antibodies (36). The results shown here suggest that at least partly, the role played by these receptors may not be solely mediated by antibody-mediated opsonization of the bacteria. In fact, we demonstrate that CD64, the high affinity Fc receptor, directly binds *B. burgdorferi* suggesting that Fc receptors mediate both antibody-dependent and

independent responses in macrophages. The role played by the opsonin-independent phagocytosis of *B. burgdorferi* mediated by Fc receptors may be more relevant at the tissue level, once the spirochetes have disseminated to tissues with poor antibody penetration (37).

Our results are suggestive, but do not provide definitive proof of the role played by BB0167 as a ligand for CD64 in the internalization of *B. burgdorferi*. In order to fully define this lipoprotein as a ligand that mediates the interaction of the spirochete and the high affinity Fc receptor, we propose to cross the CD64-deficient mice with B cell-deficient mice (μ KO), and thus eliminate the interference provided by the presence of antibodies during infection with the spirochete. Another possibility to further clarify the role of BB0167 is to generate a reconstituted strain in order to unequivocally assign the phenotype of the KO strain to the absence of this proteins and not to polar effects, that have been observed in other gene deficient spirochetes (46, 47, 48).

Our approach did not identify a surface receptor dependent on MyD88, a signaling molecule that accounts for a large portion of the phagocytic activity of macrophages to the spirochete (36, 38). In contrast, we further define the Syk-mediated pathway, probably elicited by Fc receptors and certain C-type lectins, as regulating both the internalization of and the induction of proinflammatory cytokines by *B. burgdorferi*. The role played by Syk in the internalization of the spirochete confirms previous findings (16). This signaling pathway is a positive regulator of the proinflammatory activity of macrophages, in contrast to CR3/CD14. This diversity in the role played by different surface receptors on the biosignature of macrophages is further reinforced by the presence of proteins with positive and negative modulatory effects both in the uptake of the spirochete and the ensuing induction of TNF. We previously demonstrated that phagosomes containing *B. burgdorferi* are diverse and include CR3 or not (14). It is feasible that the same would be true and a certain number of different phagosomal compositions would distinctly participate in the induction of proinflammatory cytokines. Overall, both the composition and the regulation of receptors involved in the response of macrophages to *B. burgdorferi* provide not only the capacity to eliminate the bacteria, but also the overall inflammatory output of these cells, which could be modulated over time in response to the signals that affect their expression, such as the bacterium itself.

2. REFERENCES

1. EC. Parliament calls for “alarming” spread of Lyme disease to be tackled | News | European Parliament. 2018 (Nov 29). Available from: http://www.europarl.europa.eu/news/en/press-room/20181106IPR18328/parliament-calls-for-alarming-spread-of-lyme-disease-to-be-tackled.

2. Schotthoefer AM, Frost HM. 2015. Ecology and Epidemiology of Lyme Borreliosis. Clin Lab Med 35:723-43.

3. Murray TS, Shapiro ED. 2010. Lyme disease. Clin Lab Med 30:311-28.

4. Chomel B. 2015. Lyme disease. Rev Sci Tech 34:569-76.

5. Lelovas P, Dontas I, Bassiakou E, Xanthos T. 2008. Cardiac implications of Lyme disease, diagnosis and therapeutic approach. Int J Cardiol 129:15-21.

6. Aucott JN, Seifter A, Rebman AW. 2012. Probable late lyme disease: a variant manifestation of untreated Borrelia burgdorferi infection. BMC Infect Dis 12:173.

7. Schwan TG, Karstens RH, Schrumpf ME, Simpson WJ. 1991. Changes in antigenic reactivity of Borrelia burgdorferi, the Lyme disease spirochete, during persistent infection in mice. Can J Microbiol 37:450-4.

8. Aslam B, Nisar MA, Khurshid M, Farooq Salamat MK. 2017. Immune escape strategies of Borrelia burgdorferi. Future Microbiol 12:1219-1237.

9. Montgomery RR, Booth CJ, Wang X, Blaho VA, Malawista SE, Brown CR. 2007. Recruitment of macrophages and polymorphonuclear leukocytes in Lyme carditis. Infect Immun 75:613-20.

10. Hovius JW, Bijlsma MF, van der Windt GJ, Wiersinga WJ, Boukens BJ, Coumou J, Oei A, de Beer R, de Vos AF, van 't Veer C, van Dam AP, Wang P, Fikrig E, Levi MM, Roelofs JJ, van der

Poll T. 2009. The urokinase receptor (uPAR) facilitates clearance of Borrelia burgdorferi. PLoS Pathog 5:e1000447.

11. Petnicki-Ocwieja T, Chung E, Acosta DI, Ramos LT, Shin OS, Ghosh S, Kobzik L, Li X, Hu LT. 2013. TRIF mediates Toll-like receptor 2-dependent inflammatory responses to Borrelia burgdorferi. Infect Immun 81:402-10.

12. Hawley KL, Olson CM, Jr., Carreras-Gonzalez A, Navasa N, Anguita J. 2015. Serum C3 Enhances Complement Receptor 3-Mediated Phagocytosis of Borrelia burgdorferi. Int J Biol Sci 11:1269-71.

13. Hawley KL, Martin-Ruiz I, Iglesias-Pedraz JM, Berwin B, Anguita J. 2013. CD14 targets complement receptor 3 to lipid rafts during phagocytosis of Borrelia burgdorferi. Int J Biol Sci 9:803-10.

14. Hawley KL, Olson CM, Jr., Iglesias-Pedraz JM, Navasa N, Cervantes JL, Caimano MJ, Izadi H, Ingalls RR, Pal U, Salazar JC, Radolf JD, Anguita J. 2012. CD14 cooperates with complement receptor 3 to mediate MyD88-independent phagocytosis of Borrelia burgdorferi. Proceedings of the National Academy of Sciences of the United States of America 109:1228-1232.

15. Carreras-Gonzalez A, Navasa N, Martin-Ruiz I, Lavin JL, Azkargorta M, Atondo E, Barriales D, Macias-Camara N, Pascual-Itoiz MA, Sampedro L, Tomas-Cortazar J, Pena-Cearra A, Pellon A, Prados-Rosales R, Abecia L, Elortza F, Aransay AM, Rodriguez H, Anguita J. 2018. A multi-omic analysis reveals the regulatory role of CD180 during the response of macrophages to Borrelia burgdorferi. Emerg Microbes Infect 7:19.

16. Killpack TL, Ballesteros M, Bunnell SC, Bedugnis A, Kobzik L, Hu LT, Petnicki-Ocwieja T. 2017. Phagocytic Receptors Activate Syk and Src Signaling during Borrelia burgdorferi Phagocytosis. Infect Immun 85.

17. Underhill DM, Goodridge HS. 2012. Information processing during phagocytosis. Nat Rev Immunol 12:492-502.

18. Pluddemann A, Neyen C, Gordon S. 2007. Macrophage scavenger receptors and host-derived ligands. Methods 43:207-17.

19. Dambuza IM, Brown GD. 2015. C-type lectins in immunity: recent developments. Curr Opin Immunol 32:21-7.

20. Carroll MC. 1998. The role of complement and complement receptors in induction and regulation of immunity. Annu Rev Immunol 16:545-68.

21. Nimmerjahn F, Ravetch JV. 2008. Fcgamma receptors as regulators of immune responses. Nat Rev Immunol 8:34-47.

22. Mittal R, Sukumaran SK, Selvaraj SK, Wooster DG, Babu MM, Schreiber AD, Verbeek JS, Prasadarao NV. 2010. Fcgamma receptor I alpha chain (CD64) expression in macrophages is critical for the onset of meningitis by Escherichia coli K1. PLoS Pathog 6:e1001203.

23. Ioan-Facsinay A, de Kimpe SJ, Hellwig SM, van Lent PL, Hofhuis FM, van Ojik HH, Sedlik C, da Silveira SA, Gerber J, de Jong YF, Roozendaal R, Aarden LA, van den Berg WB, Saito T, Mosser D, Amigorena S, Izui S, van Ommen GJ, van Vugt M, van de Winkel JG, Verbeek JS. 2002. FcgammaRI (CD64) contributes substantially to severity of arthritis, hypersensitivity responses, and protection from bacterial infection. Immunity 16:391-402.

24. Dunham-Ems SM, Caimano MJ, Pal U, Wolgemuth CW, Eggers CH, Balic A, Radolf JD. 2009. Live imaging reveals a biphasic mode of dissemination of Borrelia burgdorferi within ticks. J Clin Invest 119:3652-65.

25. Olson C, Bates T, Izadi H, Radolf J, Huber S, Boyson J, Anguita J. 2009. Local Production of IFN-gamma by Invariant NKT Cells Modulates Acute Lyme Carditis. Journal of Immunology 182:3728-3734.

26. Majeed M, Caveggion E, Lowell CA, Berton G. 2001. Role of Src kinases and Syk in Fcgamma receptor-mediated phagocytosis and phagosome-lysosome fusion. J Leukoc Biol 70:801-11.

27. Garcia-Cao I, Song MS, Hobbs RM, Laurent G, Giorgi C, de Boer VC, Anastasiou D, Ito K, Sasaki AT, Rameh L, Carracedo A, Vander Heiden MG, Cantley LC, Pinton P, Haigis MC,

Pandolfi PP. 2012. Systemic elevation of PTEN induces a tumor-suppressive metabolic state. Cell 149:49-62.

28. Luhrmann A, Haas A. 2000. A method to purify bacteria-containing phagosomes from infected macrophages. Methods Cell Sci 22:329-41.

29. Vinet AF, Descoteaux A. 2009. Large scale phagosome preparation. Methods Mol Biol 531:329-46.

30. Wisniewski JR, Zougman A, Nagaraj N, Mann M. 2009. Universal sample preparation method for proteome analysis. Nat Methods 6:359-62.

31. Meier F, Beck S, Grassl N, Lubeck M, Park MA, Raether O, Mann M. 2015. Parallel Accumulation-Serial Fragmentation (PASEF): Multiplying Sequencing Speed and Sensitivity by Synchronized Scans in a Trapped Ion Mobility Device. J Proteome Res 14:5378-87.

32. Meier F, Brunner AD, Koch S, Koch H, Lubeck M, Krause M, Goedecke N, Decker J, Kosinski T, Park MA, Bache N, Hoerning O, Cox J, Rather O, Mann M. 2018. Online Parallel Accumulation-Serial Fragmentation (PASEF) with a Novel Trapped Ion Mobility Mass Spectrometer. Mol Cell Proteomics 17:2534-2545.

33. Kerrigan AM, Brown GD. 2011. Syk-coupled C-type lectins in immunity. Trends Immunol 32:151-6.

34. Getahun A, Beavers NA, Larson SR, Shlomchik MJ, Cambier JC. 2016. Continuous inhibitory signaling by both SHP-1 and SHIP-1 pathways is required to maintain unresponsiveness of anergic B cells. J Exp Med 213:751-69.

35. Netea MG, Brown GD, Kullberg BJ, Gow NA. 2008. An integrated model of the recognition of Candida albicans by the innate immune system. Nat Rev Microbiol 6:67-78.

36. Belperron AA, Liu N, Booth CJ, Bockenstedt LK. 2014. Dual role for Fcgamma receptors in host defense and disease in Borrelia burgdorferi-infected mice. Front Cell Infect Microbiol 4:75.

37. Navasa N, Fikrig E, Anguita J. 2018. Host defenses to spirochetes. *In* Rich R, Fleisher T, Shearer W, Shoreder H, Frew A, Weyand C (ed), Clinical Immunology: Principles and Practice, 5th ed. Elsevier.

38. Liu N, Montgomery RR, Barthold SW, Bockenstedt LK. 2004. Myeloid differentiation antigen 88 deficiency impairs pathogen clearance but does not alter inflammation in *Borrelia burgdorferi*-infected mice. Infect Immun 72:3195-203.

39 Perez-Riverol Y, Csordas A, Bai J, Bernal-Llinares M, Hewapathirana S, Kundu DJ, et al. The PRIDE database and related tools and resources in 2019: improving support for quantification data. Nucleic Acids Res. 2019;47:D442-D50.

40 Mittal, R., Sukumaran, S. K., Selvaraj, S. K., Wooster, D. G., Madan Babu, M., Schreiber, A. D., … Prasadarao, N. V. (2010). Fcγ receptor i alpha chain (CD64) expression in macrophages is critical for the onset of meningitis by Escherichia coli K1. *PLoS Pathogens*, *6*(11), 1–19. http://doi.org/10.1371/journal.ppat.1001203

41 Lin, T., Gao, L., Zhang, C., Odeh, E., Jacobs, M. B., Coutte, L., … Norris, S. J. (2012). Analysis of an Ordered, Comprehensive STM Mutant Library in Infectious Borrelia burgdorferi: Insights into the Genes Required for Mouse Infectivity. *PLoS ONE*, *7*(10). http://doi.org/10.1371/journal.pone.0047532

42 Van Vugt, M. J., Heijnen, a F., Capel, P. J., Park, S. Y., Ra, C., Saito, T., … van de Winkel, J. G. (1996). FcR gamma-chain is essential for both surface expression and function of human Fc gamma RI (CD64) in vivo. *Blood*, *87*(9), 3593–9. http://doi.org/10.1016/j.supflu.2012.01.006

43 K. L., Olson, C. M., Iglesias-Pedraz, J. M., Navasa, N., Cervantes, J. L., Caimano, M. J,Anguita, J. (2012). CD14 cooperates with complement receptor 3 to mediate MyD88-independent phagocytosis of Borrelia burgdorferi. *Proceedings of the National Academy of Sciences of the United States of America*, *109*(4), 1228–32. http://doi.org/10.1073/pnas.1112078109

44 Yan S., Kennedy S., Koide S. 2002. Thermodynamic and kinetic exploration of the energy landscape of *Borrelia burgdorferi* OspA by native-state hydrogen exchange. J. Mol. Biol. 323**:** 363–375.

45 Studier F.W. 2005. Protein production by auto-induction in high density shaking cultures.Protein Expr. Purif.41**:**207–234.

46 Stewart, P. E., Hoff, J., Fischer, E., Krum, J. G., & Rosa, P. A. (2004). Genome-wide transposon mutagenesis of *Borrelia burgdorferi* for identification of phenotypic mutants. *Applied and Environmental Microbiology*, *70*(10), 5973–5979. http://doi.org/10.1128/AEM.70.10.5973-5979.2004

47 Hyde, J. A., Shaw, D. K., Iii, R. S., Trzeciakowski, J. P., & Jon, T. (2009). The BosR regulatory protein of *Borrelia burgdorferi* interfaces with the RpoS regulatory pathway and modulates both the oxidative stress response and pathogenic properties of the Lyme disease spirochete, *74*(6), 1344–1355. http://doi.org/10.1111/j.1365-2958.2009.06951.x.

48 Liu, J., Lin, T., Botkin, D. J., McCrum, E., Winkler, H., & Norris, S. J. (2009). Intact flagellar motor of *Borrelia burgdorferi* revealed by cryo-electron tomography: Evidence for stator ring curvature and rotor/C-ring assembly flexion. *Journal of Bacteriology*, *191*(16), 5026–5036. http://doi.org/10.1128/JB.00340-09

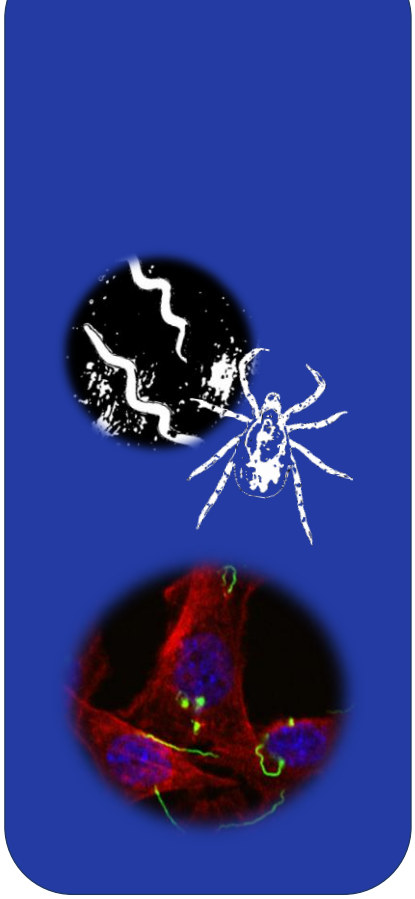

Graphical

Summary

By the use transcriptomics and proteomics we have studied innate immune responses to the spirochete using both murine macrophages and human monocytes. Based on these approaches, we have described the regulation of CD180 in response to *B. burgdorferi*. Our results show that CD180 modulates both phagocytosis and inflammation in response to *B. burgdorferi* through the transcriptional repression of complement receptor 3 (CR3) (Figure 1).

We completed our studies by performing a proteomic profile of BMMs in response to the spirochete and the identification of proteins present within *B. burgdorferi*-containing phagosomes in human macrophages. Based on the data obtained we confirmed the importance of the already reported phagocytic receptors and signalling factors as CR3, MyD88, Syk and FcRγ, which were found in the *B. burgdorferi* contained phagosomes in the proteomics study, by Immunoblot analysis and also by confocal imaging (Figure 2).

This project has also led to the identification of the Fc gamma receptor family as involved in phagocytosis of *B. burgdorferi* in the absence of antibodies. Although the common FcR γ-chain has been previously implicated in the contest of mice immune defense against the spirochete, the alpha chain (CD64) has never been related to direct phagocytosis so far. The results obtained suggest that the role played by these receptors may not be solely mediated by antibodies. Furthermore, the behaviour of other receptors of the pathway, such as CD45 and FcRG3 (low affinity α chain) or SyK/SHIP signalling molecules, confirms the relevance of this pathway (Figure 3).

We have identified a group of surface receptors that are involved in both the internalization and the induction of cytokines by *B. burgdorferi*. Some of them are implicated positively in the ingestion of this pathogen (Figure 4), others may play a regulatory role by negatively influencing phagocytosis (Figure 5), whereas the last group seems not involved in the process (Figure 6). Albeit in each group we find receptors differently modulating the inflammatory response.

Overall, our data define the specific expression traits in monocytes/macrophages in response to the spirochete, allowing the identification of components that modulate the specific interaction between the pathogen and innate immune cells.

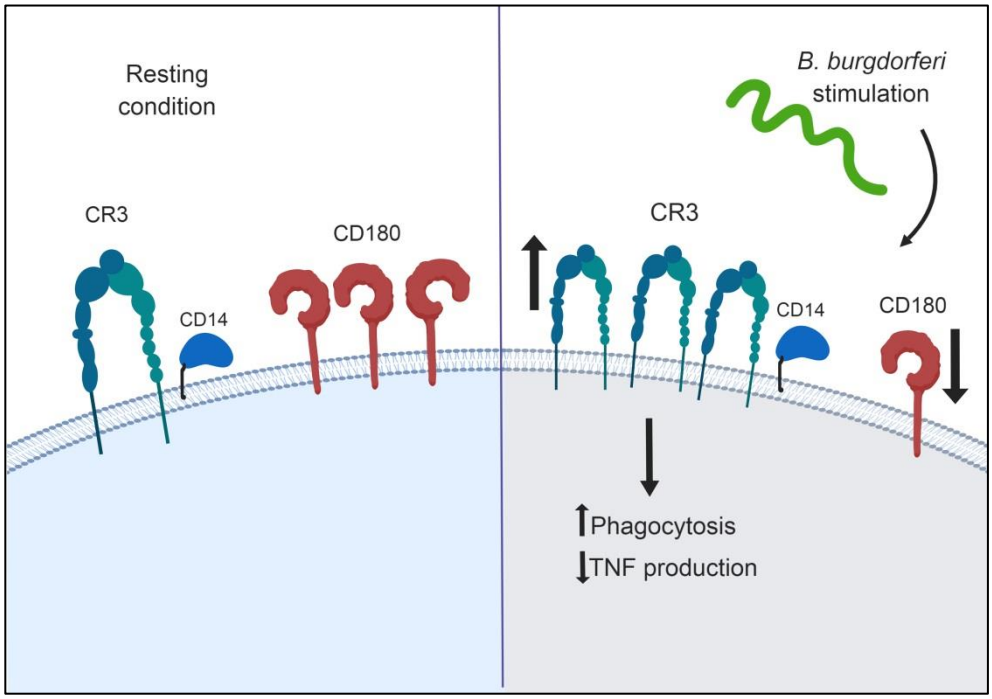

Figure 1: Negative regulatory role played by CD180 over CR3 receptor. Under resting conditions, CD180 represses CR3 expression, therefore decreasing phagocytosis and TNF production. In the presence of *B. burgdorferi*, CD180 expression decreases, releasing CR3 from its inhibitory effect and therefore increasing CR3 expression, altogether with phagocytosis and proinflammatory cytokine production.

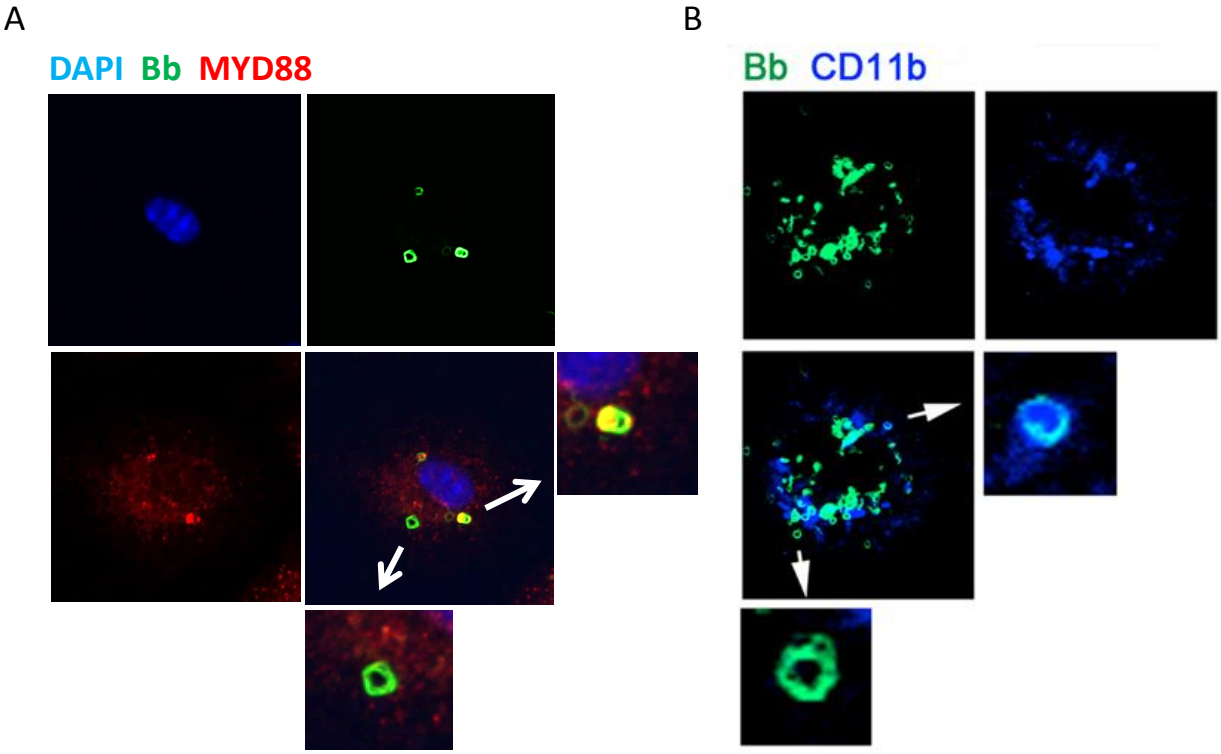

Figure 2: Confocal imagen of BMM phagosomes showing the co-localization of *B. burgdorferi* (green) and MyD88 (red) (A) and *B. burgdorferi* (green) and CD11b (blue) (B). Figure B modified from Hawley et al., 2012(3).

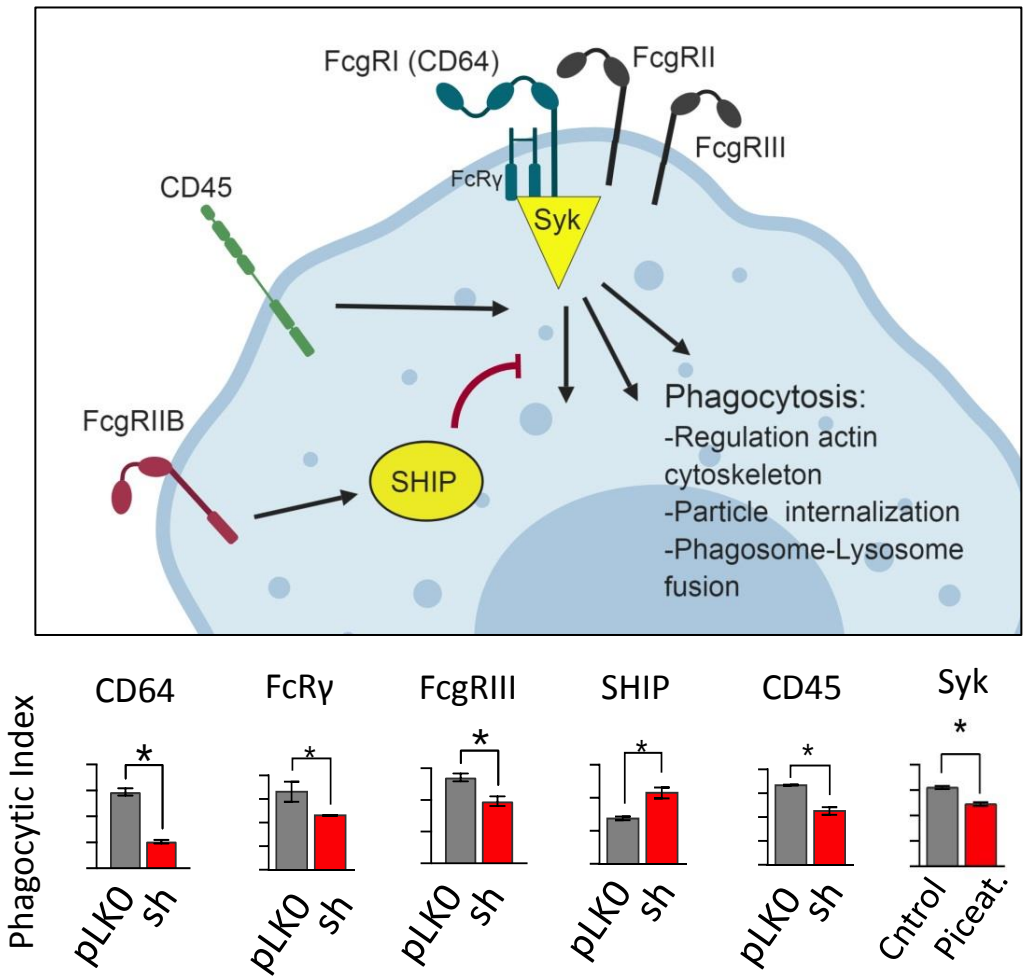

Figure 3: Simplified components of the KEGG Fc gamma Receptor pathway and the behavior of the silenced RAW 264.7 cell lines in *B. burgdorferi* phagocytosis. Bar graphics show the silencing of element positively involved in the pathway such as CD64, CD45 and FcgR3, and negatively involved, as SHIP phosphatase. The signaling molecules SyK and FcRγ show a consistent behavior when silenced (FcRγ) or when chemically inhibited (SyK) with Piceatannol.

SUMMARY OF THE RECEPTORS

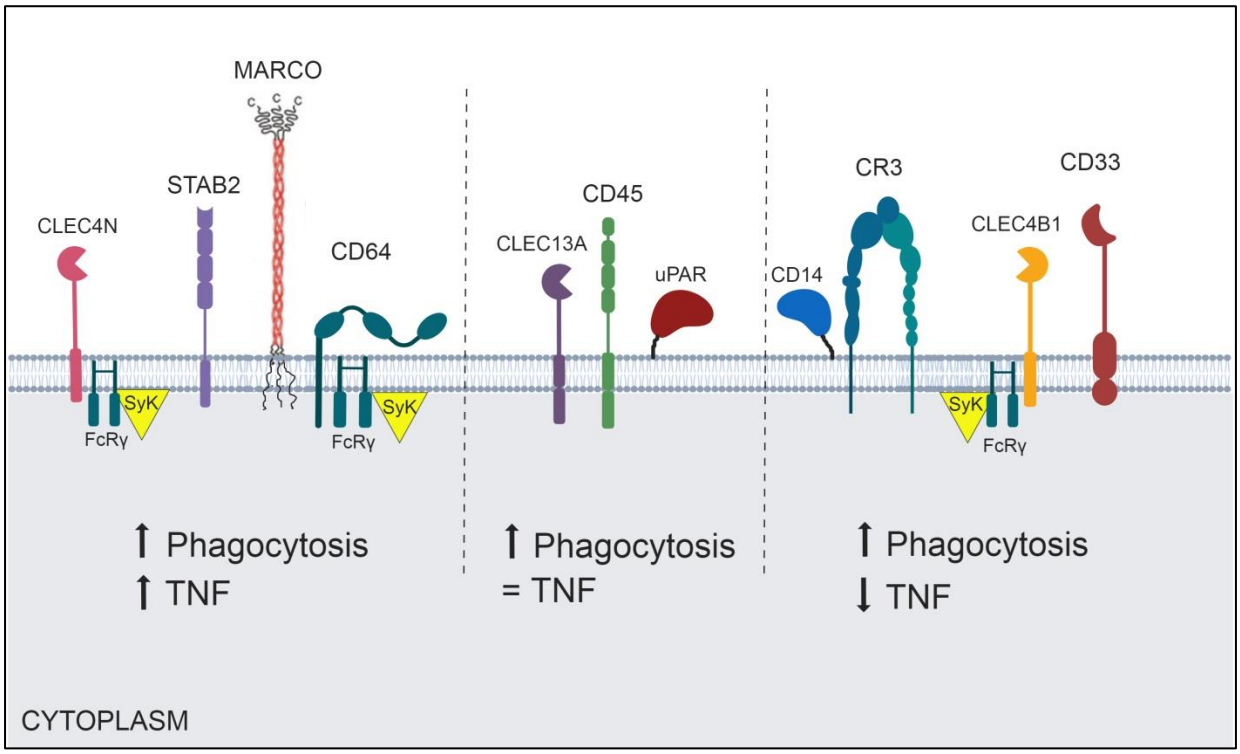

Figure 4: Representation of the receptors involved POSITIVELY in *B. burgdorferi* phagocytosis and their modulation in the TNF inflammatory response

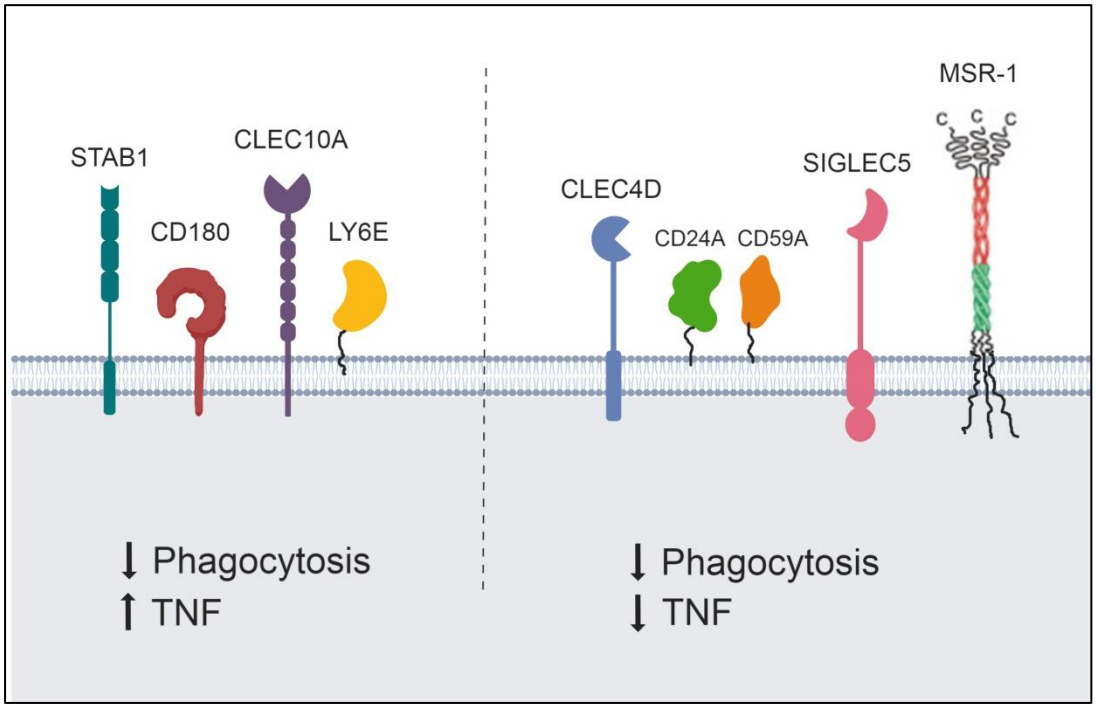

Figure 5: Representation of the receptors involved NEGATIVELY in *B. burgdorferi* phagocytosis and their modulation in the TNF production.

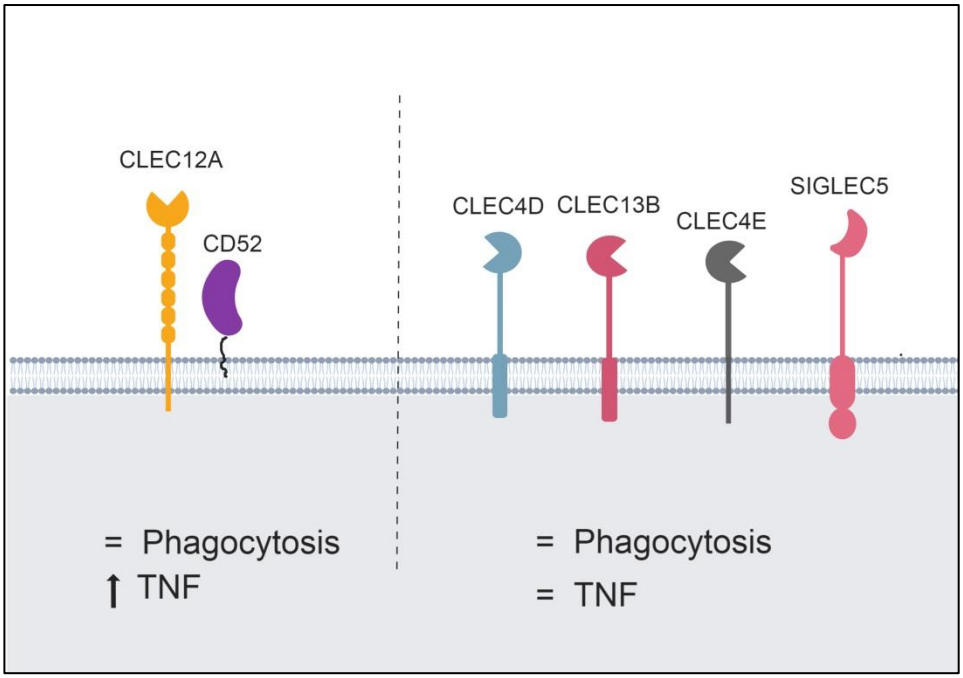

Figure 6: Representation of the receptors NOT INVOLVED in *B. burgdorferi* phagocytosis and their modulation in the TNF production.

Conclusions

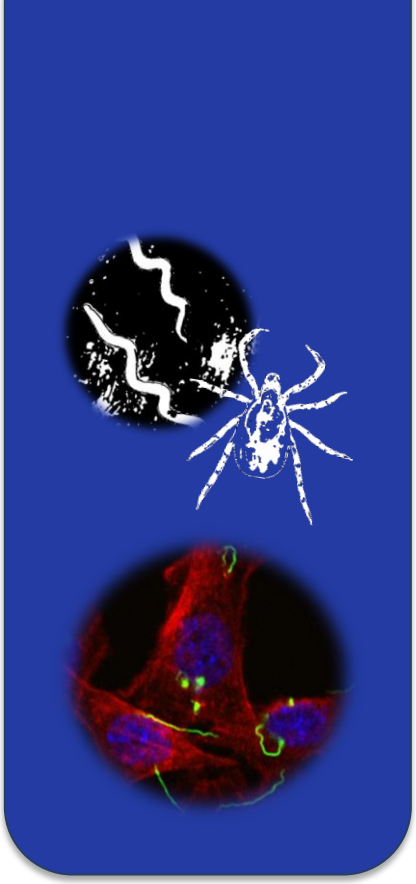

Conclusions

1. The use of large-scale analytical approaches revealed similar transcriptomics/proteomics profiles between human monocytes and murine macrophages in response to *B. burgdorferi,* showing the activation of the similar global traits and upstream activator pathways.

2. The proteome analysis of *B. burgdorferi*-containing phagosomes unveiled the regulation of macrophage activity by surface receptors involved in the ingestion of the spirochete and cytokine production.

3. CD180 modulates both phagocytosis and inflammation in response to *B. burgdorferi* through the transcriptional repression of complement receptor 3. This suggests the existence of multiple mechanisms of phagocytic and proinflammatory control that may be relevant at different phases of the response.

4. Several components of Fc gamma receptor family have been identified as phagocytic receptors for *B. burgdorferi* in the absence of antibodies, such as CD64 and CD45, revealing the implication of several signaling factors (SHIP1, FcRγ and Syk) in the process.

5. The description of a wide set of receptors belonging to the families of GPI-anchored proteins, Siglecs, C-type lectins and Scavenger receptors shows a complex mechanisms involved in *B. burgdorferi* phagocytosis and the ensuing inflammatory response.

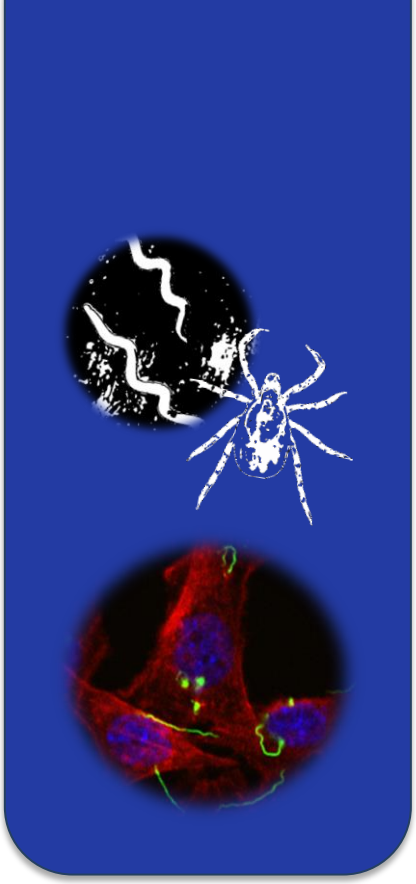

Suplemmentary material

Supplementary Table S1 Genes associated with phagocytosis and activation of phagocytes and their corresponding regulation in both BMMs and hMon stimulated with *B. burgdorferi* compared to unstimulated samples

Values in bold represent significantly regulated genes. Those genes regulated in the same direction are marked either in orange (upregulated in both analysis) or green (downregulated).

Mouse	Human	Entrez Gene Name	BMM		hMon	
			Log2(Ratio)	p-value	Log2(Ratio)	p-value
Phagocytosis						
Cd38	*CD38*	CD38 molecule	**9.924**	**3.33E-50**	0.013	9.13E-01
sf3	*CSF3*	colony stimulating factor 3	**9.086**	**1.58E-52**	**1.385**	**3.75E-05**
Il1b	*IL1B*	interleukin 1 beta	**7.704**	**7.83E-23**	**2.474**	**7.42E-07**
Il6	*IL6*	interleukin 6	**7.634**	**2.72E-22**	**6.014**	**6.61E-08**
Saa1	*SAA1*	serum amyloid A1	**6.811**	**2.75E-16**	NA	NA
Syt7	*SYT7*	synaptotagmin 7	**6.429**	**5.80E-18**	-0.069	5.17E-01
Cav1	*CAV1*	caveolin 1	**6.385**	**8.93E-69**	**1.451**	**3.80E-04**
Adora2a	*ADORA2A*	adenosine A2a receptor	**6.002**	**5.85E-70**	**2.929**	**3.23E-07**
Adora2b	*ADORA2B*	adenosine A2b receptor	**5.632**	**9.01E-136**	-0.391	1.40E-02
Lcn2	*LCN2*	lipocalin 2	**5.578**	**4.55E-11**	-0.077	5.47E-01
Tnf	*TNF*	tumor necrosis factor	**5.2**	**5.17E-77**	**3.336**	**7.92E-05**
Clec4n	*CLEC6A*	C-type lectin domain family 6 member A	**4.759**	**7.15E-33**	0.035	8.01E-01
Isg15	*ISG15*	ISG15 ubiquitin-like modifier	**4.731**	**2.97E-34**	**-1.692**	**1.93E-02**
Spic	*SPIC*	Spi-C transcription factor	**4.584**	**1.06E-23**	-0.078	3.98E-01
F10	*F10*	coagulation factor X	**4.091**	**7.04E-07**	NA	NA
Mir125a	*mir-10*	microRNA 100	**4.054**	**3.78E-04**	-0.053	7.18E-01
Src	*SRC*	SRC proto-oncogene. non-receptor tyrosine kinase	**3.85**	**2.93E-22**	**2.341**	**2.13E-07**
Hmox1	*HMOX1*	heme oxygenase 1	**3.722**	**3.37E-93**	**-1.424**	**4.92E-06**
Fpr1	*FPR1*	formyl peptide receptor 1	**3.666**	**1.18E-03**	**-1.858**	**1.12E-06**
Mirlet7e	*let-7*	microRNA let-7a-1	**3.642**	**2.10E-03**	0.145	1.06E-01
Il10	*IL10*	interleukin 10	**3.568**	**1.42E-59**	**1.929**	**3.52E-05**
Ehd1	*EHD1*	EH domain containing 1	**3.535**	**1.02E-29**	**1.261**	**4.08E-05**
Cxcl10	*CXCL10*	C-X-C motif chemokine ligand 10	**3.487**	**1.09E-04**	NA	NA
Nod2	*NOD2*	nucleotide binding oligomerization domain containing 2	**3.373**	**5.60E-62**	**-2.011**	**4.88E-05**
Pla2g4a	*PLA2G4A*	phospholipase A2 group IVA	**3.261**	**4.82E-52**	NA	NA
Fas	*FAS*	Fas cell surface death receptor	**3.204**	**6.59E-05**	NA	NA
Irf7	*IRF7*	interferon regulatory factor 7	**3.163**	**5.20E-20**	-0.353	2.17E-01
Csf2	*CSF2*	colony stimulating factor 2	**3.14**	**1.16E-02**	**3.814**	**9.01E-06**
Pf4	*PF4*	platelet factor 4	**3.13**	**2.76E-48**	NA	NA
Ly75	*LY75*	lymphocyte antigen 75	**2.954**	**9.11E-06**	NA	NA
Cebpb	*CEBPB*	CCAAT/enhancer binding protein beta	**2.768**	**3.05E-28**	0.332	5.43E-03
Fcgr2b	*FCGR2B*	Fc fragment of IgG receptor IIb	**2.708**	**2.48E-23**	0.621	1.19E-01
Camp	*CAMP*	cathelicidin antimicrobial peptide	**2.677**	**8.79E-03**	-0.293	8.35E-03

Pla2g5	*PLA2G5*	phospholipase A2 group V	**2.588**	**7.69E-03**	NA	NA
Ets2	*ETS2*	ETS proto-oncogene 2. transcription factor	**2.475**	**4.73E-94**	**1.896**	**1.80E-05**
Tlr1	*TLR1*	toll like receptor 1	**2.446**	**3.21E-11**	NA	NA
Msr1	*MSR1*	macrophage scavenger receptor 1	**2.437**	**3.36E-59**	NA	NA
Cd14	*CD14*	CD14 molecule	**2.32**	**7.36E-21**	-0.236	7.25E-01
Slc11a1	*SLC11A1*	solute carrier family 11 member 1	**2.316**	**1.79E-34**	**-1.139**	**1.24E-03**
Plaur	*PLAUR*	plasminogen activator. urokinase receptor	**2.309**	**1.07E-45**	**1.326**	**5.17E-05**
Ccl2	*Ccl2*	chemokine (C-C motif) ligand 2	**2.255**	**5.73E-12**	NA	NA
Cd302	*CD302*	CD302 molecule	**2.16**	**1.36E-08**	**-1.94**	**1.36E-04**
Icam1	*ICAM1*	intercellular adhesion molecule 1	**2.138**	**1.48E-03**	**1.319**	**5.39E-05**
Abca1	*ABCA1*	ATP binding cassette subfamily A member 1	**1.953**	**3.56E-14**	**-1.215**	**2.49E-02**
Cybb	*CYBB*	cytochrome b-245 beta chain	**1.765**	**3.11E-07**	0.19	2.85E-01
Mapkapk2	*MAPKAPK 2*	mitogen-activated protein kinase-activated protein kinase 2	**1.763**	**7.23E-16**	-0.258	1.41E-02
Eif2ak2	*EIF2AK2*	eukaryotic translation initiation factor 2 alpha kinase 2	**1.758**	**9.08E-23**	**-1.448**	**1.05E-03**
Csf2rb	*CSF2RB*	colony stimulating factor 2 receptor beta common subunit	**1.653**	**1.08E-28**	0.074	4.47E-01
Thbs1	*THBS1*	thrombospondin 1	**1.613**	**8.43E-23**	0.292	7.83E-01
Hck	*HCK*	HCK proto-oncogene. Src family tyrosine kinase	**1.561**	**3.80E-19**	**1.842**	**1.87E-05**
Tlr2	*TLR2*	toll like receptor 2	**1.556**	**1.25E-02**	0.316	1.11E-02
Syk	*SYK*	spleen associated tyrosine kinase	**1.491**	**1.74E-22**	-0.2	1.06E-01
Ptx3	*PTX3*	pentraxin 3	**1.457**	**4.10E-02**	NA	NA
Scarf1	*SCARF1*	scavenger receptor class F member 1	**1.452**	**5.74E-07**	0.562	1.65E-03
Prkce	*PRKCE*	protein kinase C epsilon	**1.378**	**1.14E-04**	NA	NA
Mif	*MIF*	macrophage migration inhibitory factor (glycosylation-inhibiting factor)	**1.367**	**3.53E-23**	-0.241	2.29E-01
Pip5k1a	*PIP5K1A*	phosphatidylinositol-4-phosphate 5-kinase type 1 alpha	**1.234**	**1.46E-14**	0.013	9.21E-01
Cat	*CAT*	catalase	**1.223**	**2.50E-08**	**-1.656**	**7.41E-06**
Treml2	*TREML2*	triggering receptor expressed on myeloid cells like 2	**1.196**	**3.56E-03**	NA	NA
Abca7	*ABCA7*	ATP binding cassette subfamily A member 7	**1.183**	**1.42E-04**	-0.933	4.90E-04
Serpine1	*SERPINE1*	serpin family E member 1	**1.126**	**1.20E-02**	0.075	4.50E-01
Myh9	*MYH9*	myosin heavy chain 9	**1.104**	**3.56E-21**	-0.25	2.47E-02
Ptger2	*PTGER2*	prostaglandin E receptor 2	**1.093**	**1.01E-04**	0.668	2.48E-03
Coro1a	*CORO1A*	coronin 1A	**-1.034**	**2.36E-05**	**-2.956**	**8.71E-08**
Itgax	*ITGAX*	integrin subunit alpha X	**-1.042**	**3.89E-05**	0.612	1.19E-02
Swap70	*SWAP70*	SWAP switching B-cell complex subunit 70	**-1.062**	**4.54E-15**	0.548	3.66E-03
Rab31	*RAB31*	RAB31. member RAS oncogene family	**-1.064**	**3.56E-13**	**1.144**	**4.86E-04**
Padi4	*PADI4*	peptidyl arginine deiminase 4	**-1.096**	**4.00E-02**	**-3.58**	**1.82E-06**

Mfge8	*MFGE8*	milk fat globule-EGF factor 8 protein	**-1.117**	**2.43E-06**	-0.324	7.07E-02
Cerk	*CERK*	ceramide kinase	**-1.159**	**5.82E-16**	-0.401	2.35E-02
Vwf	*VWF*	von Willebrand factor	**-1.173**	**1.75E-09**	-0.323	8.45E-03
P2rx7	*P2RX7*	purinergic receptor P2X 7	**-1.208**	**8.56E-06**	**2.948**	**5.35E-05**
Lgals3	*LGALS3*	galectin 3	**-1.215**	**7.76E-10**	0.936	8.72E-04
Fgr	*FGR*	FGR proto-oncogene. Src family tyrosine kinase	**-1.23**	**3.64E-02**	-0.35	1.64E-02
Ptger4	*PTGER4*	prostaglandin E receptor 4	**-1.266**	**2.12E-04**	0.485	1.76E-01
Camk1d	*CAMK1D*	calcium/calmodulin dependent protein kinase ID	**-1.28**	**5.95E-10**	-0.139	1.58E-01
Dock1	*DOCK1*	dedicator of cytokinesis 1	**-1.282**	**3.87E-06**	NA	NA
Myc	*MYC*	v-myc avian myelocytomatosis viral oncogene homolog	**-1.288**	**9.08E-04**	-0.578	7.59E-03
Rora	*RORA*	RAR related orphan receptor A	**-1.292**	**1.26E-05**	NA	NA
Mkl1	*MKL1*	megakaryoblastic leukemia (translocation) 1	**-1.326**	**1.58E-13**	-0.285	7.14E-03
Rras2	*RRAS2*	related RAS viral (r-ras) oncogene homolog 2	**-1.386**	**8.46E-03**	NA	NA
Gsn	*GSN*	gelsolin	**-1.645**	**2.84E-13**	-0.676	2.91E-03
Elmo1	*ELMO1*	engulfment and cell motility 1	**-1.783**	**3.43E-10**	-0.868	1.36E-04
Gp1ba	*GP1BA*	glycoprotein Ib platelet alpha subunit	**-1.814**	**5.75E-03**	-0.07	5.32E-01
Tecpr1	*TECPR1*	tectonin beta-propeller repeat containing 1	**-1.888**	**1.75E-32**	-0.372	5.49E-02
Trem2	*TREM2*	triggering receptor expressed on myeloid cells 2	**-2.026**	**7.70E-21**	NA	NA
Fyn	*FYN*	FYN proto-oncogene. Src family tyrosine kinase	**-2.069**	**8.63E-14**	**-1.045**	**6.38E-05**
Mcoln3	*MCOLN3*	mucolipin 3	**-2.07**	**1.08E-14**	0.561	2.10E-02
Colec12	*COLEC12*	collectin subfamily member 12	**-2.108**	**2.00E-17**	NA	NA
Plau	*PLAU*	plasminogen activator. urokinase	**-2.119**	**9.07E-10**	0.574	3.43E-03
Ucp2	*UCP2*	uncoupling protein 2	**-2.129**	**5.52E-24**	**-1.085**	**1.34E-04**
Pros1	*PROS1*	protein S (alpha)	**-2.172**	**4.41E-23**	-0.022	8.73E-01
Osbp2	*OSBP2*	oxysterol binding protein 2	**-2.175**	**1.77E-03**	NA	NA
Rapgef3	*RAPGEF3*	Rap guanine nucleotide exchange factor 3	**-2.194**	**1.30E-08**	NA	NA
Megf10	*MEGF10*	multiple EGF like domains 10	**-2.239**	**2.74E-02**	NA	NA
C1qa	*C1QA*	complement C1q A chain	**-2.259**	**1.05E-41**	NA	NA
Klf2	*KLF2*	Kruppel like factor 2	**-2.301**	**3.51E-10**	**-3.7**	**7.14E-08**
Pld4	*PLD4*	phospholipase D family member 4	**-2.302**	**9.52E-12**	0.049	6.26E-01
Mex3b	*MEX3B*	mex-3 RNA binding family member B	**-2.38**	**1.29E-07**	-0.166	1.43E-01
Anxa1	*ANXA1*	annexin A1	**-2.447**	**1.40E-51**	-0.468	6.67E-02
Hgf	*HGF*	hepatocyte growth factor	**-2.566**	**5.64E-17**	NA	NA
Rsph1	*RSPH1*	radial spoke head 1 homolog	**-2.611**	**1.03E-02**	NA	NA
Clec7a	*CLEC7A*	C-type lectin domain family 7 member A	**-2.776**	**1.84E-38**	-0.503	4.31E-04
Fgf10	*FGF10*	fibroblast growth factor 10	**-2.785**	**2.85E-02**	NA	NA
Rab27a	*RAB27A*	RAB27A. member RAS oncogene	**-2.799**	**1.36E-06**	0.072	4.95E-01

		family				
Cd4	*CD4*	CD4 molecule	**-2.824**	**1.12E-14**	**-1.278**	**1.40E-06**
Ckb	*CKB*	creatine kinase B	**-2.906**	**1.61E-21**	**1.407**	**1.02E-05**
Itgb5	*ITGB5*	integrin subunit beta 5	**-2.914**	**2.85E-20**	0.002	9.93E-01
Stab2	*STAB2*	stabilin 2	**-2.97**	**8.38E-04**	NA	NA
Gas6	*GAS6*	growth arrest specific 6	**-3.014**	**7.17E-74**	-0.645	1.88E-04
Dock2	*DOCK2*	dedicator of cytokinesis 2	**-3.063**	**2.16E-20**	**-1.4**	**1.16E-06**
Cd93	*CD93*	CD93 molecule	**-3.174**	**1.79E-50**	0.019	9.79E-01
Mrc1	*MRC1*	mannose receptor C-type 1	**-3.179**	**4.95E-27**	NA	NA
S100a9	*S100A9*	S100 calcium binding protein A9	**-3.365**	**5.19E-03**	**-3.713**	**2.40E-05**
Sirpb1b	*SIRPB1*	signal regulatory protein beta 1	**-3.403**	**5.97E-22**	-0.422	5.20E-04
Cx3cl1	*CX3CL1*	C-X3-C motif chemokine ligand 1	**-3.477**	**1.32E-04**	NA	NA
Mertk	*MERTK*	MER proto-oncogene. tyrosine kinase	**-3.498**	**1.20E-19**	-0.71	8.52E-04
Tlr9	*TLR9*	toll like receptor 9	**-3.755**	**1.24E-30**	NA	NA
Pparg	*PPARG*	peroxisome proliferator activated receptor gamma	**-3.815**	**9.15E-30**	0.307	8.52E-02
Cyp2s1	*CYP2S1*	cytochrome P450 family 2 subfamily S member 1	**-4.033**	**1.10E-06**	**-1.162**	**3.46E-05**

Activation of phagocytes

Il1a	*IL1A*	interleukin 1 alpha	**9.307**	**2.85E-222**	**6.543**	**1.43E-08**
Csf3	*CSF3*	colony stimulating factor 3	**9.086**	**1.58E-52**	**1.385**	**3.75E-05**
Ptgs2	*PTGS2*	prostaglandin-endoperoxide synthase 2	**8.664**	**4.97E-113**	**4.006**	**1.95E-05**
Met	*MET*	MET proto-oncogene. receptor tyrosine kinase	**7.953**	**3.43E-201**	**1.742**	**1.05E-05**
Ptges	*PTGES*	prostaglandin E synthase	**7.764**	**1.94E-43**	**-1.006**	**8.68E-04**
Il1b	*IL1B*	interleukin 1 beta	**7.704**	**7.83E-23**	**2.474**	**7.42E-07**
Il6	*IL6*	interleukin 6	**7.634**	**2.72E-22**	**6.014**	**6.61E-08**
Il19	*IL19*	interleukin 19	**7.603**	**4.65E-18**	**6.406**	**1.36E-08**
S100a8	*S100A8*	S100 calcium binding protein A8	**7.377**	**2.15E-89**	**-4.124**	**1.18E-05**
Cxcl2	*CXCL3*	C-X-C motif chemokine ligand 3	**6.888**	**1.71E-17**	0.191	1.07E-01
Saa1	*SAA1*	serum amyloid A1	**6.811**	**2.75E-16**	NA	NA
Inhba	*INHBA*	inhibin beta A subunit	**6.679**	**3.02E-53**	NA	NA
Il1rn	*IL1RN*	interleukin 1 receptor antagonist	**6.515**	**3.81E-176**	**3.941**	**1.35E-06**
Nos2	*NOS2*	nitric oxide synthase 2	**6.355**	**1.21E-09**	NA	NA
Edn1	*EDN1*	endothelin 1	**6.33**	**5.70E-26**	1.159	9.09E-05
Slc7a2	*SLC7A2*	solute carrier family 7 member 2	**6.219**	**1.89E-95**	NA	NA
Slpi	*SLPI*	secretory leukocyte peptidase inhibitor	**5.956**	**5.72E-19**	NA	NA
Hamp	*Hamp/Hamp2*	hepcidin antimicrobial peptide	**5.664**	**1.02E-08**	NA	NA
Adora2b	*ADORA2B*	adenosine A2b receptor	**5.632**	**9.01E-136**	-0.391	1.40E-02
Lcn2	*LCN2*	lipocalin 2	**5.578**	**4.55E-11**	-0.077	5.47E-01
Socs1	*SOCS1*	suppressor of cytokine signaling 1	**5.407**	**4.33E-46**	**1.15**	**5.85E-05**
Tnf	*TNF*	tumor necrosis factor	**5.2**	**5.17E-77**	**3.336**	**7.92E-05**
Clec4e	*CLEC4E*	C-type lectin domain family 4 member E	**5.157**	**9.73E-08**	**1.178**	**2.24E-05**

Saa3	*Saa3*	serum amyloid A 3	**5.077**	**1.26E-06**	NA	NA
Mir125a	*mir-10*	microRNA 100	**4.054**	**3.78E-04**	-0.053	7.18E-01
Ifi205	*IFI16*	interferon gamma inducible protein 16	**4.051**	**5.94E-61**	0.544	5.86E-03
Cd40	*CD40*	CD40 molecule	**4.035**	**9.00E-59**	**1.229**	**1.87E-05**
Ahr	*AHR*	aryl hydrocarbon receptor	**3.976**	**1.31E-20**	0.309	3.38E-02
Itga1	*ITGA1*	integrin subunit alpha 1	**3.956**	**4.45E-12**	**2.582**	**6.55E-07**
Ccl5	*CCL5*	C-C motif chemokine ligand 5	**3.917**	**1.69E-10**	**1.453**	**6.84E-04**
Src	*SRC*	SRC proto-oncogene. non-receptor tyrosine kinase	**3.85**	**2.93E-22**	**2.341**	**2.13E-07**
Hmox1	*HMOX1*	heme oxygenase 1	**3.722**	**3.37E-93**	**-1.424**	**4.92E-06**
Fpr1	*FPR1*	formyl peptide receptor 1	**3.666**	**1.18E-03**	**-1.858**	**1.12E-06**
Mirlet7e	*let-7*	microRNA let-7a-1	**3.642**	**2.10E-03**	0.145	1.06E-01
Il10	*IL10*	interleukin 10	**3.568**	**1.42E-59**	**1.929**	**3.52E-05**
Cxcl5	*CXCL6*	C-X-C motif chemokine ligand 6	**3.514**	**6.52E-11**	0.582	4.29E-04
Cxcl10	*CXCL10*	C-X-C motif chemokine ligand 10	**3.487**	**1.09E-04**	NA	NA
Fpr2	*FPR2*	formyl peptide receptor 2	**3.427**	**3.96E-03**	0.534	1.45E-04
Mir146	*mir-146*	microRNA 146a	**3.389**	**5.19E-03**	0.05	7.80E-01
Jak2	*JAK2*	Janus kinase 2	**3.362**	**1.54E-71**	-0.198	1.34E-01
Fas	*FAS*	Fas cell surface death receptor	**3.204**	**6.59E-05**	NA	NA
Csf2	*CSF2*	colony stimulating factor 2	**3.14**	**1.16E-02**	**3.814**	**9.01E-06**
Pf4	*PF4*	platelet factor 4	**3.13**	**2.76E-48**	NA	NA
Lta	*LTA*	lymphotoxin alpha	**3.106**	**1.92E-03**	0.245	4.64E-02
Hc	*C5*	complement C5	**2.795**	**2.88E-02**	-0.55	2.76E-04
Cebpb	*CEBPB*	CCAAT/enhancer binding protein beta	**2.768**	**3.05E-28**	0.332	5.43E-03
Tnfrsf1b	*TNFRSF1B*	TNF receptor superfamily member 1B	**2.736**	**1.22E-38**	0.875	2.12E-03
Cd200	*CD200*	CD200 molecule	**2.692**	**8.12E-28**	0.186	8.65E-02
Camp	*CAMP*	cathelicidin antimicrobial peptide	**2.677**	**8.79E-03**	-0.293	8.35E-03
Ifnb1	*IFNB1*	interferon beta 1	**2.673**	**3.87E-02**	NA	NA
Notch1	*NOTCH1*	notch 1	**2.611**	**1.09E-38**	-0.962	1.85E-03
Pla2g5	*PLA2G5*	phospholipase A2 group V	**2.588**	**7.69E-03**	NA	NA
Msr1	*MSR1*	macrophage scavenger receptor 1	**2.437**	**3.36E-59**	NA	NA
Ccl22	*CCL22*	C-C motif chemokine ligand 22	**2.409**	**3.02E-04**	**1.048**	**4.38E-06**
Snca	*SNCA*	synuclein alpha	**2.404**	**1.72E-02**	**1.564**	**7.40E-05**
Cd14	*CD14*	CD14 molecule	**2.32**	**7.36E-21**	-0.236	7.25E-01
Slc11a1	*SLC11A1*	solute carrier family 11 member 1	**2.316**	**1.79E-34**	**-1.139**	**1.24E-03**
H2-Q7	*HLA-A*	major histocompatibility complex. class I. A	**2.265**	**1.74E-22**	0.368	2.67E-01
Ccl2	*Ccl2*	chemokine (C-C motif) ligand 2	**2.255**	**5.73E-12**	NA	NA
Cd24a	*Cd24a*	CD24a antigen	**2.246**	**3.61E-03**	NA	NA
Cd1d1	*CD1D*	CD1d molecule	**2.191**	**1.81E-11**	**-3.53**	**7.41E-08**
Tnfrsf9	*TNFRSF9*	TNF receptor superfamily member 9	**2.189**	**2.86E-04**	0.938	1.22E-05
Icam1	*ICAM1*	intercellular adhesion molecule 1	**2.138**	**1.48E-03**	**1.319**	**5.39E-05**
Nfil3	*NFIL3*	nuclear factor. interleukin 3 regulated	**2.122**	**3.12E-23**	**-1.808**	**7.44E-07**

Itga5	*ITGA5*	integrin subunit alpha 5	**1.996**	**2.89E-29**	**0.999**	**7.08E-04**
Lgals9	*LGALS9B*	galectin 9B	**1.973**	**2.66E-27**	NA	NA
Ccl4	*CCL4*	C-C motif chemokine ligand 4	**1.919**	**3.46E-21**	NA	NA
Stat1	*STAT1*	signal transducer and activator of transcription 1	**1.854**	**3.69E-12**	**-1.447**	**6.77E-03**
Il4ra	*IL4R*	interleukin 4 receptor	**1.84**	**8.82E-40**	-0.149	1.67E-01
Tnfrsf10b	*TNFRSF10 A*	TNF receptor superfamily member 10a	**1.768**	**9.57E-07**	0.249	1.06E-02
Cybb	*CYBB*	cytochrome b-245 beta chain	**1.765**	**3.11E-07**	0.19	2.85E-01
Ccr7	*CCR7*	C-C motif chemokine receptor 7	**1.705**	**2.59E-02**	**5.55**	**7.66E-08**
Thbs1	*THBS1*	thrombospondin 1	**1.613**	**8.43E-23**	0.292	7.83E-01
Hck	*HCK*	HCK proto-oncogene. Src family tyrosine kinase	**1.561**	**3.80E-19**	**1.842**	**1.87E-05**
Tlr2	*TLR2*	toll like receptor 2	**1.556**	**1.25E-02**	0.316	1.11E-02
Gja1	*GJA1*	gap junction protein alpha 1	**1.549**	**1.66E-13**	NA	NA
Lcp2	*LCP2*	lymphocyte cytosolic protein 2	**1.54**	**9.11E-15**	0.454	2.64E-02
Syk	*SYK*	spleen associated tyrosine kinase	**1.491**	**1.74E-22**	-0.2	1.06E-01
Sbno2	*SBNO2*	strawberry notch homolog 2	**1.489**	**7.00E-22**	-0.199	1.76E-01
Casp1	*CASP1*	caspase 1	**1.403**	**1.42E-11**	**1.666**	**3.90E-06**
Lgals3bp	*LGALS3BP*	galectin 3 binding protein	**1.389**	**9.84E-13**	-0.378	5.48E-02
Prkce	*PRKCE*	protein kinase C epsilon	**1.378**	**1.14E-04**	NA	NA
Trpm4	*TRPM4*	transient receptor potential cation channel subfamily M member 4	**1.374**	**6.02E-12**	-0.836	3.36E-05
Clcn7	*CLCN7*	chloride voltage-gated channel 7	**1.372**	**1.34E-20**	**1.131**	**3.03E-05**
Mif	*MIF*	macrophage migration inhibitory factor (glycosylation-inhibiting factor)	**1.367**	**3.53E-23**	-0.241	2.29E-01
Osm	*OSM*	oncostatin M	**1.319**	**3.07E-09**	**1.894**	**4.00E-04**
Il1r1	*IL1R1*	interleukin 1 receptor type 1	**1.216**	**4.88E-02**	0.348	1.74E-03
Treml2	*TREML2*	triggering receptor expressed on myeloid cells like 2	**1.196**	**3.56E-03**	NA	NA
Bid	*BID*	BH3 interacting domain death agonist	**1.114**	**4.72E-06**	0.819	5.76E-05
Rabgef1	*RABGEF1*	RAB guanine nucleotide exchange factor 1	**1.114**	**8.77E-14**	0.098	2.78E-01
Ptger2	*PTGER2*	prostaglandin E receptor 2	**1.093**	**1.01E-04**	0.668	2.48E-03
Ulbp1	*ULBP1*	UL16 binding protein 1	**-1.028**	**4.99E-04**	-0.041	7.85E-01
Lrp1	*LRP1*	LDL receptor related protein 1	**-1.059**	**4.17E-05**	-0.834	1.13E-04
Cerk	*CERK*	ceramide kinase	**-1.159**	**5.82E-16**	-0.401	2.35E-02
P2rx7	*P2RX7*	purinergic receptor P2X 7	**-1.208**	**8.56E-06**	**2.948**	**5.35E-05**
Lgals3	*LGALS3*	galectin 3	**-1.215**	**7.76E-10**	0.936	8.72E-04
Apoe	*APOE*	apolipoprotein E	**-1.261**	**5.90E-15**	NA	NA
Ptger4	*PTGER4*	prostaglandin E receptor 4	**-1.266**	**2.12E-04**	0.485	1.76E-01
Rarres2	*RARRES2*	retinoic acid receptor responder 2	**-1.279**	**1.82E-05**	NA	NA
Rora	*RORA*	RAR related orphan receptor A	**-1.292**	**1.26E-05**	NA	NA
Prnp	*PRNP*	prion protein	**-1.302**	**1.77E-12**	-0.132	4.10E-01
Tyrobp	*TYROBP*	TYRO protein tyrosine kinase binding protein	**-1.303**	**4.86E-31**	**-1.629**	**1.30E-05**

Tpt1	*TPT1*	tumor protein. translationally-controlled 1	**-1.354**	**1.28E-18**	-0.68	3.60E-01
Il18	*IL18*	interleukin 18	**-1.358**	**2.47E-03**	-0.424	7.07E-03
Cd300ld	*CD300LD*	CD300 molecule like family member d	**-1.385**	**2.80E-24**	NA	NA
Ltbp1	*LTBP1*	latent transforming growth factor beta binding protein 1	**-1.643**	**2.29E-03**	NA	NA
Metrnl	*METRNL*	meteorin like. glial cell differentiation regulator	**-1.664**	**2.01E-25**	-0.377	2.31E-02
Shpk	*SHPK*	sedoheptulokinase	**-1.68**	**5.53E-05**	-0.265	1.09E-01
Tnfaip8l2	*TNFAIP8L 2*	TNF alpha induced protein 8 like 2	**-1.7**	**1.47E-29**	0.158	2.01E-01
Tspan32	*TSPAN32*	tetraspanin 32	**-1.733**	**5.32E-07**	**-3.719**	**1.03E-07**
Tnfsf12	*TNFSF12*	tumor necrosis factor superfamily member 12	**-1.797**	**1.40E-23**	-0.884	1.63E-04
Cd300lb	*CD300LB*	CD300 molecule like family member b	**-1.815**	**1.13E-31**	**-1.19**	**3.00E-06**
Havcr2	*HAVCR2*	hepatitis A virus cellular receptor 2	**-1.815**	**3.47E-06**	0.649	2.55E-02
C5ar1	*C5AR1*	complement C5a receptor 1	**-1.943**	**9.62E-17**	**-1.549**	**2.09E-05**
Fn1	*FN1*	fibronectin 1	**-1.95**	**1.80E-02**	NA	NA
Igf1	*IGF1*	insulin like growth factor 1	**-1.988**	**7.16E-35**	NA	NA
Abhd12	*ABHD12*	abhydrolase domain containing 12	**-1.992**	**1.57E-19**	0.068	5.37E-01
Trem2	*TREM2*	triggering receptor expressed on myeloid cells 2	**-2.026**	**7.70E-21**	NA	NA
Kitl	*KITLG*	KIT ligand	**-2.035**	**6.29E-03**	NA	NA
Pros1	*PROS1*	protein S (alpha)	**-2.172**	**4.41E-23**	-0.022	8.73E-01
Rapgef3	*RAPGEF3*	Rap guanine nucleotide exchange factor 3	**-2.194**	**1.30E-08**	NA	NA
Il18rap	*IL18RAP*	interleukin 18 receptor accessory protein	**-2.394**	**1.37E-02**	-0.218	2.28E-02
Ptger3	*PTGER3*	prostaglandin E receptor 3	**-2.406**	**2.31E-02**	0.153	9.53E-02
Rhoh	*RHOH*	ras homolog family member H	**-2.409**	**1.29E-16**	0.531	1.84E-04
Angpt2	*ANGPT2*	angiopoietin 2	**-2.413**	**3.97E-07**	NA	NA
Anxa1	*ANXA1*	annexin A1	**-2.447**	**1.40E-51**	-0.468	6.67E-02
Maf	*MAF*	MAF bZIP transcription factor	**-2.499**	**9.61E-64**	-0.647	5.29E-03
Kit	*KIT*	KIT proto-oncogene receptor tyrosine kinase	**-2.538**	**4.13E-13**	NA	NA
Cd300a	*CD300A*	CD300a molecule	**-2.55**	**1.79E-22**	**-1.196**	**7.74E-06**
Hgf	*HGF*	hepatocyte growth factor	**-2.566**	**5.64E-17**	NA	NA
Tnfsf13	*TNFSF13*	tumor necrosis factor superfamily member 13	**-2.661**	**1.21E-08**	NA	NA
Clec7a	*CLEC7A*	C-type lectin domain family 7 member A	**-2.776**	**1.84E-38**	-0.503	4.31E-04
Tlr8	*TLR8*	toll like receptor 8	**-2.796**	**2.88E-76**	**1.004**	**7.38E-03**
Rab27a	*RAB27A*	RAB27A. member RAS oncogene family	**-2.799**	**1.36E-06**	0.072	4.95E-01
Cd4	*CD4*	CD4 molecule	**-2.824**	**1.12E-14**	**-1.278**	**1.40E-06**
Hpse	*HPSE*	heparanase	**-2.855**	**1.86E-33**	-0.433	2.08E-02

Ccr2	*CCR2*	C-C motif chemokine receptor 2	**-2.876**	**1.33E-15**	-0.226	2.17E-02
Cd93	*CD93*	CD93 molecule	**-3.174**	**1.79E-50**	0.019	9.79E-01
S100a9	*S100A9*	S100 calcium binding protein A9	**-3.365**	**5.19E-03**	**-3.713**	**2.40E-05**
Cnr2	*CNR2*	cannabinoid receptor 2	**-3.431**	**4.98E-19**	NA	NA
Cx3cl1	*CX3CL1*	C-X3-C motif chemokine ligand 1	**-3.477**	**1.32E-04**	NA	NA
Mertk	*MERTK*	MER proto-oncogene. tyrosine kinase	**-3.498**	**1.20E-19**	-0.71	8.52E-04
Cfh	*CFH*	complement factor H	**-3.522**	**1.72E-48**	NA	NA
Tlr9	*TLR9*	toll like receptor 9	**-3.755**	**1.24E-30**	NA	NA
Cx3cr1	*CX3CR1*	C-X3-C motif chemokine receptor 1	**-6.34**	**4.64E-47**	-0.674	3.91E-04

Supplementary Table S2 Proteins identified by LnMS/MS in BMMs stimulated with *B. burgdorferi* or left unstimulated

Those proteins represented by at least 2 peptides are included. Proteins differentially regulated are indicated (upregulated: shaded orange; downregulated: shaded green).

Accession	Description	Unique peptides	Log(Ratio Borr/Unst)	ANOVA
PGH2_MOUSE	Prostaglandin G/H synthase 2	2	4.845	2.65E-06
IRG1_MOUSE	Cis-aconitate decarboxylase	4	4.215	4.48E-04
CTR2_MOUSE	Cationic amino acid transporter 2	3	3.036	5.78E-03
CLC4E_MOUSE	C-type lectin domain family 4 member E	3	2.907	6.38E-04
GBP2_MOUSE	Guanylate-binding protein 1	5	2.683	6.24E-04
SQSTM_MOUSE	Sequestosome-1	6	2.668	1.67E-03
IL1B_MOUSE	Interleukin-1 beta	4	2.407	4.79E-03
DEOC_MOUSE	Deoxyribose-phosphate aldolase	2	2.347	1.18E-02
FCGR2_MOUSE	Low affinity immunoglobulin gamma Fc region receptor II	2	2.211	7.22E-03
HMOX1_MOUSE	Heme oxygenase 1	5	2.061	2.46E-03
ICAM1_MOUSE	Intercellular adhesion molecule 1	4	1.673	6.87E-03
DDX21_MOUSE	Nucleolar RNA helicase 2	3	1.509	5.48E-03
PRDX5_MOUSE	Peroxiredoxin-5, mitochondrial	9	1.437	9.02E-03
VPS4B_MOUSE	Vacuolar protein sorting-associated protein 4B	2	1.261	1.54E-02
CD14_MOUSE	Monocyte differentiation antigen CD14	7	1.246	6.25E-03
ACSL1_MOUSE	Long-chain-fatty-acid--CoA ligase 1	12	1.210	2.80E-03
4F2_MOUSE	4F2 cell-surface antigen heavy chain	6	1.135	6.33E-03
MYO1F_MOUSE	Unconventional myosin-If	5	-1.080	3.01E-02
CD36_MOUSE	Platelet glycoprotein 4	4	-1.110	6.80E-03
NPC1_MOUSE	Niemann-Pick C1 protein	3	-1.126	4.35E-02
AGAL_MOUSE	Alpha-galactosidase A	2	-1.133	4.46E-02
LKHA4_MOUSE	Leukotriene A-4 hydrolase	6	-1.138	9.15E-03
AP3B1_MOUSE	AP-3 complex subunit beta-1	2	-1.147	4.69E-03
STOM_MOUSE	Erythrocyte band 7 integral membrane protein	4	-1.150	1.17E-02
LRP1_MOUSE	Prolow-density lipoprotein receptor-related protein 1	15	-1.166	3.84E-02
CSF1R_MOUSE	Macrophage colony-stimulating factor 1 receptor	3	-1.199	3.12E-02
SCMC1_MOUSE	Calcium-binding mitochondrial carrier protein SCaMC-1	2	-1.218	9.82E-03
ACL6A_MOUSE	Actin-like protein 6A	2	-1.268	3.67E-02
LGMN_MOUSE	Legumain	3	-1.303	2.37E-02

PP2BA_MOUSE	Serine/threonine-protein phosphatase 2B catalytic subunit alpha isoform	2	-1.349	2.60E-03
CD180_MOUSE	CD180 antigen	2	-1.349	1.65E-02
PLST_MOUSE	Plastin-3	4	-1.418	4.58E-02
WASP_MOUSE	Wiskott-Aldrich syndrome protein homolog	4	-1.665	4.06E-02
NIBAN_MOUSE	Protein Niban	2	-1.951	3.86E-02
LIPL_MOUSE	Lipoprotein lipase	2	-2.430	1.55E-02
PEBP1_MOUSE	Phosphatidylethanolamine-binding protein 1	2	2.607	1.05E-01
TXNL1_MOUSE	Thioredoxin-like protein 1	2	2.355	1.05E-01
TMA16_MOUSE	Translation machinery-associated protein 16	2	2.103	6.10E-02
MYO1C_MOUSE	Unconventional myosin-Ic	2	2.087	2.75E-01
RS17_MOUSE	40S ribosomal protein S17	2	1.834	1.95E-01
PROSC_MOUSE	Proline synthase co-transcribed bacterial homolog protein	2	1.417	3.03E-01
SUCB1_MOUSE	Succinyl-CoA ligase [ADP-forming] subunit beta, mitochondrial	3	1.328	5.97E-02
ASSY_MOUSE	Argininosuccinate synthase	2	1.108	8.46E-02
IFM3_MOUSE	Interferon-induced transmembrane protein 3	2	1.083	1.17E-01
TBA4A_MOUSE	Tubulin alpha-4A chain	12	1.059	1.46E-01
SODM_MOUSE	Superoxide dismutase [Mn], mitochondrial	2	1.042	9.68E-02
RL21_MOUSE	60S ribosomal protein L21 OS=Mus musculus GN=Rpl21 PE=1 SV=3	2	1.041	2.19E-01
HNRL2_MOUSE	Heterogeneous nuclear ribonucleoprotein U-like protein 2	2	1.031	1.59E-01
SMRC2_MOUSE	SWI/SNF complex subunit SMARCC2	2	1.018	8.13E-02
PTN1_MOUSE	Tyrosine-protein phosphatase non-receptor type 1	4	1.003	1.03E-01
FLII_MOUSE	Protein flightless-1 homolog	4	0.988	5.40E-01
XPP1_MOUSE	Xaa-Pro aminopeptidase 1	2	0.960	2.16E-01
LRC25_MOUSE	Leucine-rich repeat-containing protein 25	4	0.944	7.71E-02
VATD_MOUSE	V-type proton ATPase subunit D	3	0.941	3.90E-01
ACSL4_MOUSE	Long-chain-fatty-acid--CoA ligase 4	4	0.879	2.03E-02
TLR2_MOUSE	Toll-like receptor 2	3	0.862	8.20E-02
AGRE1_MOUSE	Adhesion G protein-coupled receptor E1	3	0.851	1.73E-01
EFHD2_MOUSE	EF-hand domain-containing protein D2	6	0.839	2.04E-01
ODP2_MOUSE	Dihydrolipoyllysine-residue acetyltransferase component of pyruvate dehydrogenase complex, mitochondrial	2	0.830	1.82E-01
CY24B_MOUSE	Cytochrome b-245 heavy chain	2	0.816	1.07E-01
E2AK2_MOUSE	Interferon-induced, double-stranded RNA-activated protein kinase	3	0.811	1.68E-01
MANF_MOUSE	Mesencephalic astrocyte-derived neurotrophic factor	2	0.807	1.31E-01
SH3K1_MOUSE	SH3 domain-containing kinase-binding protein 1	2	0.775	3.29E-01
EHD1_MOUSE	EH domain-containing protein 1	6	0.771	4.01E-02

AMPD3_MOUSE	AMP deaminase 3	3	0.765	1.08E-01
TWF1_MOUSE	Twinfilin-1	2	0.754	1.48E-01
XDH_MOUSE	Xanthine dehydrogenase/oxidase	2	0.753	3.46E-01
PLEK_MOUSE	Pleckstrin	2	0.726	2.02E-01
PSD11_MOUSE	26S proteasome non-ATPase regulatory subunit 11	5	0.725	9.64E-02
IDE_MOUSE	Insulin-degrading enzyme	2	0.712	2.79E-01
PNPH_MOUSE	Purine nucleoside phosphorylase	8	0.668	7.26E-02
NCF1_MOUSE	Neutrophil cytosol factor 1	2	0.667	2.27E-01
AT1B3_MOUSE	Sodium/potassium-transporting ATPase subunit beta-3	2	0.661	2.34E-01
FYB_MOUSE	FYN-binding protein	3	0.659	3.06E-02
IF5A1_MOUSE	Eukaryotic translation initiation factor 5A-1	2	0.653	1.37E-01
NAMPT_MOUSE	Nicotinamide phosphoribosyltransferase	6	0.647	1.30E-01
TRXR1_MOUSE	Thioredoxin reductase 1, cytoplasmic	5	0.631	5.88E-02
IFIT3_MOUSE	Interferon-induced protein with tetratricopeptide repeats 3	4	0.629	2.99E-01
EIF3D_MOUSE	Eukaryotic translation initiation factor 3 subunit D	3	0.627	1.16E-01
DCTN2_MOUSE	Dynactin subunit 2	2	0.611	1.01E-01
IFIT1_MOUSE	Interferon-induced protein with tetratricopeptide repeats 1	3	0.601	9.74E-02
PSB3_MOUSE	Proteasome subunit beta type-3	2	0.598	7.31E-03
NP1L4_MOUSE	Nucleosome assembly protein 1-like 4	3	0.579	5.27E-01
OSTF1_MOUSE	Osteoclast-stimulating factor 1	3	0.573	3.10E-01
PROF1_MOUSE	Profilin-1	4	0.569	2.63E-01
TOIP1_MOUSE	Torsin-1A-interacting protein 1	2	0.569	7.91E-02
MP2K1_MOUSE	Dual specificity mitogen-activated protein kinase kinase 1	2	0.565	3.06E-01
CHM4B_MOUSE	Charged multivesicular body protein 4b	3	0.561	1.19E-01
MIF_MOUSE	Macrophage migration inhibitory factor	2	0.516	8.67E-01
PURA2_MOUSE	Adenylosuccinate synthetase isozyme 2	3	0.500	1.96E-01
HCLS1_MOUSE	Hematopoietic lineage cell-specific protein	8	0.500	1.43E-01
VASP_MOUSE	Vasodilator-stimulated phosphoprotein	3	0.498	2.88E-01
BLVRB_MOUSE	Flavin reductase (NADPH)	5	0.496	4.31E-01
RS28_MOUSE	40S ribosomal protein S28	2	0.494	3.04E-01
DSCR3_MOUSE	Down syndrome critical region protein 3 homolog	2	0.492	2.86E-01
LA_MOUSE	Lupus La protein homolog	4	0.490	4.18E-01
RL12_MOUSE	60S ribosomal protein L12	3	0.486	4.01E-01
TPSN_MOUSE	Tapasin	3	0.484	2.60E-01
XPO2_MOUSE	Exportin-2	4	0.481	3.01E-01
PRS6A_MOUSE	26S protease regulatory subunit 6A	4	0.460	3.76E-01
LEG3_MOUSE	Galectin-3	4	0.454	5.17E-01

FPPS_MOUSE	Farnesyl pyrophosphate synthase	3	0.452	1.48E-01
PGM1_MOUSE	Phosphoglucomutase-1	3	0.430	2.56E-01
LEG9_MOUSE	Galectin-9	2	0.423	4.22E-01
RL13_MOUSE	60S ribosomal protein L13	5	0.407	4.84E-01
ASNS_MOUSE	Asparagine synthetase [glutamine-hydrolyzing]	2	0.398	5.52E-01
RS29_MOUSE	40S ribosomal protein S29	2	0.395	5.96E-01
TPM4_MOUSE	Tropomyosin alpha-4 chain	9	0.375	6.88E-02
TCTP_MOUSE	Translationally-controlled tumor protein	2	0.369	7.86E-01
MOES_MOUSE	Moesin	19	0.360	2.20E-01
AB1IP_MOUSE	Amyloid beta A4 precursor protein-binding family B member 1-interacting protein	2	0.353	1.73E-01
PTGR1_MOUSE	Prostaglandin reductase 1	4	0.344	5.43E-01
DNPEP_MOUSE	Aspartyl aminopeptidase	3	0.336	1.81E-01
BROX_MOUSE	BRO1 domain-containing protein BROX	2	0.332	2.64E-01
6PGL_MOUSE	6-phosphogluconolactonase	2	0.326	4.25E-01
COPB_MOUSE	Coatomer subunit beta	5	0.321	4.32E-01
BLMH_MOUSE	Bleomycin hydrolase	3	0.320	8.07E-01
DCTN1_MOUSE	Dynactin subunit 1	4	0.310	4.72E-01
CD44_MOUSE	CD44 antigen	4	0.297	1.44E-01
SYIC_MOUSE	Isoleucine--tRNA ligase, cytoplasmic	4	0.292	3.84E-01
PABP1_MOUSE	Polyadenylate-binding protein 1	14	0.287	6.69E-02
RS2_MOUSE	40S ribosomal protein S2	6	0.283	7.12E-01
PRDX6_MOUSE	Peroxiredoxin-6	6	0.281	4.71E-01
IF4A1_MOUSE	Eukaryotic initiation factor 4A-I	10	0.280	2.85E-01
GNA13_MOUSE	Guanine nucleotide-binding protein subunit alpha-13	3	0.280	3.38E-01
SH3L3_MOUSE	SH3 domain-binding glutamic acid-rich-like protein 3	2	0.275	6.63E-01
TPIS_MOUSE	Triosephosphate isomerase	5	0.266	3.47E-01
COR1B_MOUSE	Coronin-1B	6	0.265	5.54E-01
NONO_MOUSE	Non-POU domain-containing octamer-binding protein	4	0.262	2.25E-01
RS20_MOUSE	40S ribosomal protein S20	3	0.259	3.13E-01
COPB2_MOUSE	Coatomer subunit beta'	6	0.259	4.34E-01
TCPZ_MOUSE	T-complex protein 1 subunit zeta	10	0.252	2.30E-01
EZRI_MOUSE	Ezrin	9	0.249	2.40E-01
MVP_MOUSE	Major vault protein	13	0.247	2.05E-01
IF4G1_MOUSE	Eukaryotic translation initiation factor 4 gamma 1	4	0.240	4.64E-01
PARP1_MOUSE	Poly [ADP-ribose] polymerase 1	2	0.236	7.64E-01
KSYK_MOUSE	Tyrosine-protein kinase SYK	3	0.235	2.61E-01
RAB32_MOUSE	Ras-related protein Rab-32	3	0.235	3.29E-01
CX6B1_MOUSE	Cytochrome c oxidase subunit 6B1	2	0.228	4.85E-01

EIF3G_MOUSE	Eukaryotic translation initiation factor 3 subunit G	2	0.226	7.08E-01
RS13_MOUSE	40S ribosomal protein S13	2	0.225	5.55E-01
ITAM_MOUSE	Integrin alpha-M	11	0.225	4.27E-01
HCK_MOUSE	Tyrosine-protein kinase HCK	6	0.225	2.42E-01
RL4_MOUSE	60S ribosomal protein L4	9	0.223	5.19E-01
RS19_MOUSE	40S ribosomal protein S19	5	0.222	4.97E-01
RLA2_MOUSE	60S acidic ribosomal protein P2	3	0.221	7.54E-01
IF4E_MOUSE	Eukaryotic translation initiation factor 4E	2	0.221	4.36E-01
GSH0_MOUSE	Glutamate--cysteine ligase regulatory subunit	2	0.219	4.41E-01
PSMD2_MOUSE	26S proteasome non-ATPase regulatory subunit 2	9	0.216	5.72E-01
KPCD_MOUSE	Protein kinase C delta type	7	0.215	3.19E-01
IDHP_MOUSE	Isocitrate dehydrogenase [NADP], mitochondrial	5	0.209	5.16E-01
SNP23_MOUSE	Synaptosomal-associated protein 23	2	0.209	6.68E-01
RS4X_MOUSE	40S ribosomal protein S4, X isoform	6	0.202	2.22E-01
CAND1_MOUSE	Cullin-associated NEDD8-dissociated protein 1	6	0.197	4.48E-01
HMOX2_MOUSE	Heme oxygenase 2	2	0.197	5.33E-01
RS11_MOUSE	40S ribosomal protein S11	8	0.196	7.16E-01
PGK1_MOUSE	Phosphoglycerate kinase 1	16	0.193	5.69E-01
EIF3F_MOUSE	Eukaryotic translation initiation factor 3 subunit F	2	0.186	6.16E-01
EIF3C_MOUSE	Eukaryotic translation initiation factor 3 subunit C	4	0.178	1.32E-01
TBB6_MOUSE	Tubulin beta-6 chain	8	0.175	4.73E-01
ANXA6_MOUSE	Annexin A6	15	0.174	6.89E-01
CAPR1_MOUSE	Caprin-1	4	0.168	8.52E-01
RL28_MOUSE	60S ribosomal protein L28	2	0.166	8.18E-01
PSMD4_MOUSE	26S proteasome non-ATPase regulatory subunit 4	3	0.165	1.32E-01
LBR_MOUSE	Lamin-B receptor	2	0.164	2.37E-01
ESTD_MOUSE	S-formylglutathione hydrolase	6	0.161	7.02E-01
GPDM_MOUSE	Glycerol-3-phosphate dehydrogenase, mitochondrial	3	0.159	5.04E-01
LEG1_MOUSE	Galectin-1	4	0.157	8.38E-01
PIPNA_MOUSE	Phosphatidylinositol transfer protein alpha isoform	4	0.155	7.26E-01
ODO2_MOUSE	Dihydrolipoyllysine-residue succinyltransferase component of 2-oxoglutarate dehydrogenase complex, mitochondrial	2	0.151	5.27E-01
AP2M1_MOUSE	AP-2 complex subunit mu	4	0.151	5.43E-01
VATH_MOUSE	V-type proton ATPase subunit H	5	0.148	5.97E-01
LAMP1_MOUSE	Lysosome-associated membrane glycoprotein 1	4	0.146	7.10E-01
RL7A_MOUSE	60S ribosomal protein L7a	8	0.139	9.74E-01

RS16_MOUSE	40S ribosomal protein S16	5	0.138	5.95E-01
PP1A_MOUSE	Serine/threonine-protein phosphatase PP1-alpha catalytic subunit	4	0.137	9.48E-01
RL8_MOUSE	60S ribosomal protein L8	3	0.127	7.39E-01
AN32B_MOUSE	Acidic leucine-rich nuclear phosphoprotein 32 family member B	2	0.125	6.60E-01
LASP1_MOUSE	LIM and SH3 domain protein 1	4	0.121	6.96E-01
PSB2_MOUSE	Proteasome subunit beta type-2	2	0.117	5.67E-01
PRS8_MOUSE	26S protease regulatory subunit 8	3	0.105	7.83E-01
BCAP_MOUSE	Phosphoinositide 3-kinase adapter protein 1	3	0.101	5.58E-01
RS3A_MOUSE	40S ribosomal protein S3a	8	0.101	8.46E-01
DDX3X_MOUSE	ATP-dependent RNA helicase DDX3X	5	0.101	6.12E-01
SYDC_MOUSE	Aspartate--tRNA ligase, cytoplasmic	5	0.100	5.35E-01
SC11A_MOUSE	Signal peptidase complex catalytic subunit SEC11A	3	0.098	6.66E-01
LPPRC_MOUSE	Leucine-rich PPR motif-containing protein, mitochondrial	4	0.096	5.92E-01
ETFB_MOUSE	Electron transfer flavoprotein subunit beta	3	0.096	9.30E-01
FLNB_MOUSE	Filamin-B	8	0.090	6.19E-01
PEPD_MOUSE	Xaa-Pro dipeptidase	3	0.090	9.77E-01
G6PD1_MOUSE	Glucose-6-phosphate 1-dehydrogenase X	14	0.087	8.46E-01
ERLN2_MOUSE	Erlin-2	3	0.086	6.08E-01
HNRH1_MOUSE	Heterogeneous nuclear ribonucleoprotein H	4	0.084	9.64E-01
LRC59_MOUSE	Leucine-rich repeat-containing protein 59	5	0.082	7.42E-01
SQRD_MOUSE	Sulfide:quinone oxidoreductase, mitochondrial	2	0.080	7.14E-01
RHG17_MOUSE	Rho GTPase-activating protein 17	4	0.080	6.88E-01
TPD52_MOUSE	Tumor protein D52	3	0.080	8.95E-01
ROA1_MOUSE	Heterogeneous nuclear ribonucleoprotein A1	3	0.078	7.46E-01
RL23A_MOUSE	60S ribosomal protein L23a	6	0.077	9.91E-01
MARCS_MOUSE	Myristoylated alanine-rich C-kinase substrate	4	0.077	9.94E-01
RL5_MOUSE	60S ribosomal protein L5	6	0.075	8.27E-01
CPNS1_MOUSE	Calpain small subunit 1	2	0.070	8.65E-01
MACF1_MOUSE	Microtubule-actin cross-linking factor 1	3	0.070	7.46E-01
HSP7C_MOUSE	Heat shock cognate 71 kDa protein	21	0.065	7.28E-01
PSME2_MOUSE	Proteasome activator complex subunit 2	5	0.064	8.78E-01
DDX17_MOUSE	Probable ATP-dependent RNA helicase DDX17	8	0.063	3.65E-01
GLYG_MOUSE	Glycogenin-1	2	0.060	7.73E-01
LYN_MOUSE	Tyrosine-protein kinase Lyn	6	0.060	7.81E-01
SAR1B_MOUSE	GTP-binding protein SAR1b	2	0.050	9.01E-01
CASP1_MOUSE	Caspase-1	5	0.045	8.07E-01
PPCE_MOUSE	Prolyl endopeptidase	7	0.045	8.17E-01
SC31A_MOUSE	Protein transport protein Sec31A	5	0.043	9.20E-01

RAB6A_MOUSE	Ras-related protein Rab-6A	3	0.042	9.81E-01
IF4G2_MOUSE	Eukaryotic translation initiation factor 4 gamma 2	2	0.040	9.96E-01
U520_MOUSE	U5 small nuclear ribonucleoprotein 200 kDa helicase	2	0.040	7.06E-01
ITB1_MOUSE	Integrin beta-1	8	0.038	8.67E-01
RS3_MOUSE	40S ribosomal protein S3	9	0.037	8.36E-01
COPZ1_MOUSE	Coatomer subunit zeta-1	2	0.036	8.43E-01
NPM_MOUSE	Nucleophosmin	2	0.035	8.87E-01
PSMD6_MOUSE	26S proteasome non-ATPase regulatory subunit 6	3	0.029	9.21E-01
RL22_MOUSE	60S ribosomal protein L22	2	0.026	9.88E-01
RS15A_MOUSE	40S ribosomal protein S15a	2	0.025	8.13E-01
ABR_MOUSE	Active breakpoint cluster region-related protein	3	0.025	9.34E-01
PSB1_MOUSE	Proteasome subunit beta type-1	4	0.024	7.92E-01
RL27A_MOUSE	60S ribosomal protein L27a	3	0.023	9.77E-01
RN213_MOUSE	E3 ubiquitin-protein ligase RNF213	5	0.021	9.52E-01
SMD3_MOUSE	Small nuclear ribonucleoprotein Sm D3	2	0.019	8.99E-01
TAGL2_MOUSE	Transgelin-2	9	0.017	9.70E-01
DDX58_MOUSE	Probable ATP-dependent RNA helicase DDX58	3	0.014	8.33E-01
PSA5_MOUSE	Proteasome subunit alpha type-5	3	0.013	9.87E-01
RTN4_MOUSE	Reticulon-4	4	0.009	8.91E-01
HNRPQ_MOUSE	Heterogeneous nuclear ribonucleoprotein Q	7	0.009	9.77E-01
HNRPC_MOUSE	Heterogeneous nuclear ribonucleoproteins C1/C2	6	0.008	8.94E-01
ANXA7_MOUSE	Annexin A7	4	0.008	9.67E-01
KCD12_MOUSE	BTB/POZ domain-containing protein KCTD12	6	0.007	9.47E-01
PP2AA_MOUSE	Serine/threonine-protein phosphatase 2A catalytic subunit alpha isoform	2	0.005	7.41E-01
YBOX1_MOUSE	Nuclease-sensitive element-binding protein 1	3	0.003	8.58E-01
VATE1_MOUSE	V-type proton ATPase subunit E 1	7	0.002	9.33E-01
MAP4_MOUSE	Microtubule-associated protein 4	4	-0.007	9.48E-01
RS26_MOUSE	40S ribosomal protein S26	2	-0.011	9.14E-01
NDKB_MOUSE	Nucleoside diphosphate kinase B	5	-0.011	8.24E-01
RS12_MOUSE	40S ribosomal protein S12	4	-0.011	9.74E-01
NICA_MOUSE	Nicastrin	2	-0.017	9.72E-01
EF2_MOUSE	Elongation factor 2	19	-0.017	9.71E-01
TBB4B_MOUSE	Tubulin beta-4B chain	11	-0.019	9.98E-01
RS10_MOUSE	40S ribosomal protein S10	2	-0.020	9.22E-01
NDKA_MOUSE	Nucleoside diphosphate kinase A	5	-0.020	8.98E-01
RL31_MOUSE	60S ribosomal protein L31	3	-0.022	7.84E-01
HSP74_MOUSE	Heat shock 70 kDa protein 4	13	-0.024	8.98E-01
SYG_MOUSE	Glycine--tRNA ligase	3	-0.026	9.79E-01

BAX_MOUSE	Apoptosis regulator BAX	3	-0.027	8.34E-01
GDIR2_MOUSE	Rho GDP-dissociation inhibitor 2	3	-0.028	9.94E-01
PGAM1_MOUSE	Phosphoglycerate mutase 1	6	-0.030	8.38E-01
OAS1A_MOUSE	2'-5'-oligoadenylate synthase 1A	3	-0.031	7.97E-01
RL26_MOUSE	60S ribosomal protein L26	3	-0.032	7.81E-01
HXK2_MOUSE	Hexokinase-2	8	-0.040	7.15E-01
C1TM_MOUSE	Monofunctional C1-tetrahydrofolate synthase, mitochondrial	3	-0.042	9.64E-01
EIF3B_MOUSE	Eukaryotic translation initiation factor 3 subunit B	4	-0.048	8.20E-01
TM9S4_MOUSE	Transmembrane 9 superfamily member 4	2	-0.049	9.13E-01
EIF3L_MOUSE	Eukaryotic translation initiation factor 3 subunit L	5	-0.050	9.15E-01
TENS3_MOUSE	Tensin-3	2	-0.053	9.10E-01
ERF3A_MOUSE	Eukaryotic peptide chain release factor GTP-binding subunit ERF3A	2	-0.055	7.31E-01
PUR2_MOUSE	Trifunctional purine biosynthetic protein adenosine-3	2	-0.057	7.85E-01
RL24_MOUSE	60S ribosomal protein L24	4	-0.057	7.80E-01
PRDX1_MOUSE	Peroxiredoxin-1	11	-0.058	6.98E-01
TBB5_MOUSE	Tubulin beta-5 chain	10	-0.060	8.68E-01
VAV_MOUSE	Proto-oncogene vav	3	-0.060	7.60E-01
SGPL1_MOUSE	Sphingosine-1-phosphate lyase 1	6	-0.064	9.34E-01
RRBP1_MOUSE	Ribosome-binding protein 1	11	-0.064	7.75E-01
MYH9_MOUSE	Myosin-9	56	-0.064	9.23E-01
ARPC2_MOUSE	Actin-related protein 2/3 complex subunit 2	8	-0.065	6.73E-01
UGPA_MOUSE	UTP--glucose-1-phosphate uridylyltransferase	2	-0.065	7.14E-01
NCF4_MOUSE	Neutrophil cytosol factor 4	6	-0.065	8.68E-01
COPD_MOUSE	Coatomer subunit delta	7	-0.065	8.28E-01
EF1G_MOUSE	Elongation factor 1-gamma	7	-0.067	7.49E-01
H2B1B_MOUSE	Histone H2B type 1-B	6	-0.068	8.67E-01
RS18_MOUSE	40S ribosomal protein S18	6	-0.070	7.10E-01
SCOT1_MOUSE	Succinyl-CoA:3-ketoacid coenzyme A transferase 1, mitochondrial	4	-0.071	5.77E-01
2ABA_MOUSE	Serine/threonine-protein phosphatase 2A 55 kDa regulatory subunit B alpha isoform	2	-0.072	8.97E-01
LRRF1_MOUSE	Leucine-rich repeat flightless-interacting protein 1	2	-0.073	6.46E-01
PSME1_MOUSE	Proteasome activator complex subunit 1	7	-0.075	7.22E-01
SF3B3_MOUSE	Splicing factor 3B subunit 3	3	-0.076	7.97E-01
RAGP1_MOUSE	Ran GTPase-activating protein 1	2	-0.076	9.33E-01
RS27A_MOUSE	Ubiquitin-40S ribosomal protein S27a	3	-0.080	8.23E-01
PICAL_MOUSE	Phosphatidylinositol-binding clathrin assembly protein	3	-0.080	7.11E-01

TCPB_MOUSE	T-complex protein 1 subunit beta	6	-0.081	7.31E-01
HPCL1_MOUSE	Hippocalcin-like protein 1	5	-0.085	8.05E-01
RS8_MOUSE	40S ribosomal protein S8	6	-0.087	6.93E-01
RAP1B_MOUSE	Ras-related protein Rap-1b	5	-0.088	6.86E-01
CAB39_MOUSE	Calcium-binding protein 39	3	-0.089	6.75E-01
TCPQ_MOUSE	T-complex protein 1 subunit theta	14	-0.089	6.07E-01
SND1_MOUSE	Staphylococcal nuclease domain-containing protein 1	7	-0.096	5.52E-01
HNRPF_MOUSE	Heterogeneous nuclear ribonucleoprotein F	4	-0.096	7.29E-01
ADT2_MOUSE	ADP/ATP translocase 2	9	-0.096	7.83E-01
RL32_MOUSE	60S ribosomal protein L32	3	-0.101	7.49E-01
PSA4_MOUSE	Proteasome subunit alpha type-4	2	-0.103	9.94E-01
GSHR_MOUSE	Glutathione reductase, mitochondrial	3	-0.103	4.24E-01
DIAP1_MOUSE	Protein diaphanous homolog 1	4	-0.103	5.02E-01
SKAP2_MOUSE	Src kinase-associated phosphoprotein 2	3	-0.104	7.59E-01
RACK1_MOUSE	Receptor of activated protein C kinase 1	8	-0.104	3.92E-01
PSMD1_MOUSE	26S proteasome non-ATPase regulatory subunit 1	7	-0.105	5.77E-01
PRS10_MOUSE	26S protease regulatory subunit 10B	5	-0.106	8.79E-01
FLNA_MOUSE	Filamin-A	50	-0.108	6.45E-01
ARPC3_MOUSE	Actin-related protein 2/3 complex subunit 3	4	-0.109	7.33E-01
ADRM1_MOUSE	Proteasomal ubiquitin receptor ADRM1	2	-0.109	5.51E-01
EI3JA_MOUSE	Eukaryotic translation initiation factor 3 subunit J-A	2	-0.110	7.41E-01
PAIRB_MOUSE	Plasminogen activator inhibitor 1 RNA-binding protein	2	-0.111	2.72E-01
RLA0_MOUSE	60S acidic ribosomal protein P0	6	-0.112	5.90E-01
RL7_MOUSE	60S ribosomal protein L7	8	-0.113	3.54E-01
ANM1_MOUSE	Protein arginine N-methyltransferase 1	3	-0.113	9.01E-01
DNJC7_MOUSE	DnaJ homolog subfamily C member 7	2	-0.115	7.28E-01
RAB18_MOUSE	Ras-related protein Rab-18	4	-0.116	7.22E-01
CALX_MOUSE	Calnexin	9	-0.118	5.63E-01
EF1B_MOUSE	Elongation factor 1-beta	4	-0.119	6.34E-01
VINC_MOUSE	Vinculin	5	-0.120	7.58E-01
H4_MOUSE	Histone H4	6	-0.121	7.46E-01
LDHA_MOUSE	L-lactate dehydrogenase A chain	9	-0.122	6.59E-01
IF2A_MOUSE	Eukaryotic translation initiation factor 2 subunit 1	6	-0.123	1.47E-01
ARF1_MOUSE	ADP-ribosylation factor 1	5	-0.123	6.48E-01
PSB6_MOUSE	Proteasome subunit beta type-6	2	-0.123	4.91E-01
SEP11_MOUSE	Septin-11	3	-0.125	9.68E-01
IF2B_MOUSE	Eukaryotic translation initiation factor 2 subunit 2	6	-0.125	8.32E-01

NACA_MOUSE	Nascent polypeptide-associated complex subunit alpha	2	-0.126	7.48E-01
PPIA_MOUSE	Peptidyl-prolyl cis-trans isomerase A	7	-0.129	5.89E-01
ACTN4_MOUSE	Alpha-actinin-4	14	-0.131	6.27E-01
UBE2K_MOUSE	Ubiquitin-conjugating enzyme E2 K	2	-0.132	8.50E-01
LIS1_MOUSE	Platelet-activating factor acetylhydrolase IB subunit alpha	2	-0.134	5.84E-01
TMED5_MOUSE	Transmembrane emp24 domain-containing protein 5	2	-0.134	7.15E-01
ATPB_MOUSE	ATP synthase subunit beta, mitochondrial	12	-0.134	5.31E-01
ACADL_MOUSE	Long-chain specific acyl-CoA dehydrogenase, mitochondrial	4	-0.135	3.03E-01
FCERG_MOUSE	High affinity immunoglobulin epsilon receptor subunit gamma	3	-0.135	8.39E-01
PSA3_MOUSE	Proteasome subunit alpha type-3	3	-0.136	5.87E-01
PSA7_MOUSE	Proteasome subunit alpha type-7 O	4	-0.141	6.26E-01
GRP78_MOUSE	78 kDa glucose-regulated protein	17	-0.141	6.55E-01
SPTB2_MOUSE	Spectrin beta chain, non-erythrocytic 1	4	-0.142	8.02E-01
NIBL1_MOUSE	Niban-like protein 1	7	-0.142	5.65E-01
RAB8B_MOUSE	Ras-related protein Rab-8B	7	-0.146	6.15E-01
RS25_MOUSE	40S ribosomal protein S25	3	-0.148	6.01E-01
SERC_MOUSE	Phosphoserine aminotransferase	4	-0.148	2.17E-01
ERO1A_MOUSE	ERO1-like protein alpha	3	-0.149	8.29E-01
EF1D_MOUSE	Elongation factor 1-delta	3	-0.149	4.68E-01
AK1A1_MOUSE	Alcohol dehydrogenase [NADP(+)]	7	-0.152	5.09E-01
PSA6_MOUSE	Proteasome subunit alpha type-6	3	-0.154	5.49E-01
RL3_MOUSE	60S ribosomal protein L3	4	-0.156	5.61E-01
G3BP1_MOUSE	Ras GTPase-activating protein-binding protein 1	2	-0.158	4.00E-01
RL30_MOUSE	60S ribosomal protein L30	3	-0.158	4.05E-01
RL10_MOUSE	60S ribosomal protein L10	2	-0.160	9.72E-01
AT2A2_MOUSE	Sarcoplasmic/endoplasmic reticulum calcium ATPase 2	10	-0.160	5.13E-01
RL6_MOUSE	60S ribosomal protein L6	7	-0.160	5.85E-01
RSU1_MOUSE	Ras suppressor protein 1	3	-0.162	4.68E-01
ILK_MOUSE	Integrin-linked protein kinase	3	-0.163	4.10E-01
ADHX_MOUSE	Alcohol dehydrogenase class-3	2	-0.166	4.40E-01
TECR_MOUSE	Very-long-chain enoyl-CoA reductase	2	-0.167	9.52E-01
SP16H_MOUSE	FACT complex subunit SPT16	2	-0.167	6.01E-01
NCF2_MOUSE	Neutrophil cytosol factor 2	3	-0.167	6.41E-01
IMB1_MOUSE	Importin subunit beta-1	6	-0.169	9.97E-01
RL34_MOUSE	60S ribosomal protein L34	2	-0.169	5.25E-01
CAZA2_MOUSE	F-actin-capping protein subunit alpha-2	3	-0.174	4.78E-01
FAK2_MOUSE	Protein-tyrosine kinase 2-beta	4	-0.178	3.68E-01

IPO5_MOUSE	Importin-5	7	-0.178	5.00E-01
TADBP_MOUSE	TAR DNA-binding protein 43	3	-0.178	3.63E-01
UGGG1_MOUSE	UDP-glucose:glycoprotein glucosyltransferase 1	7	-0.178	4.59E-01
HNRPK_MOUSE	Heterogeneous nuclear ribonucleoprotein K	12	-0.179	5.76E-01
DDX5_MOUSE	Probable ATP-dependent RNA helicase DDX5	11	-0.179	2.32E-01
RS6_MOUSE	40S ribosomal protein S6	3	-0.181	3.83E-01
ALDOA_MOUSE	Fructose-bisphosphate aldolase A	10	-0.182	5.18E-01
K1C10_MOUSE	Keratin, type I cytoskeletal 10	4	-0.185	5.24E-01
IMA4_MOUSE	Importin subunit alpha-4	2	-0.185	3.37E-01
SARNP_MOUSE	SAP domain-containing ribonucleoprotein	3	-0.185	6.79E-01
GMFB_MOUSE	Glia maturation factor beta	2	-0.186	6.50E-01
1433Z_MOUSE	14-3-3 protein zeta/delta	9	-0.186	6.23E-01
G3P_MOUSE	Glyceraldehyde-3-phosphate dehydrogenase	8	-0.186	4.16E-01
FRIL1_MOUSE	Ferritin light chain 1	2	-0.189	2.24E-01
FUMH_MOUSE	Fumarate hydratase, mitochondrial	3	-0.190	5.51E-01
SAC1_MOUSE	Phosphatidylinositide phosphatase SAC1	3	-0.190	5.07E-01
CATA_MOUSE	Catalase	11	-0.190	7.26E-01
RS27L_MOUSE	40S ribosomal protein S27-like	2	-0.191	5.14E-01
COTL1_MOUSE	Coactosin-like protein	3	-0.191	7.68E-01
ENOA_MOUSE	Alpha-enolase	14	-0.192	3.96E-01
SYAC_MOUSE	Alanine--tRNA ligase, cytoplasmic	2	-0.193	7.52E-01
ARF5_MOUSE	ADP-ribosylation factor 5	5	-0.196	6.98E-01
AN32E_MOUSE	Acidic leucine-rich nuclear phosphoprotein 32 family member E	2	-0.197	5.52E-01
CISY_MOUSE	Citrate synthase, mitochondrial	6	-0.199	4.20E-01
6PGD_MOUSE	6-phosphogluconate dehydrogenase, decarboxylating	11	-0.201	4.97E-01
SERA_MOUSE	D-3-phosphoglycerate dehydrogenase	6	-0.202	5.72E-01
CATB_MOUSE	Cathepsin B	8	-0.203	4.53E-01
RRAGC_MOUSE	Ras-related GTP-binding protein C	3	-0.204	1.49E-01
DC1L2_MOUSE	Cytoplasmic dynein 1 light intermediate chain 2	2	-0.204	5.26E-01
ROA3_MOUSE	Heterogeneous nuclear ribonucleoprotein A3	5	-0.206	3.00E-01
LAP2B_MOUSE	Lamina-associated polypeptide 2, isoforms beta/delta/epsilon/gamma	3	-0.208	3.28E-01
CAPZB_MOUSE	F-actin-capping protein subunit beta	5	-0.209	4.30E-01
RHOA_MOUSE	Transforming protein RhoA	3	-0.212	3.20E-01
SYK_MOUSE	Lysine--tRNA ligase	4	-0.212	4.24E-01
RL27_MOUSE	60S ribosomal protein L27	3	-0.214	4.81E-01
PYGB_MOUSE	Glycogen phosphorylase, brain form	4	-0.215	3.96E-01
DHX9_MOUSE	ATP-dependent RNA helicase A	3	-0.216	5.73E-01
ROA2_MOUSE	Heterogeneous nuclear ribonucleoproteins A2/B1	9	-0.217	3.49E-01
SYEP_MOUSE	Bifunctional glutamate/proline--tRNA ligase	9	-0.219	3.73E-01

NSF_MOUSE	Vesicle-fusing ATPase	5	-0.220	3.64E-01
RAN_MOUSE	GTP-binding nuclear protein Ran	5	-0.220	4.25E-01
KINH_MOUSE	Kinesin-1 heavy chain	5	-0.221	4.09E-01
TCPA_MOUSE	T-complex protein 1 subunit alpha	12	-0.221	3.34E-01
RL35A_MOUSE	60S ribosomal protein L35a	2	-0.222	4.54E-01
IDHC_MOUSE	Isocitrate dehydrogenase [NADP] cytoplasmic	12	-0.223	5.14E-01
HS90B_MOUSE	Heat shock protein HSP 90-beta	20	-0.223	5.95E-01
PRS4_MOUSE	26S protease regulatory subunit 4	3	-0.224	5.07E-01
ANFY1_MOUSE	Rabankyrin-5	3	-0.227	5.15E-01
VATC1_MOUSE	V-type proton ATPase subunit C 1	4	-0.228	5.19E-01
TLN1_MOUSE	Talin-1	47	-0.228	2.19E-01
MBB1A_MOUSE	Myb-binding protein 1A	5	-0.229	4.77E-01
GSDMD_MOUSE	Gasdermin-D	3	-0.233	2.65E-01
PRS7_MOUSE	26S protease regulatory subunit 7	7	-0.234	4.85E-01
PDC6I_MOUSE	Programmed cell death 6-interacting protein	9	-0.235	1.18E-01
EF1A1_MOUSE	Elongation factor 1-alpha 1	12	-0.237	3.10E-01
TCPG_MOUSE	T-complex protein 1 subunit gamma	14	-0.239	1.25E-01
CAZA1_MOUSE	F-actin-capping protein subunit alpha-1	3	-0.239	2.98E-01
FA49B_MOUSE	Protein FAM49B	4	-0.240	4.14E-01
ACTB_MOUSE	Actin, cytoplasmic 1	12	-0.240	3.47E-01
SWP70_MOUSE	Switch-associated protein 70	2	-0.240	7.74E-01
UBP5_MOUSE	Ubiquitin carboxyl-terminal hydrolase 5	3	-0.241	1.95E-01
RBBP4_MOUSE	Histone-binding protein RBBP4	3	-0.241	4.85E-01
SODC_MOUSE	Superoxide dismutase [Cu-Zn]	2	-0.242	4.68E-01
MATR3_MOUSE	Matrin-3	3	-0.243	7.18E-01
RAB1A_MOUSE	Ras-related protein Rab-1A	6	-0.243	3.47E-01
STAT1_MOUSE	Signal transducer and activator of transcription 1	7	-0.244	4.45E-01
SDHA_MOUSE	Succinate dehydrogenase [ubiquinone] flavoprotein subunit, mitochondrial	3	-0.245	9.44E-01
CALM_MOUSE	Calmodulin	5	-0.247	5.28E-01
SYCC_MOUSE	Cysteine--tRNA ligase, cytoplasmic	2	-0.248	4.47E-01
RHOG_MOUSE	Rho-related GTP-binding protein RhoG	7	-0.249	4.05E-01
UBE2N_MOUSE	Ubiquitin-conjugating enzyme E2 N	3	-0.250	3.83E-01
GDIR1_MOUSE	Rho GDP-dissociation inhibitor 1	5	-0.250	5.24E-01
PCBP2_MOUSE	Poly(rC)-binding protein 2	6	-0.251	5.08E-01
F10A1_MOUSE	Hsc70-interacting protein	6	-0.252	1.57E-01
VATA_MOUSE	V-type proton ATPase catalytic subunit A	10	-0.254	4.84E-01
EIF3M_MOUSE	Eukaryotic translation initiation factor 3 subunit M	3	-0.254	2.17E-01
UBP14_MOUSE	Ubiquitin carboxyl-terminal hydrolase 14	3	-0.255	3.71E-01
SAHH_MOUSE	Adenosylhomocysteinase	5	-0.255	3.24E-01

VPS29_MOUSE	Vacuolar protein sorting-associated protein 29	2	-0.256	4.83E-01
HXK1_MOUSE	Hexokinase-1	6	-0.258	5.56E-01
AMRP_MOUSE	Alpha-2-macroglobulin receptor-associated protein	3	-0.258	6.16E-01
ARP3_MOUSE	Actin-related protein 3	9	-0.259	5.44E-01
ELAV1_MOUSE	ELAV-like protein 1	4	-0.260	4.02E-01
PDLI5_MOUSE	PDZ and LIM domain protein 5	2	-0.261	5.60E-01
MYO1G_MOUSE	Unconventional myosin-Ig	2	-0.261	6.86E-01
PSA_MOUSE	Puromycin-sensitive aminopeptidase	5	-0.261	1.47E-01
ML12B_MOUSE	Myosin regulatory light chain 12B	5	-0.262	5.23E-01
TCPD_MOUSE	T-complex protein 1 subunit delta	9	-0.265	5.40E-01
CYB5_MOUSE	Cytochrome b5	3	-0.265	5.27E-01
DX39B_MOUSE	Spliceosome RNA helicase Ddx39b	5	-0.268	4.54E-01
1433G_MOUSE	14-3-3 protein gamma	5	-0.268	5.31E-01
FKBP4_MOUSE	Peptidyl-prolyl cis-trans isomerase FKBP4	3	-0.270	4.84E-01
TR150_MOUSE	Thyroid hormone receptor-associated protein 3	2	-0.270	4.61E-01
DC1L1_MOUSE	Cytoplasmic dynein 1 light intermediate chain 1	3	-0.271	9.48E-02
GBB2_MOUSE	Guanine nucleotide-binding protein G(I)/G(S)/G(T) subunit beta-2	4	-0.274	4.25E-01
ETFA_MOUSE	Electron transfer flavoprotein subunit alpha, mitochondrial	4	-0.276	4.87E-01
DHRS1_MOUSE	Dehydrogenase/reductase SDR family member 1	2	-0.280	3.86E-01
GNS_MOUSE	N-acetylglucosamine-6-sulfatase	6	-0.282	7.29E-01
SMD2_MOUSE	Small nuclear ribonucleoprotein Sm D2	3	-0.283	2.87E-01
NOP56_MOUSE	Nucleolar protein 56	3	-0.285	5.34E-01
RISC_MOUSE	Retinoid-inducible serine carboxypeptidase	2	-0.288	4.64E-01
UAP1L_MOUSE	UDP-N-acetylhexosamine pyrophosphorylase-like protein 1	5	-0.289	1.33E-01
RS9_MOUSE	40S ribosomal protein S9	5	-0.289	6.01E-01
RPN1_MOUSE	Dolichyl-diphosphooligosaccharide--protein glycosyltransferase subunit 1	9	-0.289	5.39E-01
PUR6_MOUSE	Multifunctional protein ADE2	3	-0.290	3.16E-01
SEPT7_MOUSE	Septin-7	3	-0.291	1.14E-01
SC22B_MOUSE	Vesicle-trafficking protein SEC22b O	3	-0.292	1.77E-01
1433B_MOUSE	14-3-3 protein beta/alpha	7	-0.299	4.18E-01
ENPL_MOUSE	Endoplasmin	22	-0.303	3.07E-01
ERAP1_MOUSE	Endoplasmic reticulum aminopeptidase 1	3	-0.304	8.41E-01
RAB14_MOUSE	Ras-related protein Rab-14	3	-0.306	3.64E-01
NAGAB_MOUSE	Alpha-N-acetylgalactosaminidase	3	-0.306	1.95E-01
TNPO1_MOUSE	Transportin-1	3	-0.308	3.76E-01
DJB11_MOUSE	DnaJ homolog subfamily B member 11	2	-0.309	3.24E-01
HA1B_MOUSE	H-2 class I histocompatibility antigen, K-B alpha chain	5	-0.309	7.23E-01

SEPT9_MOUSE	Septin-9	4	-0.311	3.40E-01
AN32A_MOUSE	Acidic leucine-rich nuclear phosphoprotein 32 family member A	3	-0.311	2.22E-01
PFKAP_MOUSE	ATP-dependent 6-phosphofructokinase, platelet type	6	-0.313	1.61E-01
FKB15_MOUSE	FK506-binding protein 15	3	-0.313	3.85E-01
BUB3_MOUSE	Mitotic checkpoint protein BUB3	3	-0.314	3.95E-01
ACTN1_MOUSE	Alpha-actinin-1	15	-0.317	3.75E-01
THIKA_MOUSE	3-ketoacyl-CoA thiolase A, peroxisomal	7	-0.319	3.09E-01
ARF4_MOUSE	ADP-ribosylation factor 4	4	-0.322	2.59E-01
FABP5_MOUSE	Fatty acid-binding protein, epidermal	3	-0.323	8.98E-02
RL13A_MOUSE	60S ribosomal protein L13a	2	-0.323	2.61E-01
PPIB_MOUSE	Peptidyl-prolyl cis-trans isomerase B	7	-0.324	2.63E-01
SSRD_MOUSE	Translocon-associated protein subunit delta	2	-0.326	1.12E-01
ACLY_MOUSE	ATP-citrate synthase	7	-0.327	1.47E-01
SRSF1_MOUSE	Serine/arginine-rich splicing factor 1	3	-0.327	2.70E-01
UBA1_MOUSE	Ubiquitin-like modifier-activating enzyme 1	13	-0.327	9.80E-02
OTUB1_MOUSE	Ubiquitin thioesterase OTUB1	2	-0.327	3.17E-01
LAMP2_MOUSE	Lysosome-associated membrane glycoprotein 2	4	-0.328	8.61E-02
ARP2_MOUSE	Actin-related protein 2	5	-0.333	1.21E-01
USP9X_MOUSE	Probable ubiquitin carboxyl-terminal hydrolase FAF-X	5	-0.339	3.18E-01
AP2A1_MOUSE	AP-2 complex subunit alpha-1	2	-0.340	4.38E-01
RAP2B_MOUSE	Ras-related protein Rap-2b	3	-0.341	2.62E-01
SFPQ_MOUSE	Splicing factor, proline- and glutamine-rich	6	-0.343	2.51E-01
RL10A_MOUSE	60S ribosomal protein L10a	5	-0.345	6.81E-01
SHPS1_MOUSE	Tyrosine-protein phosphatase non-receptor type substrate 1	3	-0.351	9.33E-01
2AAA_MOUSE	Serine/threonine-protein phosphatase 2A 65 kDa regulatory subunit A alpha isoform	8	-0.351	2.00E-01
RL14_MOUSE	60S ribosomal protein L14	4	-0.355	2.98E-01
RB22A_MOUSE	Ras-related protein Rab-22A	3	-0.359	1.83E-01
DPYL2_MOUSE	Dihydropyrimidinase-related protein 2	11	-0.359	2.27E-01
SYVC_MOUSE	Valine--tRNA ligase	3	-0.359	4.68E-01
RL18_MOUSE	60S ribosomal protein L18	5	-0.360	3.51E-01
DYHC1_MOUSE	Cytoplasmic dynein 1 heavy chain 1	29	-0.361	3.32E-01
HA11_MOUSE	H-2 class I histocompatibility antigen, D-B alpha chain	7	-0.364	4.47E-01
DAB2_MOUSE	Disabled homolog 2	3	-0.364	1.27E-01
CALR_MOUSE	Calreticulin	11	-0.365	1.46E-01
TBB2A_MOUSE	Tubulin beta-2A chain	10	-0.365	2.07E-01
ROAA_MOUSE	Heterogeneous nuclear ribonucleoprotein A/B	5	-0.365	2.60E-01

NUCL_MOUSE	Nucleolin	13	-0.367	1.48E-01
WDR1_MOUSE	WD repeat-containing protein 1	11	-0.368	1.40E-01
SPRE_MOUSE	Sepiapterin reductase	2	-0.369	7.87E-01
SSRA_MOUSE	Translocon-associated protein subunit alpha	2	-0.370	9.22E-02
WASF2_MOUSE	Wiskott-Aldrich syndrome protein family member 2	4	-0.373	1.42E-01
TCPH_MOUSE	T-complex protein 1 subunit eta	11	-0.373	1.91E-01
SYTC_MOUSE	Threonine--tRNA ligase, cytoplasmic	2	-0.374	1.73E-01
UBC12_MOUSE	NEDD8-conjugating enzyme Ubc12	3	-0.376	6.07E-01
OST48_MOUSE	Dolichyl-diphosphooligosaccharide--protein glycosyltransferase 48 kDa subunit	6	-0.377	2.66E-01
MK03_MOUSE	Mitogen-activated protein kinase 3	7	-0.378	1.18E-01
RAB5C_MOUSE	Ras-related protein Rab-5C	4	-0.378	1.72E-01
RL23_MOUSE	60S ribosomal protein L23	4	-0.379	9.87E-01
SYFB_MOUSE	Phenylalanine--tRNA ligase beta subunit	4	-0.380	1.22E-02
MRC1_MOUSE	Macrophage mannose receptor 1	5	-0.381	5.33E-01
CYFP1_MOUSE	Cytoplasmic FMR1-interacting protein 1	10	-0.381	2.16E-01
CAP1_MOUSE	Adenylyl cyclase-associated protein 1	12	-0.382	4.42E-01
MYL6_MOUSE	Myosin light polypeptide 6	6	-0.383	1.37E-01
1433E_MOUSE	14-3-3 protein epsilon	10	-0.384	1.62E-01
MPCP_MOUSE	Phosphate carrier protein, mitochondrial	3	-0.384	4.77E-02
PERM_MOUSE	Myeloperoxidase	6	-0.385	1.81E-01
CD166_MOUSE	CD166 antigen	4	-0.386	2.01E-01
RADI_MOUSE	Radixin	8	-0.388	2.07E-01
TERA_MOUSE	Transitional endoplasmic reticulum ATPase	19	-0.389	1.09E-02
RL15_MOUSE	60S ribosomal protein L15	5	-0.389	1.91E-01
RSSA_MOUSE	40S ribosomal protein SA	6	-0.390	1.24E-01
RL9_MOUSE	60S ribosomal protein L9	2	-0.391	4.65E-01
VAT1_MOUSE	Synaptic vesicle membrane protein VAT-1 homolog	7	-0.391	2.20E-01
RL11_MOUSE	60S ribosomal protein L11	2	-0.392	2.36E-01
CORO7_MOUSE	Coronin-7	3	-0.393	2.59E-01
EIF3E_MOUSE	Eukaryotic translation initiation factor 3 subunit E	4	-0.394	2.00E-01
ARLY_MOUSE	Argininosuccinate lyase	3	-0.394	7.89E-02
MPRD_MOUSE	Cation-dependent mannose-6-phosphate receptor	3	-0.395	1.38E-01
PRAF3_MOUSE	PRA1 family protein 3	2	-0.397	1.69E-02
PRDX2_MOUSE	Peroxiredoxin-2	4	-0.401	1.84E-01
RBM39_MOUSE	RNA-binding protein 39	2	-0.402	3.40E-01
ADT1_MOUSE	ADP/ATP translocase 1	7	-0.405	6.55E-02
SET_MOUSE	Protein SET	3	-0.406	2.40E-01
PRP19_MOUSE	Pre-mRNA-processing factor 19	2	-0.407	2.39E-01

LYRIC_MOUSE	Protein LYRIC	2	-0.407	1.44E-01
APEX1_MOUSE	DNA-(apurinic or apyrimidinic site) lyase	3	-0.410	2.12E-01
RL18A_MOUSE	60S ribosomal protein L18a	2	-0.411	6.12E-01
PLD4_MOUSE	Phospholipase D4	3	-0.413	7.90E-02
CAPG_MOUSE	Macrophage-capping protein	4	-0.414	1.58E-01
ARPC4_MOUSE	Actin-related protein 2/3 complex subunit 4	4	-0.415	7.39E-02
RAB1B_MOUSE	Ras-related protein Rab-1B	7	-0.417	1.88E-01
ATPO_MOUSE	ATP synthase subunit O, mitochondrial	4	-0.418	2.00E-01
SYSC_MOUSE	Serine--tRNA ligase, cytoplasmic	2	-0.419	1.53E-01
KPYM_MOUSE	Pyruvate kinase PKM	19	-0.421	8.69E-02
PTN6_MOUSE	Tyrosine-protein phosphatase non-receptor type 6	10	-0.425	2.43E-01
ODO1_MOUSE	2-oxoglutarate dehydrogenase, mitochondrial	4	-0.425	2.34E-02
PLEC_MOUSE	Plectin	84	-0.425	6.37E-02
HXK3_MOUSE	Hexokinase-3	13	-0.427	2.00E-01
HINT1_MOUSE	Histidine triad nucleotide-binding protein 1	2	-0.428	1.76E-01
SNX1_MOUSE	Sorting nexin-1	11	-0.429	2.73E-01
NMT1_MOUSE	Glycylpeptide N-tetradecanoyltransferase 1	2	-0.429	2.28E-01
H15_MOUSE	Histone H1.5	6	-0.430	2.48E-01
VDAC1_MOUSE	Voltage-dependent anion-selective channel protein 1	3	-0.434	1.19E-01
TGM2_MOUSE	Protein-glutamine gamma-glutamyltransferase 2	8	-0.438	2.58E-01
EM55_MOUSE	55 kDa erythrocyte membrane protein	4	-0.442	1.25E-01
RINI_MOUSE	Ribonuclease inhibitor	16	-0.442	3.51E-02
RALY_MOUSE	RNA-binding protein Raly	2	-0.443	1.11E-01
SNAA_MOUSE	Alpha-soluble NSF attachment protein	3	-0.443	2.16E-01
SHIP1_MOUSE	Phosphatidylinositol 3,4,5-trisphosphate 5-phosphatase 1	2	-0.444	2.81E-01
VP26A_MOUSE	Vacuolar protein sorting-associated protein 26A	3	-0.444	2.18E-01
GLU2B_MOUSE	Glucosidase 2 subunit beta	3	-0.445	3.60E-01
INO1_MOUSE	Inositol-3-phosphate synthase 1	2	-0.447	5.93E-01
GLCM_MOUSE	Glucosylceramidase	4	-0.447	9.58E-02
NDUA4_MOUSE	Cytochrome c oxidase subunit NDUFA4	2	-0.448	8.49E-02
COPA_MOUSE	Coatomer subunit alpha	6	-0.451	1.47E-01
RHG01_MOUSE	Rho GTPase-activating protein 1	3	-0.453	3.57E-01
RL19_MOUSE	60S ribosomal protein L19	2	-0.455	2.51E-01
AMPB_MOUSE	Aminopeptidase B	6	-0.457	1.23E-01
VAPB_MOUSE	Vesicle-associated membrane protein-associated protein B	2	-0.459	5.00E-02
AT1A1_MOUSE	Sodium/potassium-transporting ATPase subunit alpha-1	15	-0.460	2.35E-01
CASP8_MOUSE	Caspase-8	4	-0.461	2.66E-01
PTPRC_MOUSE	Receptor-type tyrosine-protein phosphatase C	12	-0.462	2.23E-01

CAN1_MOUSE	Calpain-1 catalytic subunit	3	-0.464	5.97E-02
BIEA_MOUSE	Biliverdin reductase A	6	-0.467	1.84E-01
FAM21_MOUSE	WASH complex subunit FAM21	2	-0.468	5.31E-01
GNPI1_MOUSE	Glucosamine-6-phosphate isomerase 1	4	-0.470	5.17E-03
PDXK_MOUSE	Pyridoxal kinase	4	-0.471	1.74E-02
HS90A_MOUSE	Heat shock protein HSP 90-alpha	18	-0.471	3.14E-01
ECHB_MOUSE	Trifunctional enzyme subunit beta, mitochondrial	4	-0.472	1.42E-01
LMAN2_MOUSE	Vesicular integral-membrane protein VIP36	4	-0.473	1.33E-01
HPRT_MOUSE	Hypoxanthine-guanine phosphoribosyltransferase	6	-0.474	1.37E-01
CLIC1_MOUSE	Chloride intracellular channel protein 1	10	-0.474	8.68E-02
K2C1_MOUSE	Keratin, type II cytoskeletal 1	3	-0.474	3.03E-01
CDC37_MOUSE	Hsp90 co-chaperone Cdc37	4	-0.477	4.17E-01
PDIA4_MOUSE	Protein disulfide-isomerase A4	10	-0.478	6.33E-02
GRP75_MOUSE	Stress-70 protein, mitochondrial	13	-0.478	1.87E-01
SNX3_MOUSE	Sorting nexin-3	3	-0.479	1.52E-02
PA2G4_MOUSE	Proliferation-associated protein 2G4	6	-0.480	9.49E-02
TIF1B_MOUSE	Transcription intermediary factor 1-beta	4	-0.481	1.83E-02
GSTM1_MOUSE	Glutathione S-transferase Mu 1	8	-0.484	8.51E-02
AHSA1_MOUSE	Activator of 90 kDa heat shock protein ATPase homolog 1	6	-0.486	6.47E-02
DOCK2_MOUSE	Dedicator of cytokinesis protein 2	7	-0.487	1.16E-01
TPP2_MOUSE	Tripeptidyl-peptidase 2	7	-0.490	1.75E-01
IDH3A_MOUSE	Isocitrate dehydrogenase [NAD] subunit alpha, mitochondrial	4	-0.492	5.32E-02
STXB2_MOUSE	Syntaxin-binding protein 2	2	-0.496	2.04E-01
RUVB2_MOUSE	RuvB-like 2	2	-0.496	3.13E-01
DEK_MOUSE	Protein DEK	2	-0.498	1.73E-01
PDIA6_MOUSE	Protein disulfide-isomerase A6	7	-0.501	2.10E-01
RCC2_MOUSE	Protein RCC2	2	-0.502	1.60E-01
PSA1_MOUSE	Proteasome subunit alpha type-1	3	-0.502	1.45E-01
AP1M1_MOUSE	AP-1 complex subunit mu-1	2	-0.508	1.06E-01
CBR1_MOUSE	Carbonyl reductase [NADPH] 1	2	-0.510	1.61E-02
DEST_MOUSE	Destrin	2	-0.510	6.28E-02
URP2_MOUSE	Fermitin family homolog 3	9	-0.512	2.72E-02
CATZ_MOUSE	Cathepsin Z	6	-0.512	4.25E-01
EFTU_MOUSE	Elongation factor Tu, mitochondrial	3	-0.513	8.45E-02
GSLG1_MOUSE	Golgi apparatus protein 1	2	-0.513	1.64E-01
ARPC5_MOUSE	Actin-related protein 2/3 complex subunit 5	5	-0.515	2.90E-02
PP1R7_MOUSE	Protein phosphatase 1 regulatory subunit 7	2	-0.517	3.55E-01
PSB4_MOUSE	Proteasome subunit beta type-4	3	-0.517	1.41E-01
SRSF2_MOUSE	Serine/arginine-rich splicing factor 2	2	-0.519	7.47E-02

VDAC2_MOUSE	Voltage-dependent anion-selective channel protein 2	7	-0.519	1.31E-01
TCPE_MOUSE	T-complex protein 1 subunit epsilon	8	-0.522	2.84E-02
ASNA_MOUSE	ATPase Asna1	2	-0.523	3.99E-01
AATM_MOUSE	Aspartate aminotransferase, mitochondrial	7	-0.523	8.62E-02
PSMD3_MOUSE	26S proteasome non-ATPase regulatory subunit 3	6	-0.524	2.91E-01
CHIL3_MOUSE	Chitinase-like protein 3	4	-0.525	2.80E-01
SEPT2_MOUSE	Septin-2	5	-0.525	7.63E-02
ATG7_MOUSE	Ubiquitin-like modifier-activating enzyme ATG7	3	-0.525	4.65E-01
G6PI_MOUSE	Glucose-6-phosphate isomerase	7	-0.526	1.40E-01
SNX2_MOUSE	Sorting nexin-2	11	-0.528	1.40E-01
MYO5A_MOUSE	Unconventional myosin-Va	3	-0.530	2.42E-01
PDIA3_MOUSE	Protein disulfide-isomerase A3	15	-0.530	4.25E-02
VIME_MOUSE	Vimentin	28	-0.537	6.49E-02
TWF2_MOUSE	Twinfilin-2	2	-0.538	1.04E-01
EIF3A_MOUSE	Eukaryotic translation initiation factor 3 subunit A	13	-0.539	2.17E-01
CLH1_MOUSE	Clathrin heavy chain 1	34	-0.540	4.95E-02
MDHM_MOUSE	Malate dehydrogenase, mitochondrial	12	-0.544	1.81E-02
VATB2_MOUSE	V-type proton ATPase subunit B, brain isoform	7	-0.544	5.56E-02
IQGA1_MOUSE	Ras GTPase-activating-like protein IQGAP1	40	-0.545	3.25E-02
MIC60_MOUSE	MICOS complex subunit Mic60	6	-0.546	2.61E-01
ANXA3_MOUSE	Annexin A3	8	-0.548	6.09E-02
NUDC_MOUSE	Nuclear migration protein nudC	3	-0.551	2.50E-01
H14_MOUSE	Histone H1.4	6	-0.557	1.68E-01
PCKGM_MOUSE	Phosphoenolpyruvate carboxykinase [GTP], mitochondrial	2	-0.559	5.97E-02
PCBP1_MOUSE	Poly(rC)-binding protein 1	7	-0.560	1.47E-01
ANXA5_MOUSE	Annexin A5	12	-0.563	5.98E-02
1433F_MOUSE	14-3-3 protein eta	9	-0.566	9.81E-02
ATP5H_MOUSE	ATP synthase subunit d, mitochondrial	3	-0.569	2.30E-01
RAB2A_MOUSE	Ras-related protein Rab-2A	4	-0.570	6.10E-02
HYOU1_MOUSE	Hypoxia up-regulated protein 1	9	-0.571	1.55E-01
ELMO1_MOUSE	Engulfment and cell motility protein 1	5	-0.573	1.18E-01
ERP29_MOUSE	Endoplasmic reticulum resident protein 29	4	-0.575	1.20E-02
PHB_MOUSE	Prohibitin	5	-0.576	3.37E-03
HNRPU_MOUSE	Heterogeneous nuclear ribonucleoprotein U	11	-0.578	5.59E-02
UD17C_MOUSE	UDP-glucuronosyltransferase 1-7C	5	-0.578	2.04E-01
AL5AP_MOUSE	Arachidonate 5-lipoxygenase-activating protein	2	-0.578	1.32E-01
ANXA4_MOUSE	Annexin A4	14	-0.579	3.14E-02
THIM_MOUSE	3-ketoacyl-CoA thiolase, mitochondrial	4	-0.579	1.08E-01

TALDO_MOUSE	Transaldolase	10	-0.580	1.90E-01
COPG1_MOUSE	Coatomer subunit gamma-1	3	-0.582	1.78E-01
NB5R3_MOUSE	NADH-cytochrome b5 reductase 3	5	-0.583	1.42E-01
NCPR_MOUSE	NADPH--cytochrome P450 reductase	8	-0.584	2.65E-01
STIP1_MOUSE	Stress-induced-phosphoprotein 1	8	-0.585	6.27E-02
RS14_MOUSE	40S ribosomal protein S14	5	-0.585	1.86E-01
PDIA1_MOUSE	Protein disulfide-isomerase	14	-0.590	1.15E-01
PKHO2_MOUSE	Pleckstrin homology domain-containing family O member 2	3	-0.592	1.86E-01
COF1_MOUSE	Cofilin-1	7	-0.593	9.25E-02
TPM3_MOUSE	Tropomyosin alpha-3 chain	6	-0.595	5.45E-02
DLDH_MOUSE	Dihydrolipoyl dehydrogenase, mitochondrial	3	-0.597	2.97E-02
LMNA_MOUSE	Prelamin-A/C	23	-0.602	6.76E-02
DHB11_MOUSE	Estradiol 17-beta-dehydrogenase 11	2	-0.602	1.82E-02
DHE3_MOUSE	Glutamate dehydrogenase 1, mitochondrial	15	-0.602	9.26E-02
GBG2_MOUSE	Guanine nucleotide-binding protein G(I)/G(S)/G(O) subunit gamma-2	2	-0.604	7.76E-02
KCY_MOUSE	UMP-CMP kinase	4	-0.604	1.08E-02
FMNL1_MOUSE	Formin-like protein 1	7	-0.606	2.50E-01
COR1A_MOUSE	Coronin-1A	9	-0.608	2.17E-01
VPS35_MOUSE	Vacuolar protein sorting-associated protein 35	10	-0.608	4.35E-02
ERF1_MOUSE	Eukaryotic peptide chain release factor subunit 1	5	-0.610	2.63E-03
ESYT1_MOUSE	Extended synaptotagmin-1	12	-0.610	2.48E-01
C5AR1_MOUSE	C5a anaphylatoxin chemotactic receptor 1	2	-0.611	3.73E-01
MPEG1_MOUSE	Macrophage-expressed gene 1 protein	10	-0.613	1.25E-01
LMNB1_MOUSE	Lamin-B1	8	-0.616	1.32E-01
FAS_MOUSE	Fatty acid synthase	9	-0.619	2.54E-01
TMED9_MOUSE	Transmembrane emp24 domain-containing protein 9	3	-0.620	1.00E-02
AP2B1_MOUSE	AP-2 complex subunit beta	11	-0.620	7.95E-02
ATPA_MOUSE	ATP synthase subunit alpha, mitochondrial	12	-0.621	3.25E-02
VA0D1_MOUSE	V-type proton ATPase subunit d 1	3	-0.621	1.74E-01
BIN2_MOUSE	Bridging integrator 2	2	-0.623	7.42E-02
1433T_MOUSE	14-3-3 protein theta	8	-0.624	1.51E-01
USO1_MOUSE	General vesicular transport factor p115	9	-0.624	1.06E-02
HNRPD_MOUSE	Heterogeneous nuclear ribonucleoprotein D0	3	-0.627	2.78E-02
VPP1_MOUSE	V-type proton ATPase 116 kDa subunit a isoform 1	3	-0.630	6.09E-03
QCR2_MOUSE	Cytochrome b-c1 complex subunit 2, mitochondrial	2	-0.633	2.00E-01
SNX5_MOUSE	Sorting nexin-5	9	-0.634	2.40E-02
DHB4_MOUSE	Peroxisomal multifunctional enzyme type 2	4	-0.635	8.01E-02
PMM2_MOUSE	Phosphomannomutase 2	2	-0.638	4.98E-02

PCNA_MOUSE	Proliferating cell nuclear antigen	7	-0.640	3.07E-01
SYLC_MOUSE	Leucine--tRNA ligase, cytoplasmic	4	-0.642	1.66E-02
MDHC_MOUSE	Malate dehydrogenase, cytoplasmic	7	-0.642	1.29E-02
SYNC_MOUSE	Asparagine--tRNA ligase, cytoplasmic	7	-0.642	1.68E-02
PAK2_MOUSE	Serine/threonine-protein kinase PAK 2	3	-0.646	1.93E-01
MPU1_MOUSE	Mannose-P-dolichol utilization defect 1 protein	2	-0.647	7.72E-01
GBB1_MOUSE	Guanine nucleotide-binding protein G(I)/G(S)/G(T) subunit beta-1	4	-0.649	9.40E-02
CH60_MOUSE	60 kDa heat shock protein, mitochondrial	11	-0.651	5.98E-02
ANXA2_MOUSE	Annexin A2	13	-0.652	4.24E-02
UB2V1_MOUSE	Ubiquitin-conjugating enzyme E2 variant 1	2	-0.653	5.10E-02
IMPA1_MOUSE	Inositol monophosphatase 1	2	-0.654	1.34E-01
IF2G_MOUSE	Eukaryotic translation initiation factor 2 subunit 3, X-linked	6	-0.654	9.91E-02
USMG5_MOUSE	Up-regulated during skeletal muscle growth protein 5	2	-0.658	1.12E-02
GMIP_MOUSE	GEM-interacting protein	2	-0.660	8.85E-02
GPNMB_MOUSE	Transmembrane glycoprotein NMB	4	-0.663	1.74E-01
ANXA1_MOUSE	Annexin A1	14	-0.664	6.04E-02
SP100_MOUSE	Nuclear autoantigen Sp-100	2	-0.664	1.14E-01
HEXB_MOUSE	Beta-hexosaminidase subunit beta	5	-0.666	1.04E-01
ASAH1_MOUSE	Acid ceramidase	6	-0.666	1.57E-01
CO4B_MOUSE	Complement C4-B	3	-0.667	2.07E-02
ITB2_MOUSE	Integrin beta-2	12	-0.671	2.66E-02
GDIB_MOUSE	Rab GDP dissociation inhibitor beta	14	-0.676	5.78E-02
OSBL8_MOUSE	Oxysterol-binding protein-related protein 8	6	-0.679	4.33E-03
SAMH1_MOUSE	Deoxynucleoside triphosphate triphosphohydrolase SAMHD1	8	-0.686	9.29E-02
APOBR_MOUSE	Apolipoprotein B receptor	4	-0.688	1.30E-02
PLXB2_MOUSE	Plexin-B2	2	-0.689	7.24E-02
FCGR1_MOUSE	High affinity immunoglobulin gamma Fc receptor I	2	-0.693	3.79E-02
H2AY_MOUSE	Core histone macro-H2A.1	3	-0.695	3.69E-02
CALU_MOUSE	Calumenin	2	-0.697	1.62E-02
IST1_MOUSE	IST1 homolog	2	-0.697	1.72E-01
AP1G1_MOUSE	AP-1 complex subunit gamma-1	3	-0.699	1.02E-01
COR1C_MOUSE	Coronin-1C	3	-0.699	1.39E-01
TPD54_MOUSE	Tumor protein D54	2	-0.699	6.88E-02
VAMP3_MOUSE	Vesicle-associated membrane protein 3	2	-0.704	9.36E-02
GLTP_MOUSE	Glycolipid transfer protein	2	-0.706	1.41E-01
HP1B3_MOUSE	Heterochromatin protein 1-binding protein 3	6	-0.706	1.66E-01
MYO1E_MOUSE	Unconventional myosin-Ie	10	-0.709	7.29E-02
VMA5A_MOUSE	von Willebrand factor A domain-containing	16	-0.710	1.17E-01

	protein 5A			
AP2A2_MOUSE	AP-2 complex subunit alpha-2	3	-0.711	9.54E-02
BASP1_MOUSE	Brain acid soluble protein 1	3	-0.714	1.04E-01
GANAB_MOUSE	Neutral alpha-glucosidase AB	3	-0.714	6.51E-02
CNDP2_MOUSE	Cytosolic non-specific dipeptidase	11	-0.715	3.49E-02
CATD_MOUSE	Cathepsin D	6	-0.717	2.58E-03
ALDR_MOUSE	Aldose reductase	8	-0.726	2.11E-03
PSD12_MOUSE	26S proteasome non-ATPase regulatory subunit 12	4	-0.735	3.07E-02
GELS_MOUSE	Gelsolin	11	-0.739	4.69E-02
AP1B1_MOUSE	AP-1 complex subunit beta-1	3	-0.739	2.64E-02
SPB6_MOUSE	Serpin B6	11	-0.745	4.20E-02
ARC1B_MOUSE	Actin-related protein 2/3 complex subunit 1B	6	-0.752	2.80E-02
ARL8A_MOUSE	ADP-ribosylation factor-like protein 8A	2	-0.762	3.13E-02
AMPN_MOUSE	Aminopeptidase N	19	-0.773	1.70E-01
CASP3_MOUSE	Caspase-3	2	-0.775	8.42E-02
DYN2_MOUSE	Dynamin-2	6	-0.782	4.44E-03
PACN2_MOUSE	Protein kinase C and casein kinase substrate in neurons protein 2	2	-0.783	1.09E-01
H3C_MOUSE	Histone H3.3C	3	-0.785	1.34E-01
ABD12_MOUSE	Monoacylglycerol lipase ABHD12	2	-0.797	5.03E-01
HNRPM_MOUSE	Heterogeneous nuclear ribonucleoprotein M	8	-0.803	6.10E-02
EHD4_MOUSE	EH domain-containing protein 4	14	-0.811	1.58E-05
LG3BP_MOUSE	Galectin-3-binding protein	6	-0.813	1.26E-01
PLCG2_MOUSE	1-phosphatidylinositol 4,5-bisphosphate phosphodiesterase gamma-2	3	-0.814	1.22E-01
CATS_MOUSE	Cathepsin S	4	-0.817	7.78E-01
PLBL2_MOUSE	Putative phospholipase B-like 2	2	-0.821	2.29E-01
VATG1_MOUSE	V-type proton ATPase subunit G 1	2	-0.822	6.24E-02
CAN2_MOUSE	Calpain-2 catalytic subunit	8	-0.822	1.51E-02
DBNL_MOUSE	Drebrin-like protein	2	-0.823	4.93E-02
ALDH2_MOUSE	Aldehyde dehydrogenase, mitochondrial	14	-0.826	2.95E-02
SYHC_MOUSE	Histidine--tRNA ligase, cytoplasmic	4	-0.831	3.90E-02
ECHA_MOUSE	Trifunctional enzyme subunit alpha, mitochondrial	7	-0.837	1.75E-03
PLD3_MOUSE	Phospholipase D3	3	-0.842	7.59E-02
KCRB_MOUSE	Creatine kinase B-type	8	-0.843	9.61E-03
LPXN_MOUSE	Leupaxin	2	-0.848	7.88E-02
ASPH_MOUSE	Aspartyl/asparaginyl beta-hydroxylase	5	-0.852	2.68E-02
MCM4_MOUSE	DNA replication licensing factor MCM4	2	-0.857	1.12E-02
FUBP2_MOUSE	Far upstream element-binding protein 2	2	-0.860	6.05E-02
DPP3_MOUSE	Dipeptidyl peptidase 3	4	-0.866	5.21E-02

GNAI2_MOUSE	Guanine nucleotide-binding protein G(i) subunit alpha-2	9	-0.868	1.02E-01
APOE_MOUSE	Apolipoprotein E	2	-0.869	1.04E-01
FEN1_MOUSE	Flap endonuclease 1	2	-0.870	2.04E-02
SRSF7_MOUSE	Serine/arginine-rich splicing factor 7	4	-0.874	1.03E-01
RMXL1_MOUSE	RNA binding motif protein, X-linked-like-1	5	-0.877	9.14E-02
ODPA_MOUSE	Pyruvate dehydrogenase E1 component subunit alpha, somatic form, mitochondrial	2	-0.879	4.14E-02
COX2_MOUSE	Cytochrome c oxidase subunit 2	2	-0.885	3.42E-01
SRRT_MOUSE	Serrate RNA effector molecule homolog	2	-0.888	1.26E-01
NCEH1_MOUSE	Neutral cholesterol ester hydrolase 1	4	-0.926	3.71E-03
LSP1_MOUSE	Lymphocyte-specific protein 1	5	-0.930	1.06E-02
MYOF_MOUSE	Myoferlin	6	-0.932	4.41E-02
PHB2_MOUSE	Prohibitin-2	3	-0.935	2.66E-02
NUCB1_MOUSE	Nucleobindin-1	4	-0.939	7.35E-02
CPNE3_MOUSE	Copine-3	4	-0.940	2.87E-02
RB11B_MOUSE	Ras-related protein Rab-11B	7	-0.942	4.40E-02
LYZ2_MOUSE	Lysozyme C-2	3	-0.946	1.03E-02
CD68_MOUSE	Macrosialin	2	-0.946	2.28E-02
ACON_MOUSE	Aconitate hydratase, mitochondrial	10	-0.949	8.89E-03
AT2B1_MOUSE	Plasma membrane calcium-transporting ATPase 1	3	-0.958	2.91E-01
STT3A_MOUSE	Dolichyl-diphosphooligosaccharide--protein glycosyltransferase subunit STT3A	5	-0.961	3.80E-02
S61A1_MOUSE	Protein transport protein Sec61 subunit alpha isoform 1	3	-0.991	6.89E-02
TRPV2_MOUSE	Transient receptor potential cation channel subfamily V member 2	4	-1.004	7.63E-02
PSD13_MOUSE	26S proteasome non-ATPase regulatory subunit 13	8	-1.018	1.93E-01
AL9A1_MOUSE	4-trimethylaminobutyraldehyde dehydrogenase	9	-1.025	6.07E-02
SAP_MOUSE	Prosaposin	9	-1.027	5.80E-02
DHX58_MOUSE	Probable ATP-dependent RNA helicase DHX58	2	-1.052	5.39E-01
MA2B1_MOUSE	Lysosomal alpha-mannosidase	2	-1.059	1.12E-01
SORCN_MOUSE	Sorcin OS=Mus musculus GN=Sri PE=1 SV=1	3	-1.070	6.57E-02
EEA1_MOUSE	Early endosome antigen 1	6	-1.082	1.61E-01
PUR9_MOUSE	Bifunctional purine biosynthesis protein PURH	8	-1.133	9.01E-02
BZW1_MOUSE	Basic leucine zipper and W2 domain-containing protein 1	3	-1.138	8.72E-02
SH3L1_MOUSE	SH3 domain-binding glutamic acid-rich-like protein	2	-1.254	5.72E-01
PKN1_MOUSE	Serine/threonine-protein kinase N1	3	-1.510	5.76E-02
HEXA_MOUSE	Beta-hexosaminidase subunit alpha	5	-1.595	2.18E-01

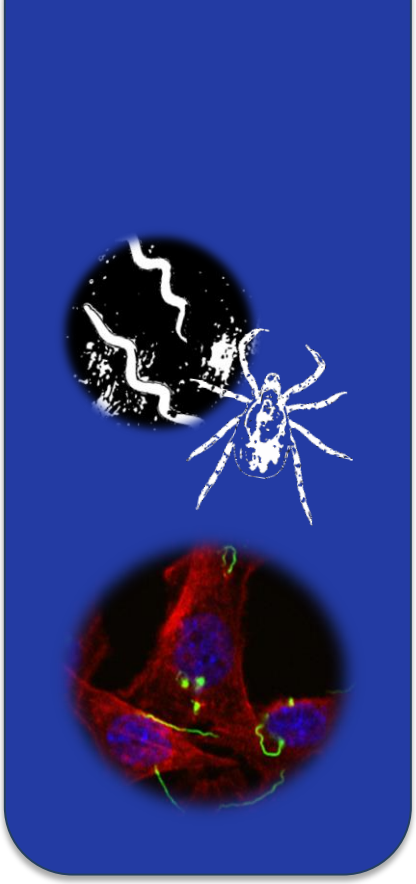

Scientific contributions

Scientific contributions

- Carreras-González, A. et al., (2019) Regulation of macrophage activity by surface receptors contained within *Borrelia burgdorferi*-enriched phagosomal fractions. *Submitted for publication*.

- Carreras-González, A., Navasa, N., Martín-Ruiz, I., Lavín, J. L., Azkargorta, M., Atondo, E., Barriales, D., Macías-Cámara, N., Pascual-Itoiz, M. A., Sampedro, L., Tomás-Cortázar, J., Peña-Cearra, A., Pellón, A., Prados-Rosales, R., Abecia, L., Elortza, F., Aransay, A. M., Rodríguez, H., … Anguita, J. (2018). A multi-omic analysis reveals the regulatory role of CD180 during the response of macrophages to Borrelia burgdorferi. *Emerging microbes & infections*, *7*(1), 19. doi:10.1038/s41426-017-0018-5

- Anguita J, Carreras-González A, Navasa N. (2018), Phagocytosis Assays for Borrelia burgdorferi. *Methods Mol Biol.* 1690:301-312. doi: 10.1007/978-1-4939-7383-5_22. PMID:29032553

- Albesa-Jové D, Romero-García J, Sancho-Vaello E, Contreras FX, Rodrigo-Unzueta A, Comino N, Carreras-González A, Arrasate P, Urresti S, Biarnés X, Planas A, Guerin ME., Structure (2017),Structural Snapshots and Loop Dynamics along the Catalytic Cycle of Glycosyltransferase GpgS. *Structure* 5;25(7):1034-1044.e3. doi: 10.1016/j.str.2017.05.009. Epub 2017 Jun 15.

- Albesa-Jové, D., Svetlíková, Z., Tersa, M., Sancho-Vaello, E., Carreras-González, A., Bonnet, Guerin, M. E. (2016). Structural basis for selective recognition of acyl chains by the membrane-associated acyltransferase PatA. *Nature Communications*, 7, 10906. http://doi.org/10.1038/ncomms10906

- Hawley, K. L., Olson, C. M., Carreras-González, A., Navasa, N., & Anguita, J. (2015). Serum C3 Enhances Complement Receptor 3-Mediated Phagocytosis of Borrelia burgdorferi. International Journal of Biological Sciences, 11(11), 1269–1271. http://doi.org/10.7150/ijbs.13395

- Navasa, N., Martin-Ruiz, I., Atondo, E., Sutherland, J. D., Angel Pascual-Itoiz, M., Carreras-González, A., Izadi, H., Tomás-Cortázar, J., Ayaz, F., Martin-Martin, N., Torres, I. M., Barrio, R., Carracedo, A., Olivera, E. R., Rincón, M., … Anguita, J. (2015). Ikaros mediates the DNA methylation-independent silencing of MCJ/DNAJC15 gene expression in macrophages. *Scientific reports*, *5*, 14692. doi:10.1038/srep14692

- Urresti S, Albesa-Jové D, Schaeffer F, Pham HT, Kaur D, Gest P, van der Woerd MJ, Carreras-González A, López-Fernández S, Alzari PM, Brennan PJ, Jackson M, Guerin ME, (2012)"Mechanistic Insights into the retaining glucosyl-3-phosphoglycerate synthase from mycobacteria, *Journal of Biological Chemistry*.